Dynamic Stability of Tunnel Elements During Immersion and Transportation



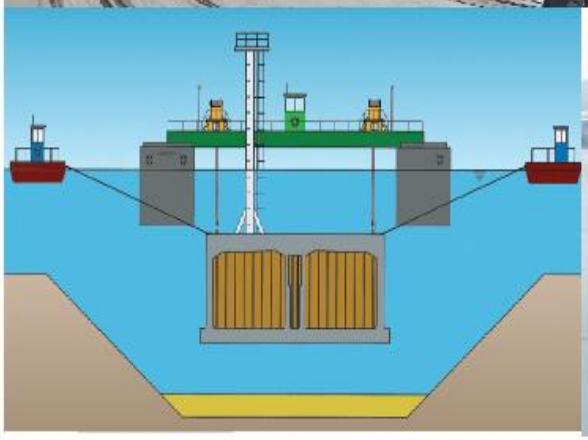


A.J Jelia

TU Delft

TU Delft Delft University of Technology

Van Hattum en Blankevoort

DELFT UNIVERSITY OF TECHNOLOGY
DEPARTMENT OF CIVIL ENGINEERING AND GEOSCIENCES

In cooperation with

Van Hattum en Blankevoort
Department of Hydraulic Engineering

Graduation committee members:

Chairman
Prof. Dr. Ir. S.N. Jonkman (Bas)
Full Professor of Hydraulic Engineering at Delft University

Supervisor TU
Ir. Zitman, T.J. (Tjerk)
Associate Professor of Costal and Hydraulic Engineering

Supervisor TU
Dr. ir. Hoogenboom, P.C.J. (Pierre)
Associate Professor Structural Mechanics

Supervisor Company
Ir. H.G. Hjelde (Hans)
Senior marine specialist at Van Hattum en Blankevoort

ABSTRACT

Immersed tunnel elements are prefabricated in the construction yard and then transported to the construction site to be integrated into the tunnel. During the transportation and immersion, the floating tunnel element is connected via cables to the immersion barges/pontoons. In this study, the hydrodynamical behavior of a floating tunnel element during construction has been modeled. The motional characteristics and stability of a floating tunnel element and twin barges during the installation are investigated.

This study aimed to investigate, how the stability of the system can be improved to make it possible to immerse a large number of tunnel elements in relatively short span of time in offshore conditions. The hydrodynamical behavior of the system and the related forces in different construction stages are analyzed. The focus of the study was on the determination of the influence of the pontoon configuration on the systems stability, the related forces, and operability. For this study, Fehmrnbelt Fixed Link tunnel project has been taken as a case study. The calculations are performed for two different pontoon configurations, namely:

- Catamaran (conventionally applied pontoon for the immersion of tunnel elements)
- Semi-submersible (platform used in offshore industry)

In the analysis, first, the main dimensions of the two pontoons are determined. The pontoons form the main piece of the immersion equipment. Subsequently, during the transport, the forces and moments on the floating element are evaluated. Two main type hydraulic external forces have been taken into consideration in the model, namely current and wave force. For different positions along transport route, the forces and moments are calculated for finite water depth and different values of flow velocity.

From the analysis, it appears that the wave-induced motions of a floating tunnel element are negligible. The relatively small waves are not able to bring the massive tunnel element into motions. The lowest natural periods of the floating tunnel element appears for roll degree of freedom, and it is about 8s. The significant current forces and moments occur during the fitting out. The stability of a floating element during transport is primary determined by the towing velocity.

During immersion, the systems stability due to waves and current forces is being analyzed. To assess the stability of the system for different current conditions, the vortex shedding periods are calculated. Then the natural frequencies of the system have been evaluated for different pontoon configurations and tunnel element length.

It appears that an immersion system with Catamaran pontoons seems to be less sensitive to vortex shedding period in contrast to the Semi-submersible barge. A Semi-submersible barge can only be used in 80% of current conditions in Fehmarnbelt. A Catamaran pontoon can be applied in 95% of the occurring current conditions.

Also, during the immersion, the wave-induced motions of the tunnel element can be ignored, provided that the wavelengths and wave periods are not too large. On the other hand, the relatively light pontoons are sensitive to wave loadings. The motions of the barges are prevented by the element, which leads to significant force fluctuations in suspension cables. In the analysis, the coupling between surge, sway, heave, roll, pitch and yaw degrees of freedom are considered. The calculations are performed for the first order responses that are valid in relatively low wave heights. Hydrodynamic effects caused by the nonlinearities are disregarded in the calculations.

The pontoons were considered as a hybrid structure. That means, concerning the horizontal degrees of freedom the pontoon structure is regarded as it is compliant and it behaves like a floating structure. While concerning the vertical degrees of freedom, it is stiff and resembles as a fixed structure, and it is not allowed to float freely. The contribution of the mooring lines to the first order response is considered of minor importance, and it is disregarded. Numerical studies are conducted to compare the dynamical behavior of the Catamaran pontoon with that of the Semi-submersible. The results of this study reveal that:

- The contribution of the first order wave force to the pontoons motions in soft degrees (surge, sway, and yaw) is limited.
- The motions in stiff degrees of freedom (heave, pitch, and roll) are normative for the immersion operation. When the tunnel element is immersed in wave conditions T>5 s and H > 1 m, then there is a significant danger that one of the suspension cables will break when applying a Catamaran pontoon. If a Semi-submersible barge is used, then the tunnel element can be immersed in wave conditions T < 6.5 s and H < 1.8 m.
- Semi-submersible pontoon has larger natural frequencies than Catamaran pontoon. The natural periods of the Semi-submersible barge are approximately a factor 1.4 larger than the natural periods of the Catamaran pontoon.
- A Semi-submersible pontoon is more sensitive to the force fluctuation in the suspension cables than the Catamaran pontoon concerning the static stability and floating capacity. Especially the floating capacity became problematic if the force fluctuations become large and therefore the pontoon can be pulled under water.
- The heave motions mainly affect the force fluctuations in suspension cables, and they can be considered as normative.
- Both barges are sensitive to the increasing wave height and period. However, the effect on Catamaran pontoon is larger. In total, a Semi-submersible barge has favorable operability in the waves and current conditions in Fehmarnbelt. Therefore, if the workability is the primary objective, then it is better to apply a Semi-submersible pontoon. Then in 77% of environmental conditions, the tunnel elements can be immersed.

For comparison of the dynamical behavior of both studied pontoons, different aspects are considered. The results are shown in the table here below.

Aspect	Catamaran	Semi-submersible
Forces in the suspension cables	-	+
Accelerations in heave	--	+
Accelerations in sway	+	-
Static stability	++	-
Floating capacity	++	-
Suite able for immersion of large tunnel elements	+	-
Stability in harsh current conditions	-	++
Stability in waves	--	++
Total operability	-	+

++	Clearly positive	--	Clearly negative
+	Positive	-	Negative
0	Neutral		

ACKNOWLEDGMENTS

This study is performed to obtain the degree in Master of Science in Civil Engineering at the Delft University of Technology, under the authority of the section of Hydraulic Engineering. The work was carried out in close cooperation with Van Hattum en Blankevoort, Department of Hydraulic Engineering.

I would like to thank all the members of my graduation committee for their great support, patience, comments, and their helpful recommendations during this study. Without them, I would not manage to finish this work. Also, I learned a lot from them.

I would also like to thank colleagues at Van Hatum and Blankervoort for their hospitality and for sharing their experiences and expertise.

Thanks also to my family and friends for their support during this period. Especially my heartfelt thanks go to the two most important women in my life my mother and my wife. And particularly to my wife Hogay for her forbearance and support during the writing of this report.

Table of Contents

LIST OF FIGURES

LIST OF TABLES

LIST OF SYMBOLS

Symbol	Definition	Units
F_d	Horizontal flow force on the system	[kN]
C_d	Drag coefficient	[-]
A_c	Effective surface of the element perpendicular to flow direction	[m^2]
ρ	Water density of flowing water	[kg/m^3]
V_R	Reference speed	[m/s]
A	Added mass matrix	
F_{lift}	Lift force per unit length of the tunnel element	[kN/m]
C_L	Dimensionless lift coefficient	[-]
f_v	Vortex shedding frequency	[1/s]
t	time	[s]
ε_{Ft}	Phase shift of the lift force	[rad]
St	Strouhal number, depending on the geometry and the Reynolds number.	[-]
V_{cur}	Undisturbed flow velocity	[m/s]
$T_{excitation}$	Excitation period	[s]
T_n	Natural period	[s]
m	Mass of the tunnel element	[kg]
m'	Added mass of the TE	[kg]
K_z	Spring stiffness for heave	[N/m]
K_{xx}	Spring stiffness for roll	[N/rad]
K_{yy}	Sprig stiffness for pitch	[N/rad]
T	Draught of the floating structure	[m]
F_{Ed}	design value of the axial rope force	[N]
F_{Rd}	design value of the tension resistance	[N]
F_{uk}	characteristic value of the breaking strength	[N]
F_k	characteristic value of the proof strength of the tension component	[N]
γ_R	partial factor.	[-]
F_{min}	minimum breaking force factor taking account of the spinning loss	[N]
k_e	spinning loss factor	[-]
K	minimum breaking force factor taking account of the spinning Joss	[N]
d	nominal diameter of the cable	[m]
R_r	rope grade	$[N/mm^2]$
f	fill factor	[-]
T_n	Natural period in n^{th} degree of freedom	[s]
I_{xx}	Moment of gyration in roll degree of freedom	[$kg \cdot m^2$]
I_{yy}	Moment of gyration in pitch degree of freedom	[$kg \cdot m^2$]
K_{heave}	Spring stiffness of the system in heave degree of freedom	[N/m]
K_{roll}	Spring stiffness of the system in roll degree of freedom	[N/m]
K_{pitch}	Spring stiffness of the system in pitch degree of freedom	[N/m]
r_{xx} and r_{yy}	Radius of gyration in the roll and pitch degree of freedom	[m]
$[M]$	The mass matrix of the system	[kg],[$kg \cdot m^2$]
$[M_a]$	The added mass matrix	[kg],[$kg \cdot m^2$]
$[C]$	The damping matrix.	[]
$[K]$	Stiffness matrix	[N]
$F(t)$	The force vector consisting from Froud-Krilov components	[N],[N·m]
$X(t)$	Displacement vector of the system	[m],[rad]
$\dot{X}(t)$	Velocity vector of the system	[m/s],[rad/s]
$\ddot{X}(t)$	Acceleration vector of the system	[m/s^2],[rad/s^2]
E	Eigen matrix of the system	[-]
ξ_i	Critical damping ratio in the i^{th} degree of freedom (taken as:0.05)	[-]
ω_i	Natural frequency in the i^{th} degree of freedom	[rad/s]
m_i	Modal mass in the i^{th} degree of freedom	[kg], [$kg \cdot m^2$]

1 INTRODUCTION

More than a half-century immersed tunnels are constructed worldwide. The majority are built in Europe, North America, and Japan. The first immersed tunnel in Europe is the Maastunnel in the Netherlands (Rotterdam). Today various types are constructed worldwide. The majority of immersed tunnels build in Europe are concrete tunnels while in North America the most of the immersed tunnels are constructed from steel. Due to many waterways and dense infrastructural network, more than half of the immersed tunnels in Europe are built in the Netherlands. For this reason, Dutch expertise has been involved in the tender phase of the Fehmarnbelt Tunnel project.

The Fehmarnbelt Fixed Link Corridor between Denmark and Germany is a spectacular infrastructure project of world-class. The fixed link is an immersed tunnel that will connect the German island Fehmarn with the Danish island Lolland. The tunnel will cross the Fehmarnbelt in the Baltic Sea at its narrowest point. The distance between the two islands is about 19 km, along with this 'shortest' distance; an immersed tunnel will be constructed.

Figure 1 Project area (DHI)

The new link is supposed to improve the travel time between Germany and Denmark. The fixed link will directly connect the two important cities in the region, Kopenhagen, and Hamburg. That's why the new link is of a large economic importance in this region.

This tunnel project has many distinctive features including its great length, its depth, offshore location, competitive marine conditions, and geographical alignment constraints. These features, combined with the overall scale of the project, make the design and construction of this massive project a distinctive challenge. Mainly its maritime site conditions and a large number of tunnel elements which have to be immersed in deep water (in deepest parts >30 m) is a great challenge for the designers and executors of the project.

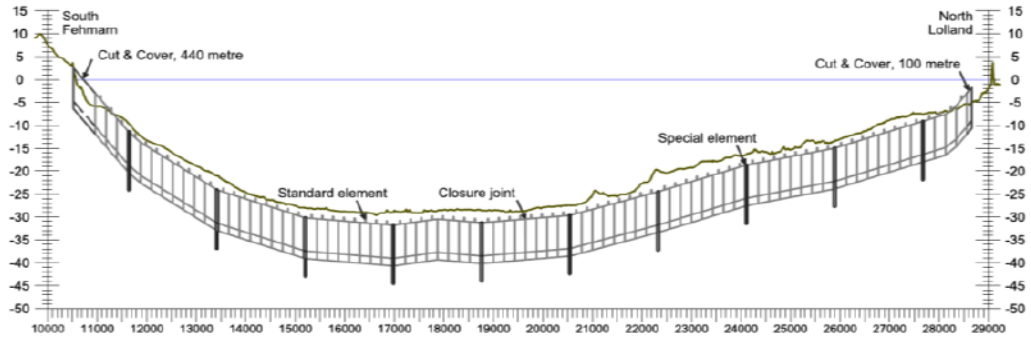

Figure 2 Fixed Link alignment (Femern A/S, 2013)

The Fehmarnbelt Fixed Link will be the largest immersed tunnel in the world. The immersion technique has never been used on this scale worldwide. The size and complexity of this project are unmatched compared to other immersed tunnel projects. The Fixed Link consists of 79 standard and 10 special immersed elements. The alignment configuration of the elements is given chapter 4.2 of this report. The production of the elements will take place in a controlled environment within a construction yard (also indicated in this report as the construction factory), which will be located on the Danish side of Fehmarnbelt

In the current design, it's been envisaged that the production site is to be located on the east side of Lolland (Denmark). After casting and hardening of the concrete, the tunnel elements will be prepared for transport and immersion. Subsequently, each tunnel element will be towed to the tunnel trench, where it will be immersed.

Figure 3 Tunnel production factory at east site of the Rødbyhavn (Femern A/S, 2013)

At the time of writing of this report, the Fehmarnbelt Fixed Link project is in the design stage. No final choices have been made yet about the length dimensions of the tunnel elements, the immersion method, and equipment. On the other hand, the hydraulic boundary conditions for immersion and transport are sufficient known.

1.1 Problem Background

The Fehmarnbelt Fixed Link will be the largest immersed tunnel in the world. The immersion technique has never been used on this scale worldwide. The longest road tunnel till the recent years was the Øresund Tunnel between Denmark and Sweden. The first immersed tunnels were relatively short, around 1 km long. The limiting factor for constructing long immersed tunnels was the ventilation system.

In structural terms, it is believed that there is no limit to the length of an immersed tunnel. Longer road tunnels are becoming possible as vehicle emissions and ventilation systems improve. The construction of the Fehmarnbelt will even encourage the development of the immersion technique and its application for an even greater scale of the immersed tunnels. The discussion is being made about the possibilities of building connections such as Bering Strait, English Chanel, and Irish Sea as immersed tunnels.

However, there are still several challenges to complete the tunnel element within a reasonable timescale and harsh environmental conditions. Till the moment, the elements are immersed in relatively calm waters during the summer months. To build very long immersed tunnel within a reasonable timescale the workability of the contractor's equipment has to be improved

There is a lot of experience gained over the years in constructing immersed tunnels. Nevertheless, most of the time the immersion process took place in river conditions, where wind waves and swells did not play an important role. For projects such as Fehmarnbelt Fixed Link and other future projects in offshore conditions, the effect of waves and swell cannot be ignored. After all the design and the execution method for an immersed tunnel must be chosen such that tunnel element can be placed safely on the bottom. Also after the placement, the tunnel element must remain stable on the ground.

During the immersion, the stability of a tunnel element is provided by the immersion rigs, which are also indicated in this report as pontoons (see, Figure 4). The pontoons and the element have to be positioned accurately over the tunnel trench when the element is being immersed. Due to external forces such as wave and current forces, the tunnel element and the pontoons will undergo some movements. Only very limited motions are acceptable for safe and accurate placement.

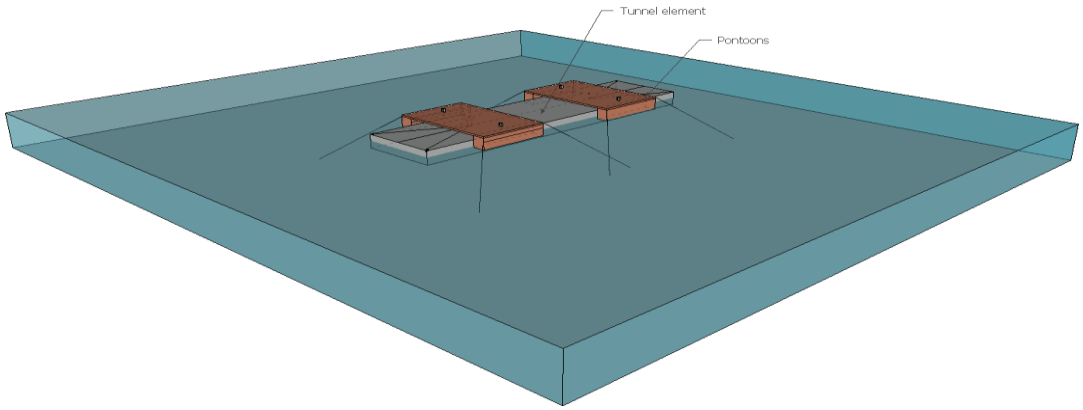

Figure 4 Tunnel element and two pontoons (also indicated as system)

As it has been mentioned before, the tunnel elements are immersed during the summer months when the wave and current conditions are mild. Nevertheless, in the case of Fehmarnbelt, this seems not to be feasible. Continuity in workability is required. Therefore, the immersion equipment and the immersion method have to be chosen such that the operability of the system has to be optimal. Also, the limiting environmental conditions have to be identified in which no immersion is possible.

The number of elements, which has to be immersed is large (89 elements). For economic reasons the chosen equipment and the immersion procedure are not chosen such that the immersion can take place in extreme weather conditions. On the other hand, in a relatively short period (3 years) all 89 elements should be immersed. In recent years three projects have been realized that have been built in the marine environment, namely:

- The Oresund Fixed Link (between Denmark and Sweden)
- Bosphorus Fixed Link (Istanbul Turkey)
- The Busan-Geoje Fixed Link (in South Korea)

When analyzing the immersion system for the three mentioned projects, one of the main differences in construction technique is the choice of the pontoon configuration (see Figure 5). From the figure, it can be seen that the configuration and dimensions of all the presented pontoons are different. Conventionally, two type pontoons are used namely a catamaran or a single pontoon (floating steel box), see also Figure 15. However, from the offshore industry it is also known that there are different types floating platforms, which are more stable in marine environment than a rectangular box-shaped pontoon.

The dynamic behavior of the system (pontoons + tunnel element) during the immersion is dictated by the size and the configuration of the pontoons. The dynamic interaction between the system and force excitation is different for distinct pontoon configuration. Therefore, the operability of the different pontoon types is also different.

Figure 5 different immersion pontoon types used in the projects (Oresund Fixed Link, Bosphorus Fixed Link and the Busan Geoje Fixed Link) [(CAPITA SYMOND)**,** (TAISEI Corporation , 2014)**,** (Hans Cozijn and Jin Wook Heo, 2009) **]**

In order to improve the workability of the contractor's equipment, the idea of investigating the effect of the pontoons configuration and its' dimensions on the workable conditions has been developed. In offshore industry, several platform configurations are used to handle the harsh environmental loads and conditions. One of the platforms frequently used in offshore industry is the Semisubmersible. It has advantageous motional characteristics, which makes it very interesting for application as a pontoon for the immersion of a tunnel element. In this thesis report the motional characteristic of two different type pontoons namely, conventional Catamaran and Semisubmersible (used in offshore industry) are investigated, see also Figure 26 and Figure 27. The dynamic stability and workability of the system with the two distinct pontoons are investigated and compared to each other, given the boundary conditions of Fehmarnbelt.

1.2 PROBLEM DEFINITION

The main problem investigated in this report is identified as:

During immersion of a tunnel element, several forces are exerted by surrounding water on the system (immersion pontoons + tunnel element) which will result in motions of the system in 6 degrees of freedom. Only very limited motions are acceptable for safe and accurate placement. On the other hand during the immersion process, only the pontoons provide the stability of the system. It is unknown what the effect of the pontoon configuration is on the total stability and workability during different environmental conditions.

1.3 RESEARCH OBJECTIVE

The main objective of this study is to investigate the effect of the pontoon configuration on total stability and workability of the system in different environmental conditions. In addition, it has to be investigated how the stability of the pontoons can be improved by adjusting its configuration.

1.4 SCOPE OF THE RESEARCH

The baseline of this research is to investigate, how the stability of the system can be improved to make it possible to immerse a large number of tunnel elements in relatively short span of time in offshore conditions. Therefore the hydrodynamic behavior of the system and the related forces in different construction stages will be determined. The focus of the study will be on the determination of the influence of the pontoon configuration on the systems stability, the related forces, and operability.

The method of execution determines the type of equipment and sequence of steps to be used. Because the choices influence each other, therefore the entire process of immersion including transport will be evaluated. The stability of the system will be evaluated from leaving the construction yard till the tunnel element is integrated into the fixed link. This report deals with how the design principles of different pontoon configurations affect the motional

characteristics in 6 degrees of freedom and operability. Two types of immersion pontoons Catamaran and Semi-submersible will be analyzed concerning operability and response in waves and current. Also, the forces and stability during the transport are investigated.

1.5 Research Question

What is the effect of the pontoon configuration on the stability and operability of the system during the immersion process?

1.6 Sub Questions

In order to answer the main question, several sub-questions are formulated. The table below also indicates where the sub-questions have been treated in the report.

Sub question	Treated in report
– What is the operational concept of immersion of a tunnel element in off shore conditions. (Which steps are involved in transportation and immersion of a tunnel element)?	2.2
– Which force mechanisms are working on the tunnel element during transportation and immersion in offshore conditions?	Chapter 3
– How can the system of tunnel element and pontoons be schematized/modeled?	
– Which aspects need to be taken into account for the determination of the pontoon dimensions?	4.3 and Appendix 1
– What are the main failure mechanisms for the immersion process?	4.7
– What is the dynamical behavior of the different pontoons configurations during the immersion process and how it can be modeled?	Chapter 7
– What is the effect of the pontoon configuration on the forces in the suspension cables?	7.6
– What is the effect of the pontoon configuration on the natural frequencies of the system?	8.2.1 and 8.3.1
– Which pontoon configuration has favorable workability/availability for the immersion of the tunnel elements?	8.2.4 and 8.3.4
– What is the effect of the dimensions of the tunnel element on the natural frequencies of the system?	6.4
– Which pontoon configuration is most suitable for the construction of the Fehmarnbelt Tunnel?	Chapter 9

1.7 Approach

The research is sub-divided into two phases. Each phase consists in its turn from several steps which are elaborated to obtain the answer to the main and sub-questions.

First, a literature survey of immersion techniques has been elaborated. Several pontoon configurations were considered for the immersion of the Fehrnbelt tunnel project. Besides, it is investigated which force mechanisms works during transport and immersion on the system. Subsequently, the boundary conditions and the requirements were determined.

Also, the important aspects which influence the dimension of the pontoons were identified. These aspects were translated to the environmental conditions in the Fehmanrbelt. Finally by taking into account the design aspects for the pontoons and environmental conditions the dimension of the pontoons were calculated.

During the transport, the forces on the system were calculated by making use of the available data from previous model tests on the tunnel elements. The influences of different environmental conditions were taken into account. The dynamic and static stability of floating element is evaluated.

The static stability was checked for the calculated pontoon dimensions. Different force mechanisms are investigated during the transport and immersion. Also, the effect of different parameters on the stability of the system has been determined. Finally, for the two different pontoon configurations, the operability in the Fehmarnbelt was investigated.

In order to study the dynamical behavior of the system, a numerical model is set up. The equation of motions has been solved in the time domain. For several environmental conditions, the response of the two types pontoon was evaluated in the time domain calculations. In addition, other parameters such as force in the suspension cables and the accelerations of the pontoons were calculated. For the operability evaluation, the system has been analyzed in the frequency domain. Response Amplitude Operators are determined as a function of wave frequency. Subsequently, the response spectra were calculated, and results were translated to statistical values of the response. The operability has been determined for the given wave scatter diagram in the Fehmarnbelt.

1.8 Thesis Outline

The report structure is given here below.

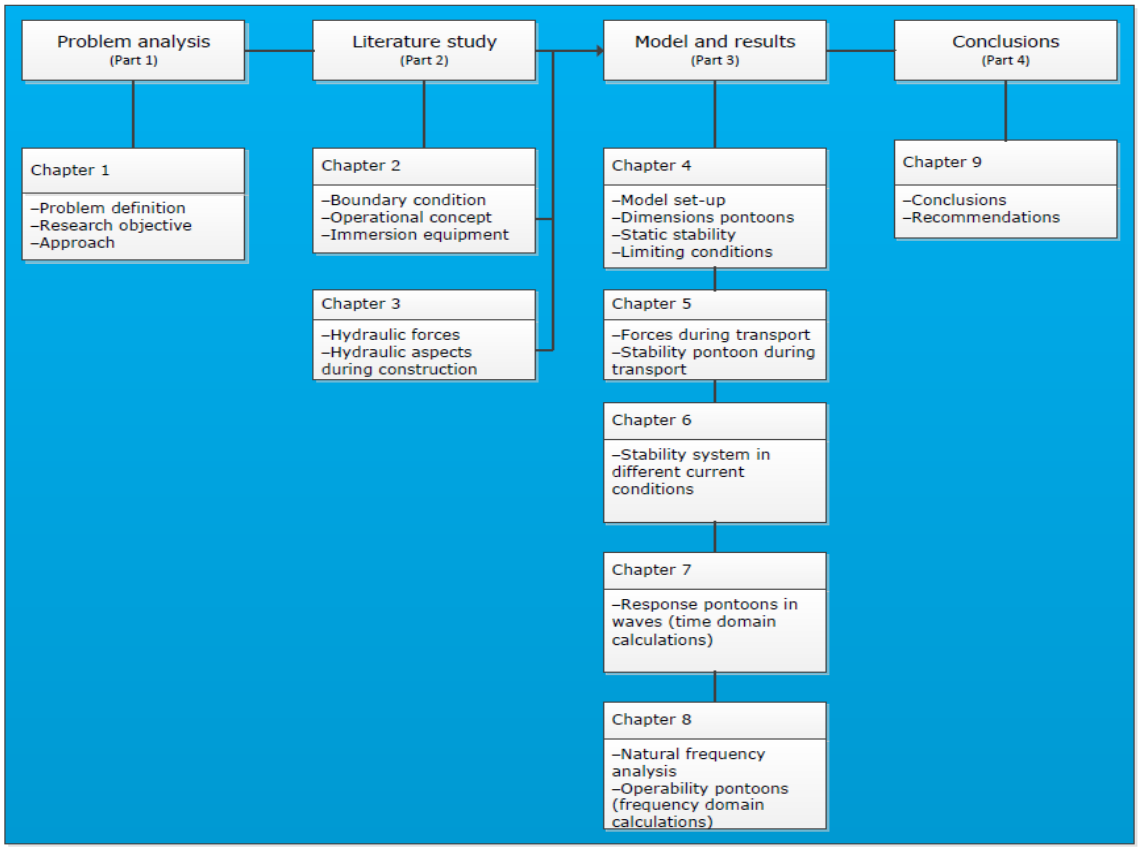

Figure 6 Report structure

2 CONSTRUCTION PROCESS AND HYDRAULIC BOUNDARY CONDITIONS

In this chapter, the construction process of the Fixed Link is described. The focus is on the immersion and transportation stages. Also, a brief explanation is given on the hydraulic boundary conditions which influence the immersion of the tunnel element. Also, the immersion equipment is discussed.

Immersed tunnels are designed such that they can float in the temporary conditions such as transportation. At the construction site, the element has to be ballasted with ballast water to immerse the tunnel element to its final destination in the trench. To overcome the positive buoyancy, the total weight of the element and the ballast has to be higher than the buoyancy force Fb.

2.1 HYDRAULIC BOUNDARY CONDITIONS

The Employer (owner of the project) provided hydrological and geological data and the draft design of the tunnel elements. The available hydrological and geological data have been developed from the investigations carried out by the owner of the project. For the calculations in this report, the relevant threshold values have been used. The following data categories are used for the analysis.

- Flow velocity
- Wave data
- Water levels
- Salinity rate

2.1.1 BATHYMETRY

The water depth is variable across the Fehmarnbelt, the bathymetry of the fairway has a greater gradient on the German side, and it is less steep near the Danish coast. In addition, from Figure 7 it can be concluded that the water depth decreased toward the coasts.

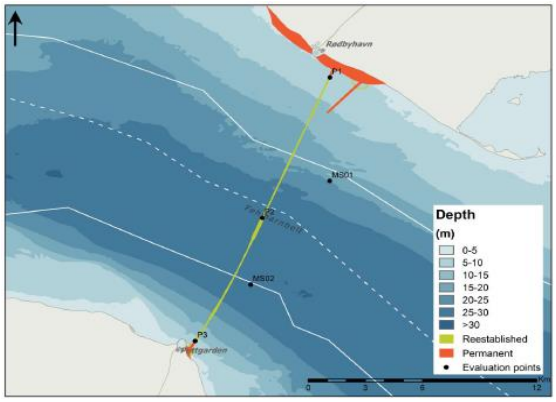

Figure 7 Water depth (Femern A/S, 2013)

2.1.2 WAVES

Waves in the project area are primarily governed by the local wind conditions and the limited fetches. The wave climate at Fehmarnbelt could occasionally be affected by the waves of the Baltic sea (southeastern: Akrona Basin). The local wind conditions primarily govern waves in the project area. The surrounding lands limit the fetches. In general, the wave climate can be considered as a mild. From the analyzed data it can be concluded that the highest waves occur in the middle of the corridor (P2). The mean wave heights near the German(P3) and Danish(P1) shores are approximately 35% and 15% lower than the mean wave height in the middle (P2). The maximum wave height measured during the 18 years measurement study is 3.6 [m] which occurred during the severe storm in December 1999 in combination with extreme wind speed (27.2 [m/s]). The annual statistics of the omnidirectional waves are presented in Table 1 .

Position	Significant wave height, Hm0 [m]	Spectral peak wave period, Tp [s]	Mean wave period,T02 [m]
	min/mean±std/max	min/mean±std/max	min/mean±std/max
P1 (near Rødby)	<0.1/0.49±0.36/2.90	1.01/3.41±1.08/8.51	0.80/2.28±0.72/5.61
P2 (Middle of the fixed corridor)	<0.1/0.57±0.40/3.58	1.01/3.44±1.01/7.38	0.81/2.42±0.73/5.13
P3 (near Puttgarden)	<0.1/0.38±0.27/2.21	1.01/3.21±1.01/9.27	0.82/2.02±0.0.56/4.67
MS01	<0.1/0.57±0.40/3.56	1.01/3.41±1.01/7.00	0.81/2.42±0.73/5.10
MS02	<0.1/0.53±0.37/3.09	1.01/3.42±0.99/8.40	0.82/2.35±0.68/4.74

Table 1 Basic Statistics of wave model data

2.1.3 CURRENT VELOCITIES

For the project area there are model values, and 18 years data measurements are available concerning the current velocities. As mentioned in Appendix 2, Fehmarnbelt is a transitional area between the North Sea and Baltic Sea. The water column is stratified associated with different flow velocity and directions. The surface flow is predominantly outgoing and the near-bed current direction is in-going. The current data include parameters of current speed and direction for the combined tidal and surge signal. The modeled current velocity values may be interpreted as representative of approximately 3-hourly averages. The current direction can be considered with an angle of 45-270° relative to the north.

The seasonal variation of the current is characterized by stronger flow velocities in the winter, fall, and weaker flow velocities in the summer for all depths. In the center of the waterway at the point P2 (see Figure 7) the flow velocities are the strongest. The distribution of the flow velocities for the 18 years modeled data are shown in Figure 8 and Figure 9.

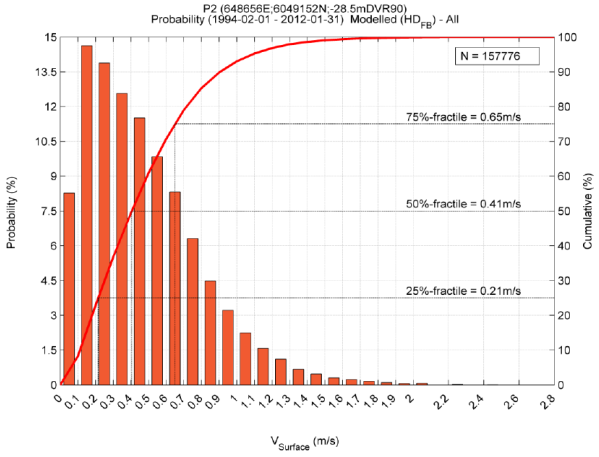

Figure 8 The distribution of surface current velocity (FEHY (Metocean Conditions), 2013)

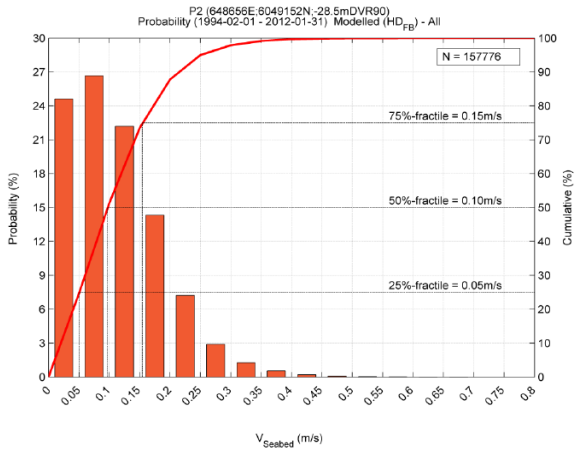

Figure 9 The distribution of near-bed current velocity (FEHY (Metocean Conditions), 2013)

2.1.4 SALINITY

The Fehmarnbelt is a transitional area between the Baltic Sea and the North Sea. The stratification in the Fehmarn Belt is strongly related to water exchange between the North Sea and Baltic Sea. The surface water flows from Baltic Sea with low salinity. The lower layer of the water column is mainly water from the North Sea with height salinity rate. The salinity of water is to be expected to increase with the incoming tide. And the salinity will reduce when the tide recedes and the saline water is flushed out by the river water. Also, seasonal variation in salinity occurs.

The water column is mainly stratified in the Fehmanrbelt, that´s why for the calculations a stratified water column is assumed. The precise shape of the stratification is difficult to predict because it is also time dependent. It can be noted that transitional area in the vertical direction is around 15 [m] (approximately). The associated water density fluctuations in the vertical of 5 [kg/m^3] (maximum) can be observed from the available data. Normally the water density fluctuation is smaller.

During a period of 19 years, the salinity rate has been measured at the Fehmarnbelt light vessel (located approximately east of the fixed link corridor). The monthly variation is originally reported and discussed in (FEHY, 2012a). Also during the period 1931-1993 the salinity of the surface water has been measured at Rødbyhavn. The extreme monthly values of the variations are presented in appendix 2. The annual mean salinity measured is 12.2 [psu]. There is large span in the variation of the extreme values of salinity. In the 62 years measured data which are available for the project locations the following extreme values are obtained:

- Minimum measured salinity 6 [psu]
- Maximum messured salinity 27 [psu]

2.2 Operational Concept

The building process of the tunnel elements is divided into four distinct building phases; each tunnel element will encounter this process. The phases refer from the leaving the construction factor till the element will be integrated into the Fixed Link. Also, attention is paid to the final phase when the tunnel will be finished. The following immersion phases should be distinguished:

I. Construction yard/fabric:

a) As discussed before, the tunnel elements are produced in a construction factory on the Danish site. After finishing the tunnel elements, each end is sealed with the aid of the bulkheads and ballast tanks are installed. Also, equipment for the remote-controlled ballast water system is installed too.

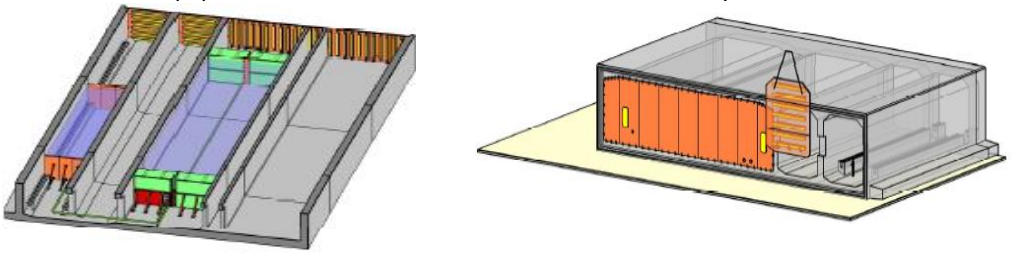

Figure 10 Principle of installing ballast tanks and bulkheads (FEHMARN BELT CONTRACTORS, 2013)

b) After installing the ballast tanks and bulkheads water will be pumped into the ballast tanks. This is done to prevent that the tunnel element will be floated in an uncontrolled way when the water basin will be filled with water. Also, the water tightness of the tunnel elements will be checked in this phase. The bollards will be installed on the deck of the tunnel elements, and the element is transported to a deeper water basin.

c) In the deeper water basin, the elements are further prepared for the transportation and immersion. Therefore the tunnel elements will be temporary moored. On the deck of the elements lifting lugs, sheaves, guide beams, and catches will be installed. The guide beams and the catches are used to guide the tunnel element sideways during the immersion. The lifting lugs and sheaves are used to pull up the tunnel element.

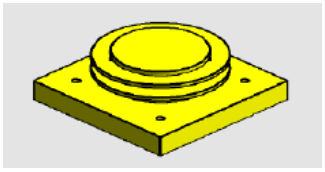

Bollards

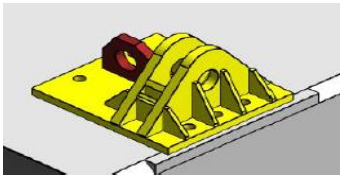

Lifting lugs

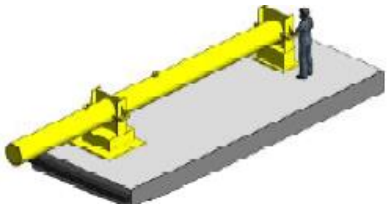

Guide beam

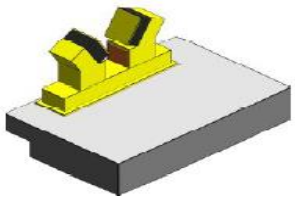

Catch

Figure 11 Overview equipment (FEHMARN BELT CONTRACTORS, 2013)

d) Before the transportation, two immersion pontoons are installed over the tunnel element. The pontoons are catamaran or semisubmersible type. The pontoon characteristics will be discussed later in this report.

e) When the predicted weather and wave conditions are within the workable window (will be discussed later on in the report) the final go decision will be made. The combined system (tunnel element + 2 pontoons) will be towed to the construction site where the preparation works (prepared trench and gravel bed) are already will be finished.

II. **Transport**

a) The system will be transported to the construction site by the aid of the tugboats. During the transport, the suspension cables will be tensioned by pulling the tunnel element a little bit. Between the tunnel element and the pontoons some blocks will be placed. This is done in order to make the three-bodied system (tunnel element and 2 pontoons) to behave as one system during the transport. This tightening will improve the floating stability and transportability of the system. During the transportation, the tunnel element will be floating with the large part under-water with a small freeboard.

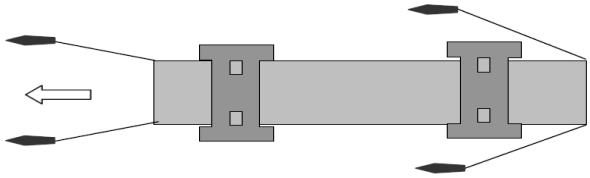

Figure 12 Tugboat configuration (FEHMARN BELT CONTRACTORS, 2013)

III. Immersion

a) After arriving on the construction site, the system is carefully shifted to the planned position above the tunnel trench. The pontoons and the element will be attached to the anchor points using the mooring lines. The element will be immersed using pumping water into the ballast tanks. When the weight of the tunnel element is larger than the buoyancy force, it will start to sink.

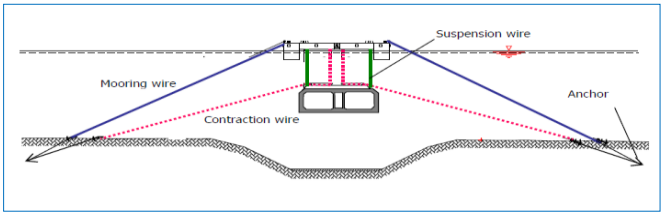

Figure 13 Tunnel element during the immersion (Wim Janssen, 2012)

b) To keep the system into the position, a spread of winch wires will be used. Three different kinds of wires are used: suspension wires, mooring wires, and contraction wires. Before the immersion, first, the wires have to be connected to the mooring points on the sea floor. Traditionally the taut mooring configuration is chosen to reduce the motions caused by the waves and current.

c) During the immersion the floating pontoons fully carry the weight of the tunnel element by means of suspension cables. The tunnel element will be connected to the previous one usingGina gasket. The Gina gasket provides also a temporary watertight seal. The newly immersed tunnel element will be placed on the gravel bed adjacent to the previously installed one. The elements will be pulled against each other, and the Gina gasket compresses and some water remains between the bulkheads. After being connected the water in immersion joint is pumped out.

The hydrostatic pressure at the free end compresses the Gina gasket further. The coupling steps are illustrated Figure 14. For the permanent water tightness, an omega profile will be installed. The deck layout used for the immersion and transportation will be removed by divers. The used immersion equipment will be returned to the fabric site for the immersion of the new element.

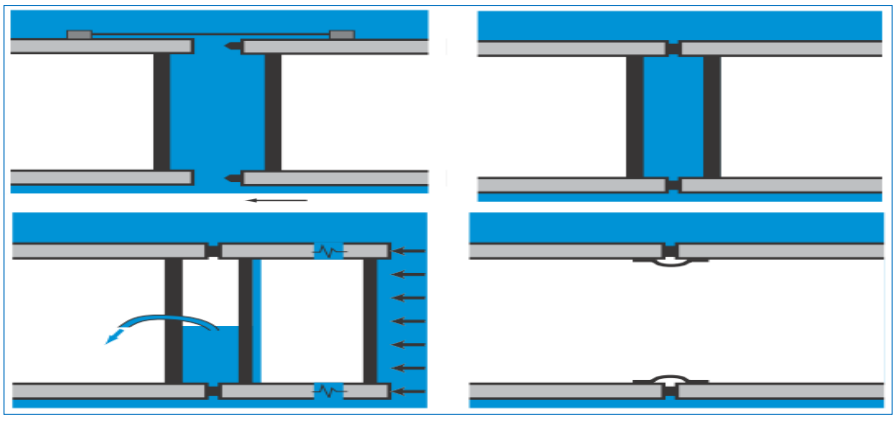

Figure 14 Connecting two elements (Lyngs, 2008)

IV. Immersed tunnel element

a) After connecting the two elements and bringing the water tight seal omega, it will be exposed to the hydraulic forces. Especially the lift force from passing ships can damage the element or its foundation. The element is not covered immediately. After placing the element on the bottom of the dredged trench, it has to be ballasted such the total weight must be 2.5% larger than the buoyancy force (temporary phase). In this temporary phase, the tunnel element will be ballasted using ballast water. This means that after the immersion extra ballast water will be pumped into the ballast tanks. In the final stage, the ballast water has to be exchanged by the ballast concrete and the ballast tanks will be removed and the dredged trench will be backfilled.

In order to be sure that the tunnel element will not float up the total weight must be 7.5% larger than the buoyancy force. Also, the trench will be refilled for a part by sand. And the roof will be protected using rock filter to prevent the erosion at the final stage. For each tunnel element, this process will be repeated until the Fixed Link is completed. This process of construction is graphically indicated in Figure 15.

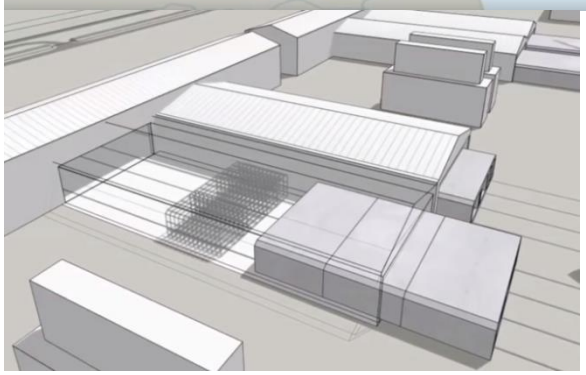

I(a)

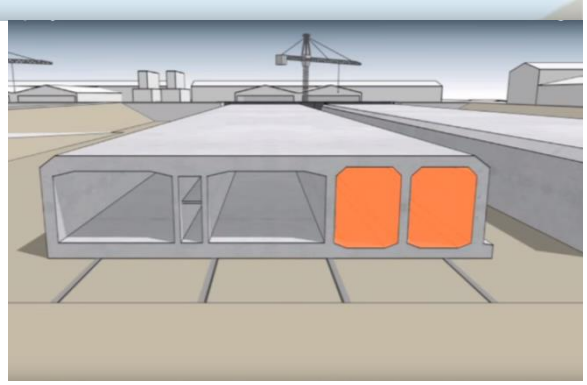

I(b)

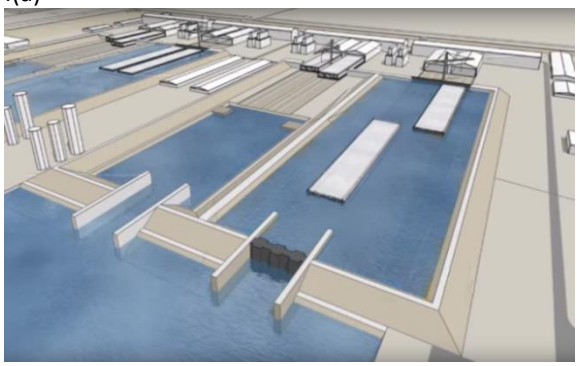

I(c)

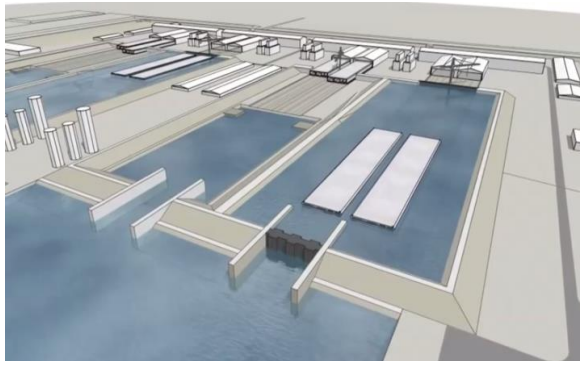

I(d)

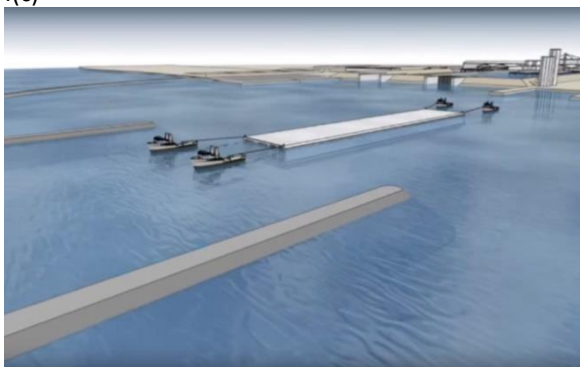

II

II

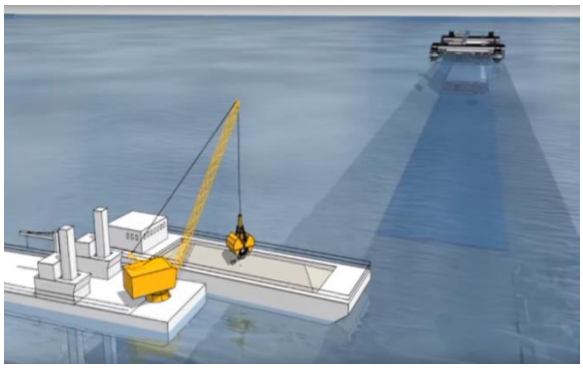

III(a)

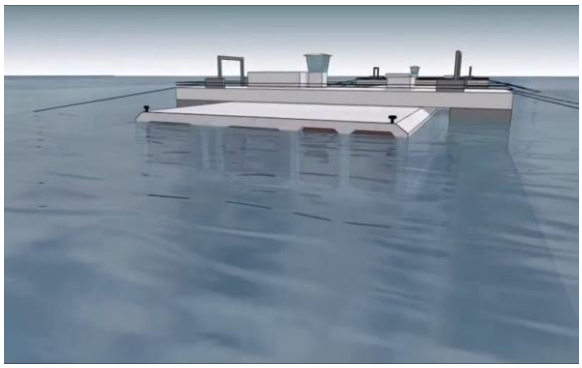

III(a)

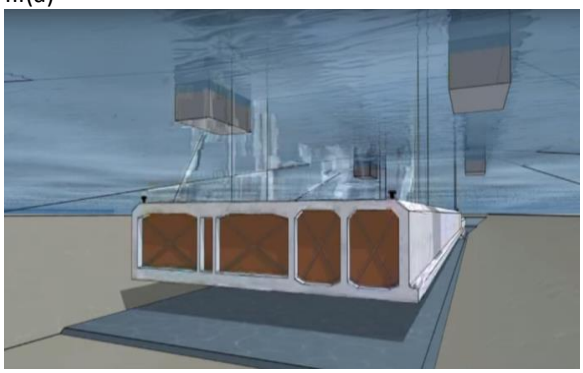

III(b)

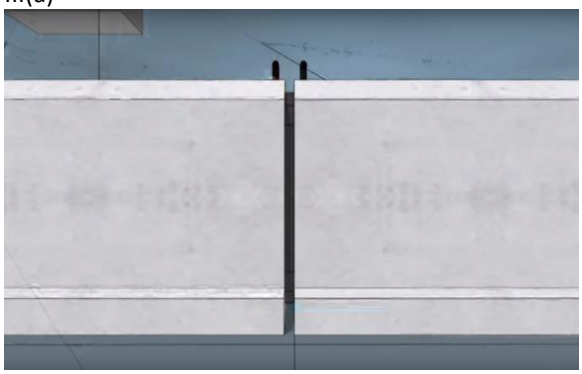

III(c)

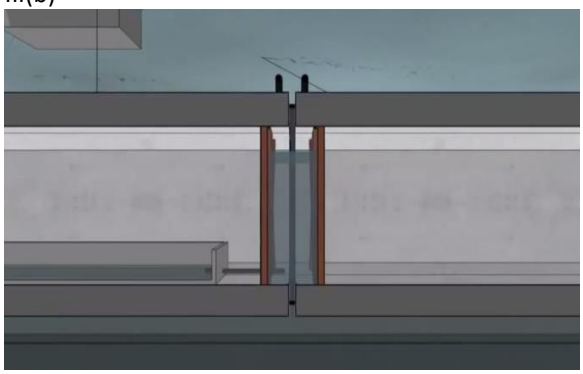

III(c)

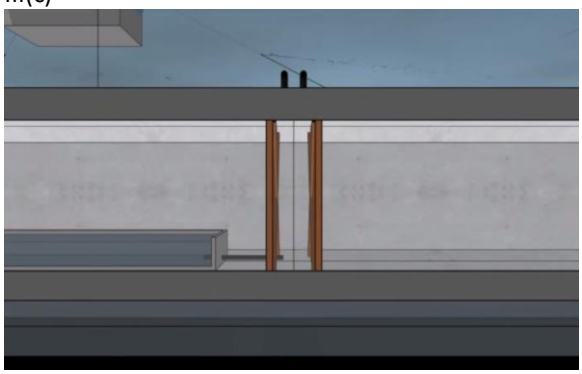

III(c)

IV(a)

IV(b)

Figure 15 Graphical presentation of the building process (Femern A/S)

2.3 IMMERSION EQUIPMENT

The immersion rigs are the main piece of equipment for the immersion. This piece of equipment is also indicated in this report as immersion pontoons or simply pontoons. The pontoon can be configured in several ways. Conventionally a single pontoon or a catamaran pontoon is used. Catamaran pontoon is an immersion rig which has two floating bodies (in this report indicated as floaters) on either side of the tunnel element connected by a beam or a deck structure

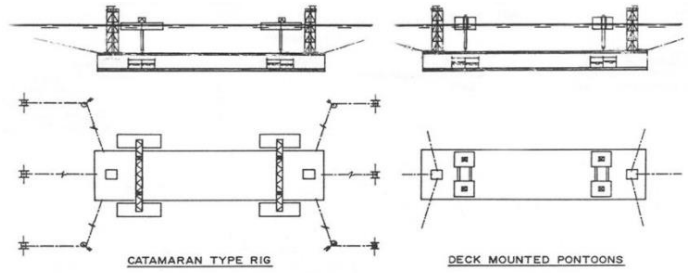

Figure 16 two type pontoons used often in construction of immersed tunnel (Gijsbert W. Nagel, 2011)l

It should be noted that a single pontoon on the deck of the tunnel element is currently not applicable anymore. The reason for that is that the element should be able to carry the weight of the pontoon during transport. Because of that, the element should have larger freeboard during the transport. In later stages of the construction, more ballast will be needed. Therefore these pontoons are not an attractive option for use in offshore or inland conditions anymore.

Generally, a set of two pontoons is used for the immersion of a tunnel element. But sometimes also one pontoon can be applied. During the immersion, the pontoons should stay stable on its position. Normally taut mooring lines are used to keep the pontoons in position. The mooring lines are anchored to the seabed. The winch stations are located at the top of the pontoons. It should be noted, that it is also possible to keep the immersion rig on position by computer-controlled thrusters. So far, no projects are known at which this technique is applied. Instead of mooring lines also large marine sheer legs can be used to keep the pontoon in the position, or a combination of both can also be used.

The immersion process is controlled from a command chamber. Normally this is a small cabin on the deck of the pontoon. All the immersion information, such as the position of the element, salinity rate, etc. is sent to the command chamber to enable the operator to control the process.

A large floating crane is another possibility, which can be used to place the elements on the bottom of the trench. But mainly the floating cranes are used for relatively small utility or metro tunnel elements. There are no reference projects known where large tunnel elements such as in the case of Fehmarnbelt have been placed by using a floating crane. Also, a single catamaran pontoon can be used for the immersion in harsh flow conditions, such in the case of Bosphorus Fixed Link (Istanbul Turkey).

Normally the tunnel elements are buoyant and thy are towed to the immersion site. It may be considering to pre-ballast the elements such that no ballast will be needed during the immersion and direct after the immersion. It can be considered to add 2.5% extra weight to the tunnel elements. During the transport the element must derive its stability from the pontoons. The main advantage of the pre ballasted TE is the reduction of the amount of activities after immersion. Summarized the following pontoon configuration could be used in the maritime conditions.

- The conventional pontoons (two catamaran pontoons)
- A jack-up platform
- A Semi-submersible pontoon
- A combination of a catamaran and a jack-up platform
- One ‘large’ single Catamaran pontoon

The mentioned pontoon configurations are given in Figure 17. In the subfigures, (g) and (h) the modeled pontoon configurations + the tunnel element are given. In order compare the dynamic behavior and stability of the pontoons two different configurations are analyzed namely: Catamaran and Semi-submersible. In offshore industry, a Semi-submersible is a commonly used type platform. It has advantageous characteristics in waves. Due to its configurations, the Semi-submersible can operate in severe weather conditions and has an advantageous response in heave. The main idea of the analysis is to investigate if the Semi-submersible pontoon has a better and advantageous dynamic behavior in waves compared to the Catamaran pontoon.

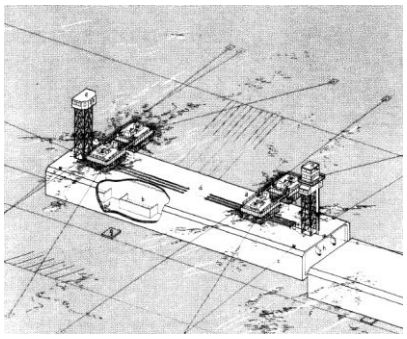

(a) Set of single pontoons (Molenaar, V.L., 1988)

(b) Catamaran pontoon (Volker CI and Strukton Immersion Projects)

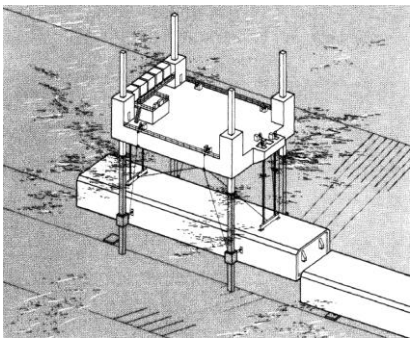

(c) Sheer leg platform (V.L. Molenaar, 1986)

(d) A set of Catamaran pontoons (Volker Construction International (immersion team), 2013)

(e) One large Catamaran pontoon (TAISEI Corporation , 2014)

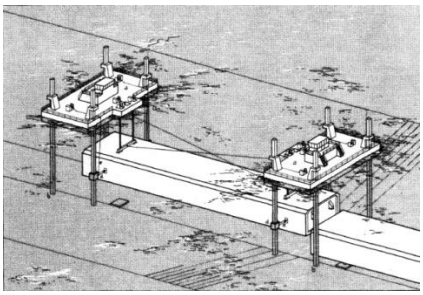

(f) Sheer leg platform applied at each end (V.L. Molenaar, 1986)

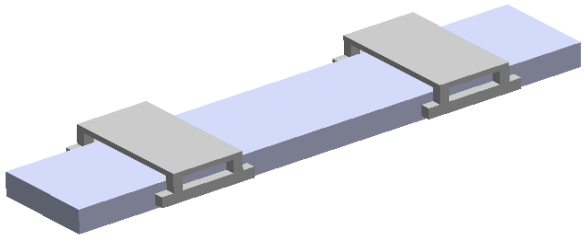

Semi-submersible pontoon

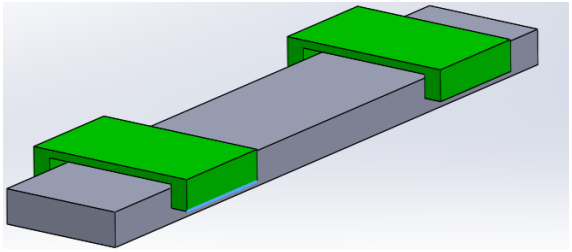

(g) Conventional Catamaran pontoon

Figure 17 Different pontoon configurations

2.4 CONCLUSION

In this chapter, the construction process, the hydraulic boundary conditions, and the immersion equipment are discussed. The main conclusions concerning the subjects as mentioned above are listed here below.

Fehmarnbelt is a transitional area between Baltic Sea and the North Sea. The water depth is variable. In the deepest part, it has a water depth larger than 30 [m].Waves in the project area are primarily governed by the local wind conditions and limited fetches. The surrounding lands limit the fetches. In general, the wave climate can be considered as a mild. The highest waves occur in the middle of the corridor; the annual significant wave height is 0.57 [m] with a peak wave period of 3.44 [s]. Also, swell waves can be neglected.

The water column is stratified associated with different flow velocity and directions. The surface flow is predominantly outgoing, and the near-bed current direction is in-going. The seasonal variation of the current is characterized by stronger flow velocities in the winter, fall, and weaker flow velocities in the summer for all depths. In the center of the waterway, the flow velocities are the strongest. For the modeling purposes, the flow velocity at the surface with an exceedance probability of 5% will be used (1.15 [m/s]). At the surface water flows from Baltic Sea with low salinity. The lower layer of the water column is mainly water from the North Sea with height salinity rate.

Further, the construction process can be divided into four distinct construction stages, namely: Construction yard/factory, transportation, immersion, and finishing works.

For the immersion operation, several pontoon configurations can be used. In this thesis report, the stability of the whole system provided two different pontoon configurations (conventional Catamaran and based on offshore industry Semi-submersible) is investigated for immersion phase.

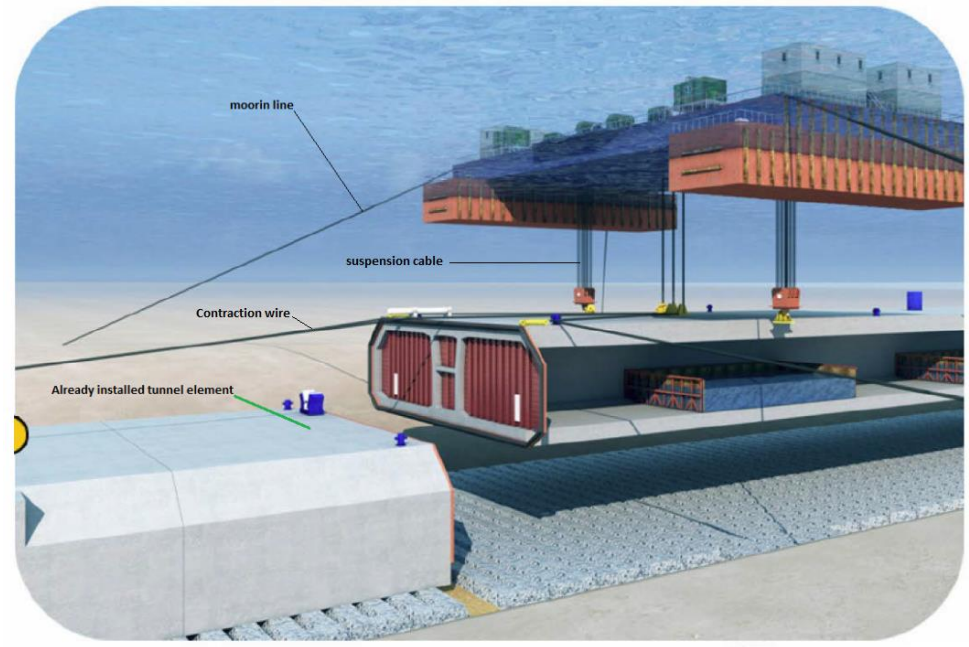

Figure 18 Tunnel element hanging on pontoon during the immersion (CAPITA SYMONDS)

3 HYDRAULIC ASPECTS AND THEORETICAL BACKGROUND.

3.1 INTRODUCTION

The forces and the resulting motion of the tunnel element during the construction can be divided into different groups. In this report, it is chosen for to separate the forces working on the system in the same manner as the building phases. Each element encounter this forces and loading from leaving the production site till it's integrated into the Fixed Link.

This chapter aims to give the reader an idea about important hydraulic aspects in each building phase. In the final situation when the tunnel is finished, it will be exposed to the pressure variation due to passing ships, wind-generated waves and tidal fluctuations. These forces are out of the scope of this study and are not considered here. The focus of this research is on the motions and forces in the construction stage. First, the forces will be categorized, and then they will be calculated quantitatively in the next chapters. Subsequently, in the last section of this chapter, an overview of the critical hydraulic forces is given, and it is indicated which of them are considered in the numerical model.

3.2 LITERATURE STUDY

Most of the available literature on immersion of a tunnel elements deal with the inland application in river conditions. The former Hydraulic Laboratory in the Netherlands which is nowadays called Deltares has conducted several hydrodynamic studies and model tests for the tunnel projects in Netherlands. The studies were carried out by using scale model tests and desk studies to predict the effect of current and waves on the tunnel element in construction. Also, other experts in the field conducted several studies to investigate the effect of the offshore conditions on the tunnel construction.

Zitman et al. (2003) investigated the probabilistic aspects of maritime transport of tunnel elements. Jongeling et al. (2001) studied the effect of passing ships over or nearby an immersed tunnel element. Thereby he evaluated the available calculation methods and accuracy of them when calculating the forces on the tunnel element by a passing ship. Rigter et al. (1989) investigated the hydraulic forces and hydraulic stability of the tunnel element during transport. Thereby he developed a 2D model which can predict the forces on floating tunnel element and its stability during transport.

Delft Hydraulic Laboratory et al. (1981) conducted model tests on the immersion of the tunnel elements in the Westerschelde (Netherlands). Thereby the forces and moments were measured in a model test. In this model test especially the effects of the current flow and tidal condition on the stability of the elements during the immersion were investigated for the Westerschelde. Eysink and de Jong et al. (1993) investigated the forces on tunnel element due to maneuvering ships during immersion. They improved and tested the existing models for accurate calculation of the forces. Eysink, Luth, De Vroeg and Wijhe et al. (1995) conducted a feasibility study on immersion for the second Benelux Tunnel.

Chakrabarti et al. (2008) conducted a dynamic simulation of the immersion of the tunnel elements for the Busan-Geoje Fixed Link project. CHEN Zhi-jie et al. (2008) has investigated the time domain response under wave actions during immersion, based on linear wave diffraction theory. He ignored the motions of the barges and investigated only the dynamic behavior of the tunnel element under wave actions. CHEN Zhi-jie et al. (2008) he calculated the dynamic behavior of tunnel element during the immersion in the frequency domain. Again, in this analysis, he ignored the motions of the pontoons and calculated the tension in the cables by a static method.

Cozijn et al. (2009) conducted model tests on the tunnel elements for the Busan-Geoje Fixed Link project and analyzed the operability of the immersion equipment in waves. Xin Li et al. (2009) carried out a dynamic simulation to compare two different execution methods. Nagel et al. (2011) performed a simplified numerical simulation of two-dimensional motions of the tunnel element and pontoon. He ignored the nonlinear terms and considered only the Froude-Krilove force. Molenaar et al. (1986) investigated the execution methods of immersed tube projects under offshore conditions.

Although the tunnel elements have been widely studied, there is still need for the evaluation of the dynamic behavior during the construction. Also, the influence of the pontoon configuration on dynamic behavior is hardly investigated. In this section of the report, the aspects, which play a role in the modeling of the hydrodynamic behavior of the tunnel elements, will be described qualitatively. In the coming up sections, these aspects are related quantitatively to the conditions in the Fehmarnbelt.

3.3 FORCES ON THE TUNNEL ELEMENT IN DIFFERENT CONSTRUCTION PHASES

The tunnel element and the floating pontoons experience effects due to moving water relative to the tunnel element and the pontoons. Three different kinds of hydraulic forces can be distinguished in different building phases see also Figure 19:

I.	Current force	(F_c)
II.	Wave force	(F_W)
III.	Buoyancy force	(F_B)

When the system undergoes dynamic movements the surrounding water exerts also extra forces on the system see also Figure 20.

I.	Inertia force (added mass)	A
II.	Damping force (added damping)	C

In order to be able to immerse and transport the tunnel element safely, the hydraulic forces must be in the balance with other system forces, namely:

IV.	Cable forces horizontal (mooring lines and contraction lines) Vertical (suspension cables)
V.	Weight of the element (adjustable with the aid by pumping extra ballast water in the ballast tanks)
VI.	Wind force (not considered here)

The surrounding water exercises different kind of forces on the tunnel element in the various construction phases. These forces are transferred via cables and anchors to the tugboats or sea bottom. There are many reasons for the emergence of these effects, which are strongly associated with the construction phase.

In general, it can be stated that the hydraulic forces during the immersion and transportation are the most relevant forces on the tunnel element and pontoons. When an element is being immersed in the particular account should be taken of the presence and quantity of ballast to hold the element securely in place. In the next sections, the main hydraulic aspects during transport and immersion are discussed qualitatively. Here only a brief notation of the aspects is given. The modeling aspects of the mentioned hydraulic phenomena are also described in the next chapters. The theoretical background is given in Appendix 5.

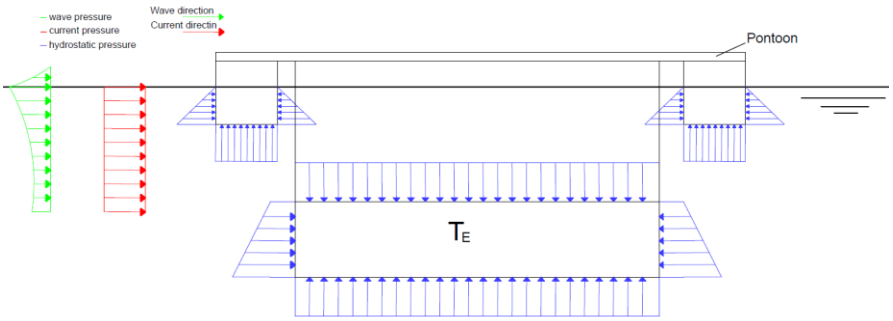

Figure 19 Main hydraulic forces working on the system

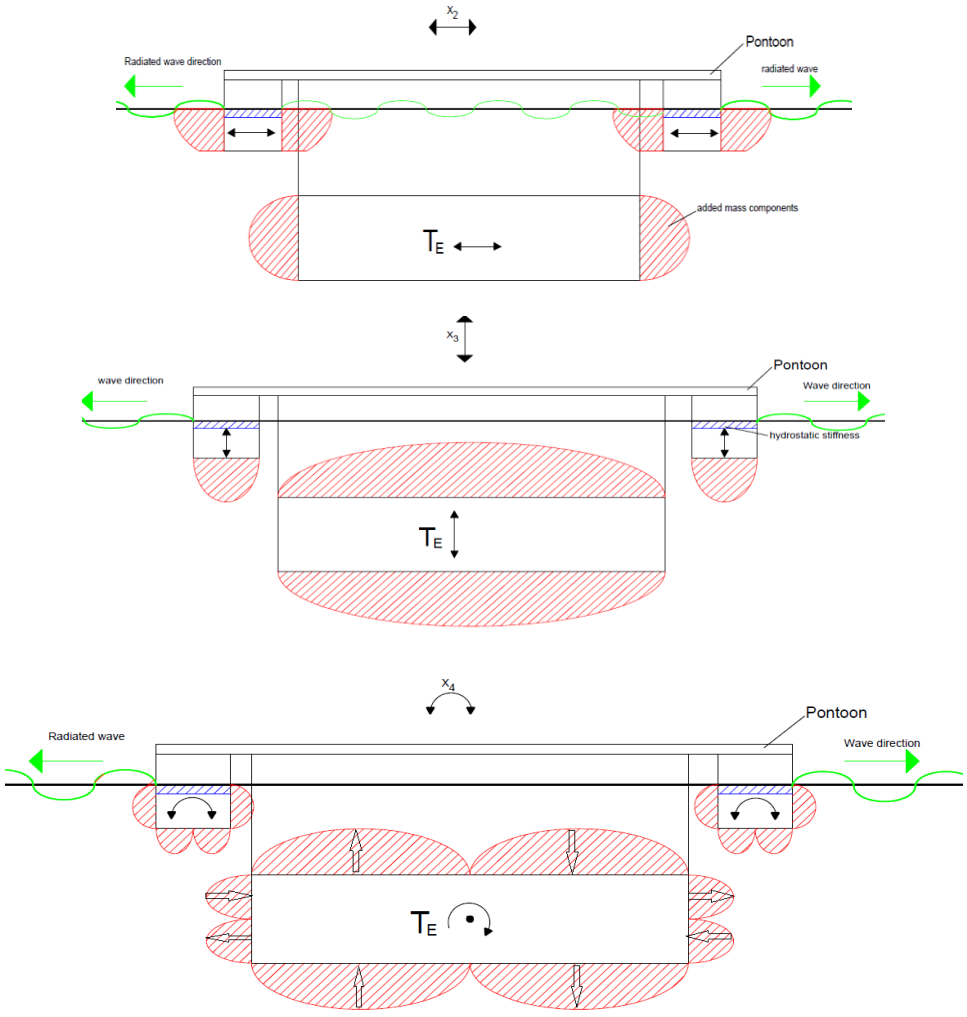

Figure 20 Extra forces on the system due to dynamic movements of the surrounding water

In Figure 20 the so-called radiation forces are depicted(see also 3.7.1). These effects are caused by the motions of a floating structure in water. The radiation force can be split into three parts namely:

- Added mass (red dashed area)
- Added damping (green line)
- Restoring force/ spring force (blue dashed area)

3.4 TRANSPORT

The tunnel element will be transported to the construction site by the aid of the tugboats. During the transportation, the tunnel element will be floating with the large part under the water with a small freeboard. Figure 21 indicates the system configuration during transport. In this construction phase, the element will be excited by the current and wave forces. Here a brief preview of the forces and the hydrodynamic mechanism will be given qualitatively. In chapter 5 the described phenomena are calculated, and the results are presented quantitatively.

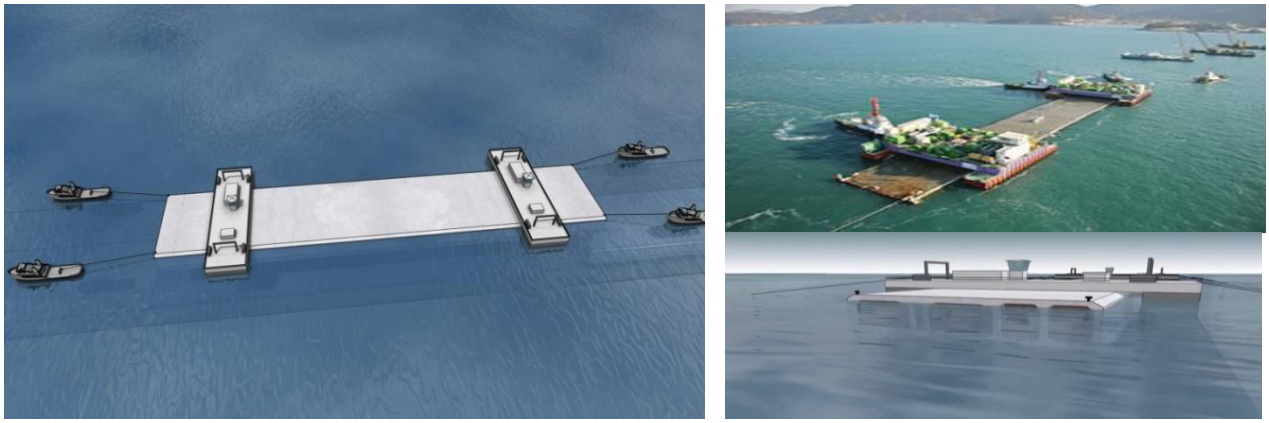

Figure 21 Tunnel element during transportation [(Femern A/S)and (Hans Cozijn and Jin Wook Heo, 2009)]

3.4.1 CURRENT FORCE

In general, the flow forces on a tunnel element can be divided into two types:

- Frictional resistance (surface drag)
- Form resistance (form drag).

The first kind of resistance/force is created by the friction between the surface of the element and running water. The second type is due to releasing/slipping of the flow along the element. Due to the last mentioned effect on the downstream side of the element, a so-called slowdown area will develop where energy losses occur and where the pressure is significantly less than on the upstream side. This effect creates a resistance force by the pressure difference between the areas upstream and downstream. The area on the upstream side is more or less in undisturbed flow (high-pressure area), and the area downstream is in the wake (low-pressure area).

For the submerged bodies (such as a floating tunnel element) the form resistance is dominant. The frictional resistance is negligible. From earlier studies, it can be deduced that the frictional resistance is less than 5% of the total. Since the estimation of the last mentioned resistance usually lesser accurate, the frictional resistance is neglected in this study. Only the form resistance has been taken into account in the calculations. The principle of the drag force is given in Figure 22.

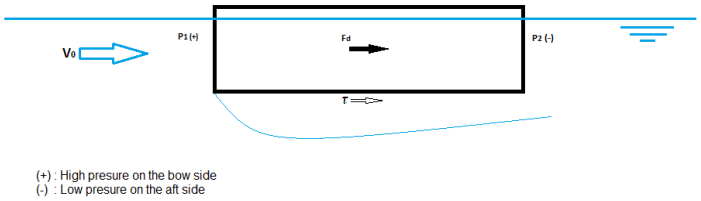

Figure 22 Principle of current force on TE during transport

3.4.2 HORIZONTAL DRAG FORCE

The horizontal flow force is determined by the flow rate, the surface area in the flow and the angle between the longitudinal axis of the element and the flow direction. The horizontal force can be divided into a stationary part and a non-stationary. The stationary part forms the main part of the horizontal drag force on the tunnel element. The non-stationary part is particularly important for the force fluctuations in the cables and the displacements of the element during transport and immersion. The stationary horizontal flow force can be expressed as:

$$F_d = \frac{1}{2} * C_d * A_c * \rho * V_R^2 \quad (1)$$

Where

F_d	Horizontal flow force on the system	[kN]
C_d	Drag coefficient	[-]
A_c	Effective surface of the element perpendicular to flow direction	[m^2]
ρ	Water density of flowing water	[kg/m^3]
V_R	Reference speed	[m/s]

When the incident flow has an angle α with the longitudinal direction of the element, the element will be excited by a resultant drag force F_s. The force F_s is not parallel to the flow direction (see Figure 23). The force component F_s can be split into two components, namely: in the x-direction (flow direction) and a component in the y-direction (perpendicular to the flow direction). The resultant force F_s makes an angle γ with the x-axis. This can be represented as follows:

$$F_{sx} = \frac{1}{2} * C_{dx} * A_c * \rho * V_R^2 \quad (2)$$

$$F_{sy} = \frac{1}{2} * C_{dy} * A_c * \rho * V_R^2 \quad (3)$$

$$\tan\gamma = \frac{F_{sx}}{F_{sy}} \quad (4)$$

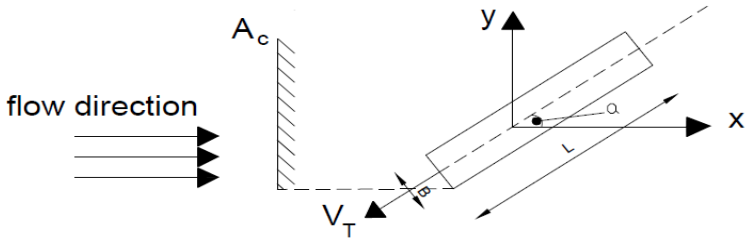

Figure 23 Area in the flow

There may be a remarkable torque about the z-axis (the vertical axis through the center of gravity of the element). This moment may occur even if the resulting current strength and the related resultant force F_s are small. Without a scale model, this torque moment is difficult to predict. Based on the measured results in previous studies, an estimate can be given with a low accuracy. From the literature, it can be concluded that this moment is difficult to determine in an analytical model with reliable accuracy.

3.4.3 HYDRODYNAMIC INSTABILITIES

During transport, the element will be ballasted such that it will have a freeboard of 0.2 [m]. Due to towing activities, the element will sink extra and rotate as result of the towing force and the related velocity. Due to small freeboard, relatively a lowl trim moment is needed to immerse the bow of the tunnel element. If the bow of the element will sink extra due to towing activities, then the longitudinal stability decreases rapidly, and the element could be pulled under water.

Therefore, the effect of the towing velocity should be investigated, and the limit velocity should be known in each part of the transport route. The forces and the related sinkage is dependent on blockage of the waterway by the tunnel element and the available water depth for the transport. The hydrodynamic instabilities are worked out in section 5.6

3.4.4 WAVE FORCE AND THE RELATED MOTIONS

The wave force on the tunnel element during the transport can be treated as a semi-stationary. The maximum bending moment will occur if two consecutive wave crests coincide with the fore and aft of the element (sagging condition) or when two wave troughs coincide the fore and the aft of the element (hogging conditions). These terms are used in maritime engineering, that's why in Figure 24 the principle of these mechanisms is given for a ship in waves.

In these conditions, the wavelength is equal to the length of the element. The sagging and hogging conditions for the tunnel elements in the Fehmarnbelt occurs when the wavelength is approximately 217.8 [m] with a correspondent wave period of 11.8 [s]. This is typical swell wave period in Fehmanrbelty. However, swells are rare in the project area.

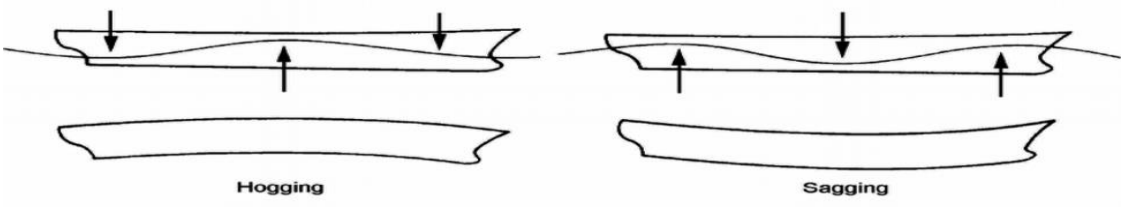

Figure 24 Principle of sagging and hogging conditions.[1]

If the solitary wave has an angle of incidence (μ), then the length of the wave corresponding to sagging and hogging conditions will be smaller than 217.8 [m]. Also, the related bending moments will be lower. Additionally, a torque moment will develop about the z-axis. In beam seas (angle of incidence μ=90˚) the same situation may occur if the length of the solitary wave is equal to the width of the tunnel element and the corresponding wave period is 5.10 [s]. However, the effect of the wave loads is limited due to small freeboard and large draught during the transport.

The wave loads may induce motions with relatively large amplitude if the wave period coincides one of the natural frequency of the element. During the transport, the floating tunnel element will have only hydrostatic stiffness in heave, roll, and pitch. For the remaining degrees of freedom the stiffness depends on the total stiffness of the system(tunnel element + tugboats). The transport cables are mostly fastened such that the relative stiffness of the wires is much lower than the hydrodynamic stiffness of the floating element. Therefore the natural frequencies of the element during the transport in sway, surge and yaw are much larger than the natural periods in heave, pitch, and roll. Therefore, the natural period of the floating element in heave, roll and pitch are normative for the dynamic response of the element during the transport. The natural periods of the floating element are calculated in chapter 5.

When the transportation is not carried out during heavy sea conditions, the tunnel element will be not sensitive to the wave forces. The relatively small wind waves are not able to bring the heavy tunnel element into motions. he wave-induced motions of the tunnel element become significant if the wave excitation frequency is near one of the natural frequencies. The natural frequencies of the floating TE are calculated in section 5.9.

[1] https://www.researchgate.net/figure/228891097_fig2_Figure-2-Hogging-and-sagging-of-ship-hull

3.5 FORCE AND MOMENTS DURING FITTING OUT CONDITIONS

During the fitting out, the element is positioned over the trench. In this phase of the building operation, the element will float. During the positioning, the current angle is changing. Due to varying angle in this step, the current forces will increase on the tunnel element. The area perpendicular to the flow direction will increase too. Also, a torque moment will work in this phase on the element.

Figure 25 TE during fitting out conditions (CAPITA SYMONDS)

3.6 IMMERSION

As mentioned before, during immersion the elements will be suspended with cables from two pontoons. In order to keep the pontoons in position each one will be fastened with the aid of 4 mooring lines (see Figure 26 and Figure 27 'blue lines'), thus in total 8 mooring lines will be applied. To control the transversal and longitudinal motions of the tunnel element 6 contraction cables will be applied (see Figure 26 and Figure 27 'black lines').

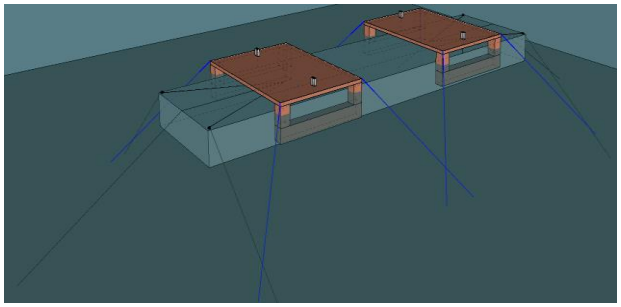

Figure 26 Semi-submersible pontoon during immersion

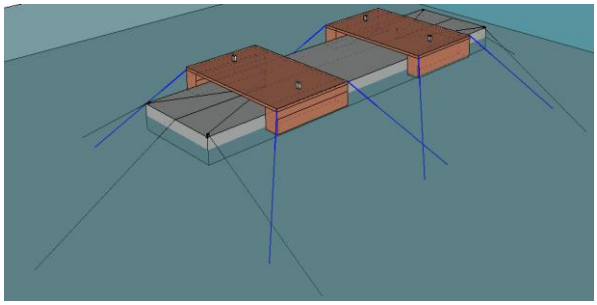

Figure 27 Catamaran pontoon during immersion

When the element is entirely underwater, it loses its stability to a large extent. From that moment, the vertical and horizontal forces should be entirely taken by the relatively small pontoons. In the first stages of the immersion, this can lead to significant vertical displacements and forces.

The horizontal and vertical forces on the tunnel elements can be determined with the aid of a desk study as a function of the flow and wave conditions. This calculation can be performed by taking into account the direction of the flow, flow velocity, the shape and the dimensions of the tunnel element and pontoons, wave conditions as well as effects due to density differences. In general, the system will be excited by three different kinds of forces, namely:

1. Hydrodynamic force
2. Current force
3. Gravitational force

For the dynamical effects, the natural frequencies should be known. The natural frequencies are the characteristics of the immersion equipment (the pontoons). These characteristics should be compared to the dominant load periods. From this comparison, the most effective dimension of the immersion rigs can be determined. From the moment that the tunnel element is just below water until the time that the element set at the bottom, the horizontal forces due to the current excitation on the element will reduce along the vertical alignment.

This is partly because the water flows both ways along the tunnel element and therefore the resistance coefficient will be reduced. Also the current velocity will reduce along the vertical alignment of the water profile. In addition, the external vertical forces on the element will decrease too along the increasing water depth.

During the immersion, an accurate positioning of the system is crucial, and this is in particular very important for the tunnel element. The significant differences compared to the transport phase are:

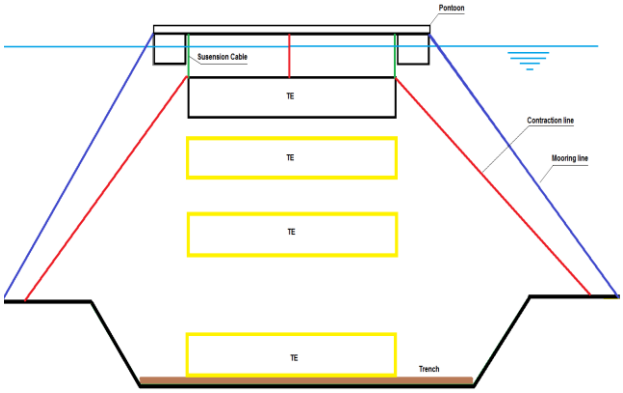

Figure 28 TE during immersion

- During the immersion, the tunnel element takes different positions in the vertical plane (see Figure 28). As a result of that, the current velocities are changing. Also, the magnitude of the forces is continuously evolving.
- During transport, the system is considered to be a floating body. But during the immersion, the element will hang on the suspension cables. The system is held in position by the contraction wires and mooring lines. In this phase, the stiffness of the entire system is changed.

It's been assumed that the fitting out and the immersion will take place under the most favorable conditions. This means that the following measures should be taken at least:

- The shipping activities should be kept at a safe distance. This means that the water level drop due to ship passage must be negligible.
- The immersion should take place under favorable weather conditions (the element is not immersed during stormy weather conditions)
- The element is not be immersed during the extreme current velocities.

3.7 HYDRODYNAMIC FORCE

In order to be able to model the wave loads, two essential assumptions are made. The first assumption is that a floating structure oscillates in still water and hydrodynamical loads and moments are calculated by assuming that only the forces working on the floating body are the forces due to oscillation in still water. The second assumption is that the waves are acting on a fixed structure. The total wave force is calculated by adding these two components. The theoretical background of the theory presented here is treated in Appendix 5.2 and 5.3. And a distinctive description of the method is given in [1], J.M.J. Journée and W.W.Massie, "SHIP HYDROMECHANICS."

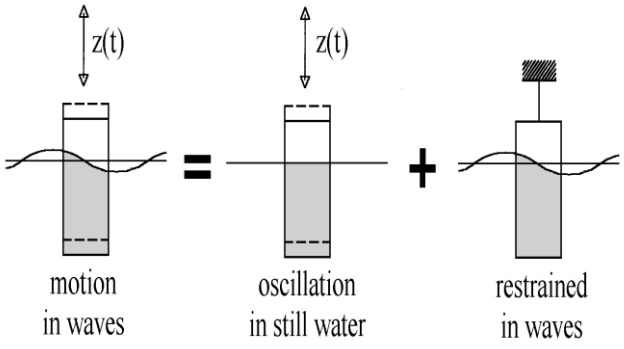

Figure 29 Summation of the two motional components (J.M.J. Journée and W.W.Massie, First Edition, January 2001)

3.7.1 Radiation Force

The force due to the motions in still water can be split into three parts.

- Force in phase with the acceleration of the floating body (added mass force)
- Force in phase with the velocity of the floating body (added damping)
- Force in phase with displacement of the floating body (restoring force, spring force)

The first two elements of the force form the hydrodynamical part. The third part is the hydrostatic part of the force. The free oscillation of the body in still water causes an extra force on the floating body. This force has terms which are proportional to the mass and damping. The force term which is proportional to the velocity is called added damping, and the term which is proportional to the acceleration is called added mass. The components of added damping and added mass are indicated with the letters a and b in the equation of motion. The coefficient a has a dimension of mass, and the coefficient b has a dimension of mass per unit of time. In general, these coefficients are not constant and depend on the frequency of the motion.

The free motions of the floating body will generate weaves, which radially propagate from it. The generated waves will transport energy which is withdrawn from the oscillations of the body. The withdrawal of the energy will cause that the oscillation of the body will decrease in time and finally it will die out. The wave damping is linearly proportional to the velocity of the oscillation in the linear systems. The actual damping will be higher than the linear damping because of the viscosity of the fluid. For the linear systems, the effects of the viscosity can be neglected because this effect is small. The added damping or the so-called radiation damping decreases from the water surface. The wave generation will be less if a body is lying deep under the surface.

The hydrodynamical reaction force which is proportional to the acceleration term as mentioned before is called the added mass. This force is the result of the accelerations which are given to the water particle near the floating structure. The difference with the previous hydrodynamical load type is that added mass-energy doesn´t dissipate energy it behaves like a standing wave.

When the amplitudes of the waves are small, the accelerations and velocity behave quite linear. It can be stated that the terms are linear for the wave heights in the project area. The hydrodynamical forces are the total reaction forces which are performed in the still standing water can be expressed as:

$$m\ddot{x} = F_h \qquad with \qquad F_h = -a\ddot{x} - b\dot{x} - cz \tag{5}$$

In the equation of motion for the translational motion, the force balances have to be implemented. For the rotations, the moment balances have to be taken into the considerations.

The radiated force caused by the motion of the floating bodies in still standing water can be calculated by integrating the pressure over the body surface.

$$F_k = -\iint_{S_0} P n_k dS = -\rho\omega^2 \overline{\eta_j} \iint_{S_0} \left(\phi_j\right) n_k dS \tag{6}$$

Restoring spring terms of a floating body

For free-floating bodies, only the restoring spring terms in the following degrees of freedom are present: heave, roll, and pitch. The other degrees don't have a restoring moment. The restoring spring term for the heave follows from the waterplane area. For the angular motions, the terms follow from the static stability phenomena. The terms of the free-floating structure can be expressed as:

Heave	$c_{zz} = \rho g A_{WL}$	(7)
Roll	$c_{\phi\phi} = \rho g \nabla * \overline{GM}$	(8)
Pitch	$c_{\theta\theta} = \rho g \nabla * \overline{GM\_L}$	(9)

In which $\overline{GM}$ and $\overline{GM_L}$ are the transverse and longitudinal metacentric heights of the floating structure.

3.7.2 WAVE FORCE

During the immersion, the wave force will excite the system. As described before to calculate the wave loads on a floating structure, it's been assumed that the structure is fixed in its location. The exiting wave force is determined by the pressure integration over the wetted body. The pressure P on the surface of a floating structure is given by the Bernoulli equation.

$$P = -\rho \frac{d\Phi}{dt} \tag{10}$$

In this equation, the hydrostatic terms have been neglected, because the hydrostatic pressure doesn't contribute to the oscillation of the floating structure. In the equation above ρ is the water density and Φ is the wave potential. The unknown wave force can be calculated by integrating the pressure over wetted surface S_o.

$$F_k = -\iint_{S_0} P n_k dS = \iint_{S_0} i\rho\omega(\phi_0 + \phi_7) n_k dS\, e^{i\omega t} \tag{11}$$

$$(f_{0k} + f_{7k}) * e^{i\omega t} = f_k * e^{i\omega t} \qquad with \qquad k = (1,2,\ldots.6) \tag{12}$$

In this equation, f_{0k} represent the undisturbed wave force or the so Called Froud Krilov Force. The under script k indicates in which degree of freedom is the force considered. The f_{7k} is the diffracted force. These forces have harmonic character. The diffracted force is included in the equation because of the diffracting of the waves due to the presence of the structure. The total external wave force on a floating structure is the sum of Froude-Krilov Force and diffracting force. For the low frequencies (long waves) the diffracted part of the force is smaller compared to the undisturbed wave force part (Froude-Krilov Force). At the higher frequencies, the diffracted part of the force getting more important.

3.7.3 CURRENT FORCE

Also during the immersion, the system will be exposed to the current excitation. Again, the frictional resistance (surface drag) can be neglected as it is less than 5 % of the total resistance. The form resistance (form drag) will cause the main current forces on the tunnel element. During the immersion, the main angle of the current direction and the longitudinal axis of the tunnel element can be assumed as 90°. The horizontal drag force can be calculated at the same manner as for floating tunnel element. The derivation of drag coefficient will be different as it is explained in section 5.3. The current drag force can be decomposed into two components namely, a drag force acting in the current direction and a lift force acting perpendicularly to the flow direction.

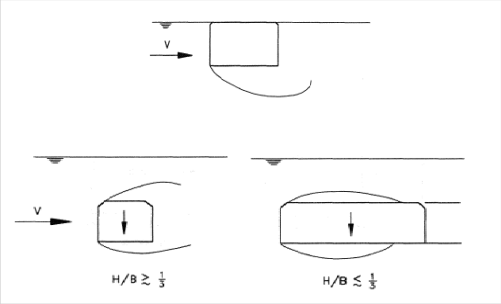

Figure 30 flow pattern (W.D. Eysink, maart 1981)

The horizontal drag force has stationary character, and it is of main importance for the determination of the capacity of the contraction cables. The dynamic component of the horizontal drag force is much smaller than the stationary part. Due to large inertia of the tunnel element it is to be expected that the dynamic component would not be able to bring the heavy tunnel element into motions if the vortex shedding frequency is not close to the natural frequency of the system. The results of the calculated drag force during immersion are given in section 5.5.

3.7.4 LIFT FORCE

During the immersion, the tunnel element is variously exerted by the current force at the top and the bottom. Due to this phenomenon, a vertical lift force will be generated on the submerged tunnel element. This vertical lift force causes a vertical translation and rotation of the tunnel element.

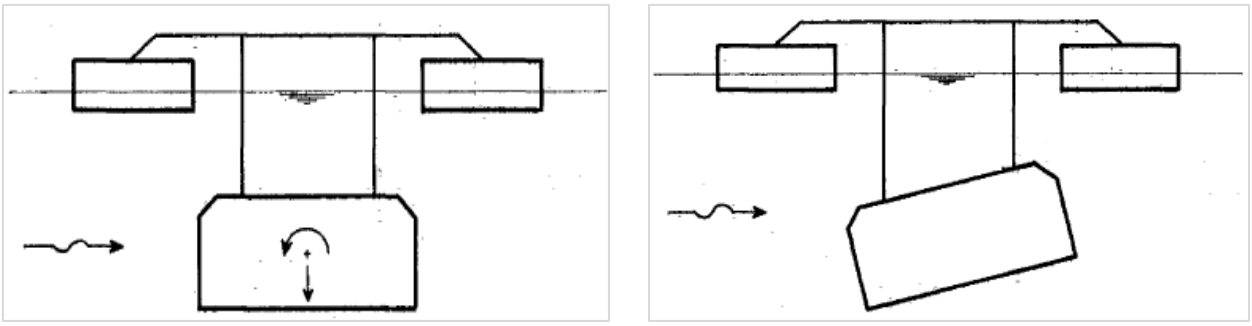

Figure 31 tunnel element in the flow (W.D. Eysink, maart 1981)

The lift force is defined as a force perpendicular to the flow velocity, and therefore it is also perpendicular to the drag force. Due to alternately vortex shedding behind the tunnel element, a cyclic pressure variation will occur in the wake. Because the vortices are shed alternately, the lift force will alternate in the direction as well. The strength of the force will vary in correspondence with the vortex shedding frequency. In formula form the relation of the lift force and the vortex shedding frequency can be given as:

$$F_{lift} = \frac{1}{2} \cdot \rho \cdot V_R^2 \cdot H_{TE} \cdot C_L \cdot \sin(2\pi \cdot f_v \cdot t + \varepsilon_{Ft}) \qquad (13)$$

Where

F_{lift}	Lift force per unit length of the tunnel element	[kN/m]
C_L	Dimensionless lift coefficient	[-]
f_v	Vortex shedding frequency	[1/s]
t	time	[s]
ε_{Ft}	Phase shift	[rad]

Given the vortex shedding frequency, the Strouhal number can be defined as:

$$St = \frac{f_v \cdot D}{V_R} \qquad (14)$$

The Strouhal number is dimensionless, and it is dependent on the Reynolds number (Re). In Figure 32 is the Strouhal number given as a function of the Reynolds number. The given Strouhal numbers are valid for circular cylinders perpendicular to the flow direction.

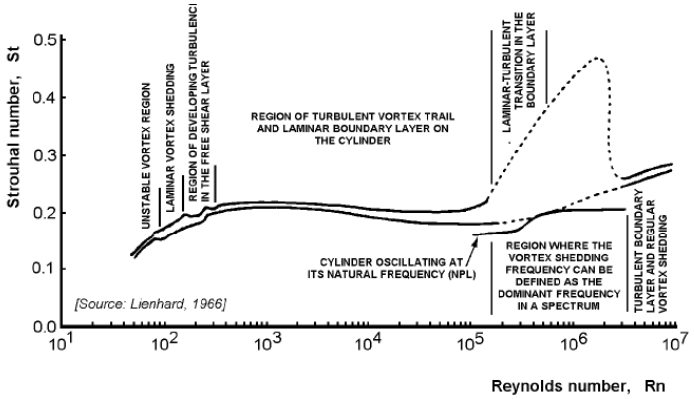

Figure 32 Strouhal number as function of Reynolds number for circular cylinder (J.M.J. Journée and W.W.Massie, First Edition, January 2001)

The lift force varies with time, the magnitude and direction of this force is dependent on the position of the vortices in the wake. The lift force oscillates back and forward with the vortex shedding frequency. In contrast to the lift force the drag force varies only slightly with the vortex shedding frequency, this is often neglected in the calculation. The magnitude of the lift force per unit length can be of the same order as the drag force.

However, the lift force is mostly not of great concern for structures like the tunnel element. By integrating all the segmental forces will result in a resultant drag force. However, for the lift force, this is more complex. The total lift force is dependent on the direction and the position of the vortices at every time instant. The segmental lift forces may differ in direction, which is dependent on the orientation and location of the corresponding vertex. This will lead to the fact that by integrating all the forces over the entire structure it will lead to much smaller resultant lift force than the resultant drag force.

However, the lift force may become of great importance when the natural frequency of the system coincide the vortex shedding period. Then the tunnel element will undergo large and uncontrollable motions. A significant effect of the massive tunnel element oscillations is that it will distort the local flow pattern. Therefore, more vortices will be shed behind the tunnel element. Since all the segments of the tunnel element will move, in more or less the same way at any instant in time, this, in turn, stimulates the vortices to become more coherent along the tunnel elements length. The lift forces on different segments will start to work in phase with each other. The tunnel element will respond to this by oscillating with a larger amplitude and reinforcing this process, in hydraulic engineering is this effect also known as lock-in effect. When the flow velocity continues to increases the lock-in effect will stop.

3.7.5 RESONANCE

The element may be sensitive to some periodic movements during the immersion. For this purpose, the possible excitation frequencies due to current and wave loads should be determined. From two pontoons configurations, the natural frequencies of the system (pontoons and the tunnel element) will be determined too. The excitation frequencies and the natural frequencies of the system will be compared. In general, it can be said that a pontoon configuration should be selected such, that the natural frequencies should lie outside the excitation frequencies of waves, swell and flow.

3.7.6 EXCITATION FREQUENCIES

During the immersion, the system will be excited by different periodic forces. The excitation forces are wave loads and current loads. The excitation period of the expected wind waves under normal conditions will be in the order of 3-5 s. Possibly also swell waves can penetrate the construction area. From the results given in (FEHY (Metocean Conditions), 2013) it can be concluded that the swell waves don't play an important role in the wave spectrum. They can be almost ignored. Nevertheless, the impact will be great if the swell waves will not be taken into account in the design of the pontoons.

The swell waves will have a period around 10-16 [s]. Another source of periodic excitation is the potential instability in the flow pattern. This instability is caused by the formation of vortices around the element, the so-called Von Kármán vortex street. The frequency at which these eddy formations take place depends mainly on the geometry of the element and the flow rate. The vortex shedding frequency equation has already been given. The Strouhal number can also be provided as in equation (15) which is characteristic of this vortex formation.

$$St = \frac{H_{TE}}{V_{cur} T_{excitation}} \tag{15}$$

In which

St	Strouhal number, depending on the geometry and the Reynolds number.
H_{TE}	Typical dimensions of the object in the flow (height of the element)
V_{cur}	Undisturbed flow velocity
$T_{excitation}$	Excitation period

In Figure 33 is the Strouhal number given as a function of the width/height ratio of a perpendicular element in the current. The most relevant element is located in the middle of the fairway, and it has during the immersion an angle of 90° with the current. The elements which will be immersed close to the banks will have a greater angle than 90° with the current. Due to the low flow velocities, the tunnel elements close to the banks are not normative. The height/width ratio of the element is calculated with the effective width B_{eff} (in this case equal to B_{TE}). With a height of 8.9 [m] and a width of 41.2 [m], the width-height ratio is 4.6.

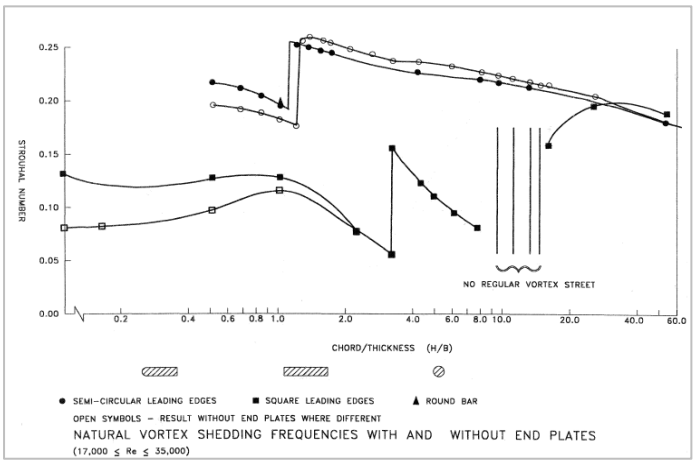

Figure 33 Strouhal number (Parker 1981)

For different flow velocities, the excitation periods are calculated. Generally, from the calculations, it can be concluded that when the de flow rate is low the excitation period increases. With the increasing flow velocities, the excitations period will decrease. If the natural frequencies of the system are outside these areas, there is little chance for the resonance to occur.

3.7.7 NATURAL PERIODS OF THE SYSTEM

The natural frequencies of a tunnel element during the immersion are primarily determined by the dimensions of the pontoons, where the element is attached to it by the suspension cables. When the element floats(during the transport), the dimensions of the elements determine the natural periods. The dimension of the pontoons during transport has little effect on the natural periods of the system. In the floating phase, the water plane area of the element is determinative.

During the immersion phase, the tunnel element will be under water and only water-cutting area of the pontoons is of influence on the spring stiffness of the system and therefore, also determines the natural frequencies. The barges consist of two floating bodies interlinked to each other. The normative dimensions of the system (hanging element on two pontoons) for the natural frequencies are, apart from the dimensions of the element itself:

- The distance (center to center) of the pontoons in the longitudinal direction of the tunnel element
- The distance (center to center) of the pontoons in the width direction of the tunnel element
- The total water-cutting area of the pontoon groups.

The three main directions of movements are:

- Heave (vertical movement)
- Roll (rotation about the x-axis)
- Pitch (rotation y-axis)

The natural periods of these three movement directions can be calculated as:

$$T_{n,heave} = 2\pi * \sqrt{\frac{m + m'}{K_z}} \qquad (16)$$

$$T_{n,roll} = 2\pi * \sqrt{\frac{I_{yy}}{K_{yy}}} \quad (17)$$

$$T_{n,pitch} = 2\pi * \sqrt{\frac{I_{xx}}{K_{xx}}} \quad (18)$$

In which:

Nr	Symbol	Description
1)	T_n	Natural period
2)	m	Mass of the element
3)	m'	Added mass
4)	I_{xx}	Inertia moment for roll
5)	I_{yy}	Inertia moment for pitch
6)	K_z	Spring stiffness for heave
7)	K_{xx}	Spring stiffness for roll
8)	K_{yy}	Sprig stiffness for pitch

A number of these values can be determined fairly accurately. Some of the parameters will be estimated from the previously conducted studies. One of the variables which is difficult to determine for analytical evaluations is the added mass. Therefore, the values of the added mass are estimated from the results of the previously conducted studies. For the added masses, the following values will be used:

$$m' = 2m\ (heave) \quad (19)$$
$$m'_{yy} = 1.6m\ (pitch) \quad (20)$$
$$m'_{xx} = 0.4m\ (roll) \quad (21)$$

The moments of inertia are found by making use of the following radii of gyration:

$$r_{yy} = \frac{L}{3{,}4} \quad (22)$$
$$r_{xx} = \frac{B}{2{,}2} \quad (23)$$

And the moments of inertia can be expressed as:

$$I_{xx} = r_{xx}^2\ (m + m'_{xx}) \quad (24)$$
$$I_{yy} = r_{yy}^2 (m + m_{yy}) \quad (25)$$

The spring stiffness can be represented as:

$$K_z = \rho g A_p \quad (26)$$
$$K_{xx} = \frac{1}{4} b_p^2 K_z \quad (27)$$
$$K_{yy} = \frac{1}{4} l_p K_z \quad (28)$$

With the aid of the formulas as mentioned earlier, the natural periods of the system can be displayed as a function of the pontoon dimensions. It can be checked whether the natural frequencies of the pontoons are near the excitations periods of the loads. Also for the different pontoon dimensions, it can be determined if it's possible that resonance can occur.

From the model studies carried out in the past, it can be concluded that the immersion system (tunnel element hanging on the pontoons) is sensitive to oscillations in the vertical direction..

The amplitude of the vertical movements and vertical forces turns out to be dependent on the immersion position and the flow rate. The model studies show that significant flow velocity leads to the considerable fluctuations in the vertical force and displacement. Approximately at the middle of the vertical alignment where the boundary between fresh and salt water is located large vertical forces can be expected.

In this position, the element is located approximately in the middle of the current-carrying depth. In this situation, the current layer may become unstable, and the mass-spring system (the tunnel element hanging on the pontoons) can be excited by this instability. Whereby the system is going to move unstable. This instability is caused by the passage of the vortices behind the element. The frequency with which this happens is dependent on the geometry and the turbulence rate (Reynolds number). The excitation frequency can be determined from the Strouhal number. It turns out that, the frequency increases as the flow rate also increases. This also leads to increase of the excitation force.

The situation becomes dangerous when the excitation frequency is close to the natural frequency of the heave, pitch, and roll of the system. When it's too close to the natural periods of the system, resonance will occur. The force fluctuations can become so large that the suspension cables (where the element is attached to it) will break. In this situation, there is also the possibility that the movements of water are going to be controlled by the movements of the element. The excitation frequency can be so close to the respective natural frequency that the element will make substantial movements relative to the remaining water depth. This will lead to: the release of the vortices will be controlled by the movements of the tunnel element. Finally, this will lead to: the excitation frequency will be 'sucked' to the natural frequency.

The occurrence of resonance is determined by the ratio between the excitation frequency N and the natural frequency (s) of a mass-spring system. If this ratio is 1, full resonance occurs, with potentially significant risk to the system. As the ratio deviates far enough from 1, the degree of resonance can occur is limited. And if the ratio is at a sufficiently large deviation even no resonance will occur at all. The natural frequencies of the system depend on the characteristics of the system as explained before.

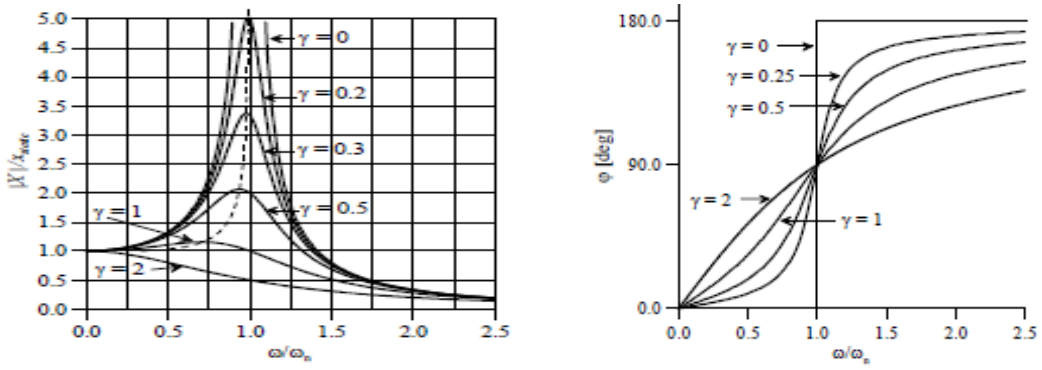

Figure 34 Amplification factor and phase lag (Spijkers, J.M.J., A.C.W.M. Vrouwenvelder, and E.C. Klaver., 2006)

In addition, the spring stiffness of the system also depends on the added mass and the added damping of the system. In particular about the last factor is very little known. The damping of the system can be determined in the numerical or a physical model. In general, it can be stated that attenuation causes a delay in the occurring oscillations, so an increase of the natural period.

It can also be stated that in the considered system damping will play an important role. In the given formulas for the natural periods, the impact of damping is not included in the calculation. Therefore, it can be said that the analyzed natural periods of the system are somewhat conservative approached. It is expected that the natural periods calculated in the numerical model will be slightly higher. Also, in reality, the natural periods of the system in different degrees of freedom will be higher.

The model research on Westerschelde tunnel shows that the system can be stabilized by taking the following measures.

- To make sure that the force from the suspension cables will apply low on the pontoon. (low-lying coupling beam).
- To apply a rigid coupling between the two floaters of a pontoon (no hinged connection between the pontoon and beam). This measure increases the stability of the pontoon in the transverse direction of the element.
- Choosing pontoons with a larger dimension in the longitudinal direction of the element than on the transverse of the element. In this way, the pontoons will be more stable in the longitudinal direction of the element.
- Choosing pontoons with larger water-cutting area A_p, whereby both the stability of the pontoon increases as the buoyancy by pontoon.

Moreover the last point, it results in that the "spring stiffness" of the system will be increased, it leads to that the dynamic behavior becomes more favorable. Also, it results that the floaters will be less submerged in water. It can lead to, the floaters will catch less flow, and that's why the force on the pontoons will also be reduced under the same circumstances when the A_p is not increased. This expectation is based on results of physical model conducted for Westerschelde tunnel project.

From the conducted model tests, it can be also concluded that the heavy tunnel elements hanging on relatively light pontoons barely moves through the wind waves. The relatively small and short-acting wave forces are not able to convert the heavy element into motion. In contrast, the relatively lighter pontoons will oscillate a lot in wind waves.

A shallow lying pontoon will be affected a lot by the wave load. The pontoon will move up and down. This leads to larger vertical forces by waves in the suspension cables, which is proportional to the wave height and the size of the pontoons. This effect will also be included in the modeling of the problem. For the project areas with a relatively low level of current velocities and a lot of wave action in the construction area, it's expected that this effect will dominate the forces on the pontoons and the forces in the suspension cables.

In addition to the above recommendations, it's also recommended to bring the suspension cables laterally as far as possible from each other. As a result of this measure, the internal forces in the roof of tunnel element will be reduced (a reduction of 20% is considered to be feasible). This measure affects the external forces on the system hardly. This aspect is also taken into account during modeling of the problem. That's why for the modeling purposes it's assumed that the suspension cables will be fastened in the outer walls of the element.

3.7.8 FORCE IN THE SUSPENSION CABLES DUE TO MOTIONS OF THE TUNNEL ELEMENT

The suspension cables should carry the extra ballast weight of the tunnel element during the immersion. The strength of these cables is of essential importance. If one of the suspension cables will break, then the tunnel element will hang unstable in the remaining wires. It is even possible that the pontoons will capsize and the

whole immersion operation will fail resulting in great damage. For the modeling purposes, it's been assumed that the tunnel element will hang on 4 or 8 suspension cables (2 or 4 wires per pontoon). It should be avoided that the natural frequency of the system coincides the vortex shedding period. If this happens, the motional amplitude of the element will become such high that it will be impossible to control the element and not to damage it. If the natural period of the element will not coincide the vortex shedding period, it is more likely to assume that the lift force on the tunnel element will be of limited value. And due to the large mass of the element, it will be not possible to accelerate such that the element will oscillate.

The element will be immersed in relatively mild wave conditions, which means that the wave forces on the tunnel element will be relatively small. From linear wave theory, we also know that the wave forces decreased exponentially with increasing depth. On another hand the elements have considerable mass and in relatively mild wave condition let say till wave height of 2 [m] approximately the tunnel element will not undergo large motions in waves and the motional amplitude can almost be neglected.

On the contrary, the pontoons have a much smaller inertia than the tunnel element. Due to wave excitation, the pontoons will tend to move with the waves. But due to the connection via the suspension cables with the tunnel element, the prevented motion of the pontoons will cause large force fluctuations in the suspension cables. The movements and sensitivity of the applied pontoons are determinative for the force fluctuation of the tunnel element. In the dynamic analysis of the pontoons, this aspect will be treated in more detail, and the results will be presented quantitatively.

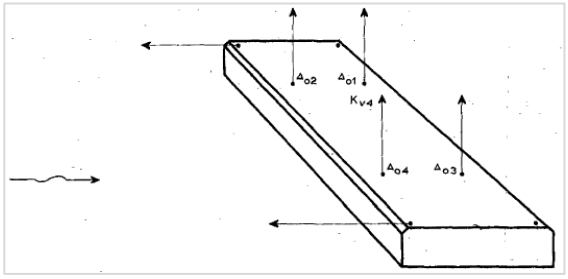

Figure 35 Vertical forces in the 4 suspension cables (W.D. Eysink, maart 1981)

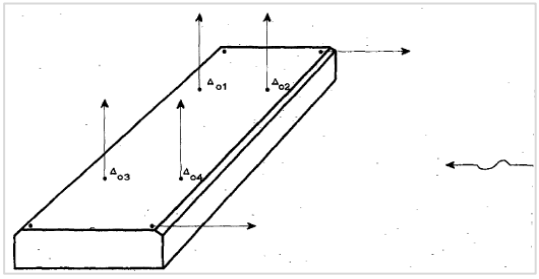

Figure 36 Vertical forces in the 4 suspension cables (W.D. Eysink, maart 1981)

Various executed model studies have shown, that during the immersion phase, the normative forces and displacements in the suspension cables occurs when the tunnel element is located just below the water surface. As the element is further immersed, the vertical forces and displacements, therefore, decreases too. Just before the bottom of the trench where the tunnel element is placed against its predecessor, the forces and movements are relatively small even at high flow velocities.

3.8 FORCES ON MOORING SYSTEM

The mooring system will mainly consist form mooring lines and contraction cables (see also Figure 41 and Figure 42). The function of the mooring lines is to keep the pontoons in position. The purpose of the contraction lines is to control the motions of the tunnel element during the immersion. The contraction lines are connected to the pontoons, tunnel element, and sea bottom. The contraction lines are guided from pontoons through the pad eyes on the tunnel element and fixed to the bottom of the sea.

The capacity of the mooring system is mainly determined by the horizontal drag force and wave Drift force. These forces have stationary character. The wind load also plays a role in the determination of the mooring capacity. However, the immersion of the element will be carried out in relatively mild windy conditions, and therefore it is disregarded in the calculations. The total transversal force which has to be taken by the mooing system is the sum of two mentioned forces, and it can be expressed as:

$$F_{mooring} = F_{drift} + F_{drag} \quad (29)$$

For the design load on the mooring system, it is looked at a situation when the tunnel element will be positioned above the trench, and the immersion is not started yet. At this position, the forces on the mooring system are maximal and also determinative.

For the determination of the drag force, the same approach has been followed as explained in section 3.4. For the exact calculations of the drag force, sophisticated model calculations are needed. In this thesis report, a simple but enough accurate approach is preferred. Because the mooring lines and contraction cables do not contribute to the first order wave motion which is essential for the dynamic analysis. The drift force is approximated as follows;

The waves can be described as irregular and can be characterized by the significant wave height Hs and Tp. For the calculation of the wave drift force, the freeboard of the tunnel element has been disregarded. From the wave potential and the Bernoulli equation, the transfer function of the time-averaged force on a vertical wall (with infinite depth) can be found by:

$$\bar{\bar{F}} = \frac{1}{2} \cdot \rho \cdot g \cdot \zeta_a^2 \cdot L \quad (30)$$

$$\frac{\bar{\bar{F}}}{\zeta_a^2} = \frac{\rho \cdot g \cdot L}{2}$$

L is the length of the wall. This transfer function is used here as a rough approximation for the tunnel element and pontoons in beam waves. The mean second-order wave force on the system can be given as:

$$\begin{aligned} \bar{\bar{F}}_{drift} &= 2 \cdot \int_0^{\infty} \frac{\bar{\bar{F}}}{\zeta_a^2} \cdot S_\zeta(\omega) \cdot d\omega \quad (31) \\ &= \rho \cdot g \cdot L_{TE} \cdot \int_0^{\infty} S_\zeta(\omega) \cdot d\omega \\ &= \rho \cdot g \cdot L_{TE} \cdot m_0 \end{aligned}$$

The significant wave height of the irregular waves can also be defined as:

$$H_s = 4 \cdot \sqrt{m_o} \quad \Rightarrow \quad m_o = \frac{1}{16} \cdot H_s^2 \quad (32)$$

Then the wave drift force can be expressed as:

$$\bar{\bar{F}}_{drift} = \frac{1}{16} \cdot \rho \cdot g \cdot L_{TE} \cdot H_s^2 \quad (33)$$

3.9 *Effect of passing ships*

Due to passing ships, the system may undergo undesired movements during the immersion, particularly in the vertical direction. The element and the pontoons can move suddenly through the water drop, which is initiated by a passing ship. This water level fall can occur long enough to put the tunnel element into motion. This phenomenon is dependent on several factors such as vessel size, speed, and the passing distance. In the model considered in this master thesis, this aspect has not been taken into account. For the model, it's been assumed that the shipping is stopped during the immersion process. Because Fehmarnbelt is an often used fairway, shipping cannot be stopped over the entire length. Further research into the effect of passing vessels during the immersion is needed.

An important parameter in this aspect is the movement of the element. The normative passing ship-generated movement should be analyzed in a model for multiple situations. From the results, the influence of the passing distance and the ship speed to be understood for the decisive decrease of the water level. On the water with a large surface, as is the case for the Fehmarnbelt, the return current and water level decrease can be set to be

proportional to water cutting area of the ship. Extrapolation of these in proportion to the movements of the element may be a reasonable first order approximation of the effect of the size of the vessel.

3.10 DENSITY VARIATION

Water densities play an important role in both the temporary conditions and the permanent conditions as mentioned before. In the temporary conditions during the immersion, the salinity rate determines the amount of ballast which has to be added. In the permanent conditions, the water density determines the water pressure on the bottom of the tunnel element. For the Fixed Link project, the salinity levels are quite predictable. For the Fehmarnbelt area there is sufficient amount of data to predict the salinity (see also appendix 8 and (FEHY (Metocean Conditions), 2013).

It's important to know the salinity variation over the depth. The salinity variation determines the amount of ballast water which has to be pumped into the ballast tanks to still have negative buoyancy during the immersion process. Also, there is a tendency that the saline water will accumulate in the trench. So before the tunnel element is uncoupled, there must be enough overweight to overcome the buoyancy force. It is dependent on the choice of the execution method. One can put the extra ballast when the tunnel element is near the surface. That will lead to an additional capacity of the floating pontoons and the winches and the suspension cables. It's also possible to measure the salinity during immersion across the water depth and when the increase of the salinity is analyzed then extra ballast water will be pumped into the ballast tanks.

When the tunnel element is uncoupled from the pontoons, it will be quite sensitive to the uplift forces. No extra material is put on the roof of the tunnel. Also, the ballast concrete will be not present in sufficient amount. That's why an additional amount of water will be pumped into the tunnel element to get extra vertical stability. The tunnel will be ballasted with an overweight of 2.5%. The salinity rate on the bottom influences the safety against the uplift in the temporary and final conditions. The salinity rate of the surface water influences the floatability of the tunnel elements. In saline water, the freeboard of the tunnel element will be higher than in fresh water.

3.10.1 *FORCE DUE TO DENSITY VARIATION*

The variation of density with depth due to the stratified condition in the Fehmarnbelt has been taken into account. The density variation over the vertical has been assumed to be 5kg/m3. If the tunnel element is lowered from a layer with lower density to a layer with higher density, the buoyancy force will be increased. The increase in the buoyancy force can be given as:

$$\Delta F_b = L_{TE} \cdot B_{TE} \cdot \Delta h \cdot \Delta \rho_w = 438.5 \cdot \Delta h \quad [kN/m] \qquad (34)$$

Where Δh is the draught in the layer with higher density. In the case of Fehmarnbelt, the water density changes approximately at a depth of 15 m under the free surface. During the immersion, the TE should be ballasted with more water approximately at a depth of 15 m to overcome the extra buoyancy force. In the case of Fehmarnbelt, it's possible that the density profile over the trench could well reach a wider density range. Once the saline bottom water from North sea with relatively a higher density has filled the trench, at least it will tend to stay there. When the tunnel element has been immersed in relatively brackish water, one should encounter a density increase of 1036 – 1007= 29kg/m3. The total increase in buoyancy force is:

$$\Delta F_b = L_{TE} \cdot B_{TE} \cdot \Delta h \cdot \Delta \rho_w = 2543 \cdot \Delta h \quad [\mathrm{kN/m}] \qquad (35)$$

Of course, this buoyancy force does not appear suddenly but builds up gradually. In reality, the density change over the depth is much less. The maximum difference measured is in time record is 5 kg/m3. To guaranty that there is

enough safety in the design stage, the value as mentioned above of $\Delta F_b = 438.5 \left[kN/m\right]$ has been taken into account in the design of the pontoons.

Another extreme situation which could occur is that half of the element length is submerged in water with higher density and another half with lower water density. This could happen if a rather sharp front passes or when a passing ship in the Fehmarnbelt causes internal waves in the two-layered. If we assume a density difference between the layers of 5 kg/m^3 the increase of the buoyancy force over the length can be given as:

$$\Delta F_b = B_{TE} \cdot H_{TE} \cdot \Delta\rho_w \cdot \Delta L = 41{,}2 \cdot 8{,}9 \cdot 5 \cdot \frac{9{,}8}{1000} \cdot \Delta L = 18 \left[kN/m\right] \qquad (36)$$

3.11 Conclusion

In this chapter, several force mechanisms have been discussed. The essential hydraulic forces on the system are given in Figure 37. The red boxes indicate the effects which are not considered in the modeling of the problem. For the low frequencies (long waves) the diffracted component of the force is smaller compared to the undisturbed wave force part (Froude-Krilov Force). At the higher frequencies, the diffracted part of the force getting more important. Because the dynamic behavior of the system is analyzed in relatively long waves, the diffracted part is not taken into account. It is assumed for now, that the influence of the diffracted part in the observed range of frequency can be ignored. Also, the frictional resistance and the dynamic part of the drag force are neglected for the calculations. The contribution to the total drag force is small. Further, the lift force is disregarded in the calculations. For structures like the tunnel element, integration of all the segmental forces will result in very small resultant force. Due to the different directionality of the segmental forces, they will cancel each other and will result in a small resultant lift force.

The blue boxes indicate the forces which are approximated by simplified methods given in the literature. The values of the radiation force are estimated by the aid of simplified methods. The green boxes indicate forces which are calculated relatively accurate in contrast to the blue boxes. Both of them are taken into consideration in the modeling of the problem.

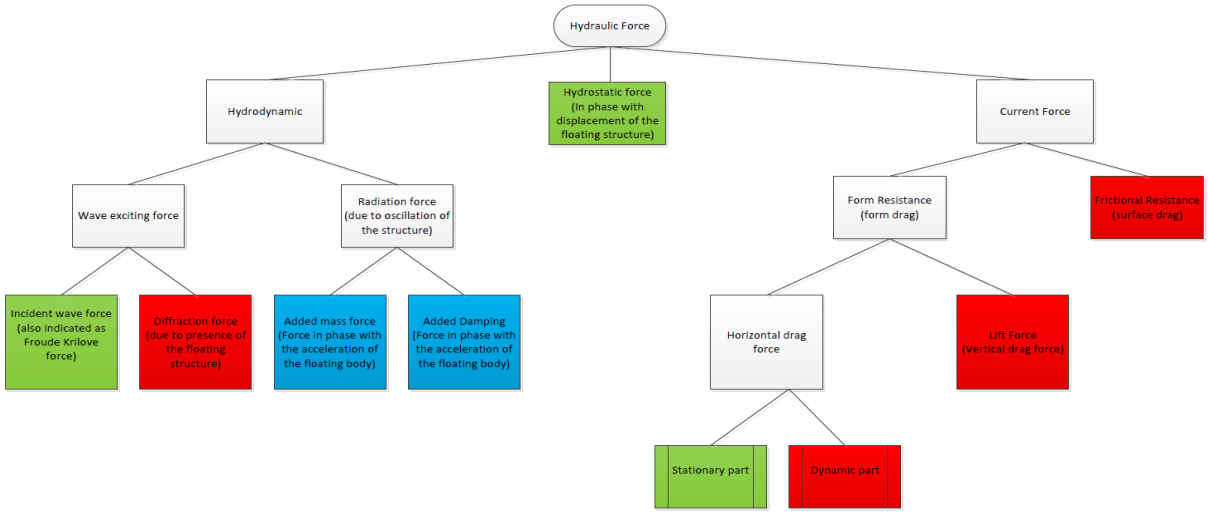

Figure 37 Overview of the Hydraulic forces during immersion

4 MODELING

4.1 INTRODUCTION

In order to answer the main and sub-questions, a numerical model is set up. The essential loads and different stability aspects are discussed in the previous chapter for each construction stage. The considered forces in the model are given in Figure 37 with green and blue boxes. This section provides an overview of the numerical model. Besides, the results of static stability and the limiting conditions are discussed too.
Modeling all the physical phenomena in one single model is difficult. Therefore three different modeling steps have been distinguished with the corresponding assumptions and simplifications. The distinguished modeling steps can be summarized as:

- Modeling parameters (section 4.2)
- Transport (section 4.4)
- Immersion (section 4.5)

In Figure 38 the flow chart of the entire model is given. In the next sections, the modeling steps are described in general, and the main modeling assumptions and simplifications are mentioned. The main modeling parameters are described in section 4.2. Section 4.3 describes how the dimensions of the pontoons are derived. In sections 4.4 and 4.5 the model principles of phases transport and immersion are described. Section 4.6 deals with how the static stability of the element and the two pontoons is verified in different construction stages. And finally, the used limiting conditions for the modeling purposes are described in section 4.7.

Detailed analysis steps and results are given in the following chapters. The pontoon dimensions and the limiting conditions are calculated in Appendix 1. For the calculations computer programs Maple, and Ansys Aqwa have been used. The calculated RAO's for the TE are given in Appendix 6, and the Maple calculation files are given Appendix 7.

4.2 MODELING PARAMETERS

In modeling step 1, the given boundary conditions for Fehmarnbelt (mentioned in chapter 2) and the dimension of illustrative design are used to calculate the dimensions of the two distinctive type pontoons. Subsequently, the static stability of the chosen dimensions and the entire system during different construction stages has been checked (paragraph 4.6). If necessary, the pontoon dimensions were altered to fulfill the static stability requirements. Finally, the limiting conditions and capacity of the mooring lines, suspension cables, and contraction cables were identified for the chosen dimensions of the system (paragraph 4.7).

4.2.1 DIMENSIONS TE ILLUSTRATIVE DESIGN:

The tunnel elements consist of a combined road and rail cross-sections all at one level. For the fixed link two types of the elements will be used:

- Standard element
- Special element.

The majority of the elements are of standard type (79 elements). Also (10) special elements will be used across the fixed link see also Appendix 1. For the modelling purposes, only the dimensions of the standard elements are used. All elements have the same layout and geometry. The details of the geometry are depicted in Figure 39; they are to a high level interchangeable.

Each element is approximately 217 m long and will be constructed from a chain of smaller segments which are temporarily connected longitudinally by using a post-tensioning system for transportation and immersion. The dimensions of the standard elements are given in Figure 39 and Table 2. The pretension cables will be cut after the tunnel elements are placed on its foundation.

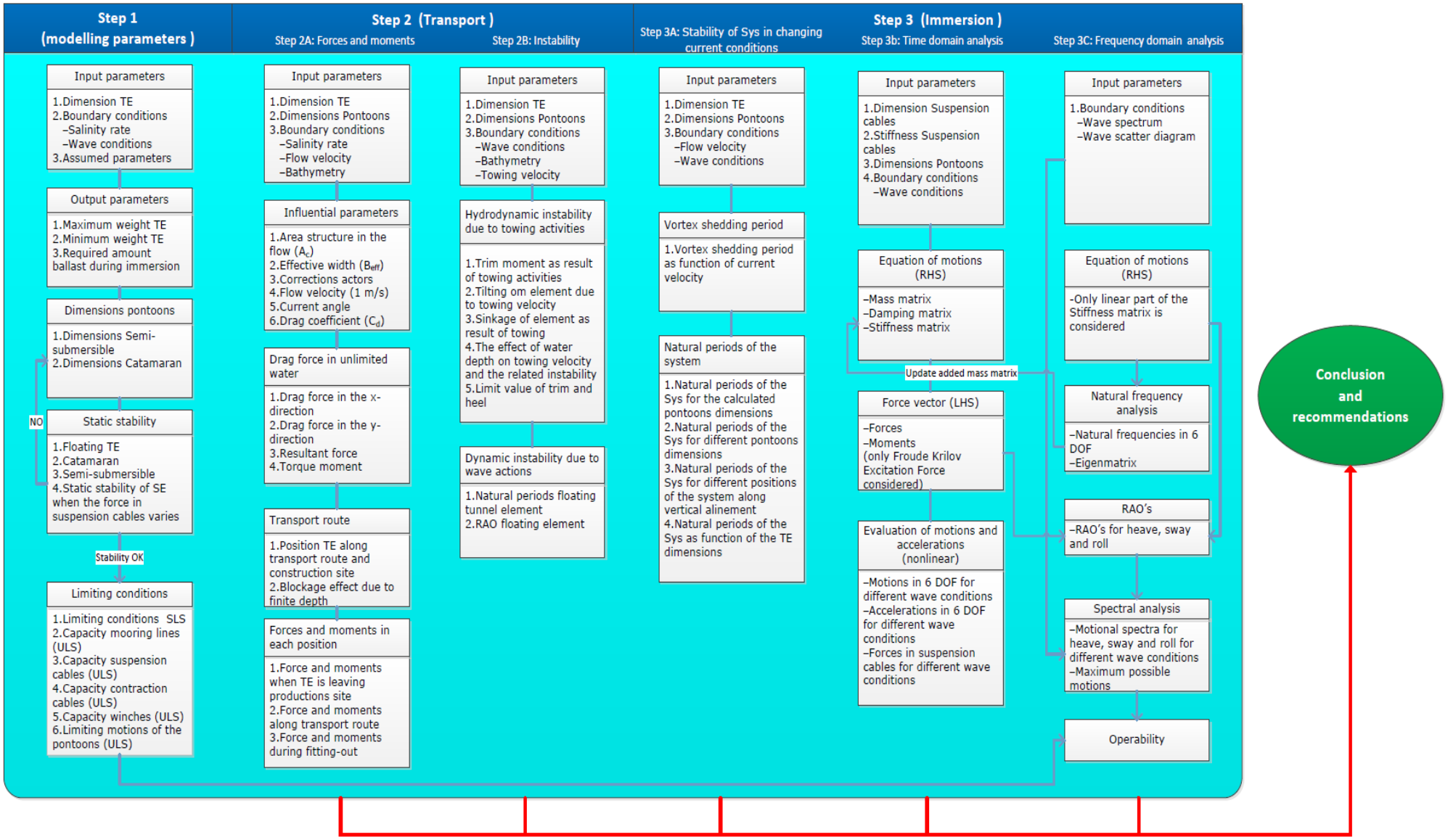

Figure 38 Flow chart of the numerical model

For the modeling purposes, the real shape of the standard elements has been simplified. The shape of the elements has been assumed to be rectangular. The cross-section which is modeled is depicted in Figure 40. The tunnel will be longitudinally ventilated, with ventilation fans spread throughout the length of the tunnel. Niches are provided above the road tubes to accommodate the ventilations. For the modeling purposes, the ventilation niches are disregarded.

	Symbol	Value	Units
Length	LTE	217.8	m
With (deck)	BTE(deck)	41.2	m
With (floor)	BTE(floor)	42.2	m
Height	HTE	8.9	m
Position Centre of Gravity			
	X	y	Z
G(x,y,z)	108.5	0.06	4.47

Table 2 Dimensions illustrative design

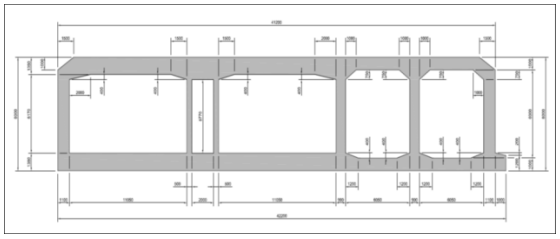

Figure 39 Actual cross-section tunnel element (Femern A/S, 2013)

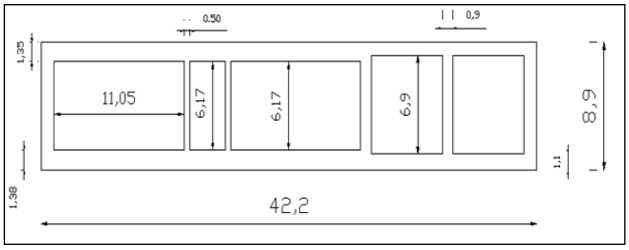

Figure 40 Simplified cross-section used in the calculations

4.2.2 TOTAL WEIGHT

For the transportation and immersion of the element, the minimum and maximum possible weights are of interest. In evaluating the buoyant behavior of the tunnel element, the nominal values of the weights and the water densities are considered. No load factors have been applied to this calculations.

Two conditions have been assed, namely:

- Lightweight condition (Considering the maximum possible water density and the minimum element weight)
- Heavyweight Condition (Considering the minimum possible water density and the maximal element weight)

When considering the Lightweight condition, the freeboard of the tunnel element will be maximal. The Heavyweight condition is the opposite of the Lightweight condition. In this state, the minimum water density and the most substantial structural weight has been considered. The heavy condition determines the minimum freeboard of the element during the transportation. The minimum freeboard is assumed to be 0.2 [m]. It has been verified in the heavyweight condition, that there still some ballast has to be applied to get this freeboard. Further, for determination of the buoyancy force three situations are considered:

1) Phase 1: When the element is floated up in the construction area, the freeboard is dependent on the weight of the element and water density.
2) Phase 2: When a floating element will have a freeboard of 0,2 m in fresh water after trimming
3) Phase 3: When the entire element is submerged.

The nominal values of the different calculated weights are given in Table 3.

Nr.	Weight component	$G_{(max)}$ [ton]	$G_{(min)}$ [ton]
1.	Structural concrete	75183	71141
2.	Bulkheads	380	380
3.	Immersion equipment	50	50
4.	Ballast tanks	250	250
5.	Immersion chambers	638,4	620
6.	Trimming concrete	598	565
	Total weight TE	77100	73006

Table 3 Total weight TE

4.3 DIMENSIONS OF THE PONTOONS

The main piece of equipment during the immersion is the immersion rigs, which takes the weight of the negative buoyant element when it is placed on the bottom of the dredged trench. Different kind of pontoons are used to support the weight of the tunnel element in its immersion condition with the required overweight. There are several options how the immersion pontoons will be configured. In this case study, it's been chosen for two types of pontoons.

- Catamaran pontoons (see Figure 41)
- Semisubmersible (type) pontoons (see Figure 42)

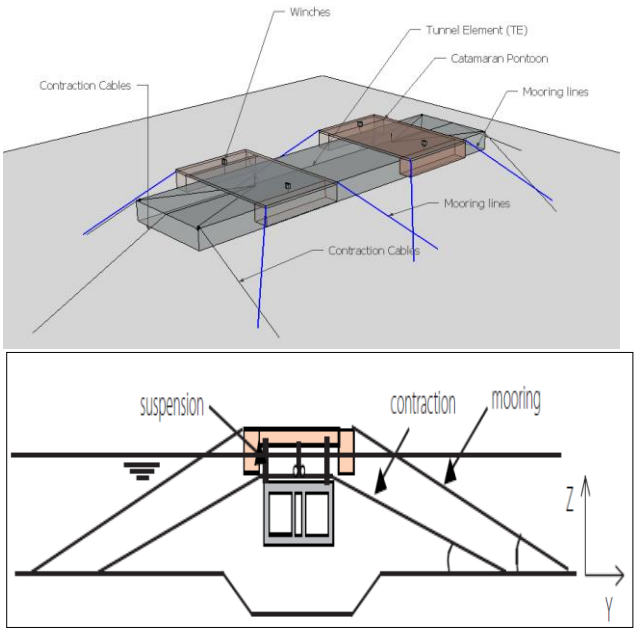

Figure 41 Catamaran Pontoon

Both types of pontoons float either side of the element, with a deck spanning over the element between them. The element is then suspended from the deck. Two sets of Semisubmersible pontoons and Catamarans are needed—one at each end of the element. The floating bodies of the both pontoon types are modeled as a floating steel box that can support the weight of the tunnel element during the immersion.

In the design of the pontoons, the following aspects are considered

- Dimensions tunnel elements (only the standard elements are considered in this study)
- The weight of the tunnel elements 'which depends on:
    1. Amount of the reinforcement
    2. Density of concrete
    3. Construction inaccuracies
    4. Weight for the extra facilities needed for the immersion.
- Salinity of the water (difference in water density in time and depth)
- Amount of the required Ballast 'which depends on:
    1. Dynamic wave force
    2. Difference in weight (of the TE)
    3. Difference in salinity rate
- Weight Bulkheads
- Weight trimming concrete (can also be used as ballast concrete)
- Weight immersion equipment
- Weight ballast tanks
- Weight immersion chamber

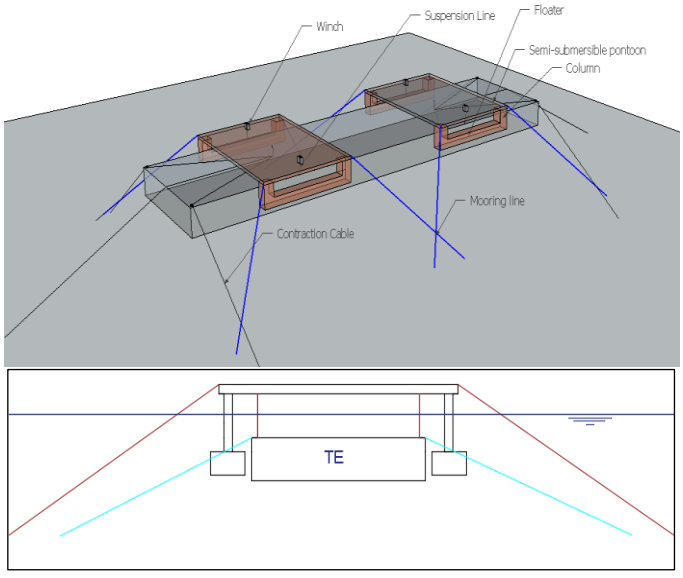

Figure 42 Semisubmersible pontoon

For determination of the dimensions of the pontoons, different load situation are considered. For the determination of the pontoons dimensions, the floating capacity of the pontoons is being taken as strength parameter, and the loads are different weights which are acting on the pontoons during the immersion.

Also, current forces and wave loads which are acting on the pontoons have been taken into account. The structural design of the pontoons and the tunnel element is not considered in the model. The design rules for the required floating capacity are taken into consideration. Then three design situation was observed. The applicable design situations are chosen such that the pontoons can fulfill its function during the immersion operation. For determination of the floating capacity of one pontoon, the freshwater density is used for the calculations.

The pontoon should also have a freeboard to prevent that wave will pass over the pontoon. The freeboard is chosen such, that if the pontoon fully reflects a design wave, then it still has enough freeboard, to prevent 'green' water on the deck of the pontoon. The reflected wave is assumed to be a standing wave. The detailed analysis is given in Appendix 1. The following pontoon dimensions are calculated for the Catamaran and Semi-submersible pontoon.

Dimension	Value	Units
With pontoon B_p	60	m
Length pontoon L_p	38	m
Height pontoon h_p	8.5	m
With floater B_f	7	m
Length floater L_f	38	m
Height floater h_f	7.5	m
With pontoon deck B_D	60	m
Length pontoon deck L_D	38	m
Height pontoon deck h_d	1	m

Table 4 Overall dimensions of the Catamaran pontoon

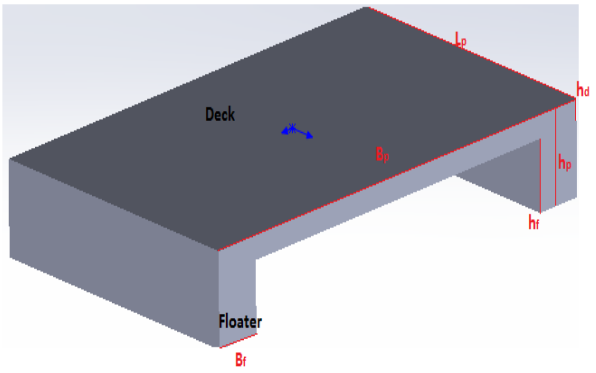

Figure 43 Catamaran pontoon

Dimension	Value	Units
With pontoon B_p	54	m
Length pontoon L_p	40	m
Height pontoon h_p	10.5	m
With floater B_f	4	m
Length floater L_f	40	m
Height floater h_f	4	
With pontoon deck B_D	54	m
Length pontoon deck L_D	30	m
Height pontoon deck h_d	1	m
Columns (L·B·hc) → (4 x 4 x 5.5)		m3

Table 5 Overall dimensions of the Semi-submersible pontoon

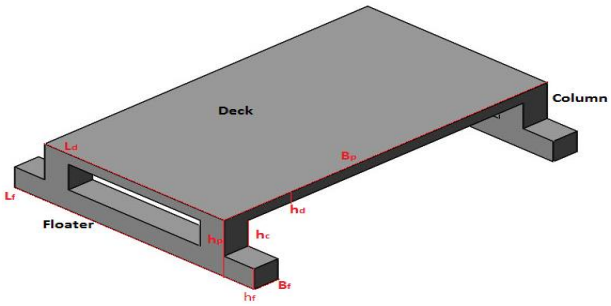

Figure 44 Semi-submersible pontoon

4.4 Modeling Transport Phase

In step 2 the forces and moments on the floating element are evaluated. Two main type hydraulic external forces have been taken into consideration in the model, namely current and wave force. The tunnel element is modeled as a rectangular box (see also Figure 87). The configuration of the tunnel element and the pontoons during transport is given in Figure 12 and Figure 21 The forces and moments on pontoons are not considered during transport. The element will have a freeboard of 0.2 [m]. For the calculations of the drag force and torque, moment freeboard has been disregarded.

First, all the relevant, influential parameters are identified and calculated. For the calculations, data provided in different literature are used. Secondly, the forces and the moments are determined in unlimited water depth for a flow velocity of 1 [m/s]. Then for different positions along transport route, the forces and moments are calculated for finite water depth and different values of flow velocity.

Subsequently, the hydrodynamic stability of a floating element was evaluated. Some hydrodynamic phenomena have been taken into account during the transportation of the tunnel elements from the factory to the immersion site. The limiting effect of the hydrodynamic stability on towing velocity has been determined for the different positions.

The natural frequencies were calculated to assess the dynamic stability. Then the wave-induced motions of the floating tunnel element are calculated in computer software Ansys Aqwa. Based on standard three-dimensional frequency-domain diffraction/radiation theory. The RAO's for 6 degrees of freedom of the floating tunnel element are calculated. These calculations are performed for 30 m water depth and 1m wave height. Different wave attack angles have been analyzed.

4.5 Modeling Immersion phase

During immersion, the system will be excited by the wave and current forces. The pontoons provide the stability of the system. The relatively light pontoons are sensitive to the wind waves in contrast to the heavy tunnel element. In step 2 the sensitivity of the floating TE to wind waves has been calculated for different wave angles. It appears that due to its large inertia TE is insensitive for relatively mild wave climate, the wave climate in the Fehmarnbelt can be considered as calm during 'normal' weather conditions. That's why the following modeling approach has been chosen.

4.5.1 Current conditions

To assess the stability of the system due to vortex shedding the following approach has been applied. For a first estimate of the current drag force, torque moment and Strouhal number again data presented in the literature are used to get an impression of the magnitude. With the aid of the tunnel element dimensions, Strouhal number and the normative current velocities in the Fehmarnbelt the vortex shedding periods are calculated.

It is assumed that the tunnel element and the pontoons behave as one body. The contribution of the pontoons to the inertia of the system is neglected. This justified by the fact (Mpontoon/MTE <0.018). On the other hand, the stability of the system is entirely contributed by the pontoons. The stability of the submerged element is neglected. Further, it is assumed that the waterplane area of pontoons determines the vertical, and rotational stiffness of the system. It means that the pontoons and TE behave as one rigid body. In reality, the connections between pontoons and tunnel element are such that motions relative to each other are possible. But this aspect is disregarded for this calculations. Only the stiffness of the waterplane area is been taken into account. The suspension cables are modeled as infinitely stiff and the stiffness of the mooring system is disregarded (see also Figure 87). Detailed elaboration and results of this analysis are given in chapter 6.3.

4.5.2 Time domain analysis

For the prediction of the global hydrodynamic response of the pontoons to wave excitation the following approach has been followed. In the analysis the coupling between surge, sway, heave, roll, pitch and yaw degrees of freedom is considered. The calculations contain typical response of the system to waves. The calculations are performed for the first order responses that are valid in relatively low wave heights. Hydrodynamic effects caused by the nonlinearities are disregarded in the calculations.

To be able to perform the calculations the system has been simplified. During the immersion phase, the tunnel element has been assumed stationary. And only the response of the pontoons has been considered. In this analysis, only the motions due to wave excitation of the pontoons are studied (see also Figure 97). The pontoons are regarded as a hybrid structure. It means that concerning the horizontal degrees of freedom the pontoon structure is considered as it is compliant and behaves like a floating structure. While concerning the vertical degrees of freedom, it is stiff and resembles as a fixed structure and is not allowed to float freely.

The contribution of the mooring lines for the first order response is considered of minor importance, and it is disregarded in the calculations.

First, the equation of motion is determined for both types of pontoons. Subsequently, the dynamic behavior for both pontoons is analyzed separately. In the analysis, the coupling between the six degrees of freedom is considered. The analysis considers various nonlinearities produced due to change in the suspension cable tension. The wave forces on the pontoons are calculated by using linear wave theory thereby ignoring the diffraction effects. The diagonal radiation terms such as added mass and radiation damping are approximated by the given values in the literature, whereby the non-diagonal terms are disregarded. The wave forces are estimated at the instantaneous equilibrium position.

Numerical studies are conducted to compare the dynamical behavior of the Catamaran pontoon with that of the Semi-submersible. The dynamic behavior of both pontoons is analyzed close to the natural frequencies of each pontoon in a wave height of 1 m and the tunnel element 1 m below the sea surface. In this way, the near-resonating behavior of the pontoons is analyzed.

4.5.3 *Frequency domain analysis*

For this analysis the dynamic response characteristics of the pontoons are presented as Response Amplitude Operators (RAO's). To apply the concept of RAO's the system is considered to be linear. This means that only the linear coefficients in the stiffness matrix are taken into account. The concept of linearity can only be applied if the motions are small enough and that the nonlinear terms in the stiffness matrix can be ignored. In the time domain analysis, it is proven that for both pontoons the motions are small enough so that the system can be assumed as linear.

For the analysis the JONSWAP spectrum is used which is adjusted for the project location (see also (FEHY (Metocean Conditions), 2013)). The response spectrum of the motions is determined by multiplying the RAO's of the motions with the provided wave spectrum. For each given environmental condition is the most probable maximum of motion in N peaks is determined.

Given the fact that the system can be assumed as linear, the equation of motion is solved in the frequency domain. Due to the character of the load (beam waves) only the response in 3 main activated modes namely, sway, heave and roll have been determined. The equation of motion is solved by using the Modal analysis. The RAO's are determined for sway, heave, and roll. The motional amplitudes are used for determination of the response spectrum. The wave scatter diagram is used for the determination of the workability of the pontoon in the given environmental conditions. For each combination of the significant wave height and wave peak period, the spectrum of the motion for each studied degree of freedom is calculated. If the most probable value of the motion exceeds the limit value, then those conditions are considered as a not working condition.

4.6 Static Stability

So far only the vertical stability of the tunnel element and the pontoons has been discussed. In the design of the tunnel element and the pontoons, there is another aspect to stability, which is stability against the overturning of the floating structures (tunnel element either the pontoons). During the construction operations, the tunnel element and the pontoons will be subjected to external forces or may not float evenly. It is essential to check that the tunnel element will stay stable in all constructions stages. The risk of the overturning or rolling must be minimized. In order to assess the static stability of the tunnel element and the pontoons, the following check calculations will be carried out in this respect:

1. Calculating the metacentric height of the tunnel element during the transport and immersion phases.
2. Calculating the static stability of the empty pontoons (without hanging tunnel element). This is done to ensure that the chosen dimensions of the pontoons are chosen properly concerning the overturning stability.

3. The static stability, of the pontoons will be checked for the immersion phase when the tunnel element will hang on the pontoons.

For checking the static stability, the metacentric height is an important parameter. The metacentric height is defined as the distance between the metacenter M and the center of gravity G (see also Figure 85). The center of gravity doesn't change its position when the floating body will have an angle ϕ or θ respectively for roll and trim degree of freedom. The point M is defined as the point on the vertical line through the G, and when the floating body is inclined, the line through the shifted center of buoyancy will intersect the line through the G at the point M. The principle of the static stability is further describes in Appendix 5.1. In all the stages the metacentric height (h_m) has to be higher than 0. Only then, the structure can return to its position when the load is removed. The metacentric height requirements vary considerably for different types of floating structures.

It is important to consider that the tunnel element has to be stable during the floating up and immersion operations. There must also be an assurance that the elements do not tilt in an unacceptable degree during the transport or the immersion. The unstable elements, tilting can be initiated by, towing velocity, mooring forces, wave motions, an inlet of water during immersion. The element must, therefore, be designed such a way that rotation, caused by external factors, is corrected by a righting moment that will return the element to its original position. Therefore the minimum h_m for the tunnel element is defined as: $h_m > 0.5$ m.

The function of the pontoons is to guide the tunnel element during the immersion operation. The pontoons can fulfill this demand only if the pontoons are afloat and have sufficient freeboard for stability (and no green water on the deck). The two pontoons, composed from a top deck and two floaters. The equipment will be installed on the deck of the pontoons. During the immersion, the floaters will carry the overweight of the tunnel element. For the determination of the static stability of the pontoons the required minimum metacentric height is deduced from BS6349 (Part 6). The meta centric height for the pontoons in all stages should be: $h_m > 1$m.

4.6.1 TUNNEL ELEMENT

The principle of the static stability of the TE is depicted in Figure 45. The static stability of the tunnel element is calculated as follows:

The freeboard during the transportation is chosen as 0.2m; this leads to a draught of the TE of (T=8.7m). The metacentric height h_m can be expressed as:

$$h_m = KB + BM - KG \qquad (37)$$

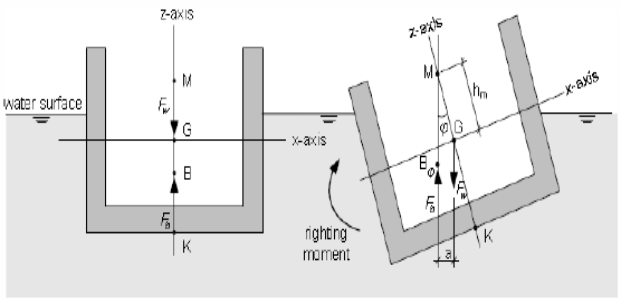

Figure 45 Static stability of the TE during the transport (M.Z. Voorendt, W.F. Molenaar, K.G. Bezuyen, 2011)

where:

$$KB = \frac{T}{2} \qquad (38)$$

$$BM = \frac{I_{TE}}{displace\ volumne} = \frac{I_{TE}}{\nabla} \qquad (39)$$

Transport

The metacentric height is calculated for trim and heel. The following values have been obtained:

	KB [m]	KG [m]	I_{TE} [m^2]	∇ [m^3]	h_m [m]
Heel	4.35	4.47	$1.27 \cdot 10^7$	78300	16.1
Trim	4.35	4.47	$3.57 \cdot 10^7$	78300	456.

Table 6 Static stability of the TE

It appears that the metacentric height is much greater than 0.5 m. From the calculated results it can be concluded that the tunnel element is statically stable during the transport.

Immersion

For fully submerged floating bodies as in case of the tunnel element, during the installation, there is no waterplane area. It means that the metacenter of the body coincides buoyancy center. In this case, the metacentric height can be calculated as:

$$h_m = KB - KG = H_{TE} - KG = 0.05\ [m] \quad (40)$$

The metacentric height during the immersion is minimal. It means that when the tunnel element undergoes small rotations, it has little capacity to return to its stability state. It should be mentioned that in the calculations the effect of the ballast water and ballast concrete hasn't been taken into account. By adding more weight to the element, the center of gravity will shift. The new position of the COG of the element can be determined by looking at the first moment of masses. The location and the z coordinate of the masses are not known at this stage. That's why the effect of the ballast water is not considered further in this research.

It has to be mentioned that a small metacentric height should be not considered as a problem during the immersion phase. The pontoons will completely determine the stability of the tunnel element. If the pontoons are correctly designed, this should be not a problem.

4.6.2 CATAMARAN PONTOON

The immersion equipment consists mainly from two floating pontoons. Here the static stability of the two types of pontoons will be determined. Previously the floating capacity and the dimensions of the pontoons have been established. Now the chosen dimension will be controlled concerning the overturning stability. In order to check the static stability the following assumptions have made:

Structural element	Weight	Units	Z-position above the keel [m]
The total weight of 1 pontoon	1500	ton	
The weight of each floater	350	ton	3.75
Weight of the deck	400	ton	8
Weight equipment	400	ton	9

Table 7 Assumes mass properties Catamaran pontoon

From the assumptions, the position of the center of gravity (COG) follows as: COG (x, y, z)→(19, 30, 6.28)

The vertical position of the center of gravity is determined by taking the first moment of mass about the keel and then dividing the moment by the total mass.

The following parameters are calculated, to determine the metacentric height.

The water plane area of the pontoon is:

$$A_{w-pontoon} = 2 \cdot B_f \cdot L_f \quad (41)$$

Draught empty pontoon + the equipment:

$$T_{pontoon} = \frac{M_{pontoon}}{\rho_w \cdot A_{w-pontoon}} \quad (42)$$

Distance from keel to the center of buoyancy:

$$KB = \frac{T_{pontoon}}{2} \quad (43)$$

The transverse and longitudinal moments of inertia are the second moments of area of not heeled water plane area about the x-axis and y-axis. For the pontoon consisting of two floating bodies it can be expressed as:

$$I_T = \left(\frac{1}{12} \cdot L_f \cdot B_f^3 + L_f \cdot B_f \left(\frac{B_p}{2} - \frac{B_f}{2}\right)^2\right) \cdot 2 \quad (44)$$

$$I_L = \left(\frac{1}{12} \cdot B_f \cdot L_f^3\right) \cdot 2 \quad (45)$$

Distance center of buoyancy till metacenter:

$$BM = \frac{I_{pontoon}}{\nabla_{pontoon}} \quad (46)$$

In the above equation, the ∇ represents the displaced volume.The metacenter is given as:

$$h_m = KB + BM - KG \quad (47)$$

With the given dimension of the pontoons the following values has been calculated for the Catamaran pontoon:

	KB [m]	KG [m]	BM [m]	I_{TE} [m^2]	∇ [m^3]	h_m [m]
Roll	1.41	6.28	251	$3.76 \cdot 10^7$	1460	253
Pitch	1.41	6.28	21.3	$3.2 \cdot 10^4$	1460	17

Table 8 Static stability of the empty Catamaran pontoon

From the results, it can be concluded that the empty (no tunnel element hanging) pontoon has enough static stability. This means that when the pontoon is loaded asymmetric, then there is enough capacity in the pontoon to produce a proper righting moment and not to capsize.

Static stability pontoon during immersion

In the second step is the static stability checked when the load from the suspension cables would work on the pontoons. For the calculations is the same approach has been followed as for the calculations of the empty pontoon. The position of the suspension cable winch is assumed to be 1m above the deck. The element would be ballasted such that per pontoon an extra weight of 984 ton should be carried. Therefore, per suspension cable, a force of 492 ton should be transmitted.

	KB [m]	KG [m]	BM [m]	I_{TE} [m^2]	∇ [m^3]	h_m [m]
Roll	2.26	7.58	157	$3.76 \cdot 10^7$	2400	151
Pitch	2.26	7.58	13.3	$3.2 \cdot 10^4$	2400	8.02

Table 9 Static stability of the Catamaran pontoon with hanging tunnel element

As we can see the pontoons are still stable, but it should be noted that the static stability in the pitch direction is decreased. Also, the effect of the water density is investigated. If the surface water has fresh water density, then the metacentric height of the pontoons will slightly decrease. The values are given in table here below.

	KB [m]	KG [m]	BM [m]	I_{TE} [m^2]	∇ [m^3]	h_m [m]
Roll	2.47	12.2	144	$3.76 \cdot 10^7$	2620	149.5
Pitch	2.47	12.2	12.2	$3.2 \cdot 10^4$	2620	7.85

Table 10 Static stability of the Catamaran pontoon with hanging tunnel element in fresh water

The effect of fluctuating suspension cable force

The force in the suspension cables is variable. Due motions of the pontoons as a result of wave and current attack on the system the forces will fluctuate. The effect of the fluctuating suspension cables force has also been investigated. The calculations steps are the same as it is given by equation (41) till equation (47). Here above the static stability is calculated for only one value of suspension cable force. In the following, the static stability is calculated for different values of the suspension cable force (see also Figure 46). For the calculations, it is assumed that the forces in both cables are equal to each other and that they are working symmetrically on the pontoon.

From calculations it appears that the static stability of the pontoons in the pitch/heel direction is sensitive to the force fluctuations. The effect of the fluctuating force in suspension cables on the metacentric height in longitudinal/transversal directions, distance BM and the draught of the pontoons is given in Figure 47. As we can see that with increasing force the metacentric height of the pontoon decreases. But also for large values of the cable forces, the pontoons are still stable. The pontoons have to stay stable, even for large force fluctuations and not to capsize during the operation. The floating capacity seems to be sufficient also for large force fluctuations. It means that the dimensions of the pontoons are properly chosen for the given operational limits concerning the static stability..

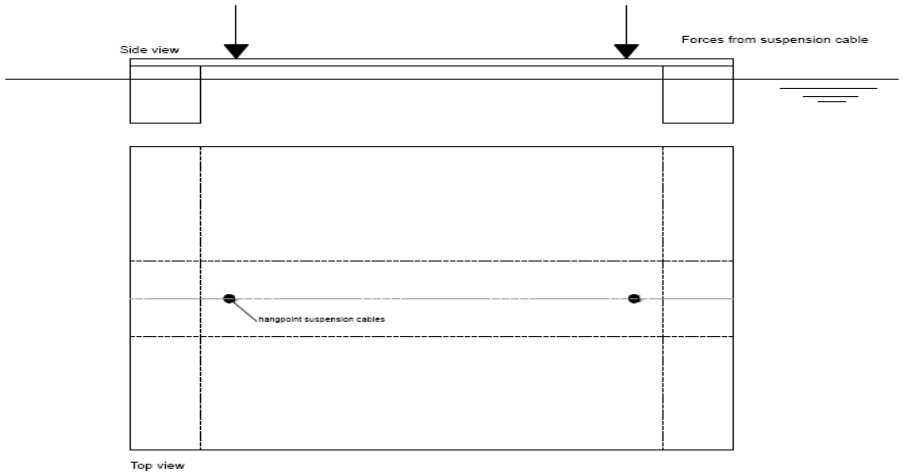

Figure 46 Principle of: working force from suspension cables on pontoon

The dynamic stability will also be checked later on. As we can see from Figure 47 the metacentric height in the roll/trim direction is also sufficient for the given force fluctuation.

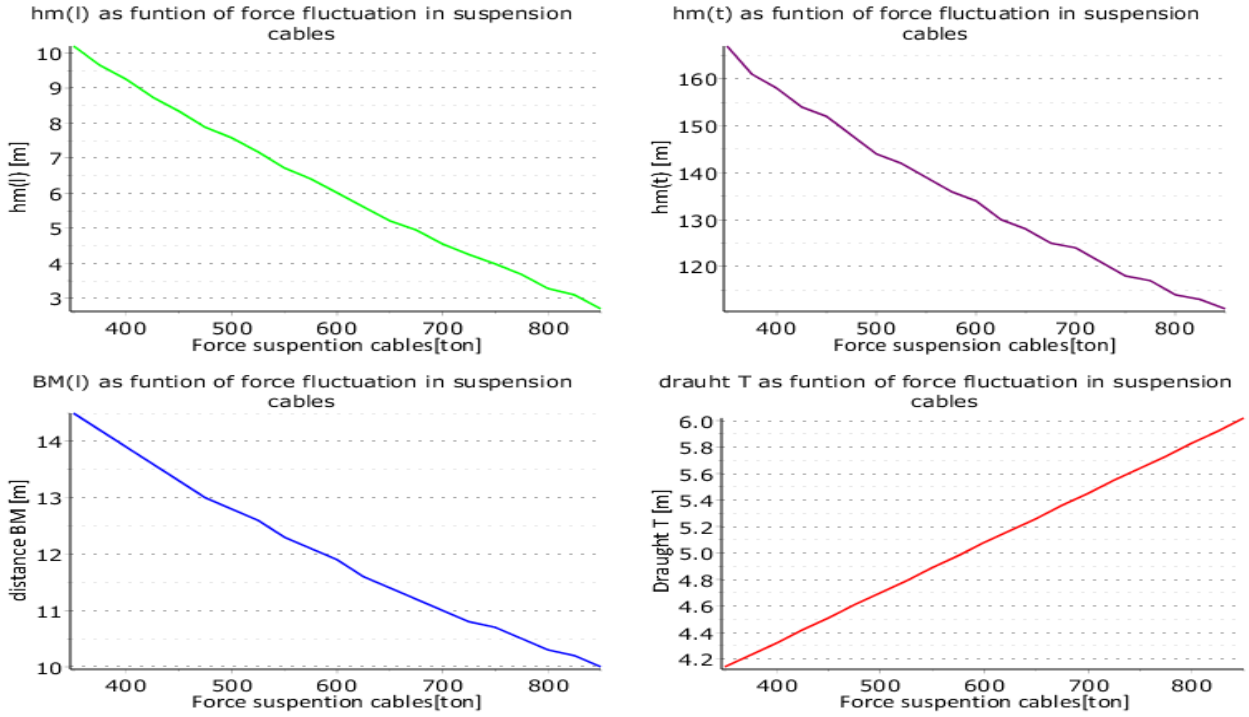

Figure 47 Effect of the fluctuation of the force in suspension cables on static stability

4.6.3 *SEMI-SUBMERSIBLE TYPE PONTOON*

The same approach is also followed to determine the static stability of the Semi-submersible type pontoon. The calculation procedure is slightly different due to changing water plane area during various stages. That's why the calculation procedure will also be presented again. The dimension of the semisubmersible pontoon has been determined earlier. To check the static stability, assumptions are made concerning the weight of the structural elements and the local z-coordinate.

Because the semisubmersible pontoon will be subjected to minor wave load, the dimensions are smaller and also the weight. The following assumptions are made for the calculations:

	Weight	Units	Z-position above the keel [m]
The total weight of 1 pontoon	1000	ton	
The weight of each floater	170	ton	2
Weight of the deck	200	ton	10
Weight of one column	20	ton	6.75
Weight equipment	400	ton	11

Table 11 Assumes mass properties Semi-submersible pontoon

Form the assumed mass and elementary coordinate of the center of gravity the position of the pontoons center of gravity (COG) is determined as: COG (x, y, z)→(20, 27, 8.79).

Due to the symmetry the position of the x and y coordinate of the pontoon lies in the middle of the pontoon. Due to different vertical distribution of the load in the z-direction the first moment of mass in z-direction has been used to determine the position of the z-coordinate. This can be expressed in the formula form as:

$$z_{cog} = \frac{\sum_{i=1}^{n} M_i * z_i}{\sum_{i=1}^{n} M_i} \quad (48)$$

First, the static stability of the empty pontoon is determined the following procedure and equation are used for the calculations: For the calculations, a water density of 1000 kg/m3 is used. Also, the static stability for the maximum water density will be calculated. The steps are the same; only the results are presented. The displaced mass of water is equal to the weight of the pontoon. The displaced volume water can be calculated from Archimedes with the following equation.

$$\nabla_o = \frac{M_{pontoon}}{\rho_w} \quad (49)$$

∇_o represents the initial displaced volume water. Given the dimensions of the floaters and the mass of the pontoon, it is obvious that initially the pontoons will be not submerged under water. And therefore the initial draught can be calculated as:

$$T_o = \frac{\nabla_o}{B_f \cdot L_f \cdot 2} \quad (50)$$

The remaining calculation steps are the same as those for catamaran pontoon. The results of the calculations are given in the table below.

	KB [m]	KG [m]	BM [m]	I_{TE} [m^2]	∇ [m^3]	h_m [m]
Roll	1.56	7.48	200	$200 \cdot 10^5$	1000	195
Pitch	1.56	7.48	21.3	$2.13 \cdot 10^4$	1000	15.4

Table 12 Static stability of the empty Semi-submersible pontoon

From the results, it can be concluded that the pontoon is initially statically stable. Now the static stability will be calculated when the pontoons will be subjected to the force from suspension cables during the immersion. The total force in the cables will be 437 [ton]. Per cable, a force of 218.5 [ton] will work on the pontoon. The forces will work symmetrically to the COG of the pontoon. As a result of that, the pontoon will sink but will not rotate about its axes. The displaced mass and displaced volume will be equal to:

$$M_{total} = M_{pontoon} + 2 \cdot F_{cable} \quad (51)$$

$$\nabla_1 = M_{total}/\rho_w \quad (52)$$

From the displaced mass it can be concluded that the pontoons will be submerged and that the columns will be submerged for a part. To determine the draught of the pontoon the following equations are used.

$$\Delta T = \frac{\nabla_1 - (L_f \cdot B_f \cdot h_f \cdot 2)}{4 \cdot A_{col}} \quad (53)$$

$$T_1 = T_o + \Delta T \quad (54)$$

With the aid of the first moment of volume, the position of buoyancy center will be determined. And the related distance KB_1.

$$KB_1 = \frac{\left(2 \cdot (L_f \cdot B_f \cdot h_f) \cdot \frac{h_f}{2}\right) + 4 \cdot \left(A_{col} \cdot \frac{T}{2}\right)}{\nabla_1} \quad (55)$$

The transverse and longitudinal moments of inertia are determined by the water plane area of the columns. And they are defined by the following equations.

$$I_T = \left(\frac{1}{12} \cdot B_{col}^4 + B_{col}^2 \left(\frac{B_p}{2} - \frac{B_{col}}{2}\right)^2\right) \cdot 4 \quad (56)$$

$$I_L = \left(\frac{1}{12} \cdot B_{col}^4 + B_{col}^2 \left(\frac{L_d}{2} - \frac{B_{col}}{2}\right)^2\right) \cdot 4 \quad (57)$$

The remaining stability terms in this loading condition are:

$$BM_T = \frac{I_T}{\nabla} \quad (58)$$

$$BM_L = \frac{I_L}{\nabla} \quad (59)$$

$$h_{m-roll} = KB_1 + BM_T - KG_1 \quad (60)$$

$$h_{m-pitch} = KB_1 + BM_L - KG_1 \quad (61)$$

With the aid of the given equations the following results are obtained:

	KB [m]	KG [m]	BM [m]	I_{TE} [m^2]	∇ [m^3]	h_m [m]
Roll	1.90	8.68	27.8	$4.01 \cdot 10^4$	1440	21.0
Pitch	1.90	8.68	7.57	$1.09 \cdot 10^4$	1440	0.79

Table 13 Static stability of the Semi-submersible pontoon with hanging tunnel element in fresh water

In addition, the results for the saline water density are:

	KB [m]	KG [m]	BM [m]	I_{TE} [m^2]	∇ [m^3]	h_m [m]
Roll	1.94	8.68	28.6	$4.01 \cdot 10^4$	1400	21.8
Pitch	1.94	8.68	7.79	$1.09 \cdot 10^4$	1400	1.05

Table 14 Static stability of the Semi-submersible pontoon with hanging tunnel element in saline water

From the results, it can be concluded that the static stability in the pitch direction is decreased considerably. Especially during the freshwater condition, the metacentric height is below the required 1m. This means that the pontoon can become unstable by force fluctuations in the suspension cable.

The effect of the fluctuating force in suspension cables on the metacentric height in longitudinal/transversal directions, distance BM and the draught of the pontoons is given in Figure 48 . From the figure, it can be seen that with increasing force the metacentric height of the pontoon decreases it becomes even negative. Which means that the pontoon is unstable and will be capsized. From the figure, it may also be concluded, that for a force fluctuation of 50 [ton] the draught of the pontoons of 7[m] will be exceeded. This means that the pontoon will not have the ability to restore its position and may capsize or submerged by force fluctuations. The stability in the roll direction is not a problem. As we can see from Figure 48 the metacentric height in the roll direction is sufficient for the given force fluctuation.

The dimensions of the structural elements play an important role for the determining of the static stability. That's why the chosen dimensions are altered with the aim to improve the static stability and floating capacity. As mentioned before the stability in the pitch direction is sensitive for the fluctuating cable forces. That's why the columns are placed in the corners on the floaters see also Figure 49. In order to add extra floating capacity the dimensions of the floaters are changed. The new dimensions of the pontoons are:

Dimension	Value	Units
With pontoon B_p	54	m
Length pontoon L_p	40	m
Height pontoon h_p	10.5	m
With floater B_f	5	m
Length floater L_f	40	m
Height floater h_f	4	m
With pontoon deck B_D	54	m
Length pontoon deck L_D	40	m
Height pontoon deck h_d	1	m
Columns	(L·B·H) → (5 x 5 x 5.5)	m^3

Table 15 Overall dimensions of the Semi-submersible pontoon (altered)

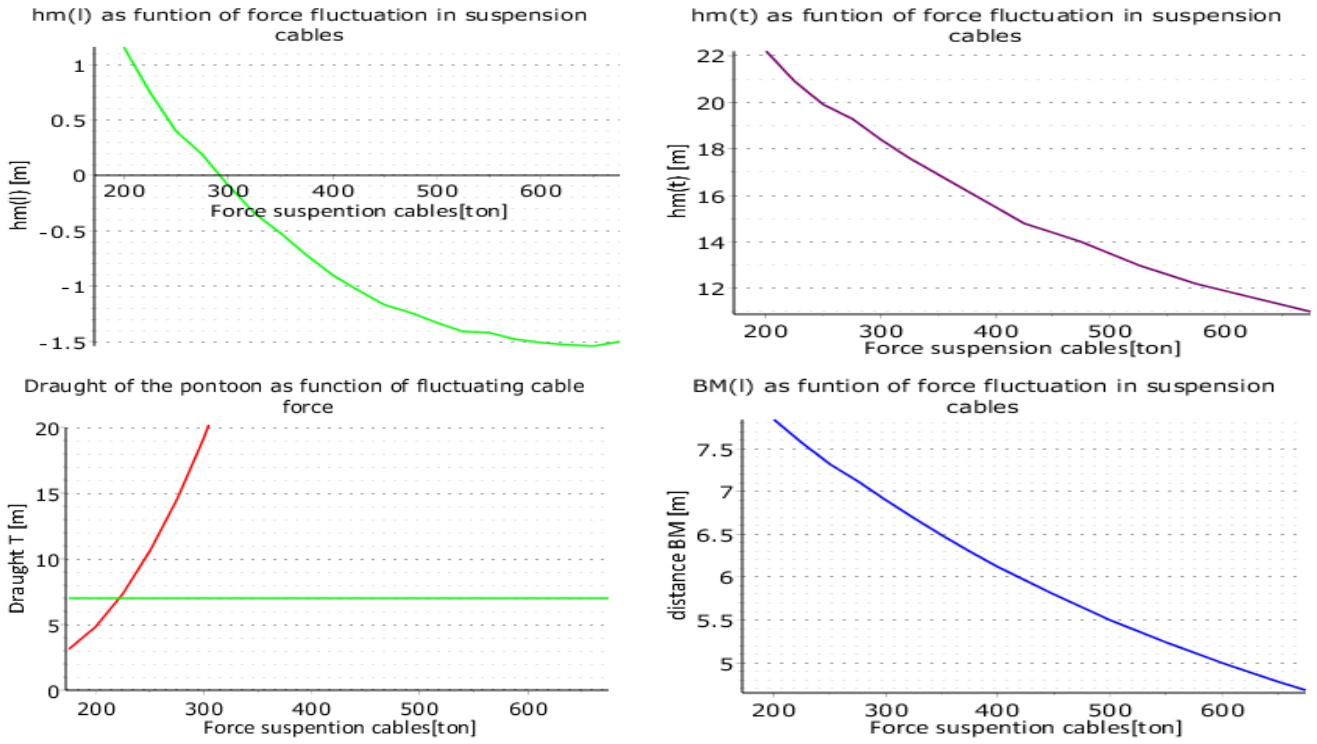

Figure 48 Effect of fluctuating cable force on static stability (Semisubmersible type pontoon)

By altering the dimensions the static stability and the floating capacity of the pontoon are improved. For the calculations the same procedure as described earlier has been followed. To analyze the behavior of the pontoon during different forcing stages, a computer program in Maple software is written (see Appendix 7.1). The results from the recalculations are presented in Figure 50.

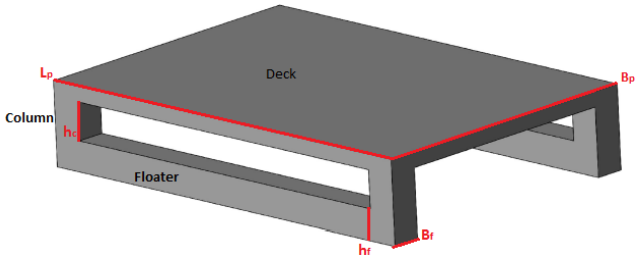

Figure 49 Altered pontoon layout

During the immersion of the tunnel element, the floaters will be fully submerged. In order to have enough floating capacity, the dimension of the columns and the floaters have been increased. In order to remain, the advantage of the Semisubmersible pontoon is the height of the floaters kept the same namely 4m. It appears that the pontoon can handle force fluctuation in the order of 160 ton. By exceeding this value, there is a danger of not having enough freeboard during the operation. In extreme cases, the pontoon can also be drawn by higher fluctuations. In the dynamic analysis of the pontoons, the forces in the cables will be determined. But for now, it is assumed that a maximal force fluctuation of 160 is acceptable.

Due to increased waterplane area of the columns, the wave forces acting on the pontoon during the immersion will also be higher. The dynamic wave force is recalculated, and the required amount of ballast is for the altered pontoons dimensions 480 [ton]. The new suspension cable force becomes 240 [ton]. It should be noted that in this report it is assumed that TE will hang on 2 or 4 suspension cables. But in reality instead of 1 wire also more cables could be used. The overall area of the cable will not change. And even the cable stiffness will remain the same.

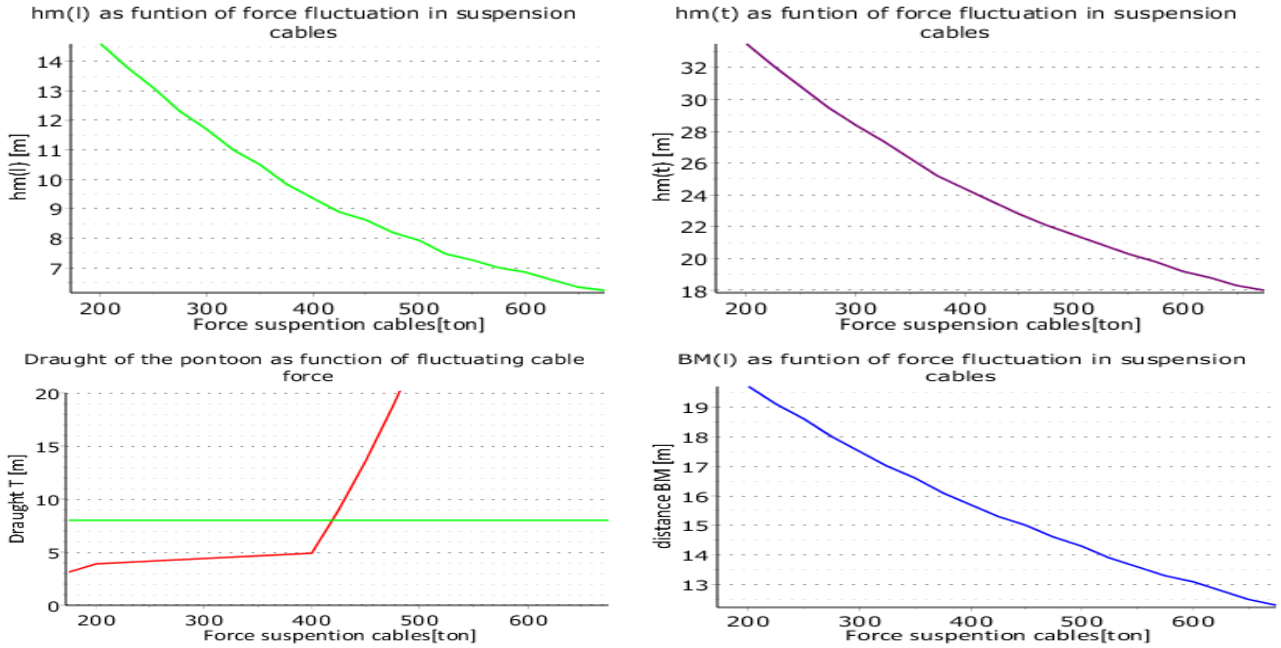

Figure 50 Static stability Semisubmersible pontoon

4.7 LIMITING CONDITIONS

The limiting conditions are determined by the loading regime and the functional requirements. If these conditions are exceeded, then the tunnel element cannot be immersed safely. For the analysis, only the floating conditions for the three structures (tunnel element and two floating pontoons) are considered. The physical parameters such as wave load and current load which govern the response of each of the three floating structure have a wide range of values. Choices should be made concerning the acceptable conditions, and economically optimization.

For the workability analysis, some limiting conditions are determined for both pontoon types. The limiting conditions are subdivided into two categories. Type 1 is the operational conditions if they are exceeded then the system cannot operate properly, and the operation should be interrupted. These kinds of limiting conditions are linked to safety and operability of the personnel and equipment on the pontoons. Type 2 operational conditions are linked to the failure of the system. If these type conditions are exceeded, then the operation will be failed. These types of conditions are related to the structural capacity of the components. In this part of the report, only the results are presented. The elaborated calculations are given in Appendix 1.6.

Limit states

Limit states are conditions which appear before the failure mechanism. For the floating system (the pontoons and the tunnel element) two limit states are distinguished.

- Ultimate limit state (ULS)
- Serviceability limit state (SLS)

4.7.1 SERVICEABILITY LIMIT STATE (SLS):

The Serviceability limit states are the boundary conditions relating to the functioning of the structure or parts thereof under normal use. The serviceability limit in the modeled case here is described as the disruption of the immersion process. As mentioned before the exceedance of this kind of restrictions will result in an interruption in the immersion process. The SLS conditions are linked in this report to the motional characteristics of the system.

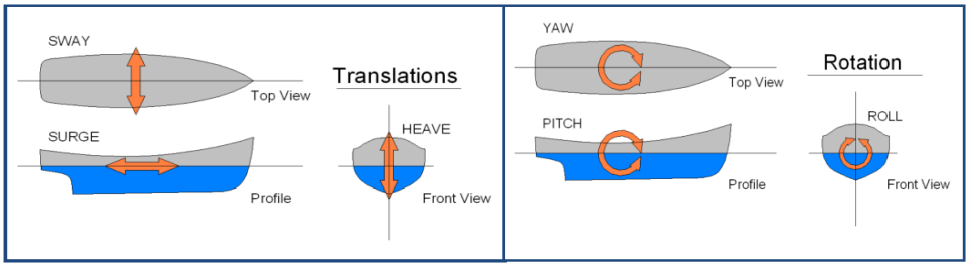

Figure 51 six degrees of freedom of a floating structure

For the SLS the limiting conditions are defined such if one of the motional amplitudes is exceeded the maximum allowable value, then the immersion operation has to be interrupted. When it is clear from the analysis that in given environmental condition the exceedance is likely to occur then those conditions will be classified as not working conditions.

In the SLS velocities and accelerations of tunnel element and pontoons are essential parameters. In the SLS the comfort for the personnel and the operability of the system is considered to be determinative. For the comfort of the staff and functioning of the electrical devices on the pontoon, some general operability limiting criteria for ships has been used to check the conditions in SLS. The requirements are copied from [J.M.J. Journée and W.W. Massie; OFFSHORE HYDRODYNAMICS; January 2001]. The values are given in….. This limits can be applied as motional constraints in the workability analysis of the pontoons.

	Motion/acceleration
Maximum roll angle	3°
Maximum pitch angle	3°
Surge (acceleration/velocity)	0.05g
Sway (acceleration/velocity)	0.05g
Heave (acceleration/velocity)	0.10g

Table 16 Limiting conditions in SLS for the pontoons

4.7.2 ULTIMATE LIMIT STATE (ULS):

In general, the boundary conditions in ULS are related to the safety of persons and the safety of the structure. In this analysis, only the structural safety is considered. When the ULS conditions are exceeded, it indicates that the immersion operation will be failed. The result of this kind of exceedance is much more dangerous than exceedance of the SLS limit conditions.

The exceedance of this type of boundary conditions indicates that the tunnel system or a component will undertake severe damage. The ULS conditions for this case study are translated to the following:

- The floating capacity of one of the pontoons will be less than required. This will lead that the pontoon will sink.
- The pontoon will be capsized during the immersion (statically not stable)
- The suspension cables will be slackening due to the dynamic wave force (zero force in one of the suspension cables).
- Allowable line tensions will be exceeded (suspension cables, mooring lines, and contraction cables)
- The force in the wires will be more than the capacity of the winch, which will lead to the failure of the winch.
- The motions and the related velocities of the tunnel element will exceed the allowable values which will cause that the guide beam/catch will be damaged. Or the tunnel element will clash to the already installed tunnel element.

The floating capacity, static stability, and minimum required cable tension has already been determined for both type pontoons considered in this study. In this section of the report, the structural capacity of the components is discussed. For the analysis purposes, it is also assumed that the capacity of the winches should be at least equal to the maximum cable force.

The total operability of the immersion process is based on the limited motion and the capacity of the system and the duration of the immersion process. Regardless the pontoon configuration the limits are applied for both pontoon types. If in specific environmental conditions the limiting motions are exceeded, then the immersion process has to be interrupted. In practice, it means, before the immersion process is initiated the hydraulic conditions have to be checked. If the limiting conditions are expected to exceed then no immersion will take place in those conditions.
To determine the workability and to compare it for the two pontoons, structural limiting conditions will be determined for the analysis purposes. First, the maximum allowable forces in the cables are determined (see Appendix 1.6). Subsequently, the allowable forces are translated to the maximum allowable transversal motions and rotations of the pontoons. Off course for the detailed design more parameters has to be determined. But for this analysis, the required parameters are sufficient to perform the dynamic analysis and check the workability. The main dynamical characteristics of the system and the dynamic analysis will be described in the next part of the report. The focus of this part is to determine the maximum allowable motions of the system for the chosen structural dimensions. The workability of the system is analyzed in beam waves. Therefore the main motion of the system will occur in three degrees of freedom, namely:

- Sway
- Heave
- Roll

For the derivation of maximal elongation is the same principle has been used as for derivation of the stiffness matrix. The maximum elongation of a cable is given in Table 18 (Appendix 1.6). The maximum force fluctuation in a cable due to motion in ith direction can be expressed as:

$$dT_i = \frac{EA \cdot \Delta l_i}{l} \tag{62}$$

Where dT_i represents the force fluctuation in the cable and *l* is the length of the cable. By substituting the values from Table 18 (Appendix 1.6) in the above-mentioned equation, the maximum force in elastic deformation region can be determined for each cable.
The maximum forces can be translated to the maximum displacements and rotations by the force and displacement relationship. In the dynamic analysis, the effect of the mooring lines and contraction wires is not taken into account. That is why only the maximal allowable forces in the suspension cables are translated into the maximal motions of the pontoons. For the determination of the maximum displacement, the relations are used for the motions in sway and roll (see also Figure 102 and Figure 104). For heave, the maximum displacement is equal to the maximum elongation of the suspension cable (see also Figure 103).

$$dT_2 = \left(\sqrt{x_2^2 + l^2} - l\right) * \frac{AE}{l} \tag{63}$$

$$dT_4 = \frac{AE}{l} \cdot \left(\frac{B_p}{2} - B_f - tolerance - \frac{W_1}{2}\right) \cdot \cos(\varphi) \cdot \varphi \tag{64}$$

Where

dT_2	Force Fluctuation in each cable due to sway motion
x_2	Displacement in sway degree of freedom
l	Length of the suspension cable
AE	Axial stiffness of the cable
B_p	Width of the pontoon
B_f	Width of the floater
$tolerance$	Transversal distance between the pontoon and the tunnel element(=2m)
W_1	Wall thickness of the tunnel element of the outer wall
φ	Rotation in Roll degree of freedom.

The maximal motion of the system are given in Table 19 (Appendix 1.6) for the ULS for two or four suspensions cabled system. The SLS conditions are not considered further because these conditions are meant to limit strains such that the corrosions control measures, cracking of the sheaths, and hard fillers are not damaged.

Due to temporary character of the immersion operation, it is most probable that these conditions are not restrictive for the immersion operation. The subscript 2,3,4 in the results indicated the motions in sway, heave and roll degrees of freedom. The subscripts C and S indicate the Catamaran and Semi-Submersible pontoons.

Limit Motions	Value when 2 suspension cable are applied		Valued when 4 suspension cables are applied	
Catamaran pontoon				
$x_{2\text{-}C}$	0.8771	[m]	0.7693	[m]
$x_{3\text{-}C}$	0.06377	[m]	0.0638	[m]
$x_{4\text{-}C}$	0.003149	[rad]	0.003149	[rad]
Semi-submersible pontoon				
$x_{2\text{-}S}$	1.3516	[m]	1.1695	[m]
$x_{3\text{-}S}$	0.08503	[m]	0.08503	[m]
$x_{4\text{-}S}$	0.00556	[rad]	0.00420	[rad]

Table 17 Limit motions pontoons for the ULS

4.7.3 CONCLUSION

In this chapter, the general model setup is discussed. Subsequently, it is being explained how the main dimensions of the pontoons were calculated, and the values have been presented.

To ensure that the system or components of it are stable and will not capsize, the static stability is analyzed. From the calculations, it can be concluded that the floating element is stable enough during the transport, even with a very small freeboard of 0.2 [m].There is little chance for the floating tunnel element that it will capsize. On the other hand during immersion, when TE will be entirely submerged it will lose its stability. The overturning stability should be provided by the pontoons. Also, it can also be concluded that the empty pontoons are stable concerning the overturning stability. This means that when the barge is loaded asymmetric, then there is enough capacity in the pontoon to produce a proper righting moment and not to capsize.

But during the immersion operation, the Semi-submersible pontoon becomes unstable, and it can capsize. It appears that the static stability of the pontoons in the pitch direction is sensitive to the force fluctuations. With increasing force, the metacentric height of the pontoon decreases it becomes even negative. Also, the floating capacity of the pontoon was insufficient to handle force fluctuations.

The dimensions of the structural elements play an essential role in the determination of the static stability. That's why the chosen dimensions are altered with the aim to improve the static stability and floating capacity. The columns are placed in the corners on the floaters to increase the longitudinal moments of inertia. To add extra floating capacity the dimensions of the floaters were enlarged. By altering the dimensions the static stability and the floating ability of the pontoon are improved. It appears that the barge can handle force fluctuation in the order of 160 ton. By exceeding this value, there is a danger of not having enough freeboard during the operation. In extreme cases, the pontoon can also be drawn by higher fluctuations. Overall it can be concluded that the Semi-submersible barge is more sensitive to the force fluctuation in the suspension cables than the Catamaran pontoon concerning the static stability and floating capacity.

Finally, the limiting conditions were determined for the calculated pontoon dimensions. Before doing that the capacity of the mooring system (which consist form mooring lines, contraction cables) and suspension cables were determined. The capacity of the mooring lines was translated to the maximum allowable motions of the pontoons. From the calculations, it can be concluded that the Semi-submersible barge has slightly larger motional limits compared to the Catamaran pontoon.

5 TRANSPORT

5.1 INTRODUCTION

During the construction stage different loads works on the tunnel element. The main two type hydraulic external forces working on the tunnel element during the transportation are current and wave forces. Here a quantitative overview will be given. Additionally, the hydrodynamic stability and the natural periods are discussed too. The boundary conditions are given in chapter 2 and Appendix 2. For the detail explanation of the boundary conditions, please see also (FEHY (Metocean Conditions), 2013).

This chapter aims to give a first estimate of the hydraulic forces and tunnel element motions during the transportation. The results of the calculations must also provide an insight into the circumstances in which the element becomes unstable.

From the results, it can be concluded what type of equipment is needed for the operation. And under which circumstances, the transport can take place. Also, the forces calculated here can be used as verification of the calculated forces by software. If the values differ a lot, it will mean two things.

- The nonlinear effects become important and they cannot be neglected.
- The model setup in the computer program is not proper enough to predict the behavior of the TE.

Due to nonlinearities, it is difficult to predict some aspects described here with high accuracy. That's why for a final design stage a scale model tests are preferred. The values presented here can be seen as a first estimate.

5.2 TRANSPORT OPERATION

Construction operation is outlined in Chapter 2. For completeness, here some steps are pointed out related to the transport of the tunnel element. In the current design it's been envisaged that the production site is to be located on the eastside of Lolland (Denmark). After casting and hardening of the concrete, the tunnel elements will be towed to the deeper part of the launching basin. After outfitting and preparing of the tunnel elements for the immersion the sliding gate will be opened. And the element will be towed to the tunnel trench, in order to be immersed ((CAPITA SYMONDS) and (FEHMARN BELT CONTRACTORS, 2013))

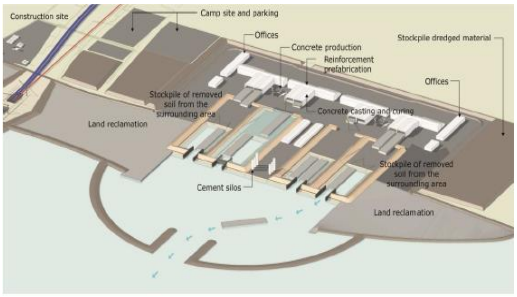

Figure 52 Schematic of tunnel production factory (Femern A/S, 2013)

The first towing operation will take inside the tunnel factory, when the tunnel element will be towed to the deeper part of the launching basin. This phase will not take limitation on the working conditions because the flow velocities inside the basin are negligible.

The second phase is the transport form the factory to the tunnel site. Although the factory is situated near the tunnel site, the voyage for the elements which has to be placed on the German side of the Fixed Link will be almost 20 [km] long (Femern A/S).

The third phase is the positioning of the element over the trench and lowering the element to its final position. It has to be considered when the tunnel element leaves the factory there are no escape locations where the tunnel element can be positioned till workable conditions occur. Because of the different character between the transportation and immersion operation, it can be considered to allow the transportation in some severe conditions, position the element over the trench, and then wait till workable conditions occur for the immersion.

The forces during the different transport stages are calculated here for different environmental conditions. That's why the presented calculation can be used for the selecting the proper workable conditions. And the results presented here can also be used for choosing proper auxiliary equipment. The choice of the auxiliary equipment is outside the scope of this analysis.

Towing Force

The towing force must counteract the wave forces and the resistance of the element. The wave force is discussed later on. The towing resistance can be considered as a semi-stationary condition. Wind force is neglected in the calculations because of small freeboard of the element. Dynamic forces in the towing cables are not considered here. Due to the motions of the tugboats, some dynamic components will be present. In the design of the bollards, this force has to be taken into account.

5.3 Flow Force on floating TE

The flow force on the floating element can be estimated as drag force. From the literature (A. Glerum, B.P. Ritger, W.D. Eysinik, W.F. Heins, 1967), it has been observed that the skin friction is less than 5% of the total towing force. Therefore the skin friction has not been taken into account. The horizontal drag force on the tunnel element can be estimated with the following formula. In the formula, the presented horizontal drag resistance is observed in a 2-D vertical plane.

$$F_d = C_D \cdot \frac{1}{2} \cdot \rho_w \cdot V_r^2 \cdot A_c \qquad (65)$$

During the transport, the tunnel elements will float and it will have a freeboard. As result of this freeboard, the deck of the element will be above water. Only the bottom of the element will be in contact with the flow. On the sharp edge upstream, the flow will release. For the calculations, it is assumed that the element will not undergo large movements. Due to this assumption, the flow pattern can be treated as stable. The two-dimensional flow pattern is given in Figure 22. In addition, a downward force will also work on the element as result of towing and flow velocities. This force can lead in a combination of a small freeboard and large current or towing velocities to stability problems.

The drag coefficient is derived from the presented data in literature (S.J. Callander and S.T. Schuurmans, 1991). The shape and size of the element determine the current flow around it. At the corners of the element, the streamlines will release. For the determination of the drag coefficient, width / height ratio is important. For each given ratio, the value of the drag coefficient can be read from Figure 53. The data are applicable to a fully submerged element. However, on top of a floating element water does not flow. Only the bottom of the element is in the flow. Thus, the streamlines release only at the bottom in the upstream corner of the element. In order to be able to use the data in Figure 53 here for the same approach as named in (S.J. Callander and S.T. Schuurmans, 1991) has been chosen. The element is considered as half of an element that is completely underwater. In this situation, the resistance coefficient is determined by the ratio width / (2 * height). See also figure Figure 54. In the calculations, the freeboard of 0,2m has been disregarded and the height of element H has been taken into account. Therefore, the thickness of the element in the flow is twice the height of the element.

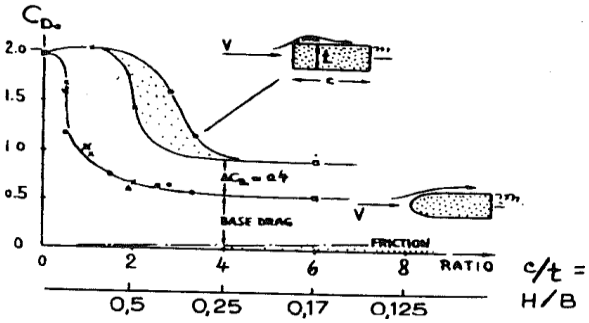

Figure 53 Drag coefficient (S.J. Callander and S.T. Schuurmans, 1991)

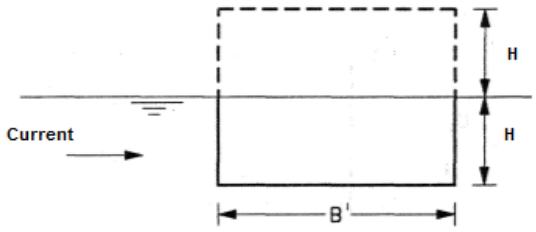

Figure 54 Principle of the drag coefficient derivation for a floating TE

Approximately at the value $B/H \approx 3$ the value of drag coefficient reduces. This can be related to the fact that boundary layer of the current attaches again to the tunnel element. This results that wake width will be reduced. At the downstream side the streamlines will release again. But the wake width and de drag coefficient will be reduced.

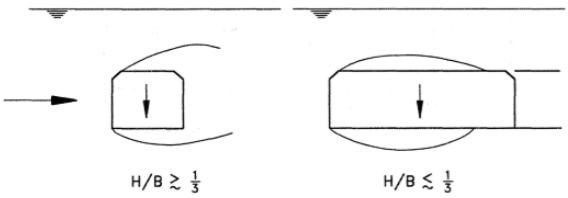

Figure 55 Reattachment of the wake (W.D. Eysink, maart 1981)

The width of the standard elements is 41.2m. A first guess is that during the transportation the reattachment doesn't occur. But during the immersion is the ratio B/H=4.6 and that the reattachment will most likely occur. This reattachment process results also in a vertical current force see also Figure 55. The vertical force is indicated in this report as Lift force and is denoted as F_L.

5.3.1 CORRECTION FACTOR FOR THE WIDTH

The drag coefficient presented in Figure 53 is valid for infinite long bodies. The tunnel element has a finite length. Therefore a correction factor has to be applied in order to get the C_d value for the finite length body. In the literature (S.J. Callander and S.T. Schuurmans, 1991) different values for the correction factors are. The values are presented in Table 18.

$\lambda = L/H$	Values from []	$\lambda = L/H$	Values from []
0-4	0.60	1	0.58
4-8	0.70	5	0.60
8-40	0.80	20	0.75
>40	1	∞	0.95

Table 18 Values of the correction factor

In this case study the ratios are:

$$\frac{L}{H} = \frac{217.8}{8.9} = 24.47 \quad \text{and} \quad \frac{L}{2*H} = \frac{217.8}{8.9} = 12.23$$

The correction factor is derived based on the presented values in Table 18. The values C_d are deduced from Figure 53 and are multiplied by the correction factors given in Table 19. The valued of the drag coefficient for the immersion and transportation stages are given here below.

	λ	C_d
Immersion	0.76	0.95
Transportation	0.69	1.6

Table 19 Values of Correction factor and drag force

5.3.2 INFLUENCE OF THE REYNOLDS NUMBER

The given drag coefficients are all valid for lower Reynolds number ($R_e = \frac{V \cdot L}{v}$). With characteristic length of 41.2 m and V= 2 m/s, we get an Reynolds number for TE during transport of $8.24 \cdot 10^7$ and $4.12 \cdot 10^7$ for a current velocity of 1 m/s. All the figures presented in this report are valid for lower Reynolds number. The main assumption here is that the drag coefficient will reach some limit and will be less dependent on Reynolds number change. The same conclusion could be made from the literature observation. In Figure 56 we can see that the drag coefficients stabilizes for higher Reynolds number.

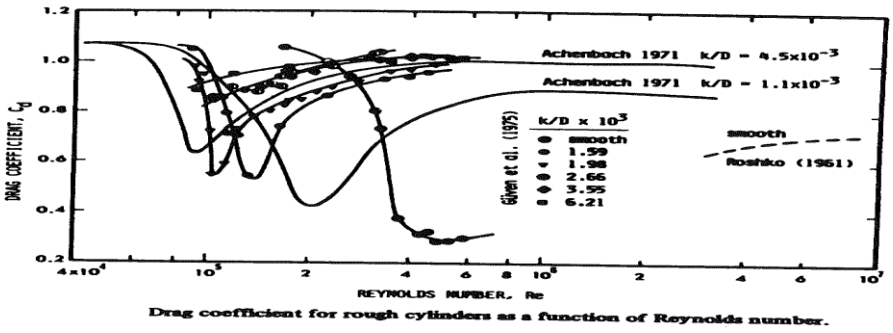

Figure 56 Cd coefficient for high Reynolds number (S.J. Callander and S.T. Schuurmans, 1991)

5.3.3 Reference Velocity

A reference velocity V_R has been defined as 1 [m/s]. In the following sections, all forces will be related to this velocity. In order to deduce the forces and moments for different position in space and time the calculated forces and moments will be multiplied by an adjusted velocity V_c^2 to get the applicable values.

5.3.4 Area A_C perpendicular to the current

The area perpendicular to the flow is dependent on the flow angle α. The flow on the surface in Fehmarnbelt is most of the time outgoing from the Baltic Sea into the North Sea. At the bottom of the water way the flow is in going from the North Sea to the Baltic Sea. Figure 57 and Figure 58 indicate the ingoing and outgoing flow in the region, graphically. The red line in the figures, indicate the Fixed Link project alignment.

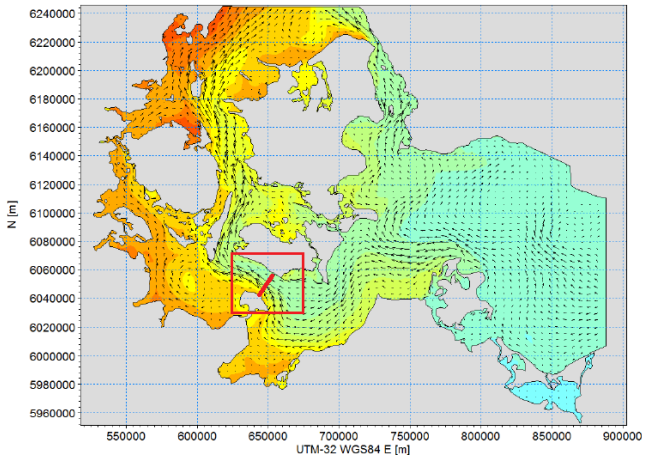

Figure 57 Outgoing flow from Baltic Sea (FEHY (Metocean Conditions), 2013)

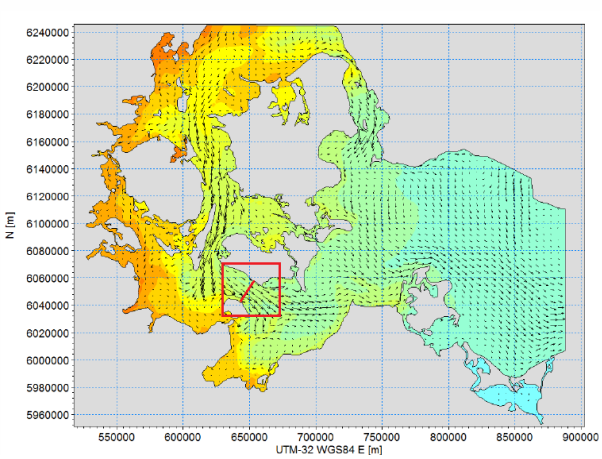

Figure 58 Ingoing flow from the North Sea (FEHY (Metocean Conditions), 2013)

Further information on the current directions and the velocity in the project area are given in Appendix 2 and FEHY (2013). Fehmarnbelt Fixed Link. Metocean Conditions. In the Figure 59 a sketch of a tunnel element during transport is given. As the figure it shows the element will have an angle with the current direction. The oblique current incidence will result in changing area perpendicular to the flow. The area perpendicular in the flow is sketched in Figure 60.

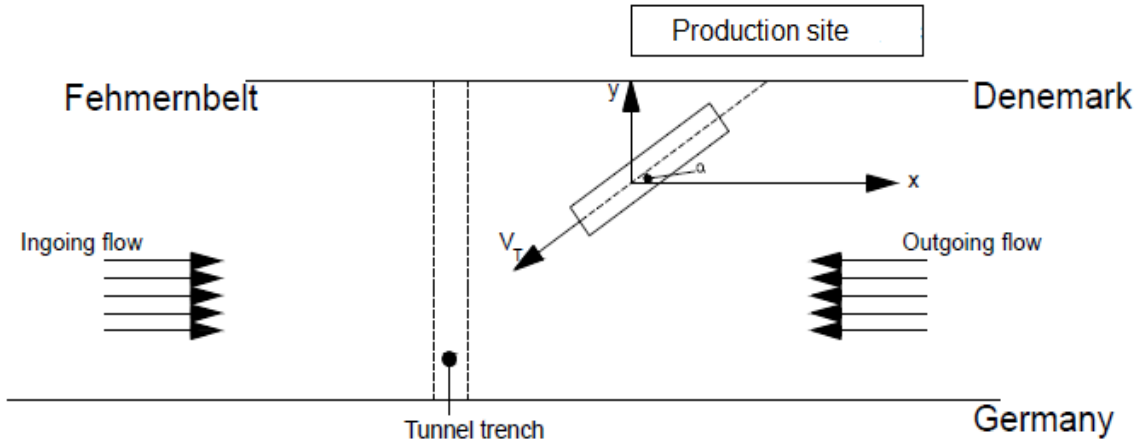

Figure 59 Schematization of the tunnel element during the transport

The total area perpendicular to the flow direction can be given by the following equation (see also Figure 60):

$$A = (L \cdot \sin\alpha - B\cos a) \cdot \mathrm{H} \qquad (66)$$

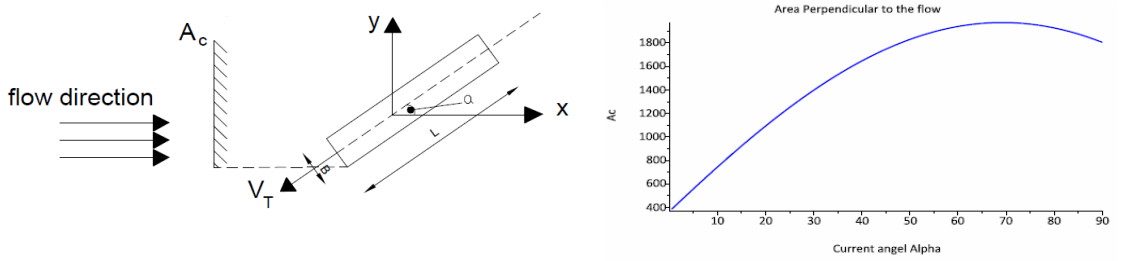

Figure 60 Area perpendicular to the current direction

For the given tunnel element dimensions the maximum and minimum values of the area are:

- Maximum area in the flow A_c=1965 m^2 (by an $\alpha = 79°$)
- Smallest area in the flow A_C=B · H = 367 (by an $\alpha = 0°$)

As mentioned before the freeboard has been disregarded in calculations. In Figure 60 the area perpendicular to the flow has been depicted as function of α.

5.3.5 WIDTH PERPENDICULAR TO THE CURRENT

When the elements are not towed perpendicular to the flow, the width B is also variable and it is denoted in this report as effective width(B_{eff}). The effective width is dependent on the flow direction. Two situations can be distinguished for the effective width (width perpendicular to the flow).

Situation 1: when the current angle $0 < \alpha \leq \arctan\left(\frac{B}{L}\right)$

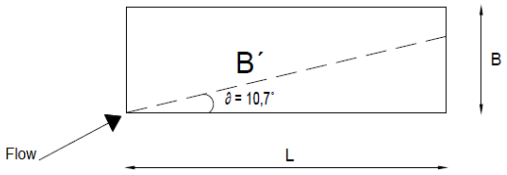

$$B_{eff} = \frac{L}{\cos(\alpha)} \qquad (67)$$

Situation 2: when the current angle $\arctan\left(\frac{B}{L}\right) < \alpha < 90°$

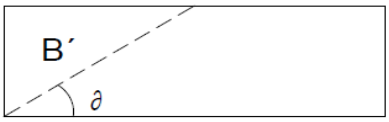

$$B' = \frac{B}{\sin(\alpha)} \qquad (68)$$

Figure 61 Effective width

In this way the minimum and the maximum values for B_{eff} can be determined. The maximum and the minimum values of B_{eff} are:

$$B_{eff(min)} = B \quad \text{When } \alpha = 90° \qquad (69)$$

$$B_{eff(max)} \quad \frac{L}{\cos 10,7} \quad \text{when } \alpha = 10,7 \qquad (70)$$

$$B'_{(min)} = 41,2 \text{ m}$$

$$B'_{(max)} = 221 \text{ m}$$

In Figure 62 the values of B_{eff} are plotted as a function of the current angle α.

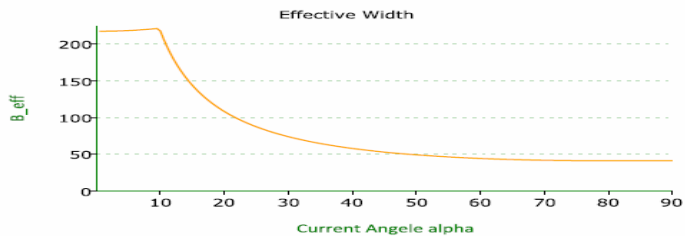

Figure 62 Effective width

Based on the above-mentioned information the values of ratios which are needed for the determination of the drag coefficient and the related parameters are recalculated.

For the two building phases, namely transport and immersion not just single values of the drag coefficient are valid but a range of values. Therefore, it is more convenient to present the limit values of the drag coefficient.

Construction phase	Drag coefficient Cd	
	Min	Max
Transport	0.95	1.6
Immersion	0.95	0.95

Table 20 Values of the drag coefficient

From the results of Figure 62 it can be concluded that, the effective width is variable and it is dependent on the current angle. As mentioned before the drag coefficient Cd is dependent on the height/width ratio of the tunnel element. That's why the ratio's for different current angels has been calculated for the immersion and transportation phase. The results are presented in Figure 63.

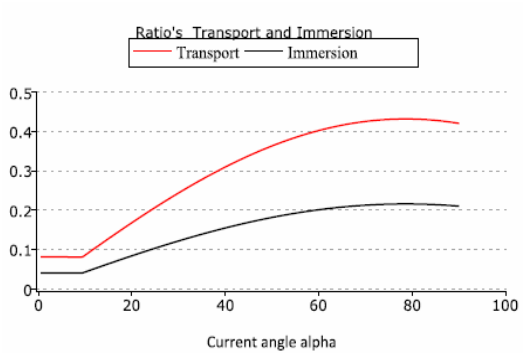

Figure 63 H/Beff ratio during transport and immersion

Based on the results from Figure 63 the data presented in Figure 53 are translated to the situations valid for the project area. In addition, for the relevant ratio's the drag coefficient has been determined. The drag coefficient for the project relevant ratio's is given in Figure 64.

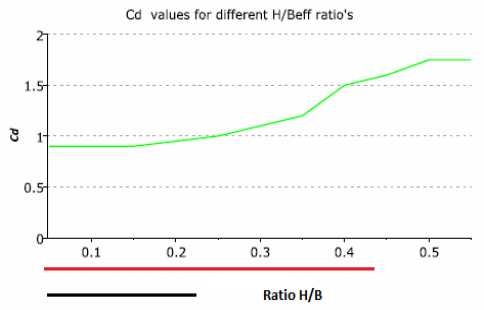

Figure 64 Drag Coefficient as function of H/B

The values presented in Figure 64 will be used for the calculations of the horizontal drag force on the tunnel element. The values till a ratio 0.21 are valid for determining the drag coefficient for the immersion phase and the values till ratio 0.43 are valid for the transportation phase. In analogy with Figure 63 the range of the ratios is been given in the figure with red and black line. It has to be noted that the values presented in Figure 64 are indicative. The site boundary conditions are determinative for the determining of the drag coefficient.

For accurate results the values of the Cd has to be determined in a scale model where the site boundary conditions can be taken into account. In order to take different uncertainties into account a load factor will be applied in the calculations. The load factors are determined in Appendix 3. The values presented in Figure 64 are transformed such that for each current direction the drag coefficient can be determined. Also a correction factor of the finite length has been applied in the calculations. The results are given in Figure 65.

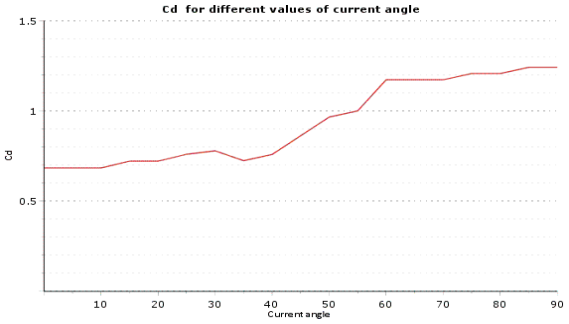

Figure 65 Drag coefficient for different current angles

5.3.6 BLOCKAGE FACTOR ß

The surrounding environment has a significant influence on the flow force on the element. The following surroundings elements have important influence on the drag force:

- shores
- bottom
- another tunnel elements
- vessels and the other objects in the surroundings of the element

The influence of the environment can be represented with the aid of the blockage factor ß. The factor ß is a ratio of the area of the element and the total flow area, which in formula form can be expressed as:

$$\beta = \frac{A_C}{A_{total}} = \frac{A_{total} - A_1}{A_{total}} \quad (71)$$

$$A_1 = A_{total} - A_c \quad (72)$$

where	
β	Blockage factor
A_C	Area TE perpendicular to the flow direction
A_{total}	Undisturbed flow area
A_1	Flow area at the location of TE

When ß (almost) equal to zero, then there is an infinitely large space around the element. Then for the drag coefficient (Cd) the values for unlimited water can be used. With increasing ß values, the influence of the blockage will be larger on the drag force. In addition, the tunnel element will experience more acceleration and deceleration in the surroundings with increasing drag force. For the Westerschelde tunnel project (see also (S.J. Callander and S.T. Schuurmans, 1991), (W.D. Eysink, H.R. Luth, J.H. de Vroeg en H.J. van Wijhe, 1995) and (H.W.R. Perdijk en A. Vrijburcht, 1990)) the following relation has been derived between the drag force in unlimited water and drag force in limited water where the blockage of the waterway do play a role.

$$\frac{F_d^*}{F_d} = 1 + \left(\frac{\beta}{1-\beta}\right)^2 \cdot \frac{1}{C_D} \quad (73)$$

Were	
F_d^*	Drag force included the effect of blakage factor
F_d	Drag force in unlimited water
C_D	Drag coefficient

From Research at Westerschelde tunnel it follows that the ß factor has very limited influence on the drag force (0.03 <ß <0.07). It follows that the ratio (F_d^*/F_d), in that case is almost equal to one. In the case of Fehmarnbelt the cross-sectional area for water to flow is even greater than in the Westerschelde (Netherlands). Therefore, it is believed that the blocking effect may be neglected for the large part of the transport route. However, for shallow parts (0-5 m and 5-10 m) the waterway has to be dragged, in order to transport the tunnel element. In the shallow parts the effect of blockage has been taken into account in the calculations of the drag force.

5.4 Drag Force

First the drag force is been calculated as a function of current angel for a flow velocity of 1 m/s. The drag force at different positions can be deduced from Figure 66, if the angle of the tunnel with the current flow is known. The drag force as a function of the current angel is presented in Figure 66.

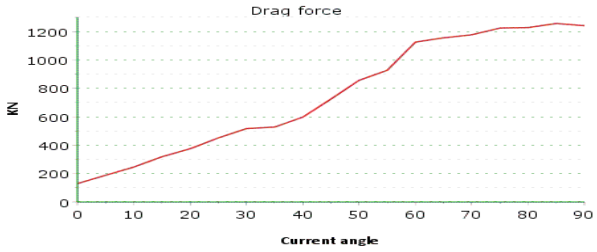

Figure 66 Drag force as a function of the current angle for a current velocity of 1[m/s]

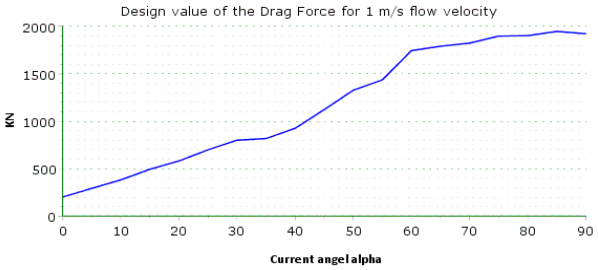

Figure 67 Design value of the drag force

As there are a lot of uncertainties about the chosen values for the drag coefficient, a load factor has been applied to the calculated values. The load factors has been calculated in Appendix 3 The value for the load factor has been chosen to be 1.55. The recalculated drag force is given in Figure 67.

5.4.1 Drag force in y direction

From studies for previous immersed tunnel projects it been obvious when the tunnel element and the current has an angle α there is also a horizontal force in the y direction (a kind of transversal force in the y-direction). There is lack of data to estimate this force. In order to be able to estimate this transversal force in the y-direction data conducted in the previous tunnel project studies (W.D. Eysink, maart 1981) has been used for determination of the coefficient C_{dy}. The idea of this force is been sketched in Figure 68

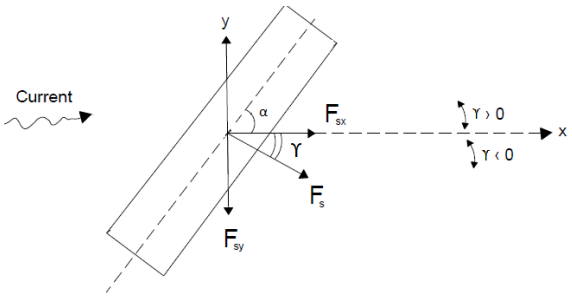

Figure 68 Transversal force in the y-direction

In analogy with Fehmarnbelt Westerschelde is also a waterway with deep and wide cross section. The motivation for the reuse of the data is, the acquired force coefficients are dimensionless. Theoretically it can be stated that they are also independent from the dimensions of the tunnel element. For the calculations the curve with the most measurement res (H.W.R. Perdijk en A. Vrijburcht, 1990)ults in that study was used.

Figure 69 has been used to calculate the values of the force in the y-direction. The results are presented in Figure 70. For the calculation is the same equation as for the drag force in the x-direction has been applied. The only difference is now that the value of $C_{d(y)}$ are taken into account instead of C_d. It has to be noted when the flow is ingoing (from the North Sea to the Baltic Sea) the angle ϒ between the Fx and Fy is negative and when the flow is outgoing (other way around) the angle ϒ will be positive.

In analogy with drag force in the x-direction also the design value of Fy has been calculated by applying a load factor of 1.55. The recalculated values of Fy are given in Figure 71. Having the values of Fx and Fy also the values of the angel ϒ between the two horizontal forces and the resultant force can be determined. The calculated values of the angel ϒ and the resultant force FR are given in Figure 72, Figure 73 and Figure 74. The current angle ϒ is valid for the outgoing flow. For the ingoing flow is the figure exact symmetric about the x-axis.

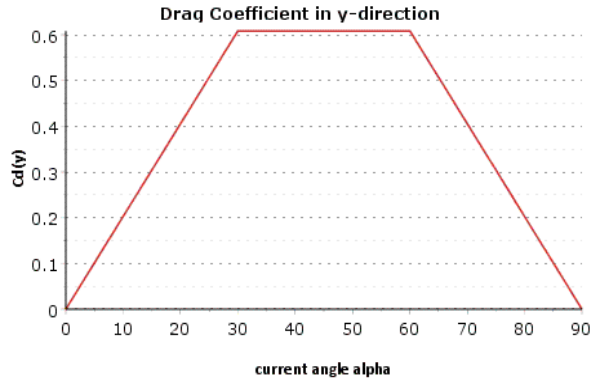

Figure 69 Drag Coefficient Cd(y) from[literatuur benomen]

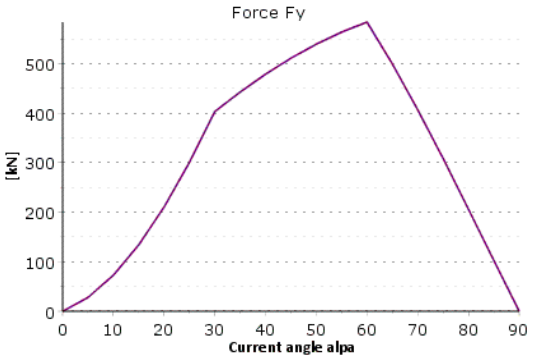

Figure 70 Force Fy as a function of the current angle alpha

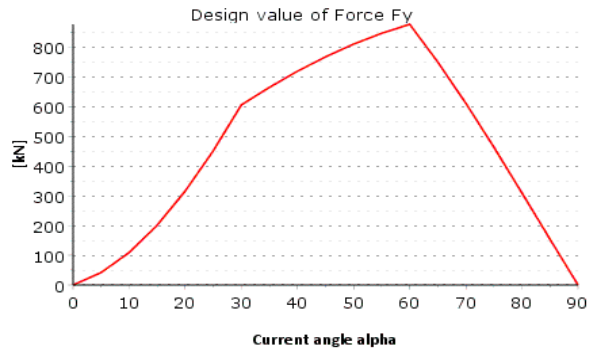

Figure 71 Design values of Force Fy as a function of the current angle alpha

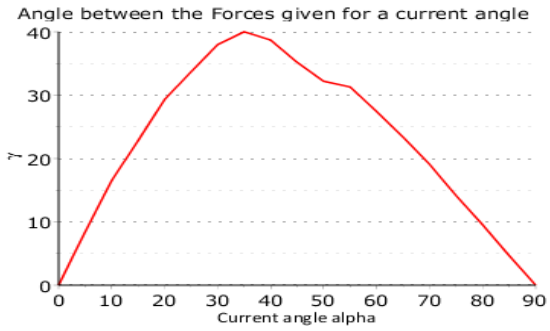

Figure 72 Current angle ϒ between the forces Fx and Fy

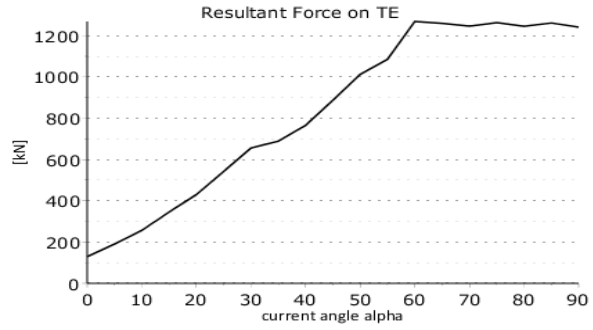

Figure 73 Resultant force FR for 1 m/s flow velocity

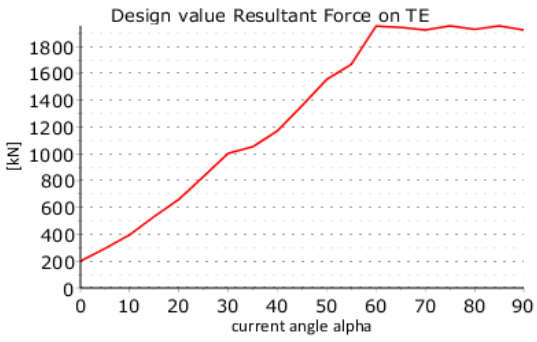

Figure 74 Design value Resultant force FR for 1 m/s flow velocity

5.4.2 MOMENT ABOUT THE Z-AXIS

The torque moment is calculated with the aid of data from laboratory tests for Westerschelde tunnel project. (See also (W.D. Eysink, maart 1981). This moment will work on the tunnel element about the z-axis. Without the model tests, this moment is difficult to calculate. Therefore, the data for the dimensionless arm are reused form the literature mentioned above. The motivation for the reuse of the data is given in the previous section. (It has to be said that the presented values should be used with caution. These values are only indicative) For the calculations, the dimensionless moment coefficient from Figure 75 is multiplied by the resultant drag force in Figure 74. The calculated values of the moment are presented in Figure 76 for the different current angles. Form the results it can be concluded that during transport a significant moment will act on the element. During the immersion for a current angle of 90°, this moment disappears.

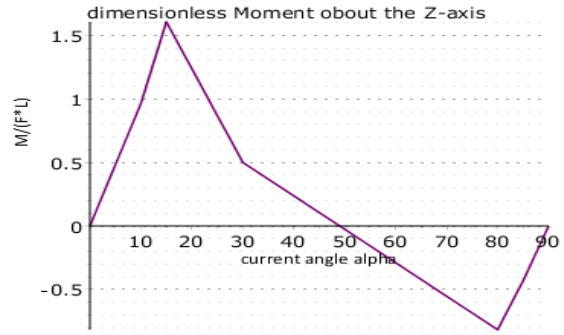

Figure 75 Dimensionless moment about z-axis (W.D. Eysink, maart 1981)

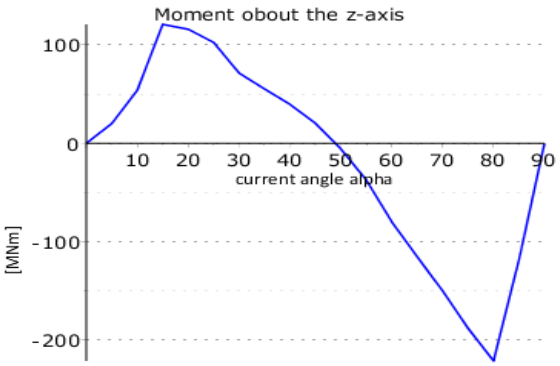

Figure 76 Moment about z-axis (design values)

5.5 FORCES DURING THE TOWING OPERATION ON FLOATING TE

Now the above estimated overall values of forces will be applied to the construction of the Fehmarnbelt tunnel. The values must be translated into specific condition of the tunnel element in the fairway. In order to do this it is necessary to do some assumptions of the course of the transport of the tunnel element. The assumptions are listed here below.

1. It is assumed that all the standard elements will be built in the factory on the Danish side. This means that also the tunnel elements must be towed to the German side of the Fehmarnbelt. The journey of a tunnel element will be then almost 20 [km].
2. During the transport all shipping activities in the navigation channel is kept at a safe distance. So the transport of the element does not suffer from the shipping activities. This means that also water level drop due to sailing ship may be neglected (not considered in calculations).
3. When leaving the factory the tunnel element will have an angle of 40 degrees with the current direction.
4. Arriving at the immersion site, the tunnel element will be maneuvered in such a way that it makes an angle of 90 degrees with the flow direction. During the maneuvering, the angle of the element will be adjusted smoothly from 40 to 90 degrees.
5. It is assumed that there is sufficient water depth to transport the tunnel element.
6. The blockage of the waterway by the tunnel element does not play a role in determining of the forces (this is valid for the transport in deeper parts)
7. For the calculations, the average depth of 30 m has been taken into account.

For the analysis of the current forces, the environmental condition have to be taken into account. The environmental boundary conditions are listed in Appendix A and more in detail described in [Metocean conditions]. In this part of the report is only a brief notation is given for motivating the choices which has to be made.

Bathymetry

The water depth is variable across the Fehmarnbelt, the bathymetry of the fairway has greater gradient on the German side and it is less steep on the Danish side. From Figure 7 it can be concluded that the waterway is less deep nearby the coasts. Because of the insufficient depth of the fairway it is more likely that there a trench will be dredged from the factory till a distance where sufficient depth will be available for the transportation of the element. That's why in the calculation of the forces in this part in the fairway a blockage factor ß=0.25 has been applied in order to bring the effect of the extra force into account due to blockage

Current velocities

For the project area there are model values and 18 years data measurements are available concerning the current velocities. As mentioned in Appendix 2, Fehmarnbelt is a transitional area between the North Sea and Baltic Sea. The water column is stratified associated with different flow velocity and direction over de water column. The surface flow is predominantly outgoing and the near bed current is ingoing. The current data include parameters of current speed and direction for the combined tidal and surge signal. The modeled current velocity values may be interpreted as representative of approximately 3-hourly averages. The current direction can be considered with an angle of 45-270° relative to the north.

Stronger flow velocities in the winter and fall and weaker flow velocities characterize the seasonal variation of the current in the summer for all depths. In the center of the waterway at the point P2 (see Figure 7) the flow velocities are the strongest. The distribution of the flow velocities for the 18 years modeled data is shown in Figure 8 and Figure 9.For the calculations, an exceedance probability of 5% has been chosen. The values of 1.1 [m/s] and 0.25 [m/s] will be used in the calculations. The values of current velocities at the locations P1 and P3 are deduced as percentage of the flow velocity at location P2. The flow velocity at P1 near the Danish cost is assumed 70% of the flow velocity at P2 and at P3 near the German cost 75%.

During the transport and fitting out at the tunnel site, seven different positions have been distinguished namely:

1. Sailing out from the construction factory in shallow water
2. Towing the tunnel element to the tunnel site trough deep water.
3. Arriving at the tunnel site/tunnel trench, the tunnel element having an angle with the current of 40°. And then fitting the element over the trench and each position is chosen as an interval 10° from 40 till 90°.

Conclusion

The results are presented in Table 21, Figure 77 and Figure 78 . It appears that the greatest force on the element works during the fitting out of the element, during stage 4 after arriving at the tunnel site. At this stage the element makes an angle of 50° with the flow direction. Also the current forces in stages 5,6 and 7 stays quite large. So it can be concluded that when the tunnel element makes a greater angle than 40° the force will grow with a factor 1.65 and then staying quite stable. The largest moment of force, occur when the tunnel element makes an angle of 80° and then disappearing when the element will be positioned perpendicular to the flow direction. It means that during the positioning operation of the element one should be aware of this force moment and take it into account by choosing the proper positioning equipment. Also during the transport phase there will be a force moment about the z-axis.

But the magnitude will be much lesser. It has to be mentioned that the presented results can only be used as indicative. There is great amount of uncertainties in the presented values. Especially the presented results for the Moment are the most uncertain.

Due to lack of data and information in the literature, the data presented in study for the Westerschelde tunnel project scale model (W.D. Eysink, maart 1981) has been reused in order to get an idea about the magnitude of the moment, which can occur. The motivation for doing this was, Westerchelde is also a broad and deep waterway with comparable environmental conditions.

However, hydraulic condition in the Fehmarnbelt are quite different. For example the current velocities in the Fehmarnbelt are controlled by the exchange of water between the Baltic Sea and the North Sea. Also the current velocities in the Fehmarnbel are lower than in the Westerschelde. Also the dimensions of the tunnel elements are different. And the geometry of the waterway plays an important role, which is off course different for both mentioned water ways.

It's advisable to use the presented data with caution. But both waterways are wide and deep water ways in direct connection to the North Sea. That's why the result from the Westerschelde has been adjusted and reused for the calculations in this section. The scale model tests should reveal a better understanding of the magnitude of this force.

Positions TE	Current velocity[m/s]	Resultant Force [kN]	Moment about z-axis [MNm]
Stage 1 current $\alpha = 40°$, shallow water	0.77	491.62	25.376
Stage 2 current $\alpha = 40°$, deep water	0.9	926.40	47.819
Stage 3 current $\alpha = 50°$, deep water	1	1225.1	-6.9376
Stage 4 current $\alpha = 60°$, deep water	1.1	1534.8	96.607
Stage 5 current $\alpha = 70°$, deep water	1.1	1507.3	-181.54
Stage 6 current $\alpha = 80°$, deep water	1.1	1506.6	-267.76
Stage 7 current $\alpha = 90°$, deep water	1.1	1501.6	0.

Table 21 Forces on the tunnel element in different stages

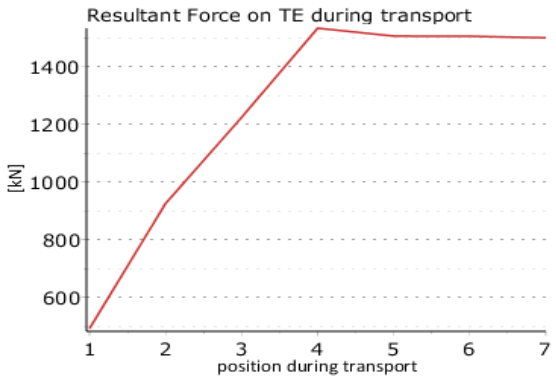

Figure 77 Resultant Forces on TE during different transport stages

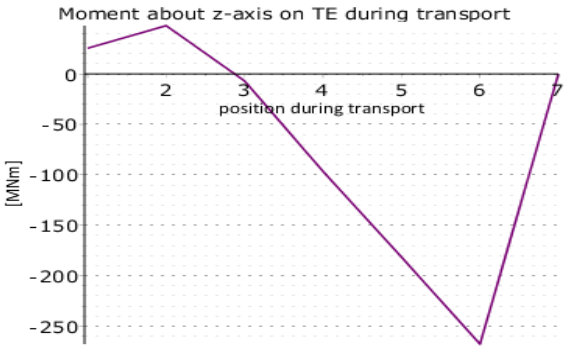

Figure 78Moment on TE about the z-axis during different transport stages

5.6 HYDRODYNAMIC INSTABILITY DURING TRANSPORT

A number of hydrodynamic phenomena has to be taken into account during the transportation of the tunnel elements from the factory to the immersion site. The phenomena leads to limiting towing velocity and also current velocity. In the previous section the effects of the flow velocity and the related forces has been determined. In this part of the report the effect of the towing velocity and the related hydrodynamic instabilities is been investigated. The following three phenomena in relation with the hydrodynamic instability will be investigated.

1. The bow-wave of the tunnel element
2. The pressure decrease due to flow acceleration.
3. The trim moment as a result of towing

Calculations for all the three of the above-mentioned phenomena will be performed. For the calculations, the same approach is used as in (H.R. Luth and E.W.B. Bolt;, 1994). The main purpose of this analysis is to determine the limiting towing velocity. If the towing velocity will be exceeded it is plausible that the tunnel element will be pulled under water and there is considerably chance that the element can become uncontrollable.

5.6.1 THE B (H.R. LUTH AND E.W.B. BOLT;, 1994)OW WAVE OF THE TUNNEL ELEMENT:

The hydrostatic head Δh due to stagnation of the towing velocity of the tunnel element is calculated with aid of Bernoulli equation, the following equation is been used for the calculation.

$$\frac{1}{2} * \rho_w * V_{tow}^2 = \rho_w \cdot g \cdot \Delta h_{bow-wave} \quad (74)$$

If we rearrange the equation, the bow wave can be written as a function of the towing velocity. Then we get the following equation :

$$\Delta h_{bow-wave} = \frac{1}{2g} * V_{tow}^2 \quad (75)$$

The values of the bow wave are presented in Table 22 and Figure 79 for different towing velocities.

Toing velocity [m/]	Bow wave in front of the tunnel [cm]
0	0.00
0.5	1.28
1	5.10
1.5	11.5
2	20.4
2.5	31.9
3	45.9
3.5	62.0
4	81.5

Table 22 Bow wave for different flow velocities

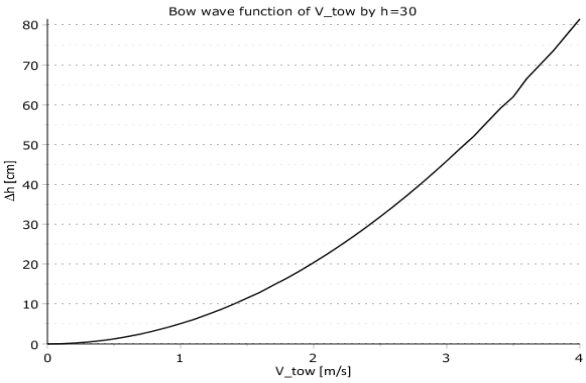

Figure 79 Bow wave as a function of towing velocity

PRESSURE DROP DUE TO FLOW ACCELERATION UNDER THE TUNNEL

In order to calculate the pressure drop under the element, it is assumed that the draught of the element is 1/3 of the water depth. For the contraction coefficient, a value of 0.75 has been assumed. The pressure drop is calculated by means of Bernoulli equation and conservation of mass. In Figure 80 is the sketch of the situation is been given.

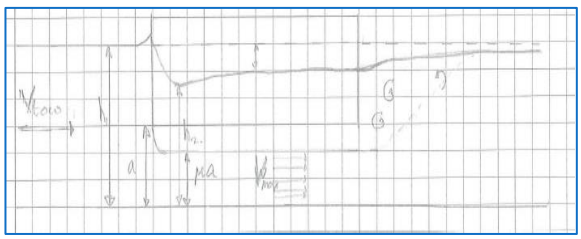

Figure 80 pressure drop under the tunnel element during the transport (B.P. Rigter, April 1989)

The maximum pressure drop is calculated as:

$$\Delta h_{max} = \frac{V_{tow}^2 - V_{max}^2}{2g} \quad (76)$$

The amount of discharge per meter width of the tunnel element and waterway can be given as:

$$q_1 = h \cdot V_{tow} \quad (77)$$

$$q_2 = \mu \cdot a \cdot V_{max} \quad (78)$$

From the conservation of mass, it follows:

$$q_1 = q_2 \quad (79)$$

By rearranging the given equations V_{max} and Δh can be expressed as function of the towing velocity.

$$V_{max} = 2.04 \cdot V_{tow} \quad (80)$$

$$\Delta h_{max} = 0.158 \cdot V_{tow}^2 \quad (81)$$

The pressure drop is assumed to be equally distributed in the width under the tunnel element. The mean value is assumed to be equal to the ($\Delta h_{max}/2$) as a rough approximation. The extent of the under pressure is assumed to be approximately 2*draught of the tunnel element. Now the values for the vertical force and the trim moment associated with pressure drop are calculated with the following equations.

$$F_{vertical} = \frac{1}{2} \cdot \Delta h_{max} \cdot \rho_w \cdot g \cdot 2 \cdot T \cdot B \quad (82)$$

$$M_{trim} = \frac{1}{2} \cdot \Delta h_{max} \cdot \rho_w \cdot g \cdot 2 \cdot T \cdot (\frac{L}{2} - \frac{2T}{2}) \cdot B \quad (83)$$

Where		
Δh_{max}	The under-pressure due to flow acceleration under the element	[m]
V_{tow}	Towing velocity tunnel element	[m/s]
V_{max}	Maximum velocity under tunnel element during towing activities	[m/s]
q_1 and q_2	Specific discharge in waterway and respectively under TE	[m/s]
a	Keel distance (under TE) (here a=1/3*water depth = 10 m)	[m]
μ	contraction coefficient = 0.75	[-]
T	Draught TE = 8.7	[m]
$F_{vertical}$	Vertical force due to under-pressure	[KN]
M_{trim}	Tilting moment due to under-pressure	[KNm]
L	Length tunnel element	[m]
B	Width tunnel element	[m]

Due to the vertical force, the element will sink extra. Due to the trimming moment, the element will rotate and the front will also sink further. From literature, it can be concluded that a 3D effect also occur. Which has an effect on the distribution of the pressure drop over the width. This effect is predominantly dependent on the flow pattern and the geometry of the water. Without the model tests this effect is hardly to determined. That's why in the calculations this effect is not been taken into account. This makes the presented calculations and result a bit to be conservative.

For different values of the towing velocity and a depth of 3xdraught the forces and the moments on the TE during transport has been calculated. The results are given in Table 23 and the following figures. As we can see from the presented results, the pressure drop increases exponentially as function of the flow velocities. Also the associated forces increases on the tunnel element quadratically with increasing towing velocity.

Velocity (V_{tow} [m/s])	Pressure drop (Δh max [m])	Pressure drop (Δh mean [m])	Vertical Force (F_z [kN])	Trim moment (M_{trim} [MNm])
0.5	0.0395	0.0198	143	14.3
1	1.58	0.0790	573	57.3
1.5	0.356	0.178	1290	129
2	0.632	0.316	2290	229
2.5	0.988	0.494	3580	358
3	1.42	0.710	5110	511
3.5	1.93	0.965	7000	700
4.0	2.53	1.26	9190	919

Table 23 Pressure drop and the associated forces as function of flow velocity

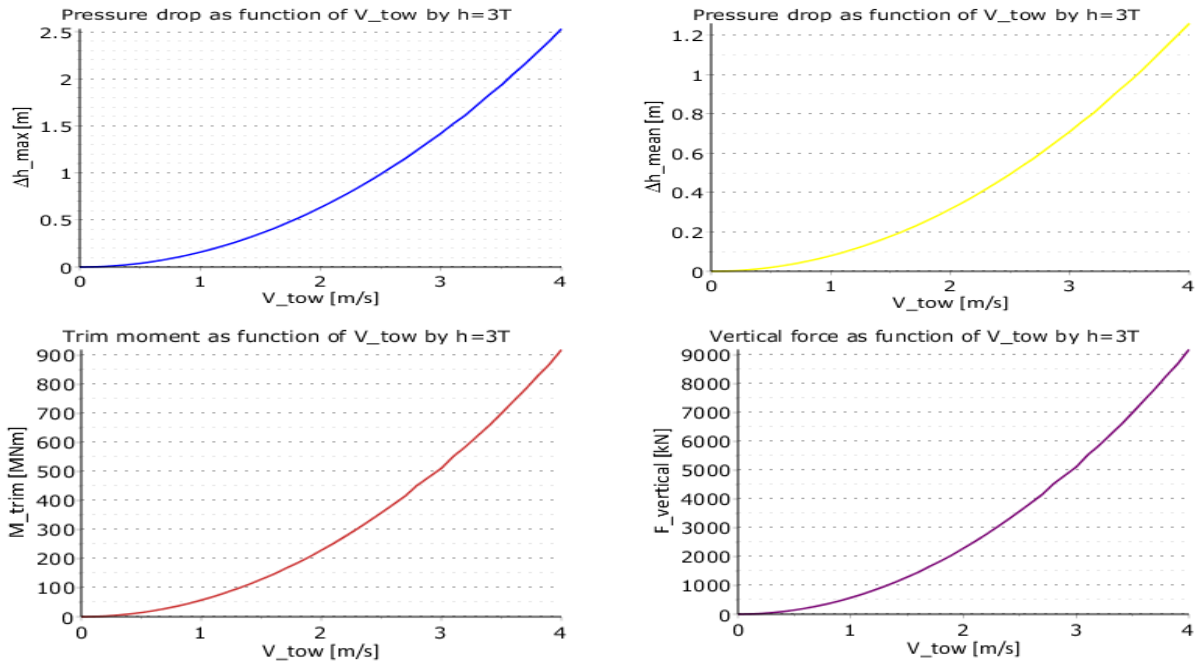

Figure 81 Pressure drop and the assciated force as function of flow velocity

It has to be noted that the water depth is an important parameter in the determination of the forces. If the draught will be half of the water depth then the coefficient for the Δh_{max} will be doubled and also the associated forces on the TE.

During the transport from the factory to the trench site, the water depth is variable. This means that also the (draught/water depth) ratio varies. In order to be able predict the tunnel elements behavior, the effect of the water depth on associated forces has been investigated. For different water depths and flow velocities the forces has been calculated.

As mentioned previously the water way on the Danish cost has to be dredged such that an appropriate depth must be available for the transport of the tunnel elements from the factory to the immersion trench. Is has been assumed that in all stages a minimal keel clearance of 1m has to be available. The freeboard is been assumed to be 0.2[m]. This leads to a draught T of 8.7 [m]. With a minimum keel clearance this leads to a minimum water depth of 9.7 [m]. This value is also been used for the calculations. The other steps are exact the same as mentioned for the calculations of the (draught/water depth) ratio of 1/3.

From the boundary conditions presented in Appendix 2, it can be concluded that the water depth in the deeper parts of the waterway > 30 [m]. That's why the calculations are performed for water depths 9.7[m]< h <30[m]. Also, to relate the influence of the towing velocity, for 5 different values of the towing velocities the forces are calculated as function of the water depth. In Figure 82, Figure 83 and Figure 84 are the values given for the pressure drop, vertical z-force and trim moment. As mentioned before the trimming moment will cause a rotation about the longitudinal direction of the TE during the transport.

From the figures, it can be concluded that effect of water depth and the associated pressure drop is quadratically. With increasing water depth, the pressure drop under the element decreases. For water depths larger than 15 m, the difference in pressure drop for different velocities decreases too. So one should be aware of the effect of shallow water and the towing velocity. In the following also the extra sinkage due to towing velocity will be calculated. But first the trimming moment due to towing force will be calculated.

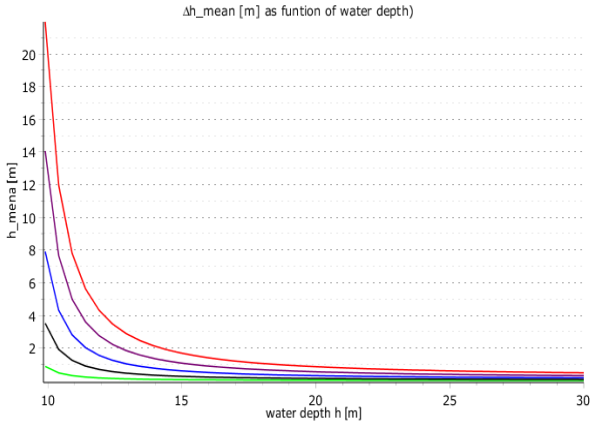

Figure 82 Mean values of the pressure drop as function of the water depth for five towing velocities (green = 0.5, black =1, blue=1.5, purple =2, red =2.5) in [m/s]

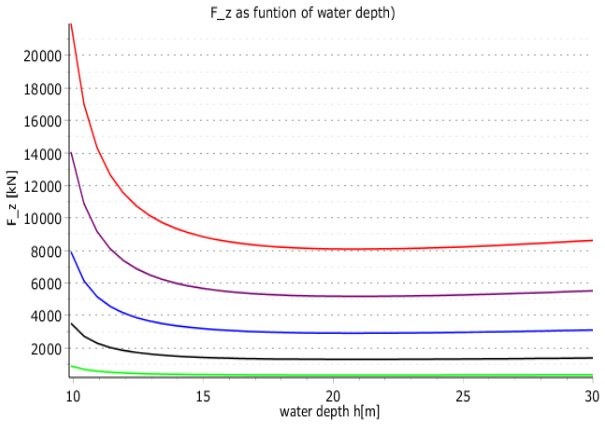

Figure 83 Vertical force as function of the water depth for five towing velocities (green = 0.5, black =1, blue=1.5, purple =2, red =2.5) in [m/s]

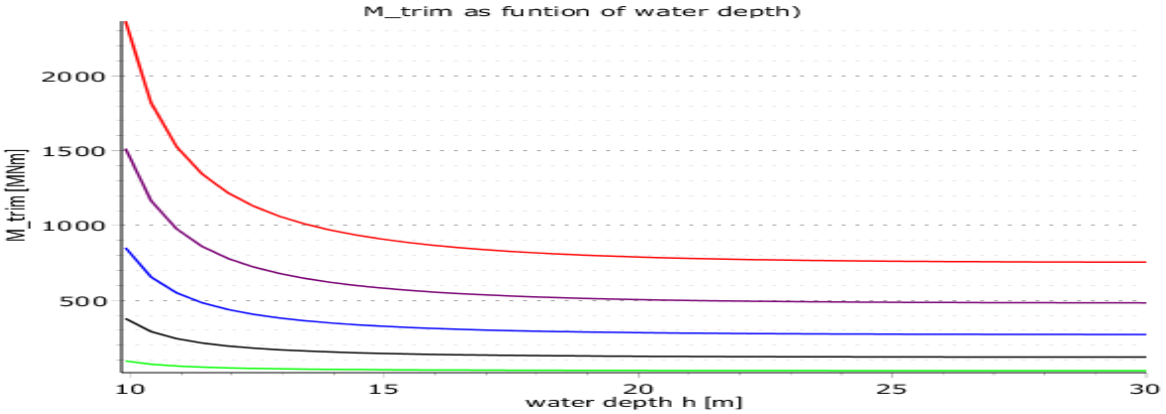

Figure 84 Trim moment as function of the water depth for five towing velocities (green = 0.5, black =1, blue=1.5, purple =2, red =2.5) in [m/s]

5.6.2 TRIMMING MOMENT DUE TO TOWING FORCE

In the previous section the towing force on the tunnel element during the transport in different stages has been calculated (see, Table 21). The resulting towing force on the TE will be 926.40 [kN]. The resultant of this force has an arm a about the COG of the element. This results also in a trimming moment on the TE. For the arm a value of 5 [m] has been assumed. The trim moment will be then:

$$M_{trim} = 5 \cdot F_{tow} \tag{84}$$

The trim moment due to towing force is: 4632 [kNm]. If we compare this to the values of the trim moment due to pressure drop then we can conclude the following: $M_{trim,towing} \ll M_{trim,underpressure}$. That is why this force moment is not been considered further in the calculations.

5.7 LIMITING MOTIONS DURING THE TRANSPORT

During the transport, the freeboard of the element is assumed 0.2m. Having the value of the freeboard, we can also define the maximum angel of trim and roll during the transportation for the tunnel element. The tunnel element may not trim or roll such that the freeboard is exceeded. The tunnel element will trim or roll about the center of floatation. Because of the symmetric box shape of the tunnel element the center of flotation is located in the middle of the water plane area, thus at the points(L/2, B/2). The maximum values of for the angle are:

$$\theta_{trim} = \sin^{-1}\left(\frac{freeboard}{0.5 \cdot L}\right) = 0.105^{\circ} \tag{85}$$

$$\varphi_{roll} = \sin^{-1}\left(\frac{freeboard}{0.5 \cdot B}\right) = 0.56^{\circ} \tag{86}$$

5.8 TOTAL SINKAGE

Due to acting forces, the element will sink and rotate as a result of the acting forces. Because off the small freeboard it is important that the total sinkage may not exceed the freeboard. That's why for different values of the water depth and towing velocity calculation has been performed, in order to be able to estimate the total sinkage. The vertical force due to the pressure drop will cause a sinkage which can be expressed as:

$$\Delta Z_1 = \frac{F_{vertical}}{\rho_w \cdot g \cdot A_w} \quad (87)$$

For the calculations it is assumed that the total weight of the TE during transport passes through its centre of gravity (G or CoG). The buoyancy force F_B acting on the TE passes through the centre of buoyancy B, which corresponds to the centre of the displaced fluid. When the TE is subjected to a trimming moment M_{trim} it will trim with an angle θ. As result of trimming of the structure, the underwater shape will be changed. The centre of buoyancy will shift from *B* to B_θ, while the centre of gravity of the TE remains unchanged at *G*. An equilibrium will be achieved when the righting moment M_S equals the external trimming moment M_{trim} . The principle of this is given in adjacent figure. The theoretical background of Figure 85 is given in appendix 5.1.

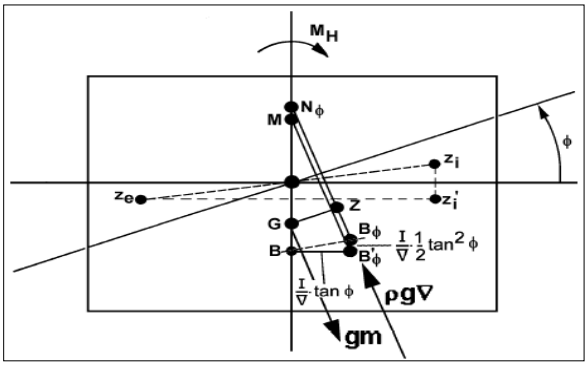

Figure 85 Principle of righting moment (J.M.J. Journée and W.W.Massie , "SHIP HYDRODYNAMICS",2001)

In formula form the equilibrium can be given as:

$$M_S = M_H \quad (88)$$

$$M_S = \rho g \nabla * \overline{\overline{GZ}}_L \quad (89)$$

The stability moment is found considering the stability moment of the edge shaped box, what actually the tunnel element also is. The stability moment can be expressed as:

$$M_s = \frac{1}{6} \cdot \rho_w \cdot g \cdot B \cdot t \cdot L^2 \quad (90)$$

In the above mentioned formula, t represents the trim sinkage. The draught of the element has to be corrected by the sinkage. In formula form can this be presented as:

$$T_{bow} = T + t + \Delta Z_1 \quad (91)$$

$$T_{aft} = T - t + \Delta Z_1 \quad (92)$$

As mentioned before for different values of de water depth, the total sinkage for different towing velocities has been calculated. Each figure shows 3 lines, which represent 3 types of sinkage namely: sinkage due to vertical force, sinkage for trimming of the element and the total sinkage as the sum of the both. The value of freeboard is also given in the figures as a horizontal line. From the figures it can be easily observed by which value of the towing velocity and water depth the freeboard will be exceeded. The calculated results are presented in Figure 86.

Conclusion

The freeboard of the tunnel element should be reduced by the values of the total sinkage. Also from the presented results it can be concluded that the water depth is an important parameter for the towing stability. From the results (Figure 86) it can be seen that when the towing velocity 2.5 [m/s] that the sinkage for all depths is greater than 0.2 [m]. In that situation the element will be permanently under water. And there is great chance that the element will become unstable. So by a freeboard of 0.2 [m] the towing velocity of 2.5 [m/s] is not an option. The same can be also concluded for the towing velocity of 2 [m/s].

For all water depths the element will be pulled under water. The towing velocity of 1.5 [m/s] can only be applied when the water depth is greater than 12 [m]. Only then the element can be transported safely. From Figure 86 we can see that 0.20 [m] freeboard is sufficient for towing velocities of 0.5 and 1.0 [m/s]. For all the water depths there is no danger for TE becoming unstable. It has to be noted that in the calculations the towing velocity is applied as reference velocity. It means that the element will move with that velocity relative to water particles. Given the current location of the construction factory it is plausible that the element will be transported in the same direction as the outgoing flow. In the case of the outgoing velocity the actual towing velocity has to be adjusted such that it will not exceed the total velocity of 1.5 [m/s]. The actual towing velocity and the current velocities has to be added as two vectors. And has to be subtracted when the towing velocity has opposite direction as the flow (ingoing flow conditions).

Also measure has to be taken for the bow wave. In the case of 1.5 [m/s] there is also a bow wave of 11.5 [cm]. In the case of not taking any measures water will constantly flow over the element. If the pontoons will be installed over the tunnel element in the factory. Then also the floating capacity of the pontoons can be added to the floating capacity of the element. In that case no extra measures needed for overcoming the bow wave. For the overall stability it is advisable to apply the towing velocity of 1.5 [m/s] only by a water depth greater than 12 [m]. In other cases the towing velocity of 1.0 [m] is preferred.

It has to be noted that the presented calculations may be considered as conservative. The 3D effect are not been taken into account. Which can lead to the reduction of the forces and the associated sinkage. But that can be better investigated in a scale model tests.

Generally the question is, if it is not better to apply a greater freeboard than 0,2 [m]. In that case the element can be transported faster to the immersion site. But the disadvantage is that the forces working on the element will increase too. Resulting in greater amount of pre-stressing and much more ballast during the immersion will be needed. For the final design model test are recommended in order to optimize the design and construction process.

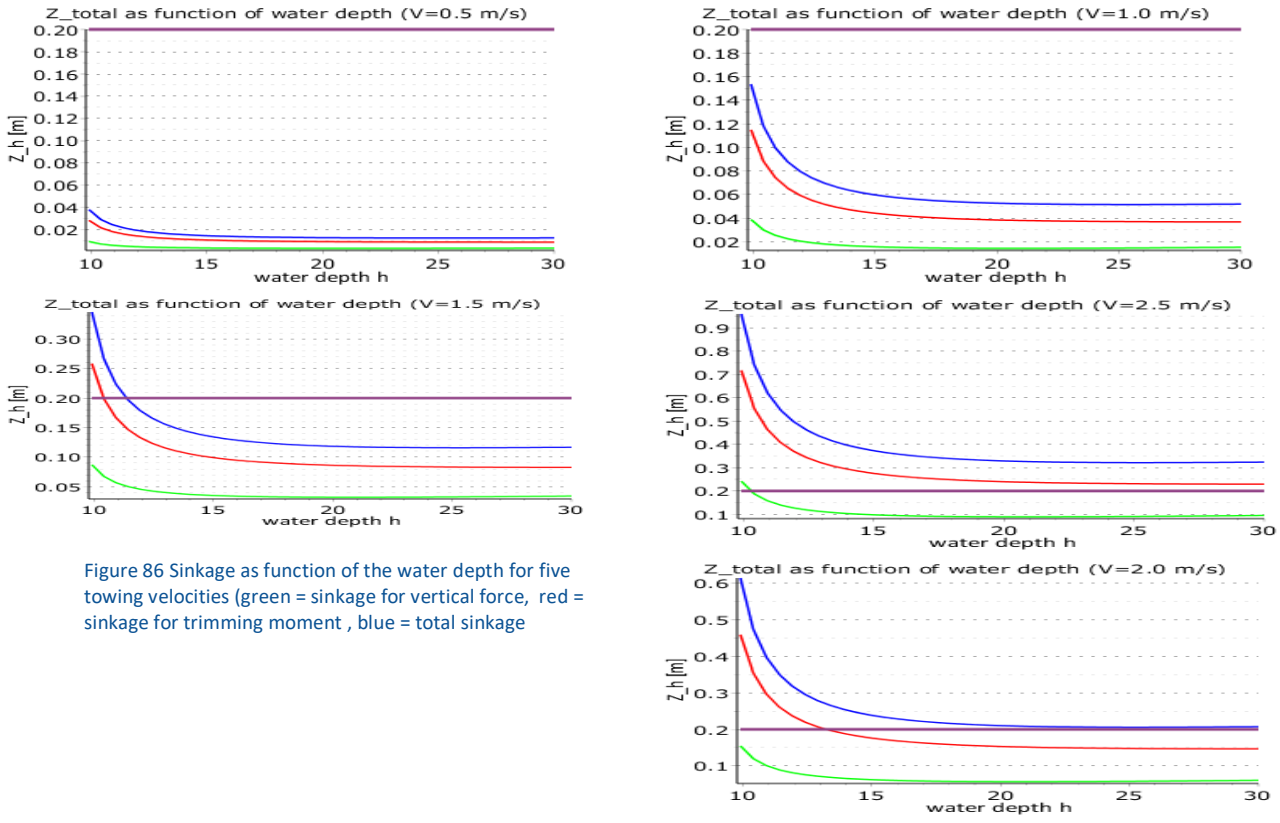

Figure 86 Sinkage as function of the water depth for five towing velocities (green = sinkage for vertical force, red = sinkage for trimming moment , blue = total sinkage

5.9 NATURAL PERIODS

The response of the TE to the wave excitation depends on its natural periods in relation with the wave periods. When the element floats (during the transport), the dimensions of the element determine the natural periods. The hydrostatic stiffness provided by the waterplane area of the element is much larger than the stiffness of the cables which connect the element to the tugboats. That is why only the natural periods in heave, roll, and pitch are calculated for this phase.

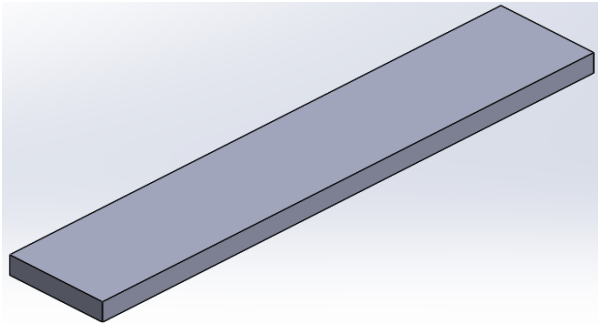

Figure 87 Modeled tunnel element

During the transport the tunnel element has been modeled as one rigid body as given in Figure 87.The following formulae are used for the calculations of the natural periods of the tunnel element during the transport. It has to be mentioned that the damping effect has been neglected in the calculation of the natural periods. The effect of damping will enlarge the natural periods. So the calculations presented here are conservative. In reality the natural periods will be slightly larger than presented here.

$$T_h = 2\pi\sqrt{\frac{m + m_a}{K_z}} \tag{93}$$

$$T_p = 2\pi\sqrt{\frac{I_y + m_{a(yy)}}{K_{(yy)}}} \tag{94}$$

$$T_{ral} = 2\pi\sqrt{\frac{I_x + m_{a(xx)}}{K_{(xx)}}} \tag{95}$$

The mass moment of inertia TE about x-axis(roll) and y-axis (pitch) can be expressed as:

$$\begin{aligned} I_{xx} &= \rho\left(\tfrac{1}{12}\cdot B^3\cdot H + \tfrac{1}{12}\cdot H^3\cdot B\right)\cdot L \\ &= \rho\cdot\tfrac{B^2+H^2}{12}\cdot L\cdot B\cdot H \\ &= K_{xx}^2\cdot\rho\cdot L\cdot B\cdot H \end{aligned} \qquad \begin{aligned} K_{xx} &= \sqrt{\tfrac{B^2+H^2}{12}} \\ K_{xx} &\approx 0{,}3\,B \end{aligned} \tag{96}$$

$$\begin{aligned} I_{yy} &= \left\{\tfrac{1}{12}\cdot L^3\cdot H + \tfrac{1}{12}\cdot H^3\cdot L\right\}B \\ &= \tfrac{L^2+H^2}{12}\cdot L\cdot B\cdot H \\ &= K_{yy}^2\cdot L\cdot B\cdot H \end{aligned} \qquad \begin{aligned} K_{yy} &= \sqrt{\tfrac{L^2+H^2}{12}} \\ K_{yy} &\approx 0{,}29\cdot L \end{aligned} \tag{97}$$

The mass moment of inertia are calculated assuming a homogeneous mass distribution over the element. For the added mass empirical approximations are used. The remaining quantities are reasonably well known. For the hydrodynamic mass terms the following values has been used. M denotes the mass of the element.

1. Added mass for heave motion → M_a = 2·M
2. Added mass for pitch motion → $M_{a(yy)}$ = 1,6·M
3. Added mass for roll → $M_{a(xx)}$ = 0,4 ·M

The following natural periods for the motions of the tunnel element are calculated for the transport phase:

Degree of freedom		Natural period	
Heave	T_{heave}	10,06	[s]
Pitch	T_{pitch}	10,35	[s]
Roll	T_{roll}	8,05	[s]

Table 24 Natural periods during transport

The calculated periods are close to the typically swell periods. These period are well above the periods of the wind generated waves. In the project area the occurrence of long-period waves (waves having periods in the range 8-16s) have been analyzed. From the results presented in (FEHY (Metocean Conditions), 2013)it can be concluded that a very small part of the wave spectrum energy belongs to long period waves (0.0625-0.125Hz) on average. In total, about 0.4% of the total wave energy belongs to long-period waves. Long-period waves like swell play a very small role in the climatology of the study area during the normal weather conditions.

5.10 Conclusion

In this chapter, the forces and moments on TE during transport are evaluated. Additionally, the hydrodynamic stability and natural periods are calculated.

The following conclusions are derived from the calculations:

1. It appears that the most significant drag force on the element works during the fitting out of the element. The maximum forces are calculated for a current angle of 50° also; the current forces stay quite large for greater angles. Therefore, it can be concluded that when the tunnel element makes a greater angle than 40°the force will grow by a factor 1.65 and then staying quite stable.

2. The most significant moments occur when the tunnel element makes an angle of 80°and then disappearing when the element will be positioned perpendicular to the flow direction. It means that during the positioning operation of the element one should be aware of this force moment and take it into account by choosing the proper positioning equipment. Also during the transport phase there will be a force moment about the z-axis. But the magnitude will be much smaller.

3. Towing velocities higher than 1,0 [m/s] can only be applied when the water depth is larger than 12 [m], in a combination of a freeboard of 0,2 [m]. For shallow water depths < 12 [m], the element is only stable if the towing velocity will be 1.0 [m/s] or smaller.

4. The natural periods of the floating element are sufficiently far enough from the wave periods. The calculated periods are close to the typically swell periods. For Fehmarnbelt very small part of the wave spectrum energy belongs to long period waves (0.0625-0.125Hz) on average. In total, about 0.4% of the total wave energy belongs to long-period waves. Long-period waves like swell play a minimal role in the climatology of the study area during the normal weather conditions. Therefore, it can be concluded that there is small chance that resonance will occur due to wave loading.

6 IMMERSION

6.1 INTRODUCTION

An overview of the forces during the transport phase and the static stability of the system is given in the previous chapters. In this chapter an overview of the forces and systems stability during the immersion will be described. In this phase the element will be positioned over the trench and it will be lowered to its final position. The main issues during this stage is the controllability of the motions of the element and the pontoons. For the calculations it is assumed that the immersion operation will be not performed in the stormy conditions and that the shipping will be stopped. Only relatively calm weather conditions are considered in the calculations.

During the immersion, two force mechanisms have been studied namely: excitation by current force and wave force. In order to assess the stability of the system the natural frequencies are calculated and subsequently they are compared to the vortex shedding periods for different environmental conditions. In addition the motional characteristics of the tunnel element due to wind wave excitation has been calculated. The focus in this chapter is on the motional behavior of the tunnel element. In the next chapter the motional of the two floating pontoons are calculated.

6.2 REACTION OF THE TUNNEL ELEMENT TO THE WAVE FORCES:

When the immersion will be not carried out in the heavy sea conditions, the semi stationary forces such as second order wave drift force will not form an important stationary loading and it does not contribute to the first order wave induced motions. In chapter 4.6 the wave drift force and in chapter 5 the drag forces on the tunnel element calculated. The natural periods of the floating element has been calculated previously. The wave induced motions of the tunnel element become important if the wave excitation frequency is near one of the natural frequencies. In the previous chapter the natural frequencies of the floating element has been determined. The smallest natural period is 8 [s] and the other two periods are approximately near the 10 [s]. If we include the damping effect then the natural periods of the element will enlarge slightly. So the natural periods of the floating element are close to the swell frequencies. From the given boundary conditions it can be concluded that the swell waves do not play an important role in the project area. The effect of the swell waves can be neglected.

From provided information it can be derived that, in the project area only the wind-generated waves play an important role for the immersion operation. The waves in Fehmanrnbelt have relatively short periods and small wave lengths. The wave parameters in the project area, are presented in Table 25.

Position	Significant wave height, Hm0 (m)	Spectral peak wave period, Tp (s)	Mean wave period, T02 (s)
	min/mean±std/max	min/mean±std/max	min/mean±std/max
P1 (near Rødby)	0.1/0.49±0.36/2.90	1.01/3.41±1.08/8.51	0.80/2.28±0.72/5.61
P2 (Middle of the fixed corridor)	0.1/0.57±0.40/3.58	1.01/3.44±1.01/7.38	0.81/2.42±0.73/5.13
P3 (near Puttgarden)	0.1/0.38±0.27	1.01/3.21±1.01/9.27	0.82/2.02±0.0.56/4.67

Table 25 Wave parameters in the project area (FEHY (Metocean Conditions), 2013)

The influence of waves decreases exponentially with increasing depth, relatively short waves will have little influence near the bottom of the trench. Also the loads acting on tunnel element are larger near the water surface and decrease with increasing immersion depth. The related motions of the element follows the same pattern.

Wave induced motions of the floating tunnel element are calculated in computer software Ansys Aqwa. Based on standard three dimensional frequency domain diffraction/radiation theory the RAO's for 6 degrees of freedom of the floating tunnel element are calculated. This calculations are performed for 30 m water depth and 1m wave height. Different wave attack angles has been analyzed. The calculated RAO's for beam waves are presented in Figure 88. The RAO's for other attack angle are shown in Appendix 6.

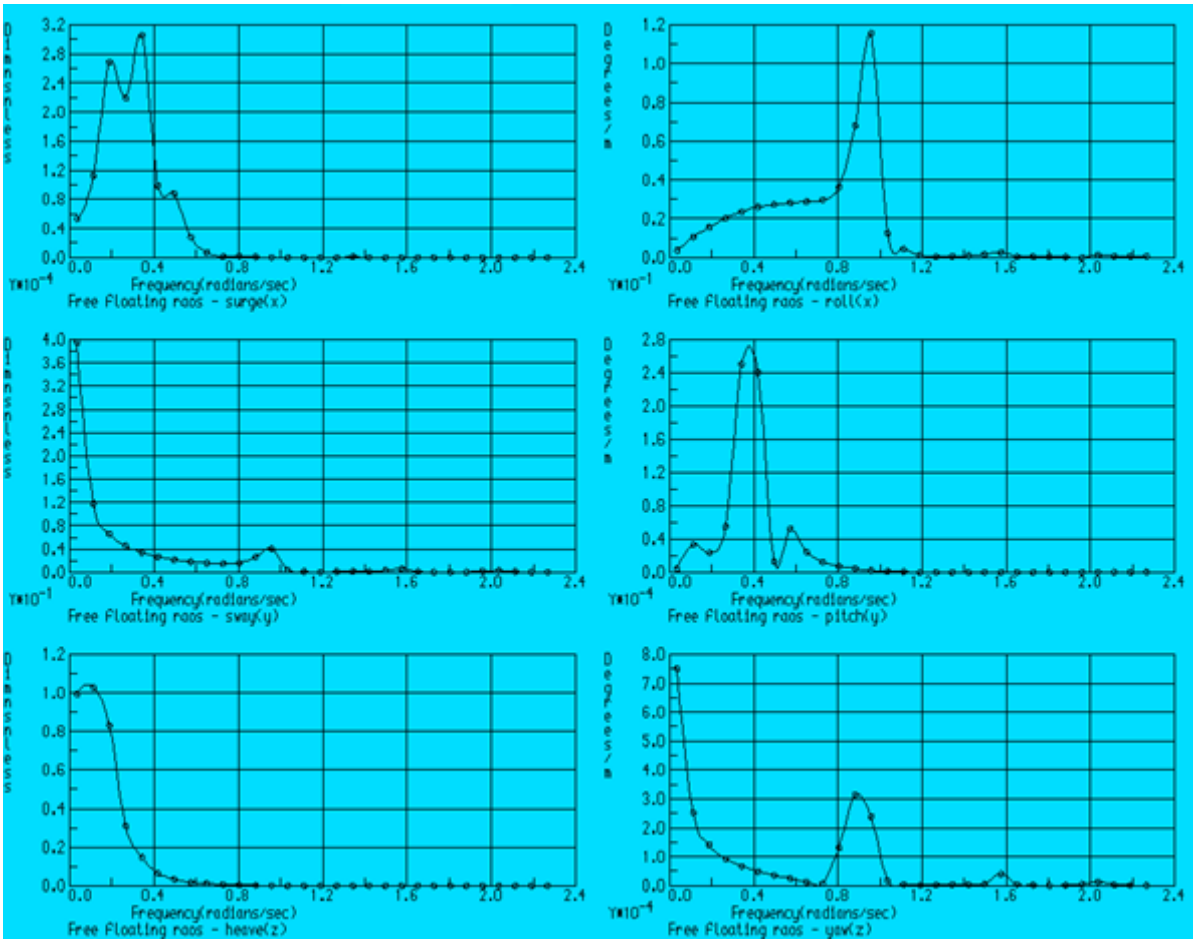

Figure 88 RAO's Tunnel motions in 6 degree of freedom

From the calculations it can be concluded that tunnel element is not sensitive to the wave forces. The wave spectrum of the project area is given in Figure 89. As we can see also from the spectrum the main energy of the spectrum lies above the a wave frequency of ω > 0.7. And the peaks in the RAO's which does matter are below a wave frequency of 0.4 > ω. This can be explained by the fact that the wave forces are quite small and leads to negligible accelerations. That's why in the further analysis the impact of the wave load will be only analyzed for the 2 types of pontoons considered in this case study.

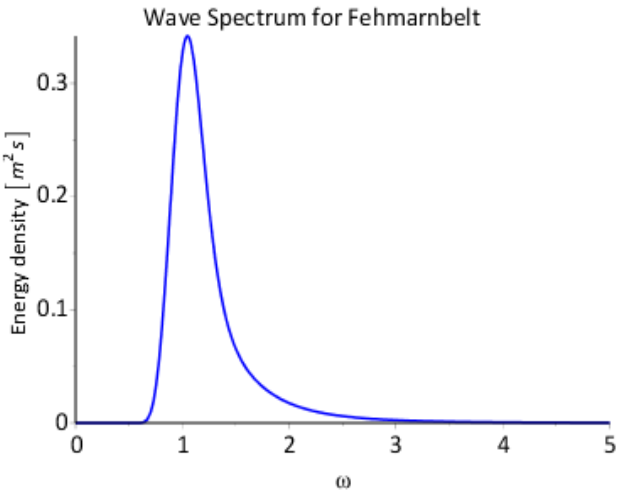

Figure 89 Wave Spectrum project area

6.3 VORTEX INDUCED MOTIONS

During the immersion the tunnel element will be predominantly exposed to the flow forces. The angle of the current flow with the longitudinal dimension of the tunnel element is predominantly 90° in the middle of waterway. Near the costs the current angle may vary, but the current velocity in the middle of the fairway are determinative for the force determination. Again the skin friction will be ignored because the total skin friction will be less than 5% of the drag force. The current drag force can be decomposed into two components namely, a drag force acting in the current direction and a lift force acting perpendicularly to the flow direction. The drag force components can be given as:

$$F_d = C_d \cdot A_c \cdot \frac{1}{2} \cdot \rho_w \cdot V_{current}^2 \quad (98)$$

$$F_L = C_L \cdot A_L \cdot \frac{1}{2} \cdot \rho_w \cdot V_{current}^2 \quad (99)$$

The drag and lift coefficients should be determined experimentally for accurate results. Also the flow velocity over the vertical profile is variable. Due to stratified conditions in the Fehmarnbelt, the flow is predominantly two directional. Namely ingoing and outgoing. For the calculations the near surface velocity will be used. For a fist estimate of the forces again data presented in the literature will be used to get an impression of the magnitude of the forces.

Drag and lift forces are produced by the fact the vortices will be shed alternately behind the tunnel element in the flow. In the area closest behind the tunnel element the pressure drop will be largest. This leads to a resulting force directed toward the vortex, which can be decomposed in drag and lift force components. Given the vortex shedding frequency a dimensionless number called the Strouthal number can be defined as:

$$St = \frac{f_v \cdot D}{U} \quad (100)$$

The values of St depends again on Reynoldsnumber (*Re*) and the flow velocity. For lower Re, St is approximately equal to 0.2 for cylinders. For higher values of *Re* the St increases slightly. In order to be able to predict the vortex shedding frequency of the tunnel element during the immersion some data from literature has been reused. On basis of the length and height ratio and the assumed flow velocities the St has been determined from Figure 90 and Figure 91.To avoid large motions of the element during the immersion, the immersion conditions must be chosen such that the vortex shedding frequency does not coincide with the natural frequencies of the system. The natural frequencies of the system will be determined later. First the vortex induced frequency and the associated period will be determined.

The tunnel element will have a height/width ratio of 0.216 and a width height ratio of 4.63. From Figure 90 for the rectangular shapes is a value of 0.18 has been read and from Figure 91 the St value for the given width/height ratio is 0.13. From the presented information it can be assumed that the value of the vortex shedding will be in between the ranges mentioned above. The vortex shedding period for given TE dimensions will be in the range of:

$$50\ [s] < T_{vortex} < 68\ [s] \quad (101)$$

The vortex shedding period decreases with increasing flow velocity. In extreme cases when flow velocity is approximately 2.5 [m/s], the vortex shedding period will decrease till a value of 19 s. In Figure 92 is the effect of the flow velocity on T_{vortex} has been given. The upper green line represents the values of St found in Figure 91 and the lower line represents the value of St derived from Figure 90. The St derived from this figures is dependent on height/width ratio. For other dimensions other St values will be found and the presented results in Figure 92 will be not applicable.

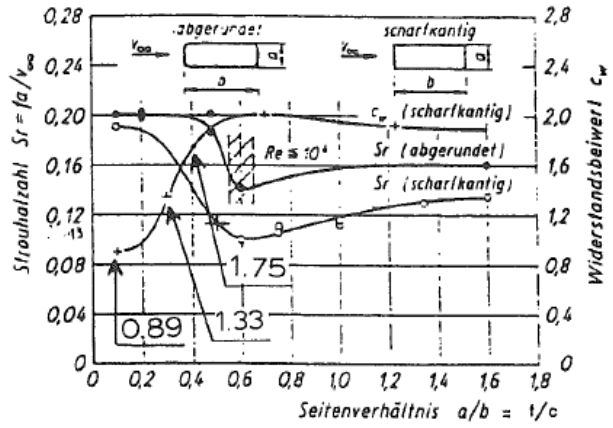

(B)

Strouhal number and drag coefficient of rectangular sections.

15 mm ≦ a 27 mm for a/b ≦ 1

$2.10^3 \leq Re \leq 10^5$

[Schramm, 1966]

Figure 90 Strouhal -number Dependency on H/B (Scharamm, 1966)

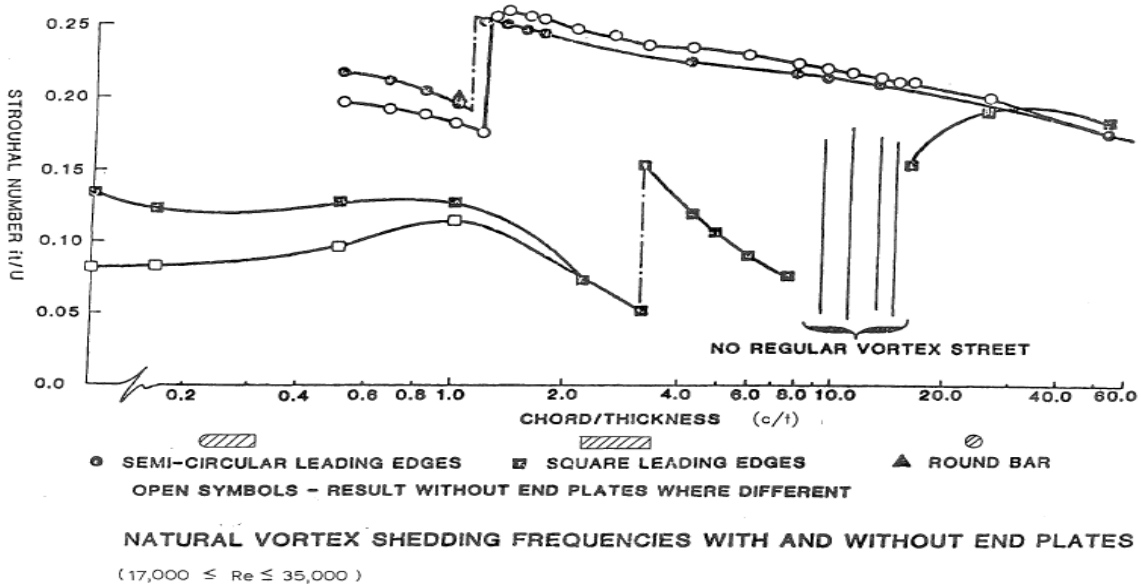

Figure 91 Strouhal -number Dependency on B/H (Parker, 1981)

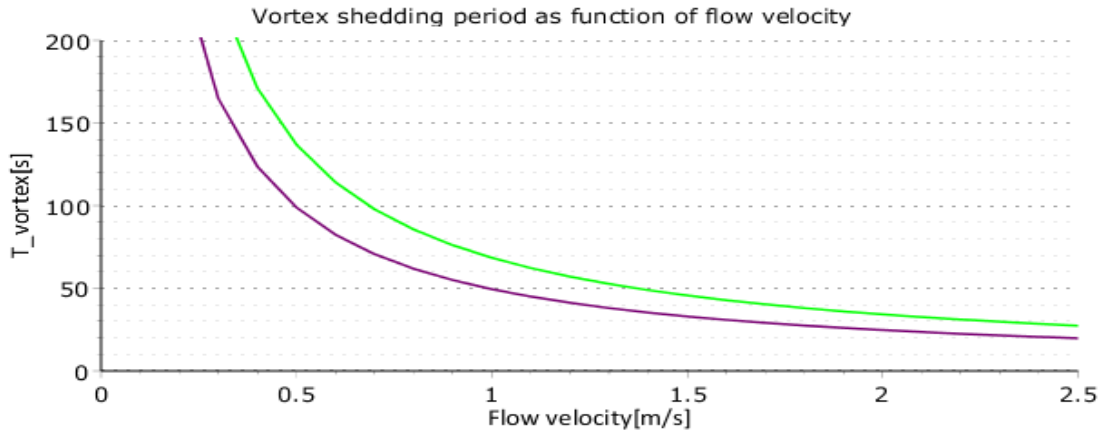

Figure 92 Vortex shedding period as function of flow velocity

6.4 NATURAL PERIODS

The response of the tunnel element to the wave excitation is determined in section 6.1. The natural frequencies of the floating tunnel element has already been calculated. In this section the natural periods of the element during the immersion are calculated. The main objective of this section is determination of the natural frequencies of the entire system and comparison to the calculated vortex shedding periods. The calculations presented in this section give an insight into resonant behaviour of both pontoons in different flow conditions.

When the TE will be fully submerged, the element doesn't have vertical stability (see also section 4.6 static stability). The pontoons will provide entirely the stability of the system. In this section the natural periods of the current excitation will be calculated for two alternative pontoon arrangements. The chosen arrangement should be such that the system does not go into resonance.

The current force may excite the tunnel element in the vicinity of the natural periods of the element. When the vortex shedding excitations frequency is close enough to the to the natural frequency of the element, then the vortex shedding may become controlled by the motions of the tunnel element. This situation can lead to a full resonant situation and in the hydraulic engineering it is indicated as "lock-on effect".

Three motional directions have great influence on the cable forces and the related systems response, namely: (heave, roll and pitch). The responses in the remaining motional directions are of stationary type and are controlled by the stiffness of the contraction cables. The natural periods of those directions are predominantly larger than the current excitation periods and there is no danger of resonance in those directions.

For the calculations the same approach has been followed as in (W.D. Eysink, H.R. Luth, J.H. de Vroeg en H.J. van Wijhe, 1995), (S.J. Callander and S.T. Schuurmans, 1991) and (H.R. Luth and E.W.B. Bolt;, 1994). It is assumed that the tunnel element and the pontoons behave as one body. The contribution of the pontoons to the inertia of the system is neglected. This is justified by the fact ($M_{pontoon}/M_{TE}$ <0.018). On other hand the stability of the system, is entirely contributed by the pontoons. The stability of the submerged element is neglected. The actual arrangement of pontoons is rather crucial in the dynamic behaviour of the system.

The waterline areas of the pontoons determine the vertical stiffness of the system, regarded as one rigid body. In reality, the connections between pontoons and tunnel element are such that motions relative to each other are possible. But this aspect is disregarded for the calculations in this section. And for now only the stiffness of the water plane area is been taken into account. The suspension cables are modelled as infinitely stiff and the stiffness of the mooring system is disregarded.

The natural frequencies of the element during the immersion are mainly determined by the dimensions and geometry of the pontoons, if we consider that the stiffness is only provided by the water plane area. The normative dimensions for the natural frequencies of the element under water suspended from the pontoons are apart from the dimensions of the element itself are:

1. l_p the c.t.c (centre to centre) distance of the pontoons in the longitudinal direction of the element.
2. b_p c.t.c distance of the pontoons in the width direction of the element.
3. A_p water-cutting (of water plane area) surface of the two pontoons.

In Figure 93 the above mentioned distances are explained.

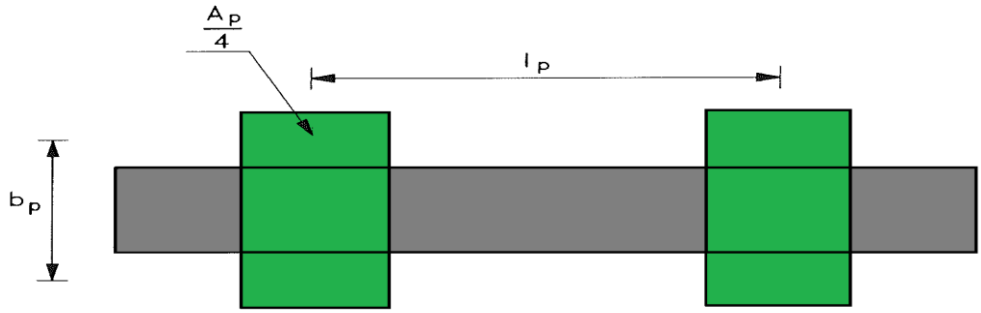

Figure 93 Tunnel element during the immersion

The natural periods of the tunnel element can be expressed as:

$$T_{heave} = 2\pi\sqrt{\frac{M_{TE} + M_{a-heave}}{K_{heave}}} \quad (102)$$

$$T_{roll} = 2\pi\sqrt{\frac{I_{xx}}{K_{roll}}} \quad (103)$$

$$T_{pitch} = 2\pi\sqrt{\frac{I_{yy}}{K_{pitch}}} \quad (104)$$

Where the moments of inertia can be expressed as:

$$I_{xx} = r_{xx}^2 \cdot (M_{TE} + M_{a-roll}) \quad (105)$$

$$I_{yy} = r_{yy}^2 \cdot (M_{TE} + M_{a-pitch}) \quad (106)$$

Where r_{xx} and r_{yy} are the radii of gyration in respectively roll and pitch degrees of freedom and they can be expressed as:

$$r_{xx} = \frac{B}{2.2} \quad (107)$$

$$r_{xx} = \frac{L}{3.4} \quad (108)$$

Now the stiffness of the system in heave, roll and pitch can be expressed as:

$$K_{heave} = \rho_w \cdot g \cdot A_p \quad (109)$$

$$K_{roll} = \frac{1}{4} \cdot b_p^2 \cdot K_{heave} \quad (110)$$

$$K_{pitch} = \frac{1}{4} \cdot l_p^2 \cdot K_{heave} \quad (111)$$

Where

a)	T_n	Natural period in nth degree of freedom	[s]
b)	I_{xx}	Moment of gyration in roll degree of freedom	[kg·m^2]
c)	I_{yy}	Moment of gyration in pitch degree of freedom	[kg·m^2]
d)	K_{heave}	Spring stiffness of the system in heave degree of freedom	[N/m]
e)	K_{roll}	Spring stiffness of the system in roll degree of freedom	[N/m]
f)	K_{pitch}	Spring stiffness of the system in pitch degree of freedom	[N/m]
g)	r_{xx} and r_{yy}	Radius of gyration in the roll and pitch degree of freedom	[m]

With the given dimensions of the pontoons and TE the natural periods in heave, roll and pitch can be expressed as:

$$T_{heave} = \frac{954.36}{\sqrt{A_p}} \quad (112)$$

$$T_{roll} = \frac{24419}{b_p \cdot \sqrt{A_p}} \quad (113)$$

$$T_{pitch} = \frac{1.138 \cdot 10^5}{l_p \cdot \sqrt{A_p}} \quad (114)$$

The position of the l_p is variable and can be chosen arbitrary. However, in the calculations the most favorable position is chosen in order to reduce the bending moment in the tunnel element due to forces in suspension cables. It is assumed that the suspension cables will be attached to the tunnel element at a distance of $(1/5 \cdot L_{TE})$ from the edge of the tunnel element. Therefore the length l_p can be expressed as:

$$l_p = L_{TE} - \left(\frac{1}{5} \cdot L_{TE} \cdot 2\right) \quad (115)$$

The distance b_p is expressed as:

$$b_p = B_{TE} - \left(\frac{1}{2} \cdot B_{floater} \cdot 2\right) \quad (116)$$

With the given expressions the natural periods of the tunnel element are calculated for the given pontoon dimensions. The following natural periods for the Catamaran pontoon and Semi-submersible pontoons are calculated.

	Catamaran	Semi-submersible
T_{heave}[s]	29.26	67.48
T_{roll} [s]	14.13	35.24
T_{pitch} [s]	26.70	59.50

Table 26 Natural periods for different types pontoons

The length of the tunnel element is determined in the illustrative design. It's being investigated what will be the effect on natural periods if the length will be changed, by keeping the width of the element and the pontoon dimensions constant. The width of the elements is determined by the functional requirements. Further the length l_p is adjusted such that for each value of L_{TE} the suspension cables will be attached to the tunnel element at distance of $(1/5 \cdot L_{TE})$ from the edge of the tunnel element. The calculations are performed from a length of 100 [m] till 220 [m]. A shorter element will also have a smaller weight. Also the mass of the tunnel element and the added mass components are changed such that they form a ratio of the calculated mass of TE for a given length of 217.8 m.

In Figure 94 the results from the calculations are presented for the Catamaran pontoon. The same calculations has been performed also for Semi-submersible type pontoon. The results are presented in Figure 95. Each of the mentioned figures gives the natural periods of both types of pontoons for different length of the TE. The result in each figure are presented in the following sequence: heave , roll, pitch. In order to be able to compare the natural periods the mentioned three natural periods are given in one figure.

From the figures it can be concluded that the size and position of the tunnel element is determinative for calculating the natural frequencies of the system. Here, it is assumed that the vertical suspension cables are infinitely stiff and do not contribute to the spring stiffness of the system. The spring stiffness is only determined by the pontoons. The location of the fastening points of the cables in the transverse direction doesn't play a role in this consideration.

It should be noted that the location of the cables is of importance for the determination of the dynamic forces in the cables. The shorter the distance between the suspension cables, the smaller the forces will be. To determine dynamic behavior of the pontoons and the cable forces the spring stiffness of the cables and the location will be included in the calculations presented in the next part of this report.

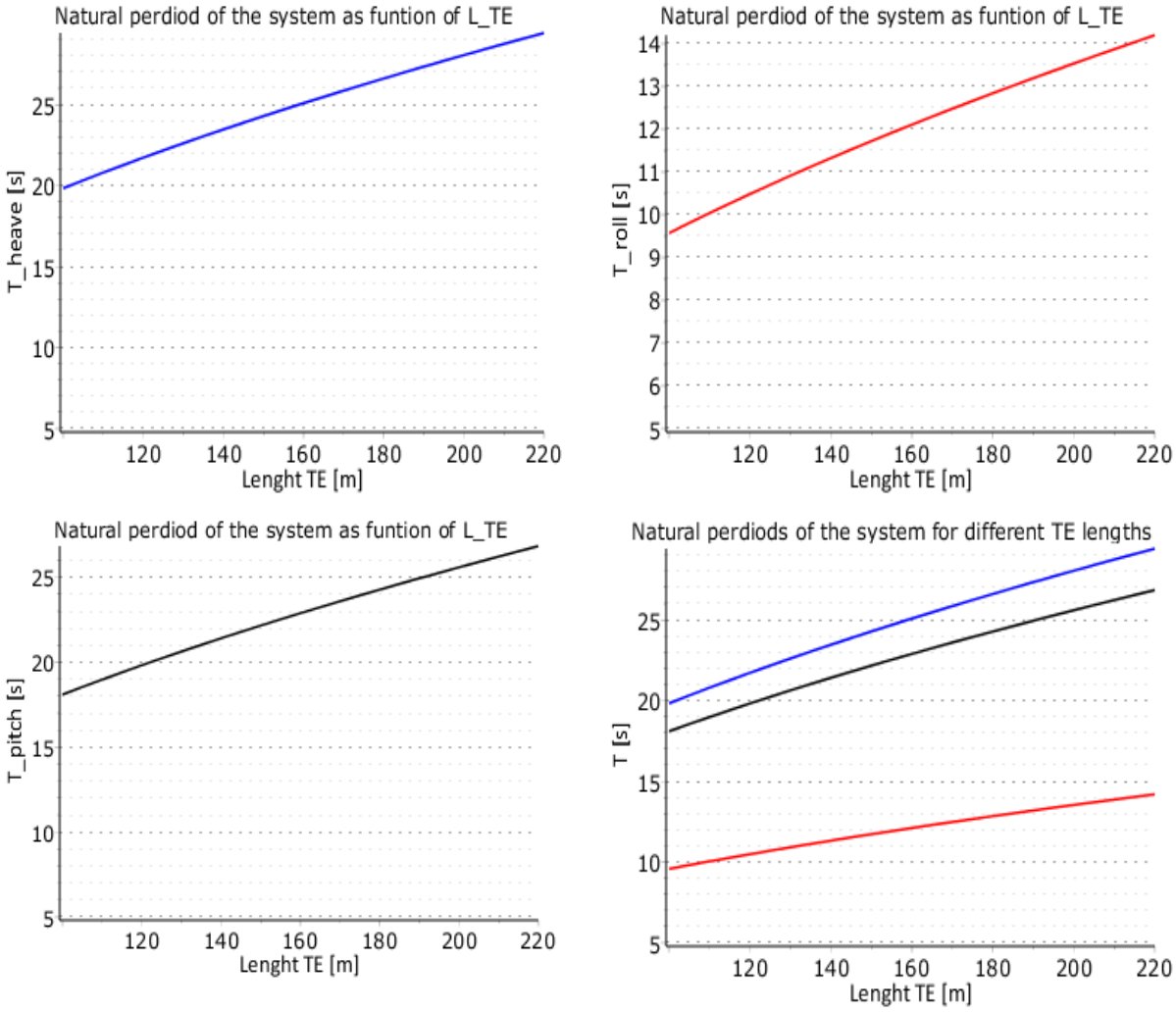

Figure 94 Natural periods of the system for the Catamaran pontoon for different lengths of TE (blue= heave; red=roll; black=pitch)

From the calculated results, it can also be concluded that the Semi-submersible has a favorable behavior concerning the flow forces. The natural periods of the system for the Semi-submersible pontoons are much larger than that for the Catamaran pontoons. However for both pontoons the roll degree of freedom is the most sensitive and less stable. For current velocities greater than 1.5 [m/s] the system may become unstable and even resonance may occur when the excitation frequency coincide the natural frequency. Especially the shorter elements are more sensitive than the longer elements. Due to greater inertia the longer elements are difficult to bring into motion. The lower band and the upper band of the vortex shedding periods are given Table 27. For the both types of the pontoons the natural periods are given in Table 28 and Table 29.

From the results it can be concluded that the workable conditions depend on the final chosen length and the pontoon configurations. For example for a current velocity of 1.1 [m/s] which is not exceeded for 95% of the time the natural periods of the system when choosing Catamaran pontoon are far from the current excitation periods. There is hardly chance that the resonance will occur.

Flwo Velocity [m/s]	Lowe bound Vortex shedding period [s]	Higher bound Vortex shedding period [s]
0.5	98.91	136.9
0.6	82.44	114.1
0.7	70.62	97.85
0.8	61.80	85.54
0.9	54.94	76.05
1.0	49.46	68.45
1.1	44.94	62.23
1.2	41.20	57.04
1.3	38.04	52.66
1.4	35.32	48.90
1.5	32.96	45.64
1.6	30.90	42.79
1.7	29.09	40.27
1.8	27.47	38.04
1.9	26.02	36.04
2.0	24.72	34.23

Table 27 Vortex shedding periods for different flow velocities

Length TE [m]	I_p	T_{heave}	T_{roll}	T_{pitch}
100	60	19.83	9.577	18.10
110	66	20.79	10.04	18.98
120	72	21.72	10.49	19.82
130	78	22.62	10.92	20.64
140	84	23.46	11.33	21.41
150	90	24.28	11.73	22.17
160	96	25.08	12.11	22.90
170	102	25.85	12.48	23.60
180	108	26.61	12.84	24.28
190	114	27.34	13.20	24.94
200	120	28.04	13.54	25.59
210	126	28.74	13.88	26.22
220	132	29.42	14.20	26.85

Table 28 Natural periods of the system for Catamaran pontoon

Length TE [m]	T_{heave}	T_{roll}	T_{pitch}
100	45.75	23.89	36.04
110	47.98	25.05	38.68
120	50.11	26.16	41.10
130	52.16	27.23	43.42
140	54.14	28.26	45.59
150	56.02	29.25	47.66
160	57.84	30.21	49.61
170	59.64	31.14	51.47
180	61.36	32.05	53.26
190	63.03	32.93	55.02
200	64.66	33.78	56.68
210	66.30	34.62	58.28
220	67.87	35.44	59.86

Table 29 Natural periods of the system for Semi-submersible pontoon

On other hand for the Semi-submersible pontoon the natural periods in heave and pitch coincide the vortex shedding period for smaller tunnel lengths. And for the greater lengths there is still danger of the resonance in the pitch degree of freedom. Decreasing of the water plane area of the pontoons will enlarge the natural periods. But as we saw in chapter 4.5, for the static stability of the system decreasing of the water plane area is not favorable. Obviously two options can be chosen, namely:

a) Enlarging the water plane area of the pontoons, so that the natural period in pitch and heave decrease and therefore it will be far enough from the vortex excitation periods.
b) Choosing the workable conditions such that the flow velocity will not exceed 0.7 [m/s].

For the dimensions of the illustrative design and the chosen pontoon dimensions for the Semi-submersible pontoon the natural period in pitch is: T_{pitch} = 59.50 s. This value is in between the upper and the lower band for the vortex shedding period. In order to avoid resonance in pitch, the flow velocity during the immersion should be lower or equal to 0.7 [m/s]. The natural periods are also recalculated by enlarging the water plane area of the columns (6x6) and greater floater length (45 m). For the tunnel element length smaller than 140 m the natural periods are fairly far from the vortex-shedding period. For the greater lengths than 150 m the natural period in heave and pitch are still close to the vortex-shedding periods. The only solution then is that the element should be immersed by low flow velocities.

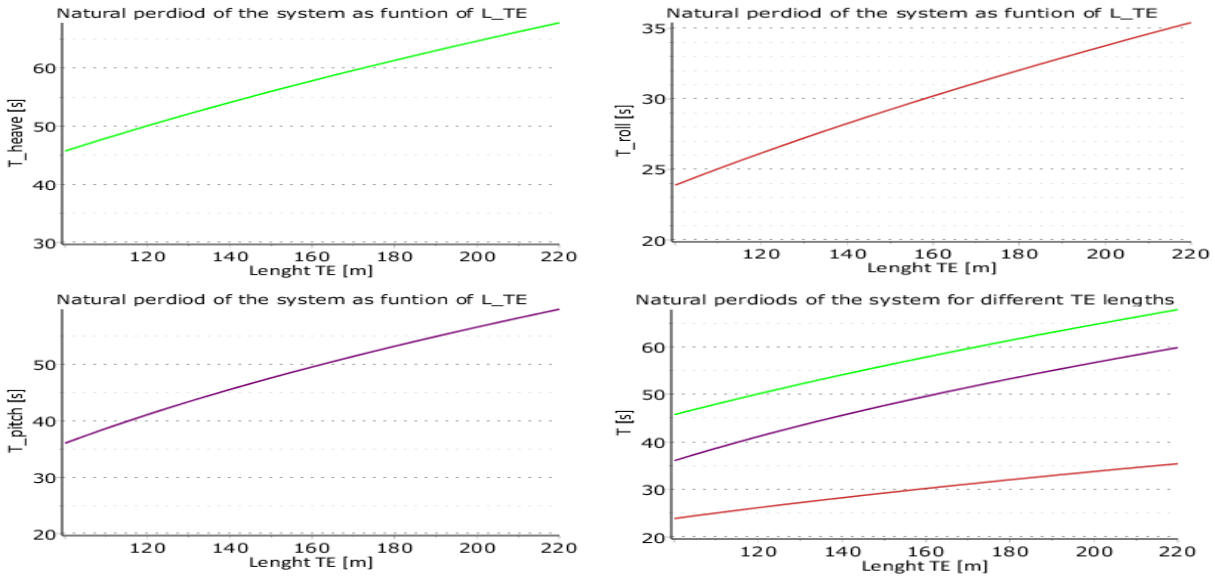

Figure 95 Natural periods of the system for the Semi-submersible type pontoon for different lengths of TE (green= heave; orange=roll; dark purple=pitch)

For both types pontoons the natural periods of the system are well between the vortex-excitation and wave-excitation periods. As explained, before the natural frequencies of the system with de Semi-submersible pontoon are quite close to the vortex shedding periods when de flow velocity > 0.7 [m/s]. It has to be mentioned that the natural periods of the system above are calculated just for the conditions when the tunnel element is just immersed. During the immersion process, the natural periods will increase. An estimate of this increase follows as: When the tunnel element is just submerged the following values are used for the added mass term for the above presented calculations:

$$M_{a-heave} = 2 \cdot M_{TE} \quad (117)$$
$$M_{a-roll} = 0.4 \cdot M_{TE} \quad (118)$$
$$M_{a-pitch} = 1.6 \cdot M_{TE} \quad (119)$$

When the tunnel element will be half way to its final position in the trench approximately at 15 m water depth the following values for the added mass are estimated.

$$M_{a-heave} = 3 \cdot M_{TE} \quad (120)$$
$$M_{a-roll} = 0.6 \cdot M_{TE} \quad (121)$$
$$M_{a-pitch} = 2.4 \cdot M_{TE} \quad (122)$$

With the above estimated values of the added mass the natural periods of the system are recalculated and resulting in the following values:

	Catamaran	Semi-submersible
T_{heave}[s]	33.79	77.92
T_{roll} [s]	15.10	37.67
T_{pitch} [s]	30.54	68.03

Table 30 Natural periods for different type pontoons at the water depth of 15 m

When the tunnel element is just above the tunnel trench the following values for the added mass are estimated:

$$M_{a-heave} = 4 \cdot M_{TE} \quad (123)$$
$$M_{a-roll} = 1 \cdot M_{TE} \quad (124)$$
$$M_{a-pitch} = 3 \cdot M_{TE} \quad (125)$$

Resulting in the following values of the natural periods:

	Catamaran	Semi-submersible
T_{heave}[s]	37.77	87.12
T_{roll} [s]	16.89	42.11
T_{pitch} [s]	33.13	73.80

Table 31 Natural periods for different type pontoons at the water depth of 30 m

The tunnel element close to the bottom, the excitation by current will not be of any consequence anymore because of the lee of the trench walls and the lower flow velocities. In addition, the flow velocities decrease with increasing water depth. Again it appears that the natural frequencies of the system with the catamaran pontoons are sufficiently far from the vortex shedding periods. With increasing water depth the flow velocity decrease resulting in larger vortex shedding period. As result of increasing added mass also the natural frequencies of the system increase. Also here the natural frequencies for the Semi-submersible pontoon still close to the vortex-shedding periods.

6.5 Conclusion

From the calculations it can be concluded that tunnel element is not sensitive to the wave force. The main energy of the wave spectrum lies above a wave frequency of $\omega > 0.7$. And the peaks in the RAO's which does matter are below a wave frequency of $0.4 > \omega$. This can be explained by the fact that the wave force are quite small compared to the tunnel element mass.

It has also been investigated what the effect of the length of the tunnel element is on the stability of the system. Because the length dimensions of the illustrative design are quite large and it may be chosen to reduce the length. For the tunnel element length smaller than 140 m the natural periods are fairly far from the vortex-shedding period. For the greater lengths than 150 m the natural period in heave and pitch are still close to the vortex-shedding periods. This is only valid for the Semi-submersible pontoon. An immersion system with Catamaran pontoons seems to be less sensitive to vortex shedding period. Despite that a system with the Catamaran pontoon have smaller natural periods in general, the natural frequencies lies far enough from the vortex shedding periods, and that makes it less sensitive.

Due to larger natural periods of the system with Semi-submersible pontoons and the flow conditions in the Fehmarnbelt it can be concluded that by applying the Semi-Submersible pontoons there is more danger for occurring of the resonance during the immersion than for a system with the Catamaran pontoons. In general it can be stated that with increasing flow velocities the vortex shedding frequencies will decrease. The vortex shedding periods will become close to the natural frequencies of the system if a Catamaran pontoon is applied. In that situations a Semi-submersible pontoon will be more stable than a Catamaran pontoon. That makes a Semi-submersible pontoon more suitable to apply in a more unfavorable climate conditions.

7 DYNAMIC ANALYSIS PONTOONS IN TIME DOMAIN

7.1 INTRODUCTION

This chapter builds on the theory presented in chapter 3 and appendix 5 and uses relatively simple approximations to predict and discuss important aspects of the global hydrodynamic response of the pontoons. In this chapter, only the immersion phase is considered. This section also provides insight into the hydrodynamic loading working on the barges/pontoons during different immersion stages. The emphasis in this chapter is on the overall behavior in the limiting conditions. Here the dynamic analysis of the pontoons to the regular waves is presented in the time domain. In the analysis, the coupling between surge, sway, heave, roll, pitch and yaw degrees of freedom are considered.

The calculations contain typical response of the pontoons to waves. In the calculations, approximate methods are used which doesn't require complicated analysis or reference published data to predict the response. That's why these calculations are not suitable for detailed design. The results presented here can be used for:

- To predict the likely response of the system
- Understand and gaining confidence in the results of the more sophisticated analysis.

The calculations are performed for the first order responses that are valid in relatively low wave heights. Hydrodynamic effects caused by the nonlinearities are disregarded in the calculations. If the model test or sophisticated analysis predict the very different response of the system from those presented here, it's possible that the nonlinear effects have become dominant.

The equations used in the calculations explain the physical phenomena which are being modeled. The calculations are very straightforward that's why relatively simple computer program such as maple has been used. This chapter deals with the time domain calculations of the system in regular waves. In the following section, the operability of the system has been determined. For the operability of the system, calculations are performed in the frequency domain. Therefore the statistics of the response in different sea states has been established. The motional RAO's are readily converted to statistical values by using spectral analysis (see, chapter 8).

7.2 SIMPLIFICATIONS OF THE SYSTEM

To be able to perform the calculations the system has been simplified (tunnel element and two pontoons). The motions are calculated for two different phases and two different floating bodies. During the floating stage, only the response of the tunnel element has been considered. That is when the tunnel element will be transported. The contribution of the pontoons has been disregarded.

During the immersion phase, the system's behavior has been analyzed in two parts. Initially, the response of the tunnel element to wave force and the stability of the system due to vortex shedding has been studied (chapter 6). The tunnel element has been modeled in a 3D diffraction program (Ansys Aqwa). From the calculations in Ansys Aqwa, it can be concluded that the motions of the tunnel element in random waves are negligible and may be disregarded when analyzing movements due to wave excitation(see also appendix 6. and the previous chapter).

For the following calculations, the element has been assumed stationary. And only the response of the pontoons has been considered for different positions along the vertical alignment. In Figure 96 the modeled pontoon configuration has been depicted (with a stationary tunnel element).

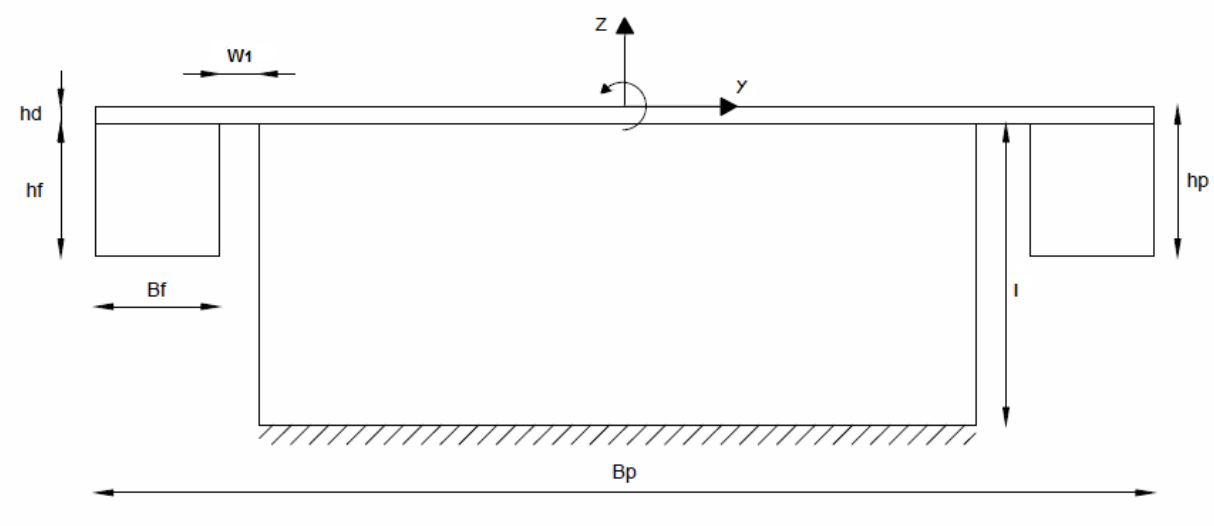

Figure 96 Modelled pontoon configuration during immersion

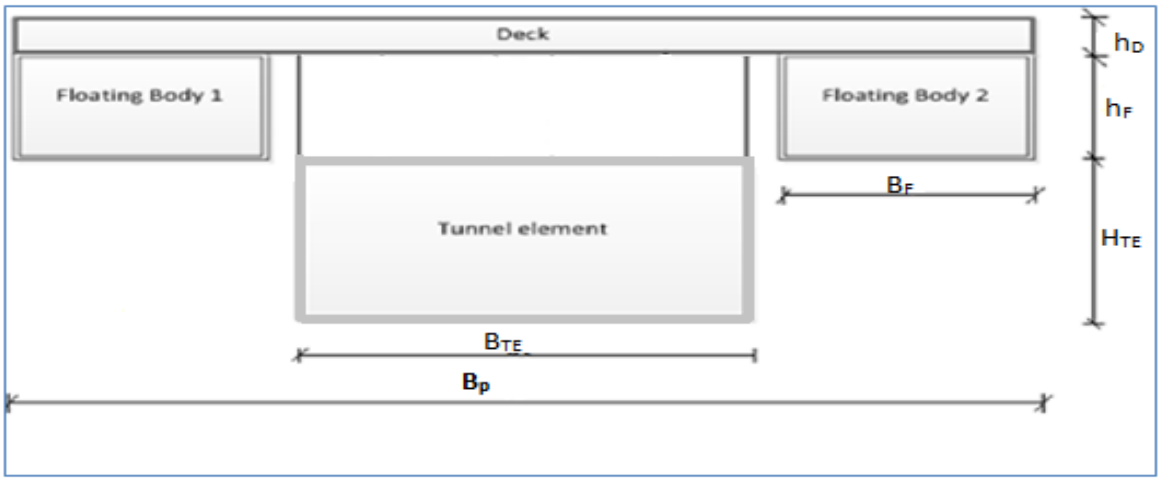

Figure 97 pontoon configuration during immersion with stationary tunnel element (drawing in not on scale)

Figure 98 Overview of the tunnel element and the two pontoons in the length direction (drawing in not on scale)

7.2.1 IMMERSION PHASE:

During the immersion phase, the pontoons are considered as a hybrid structure. Concerning the horizontal degrees of freedom, the barge is considered as it is compliant and behaves like a floating structure. While concerning the vertical degrees of freedom, it is stiff and resembles as a fixed structure and is not allowed to float freely. The contribution of the mooring lines to the first order response is considered of minor importance and is disregarded in the calculations.

First, the equation of motion is determined for both type pontoons. Subsequently, the dynamic behavior for both pontoons is analyzed separately. The procedure for the determination of the equation of motion for both pontoons is equal. The components which are dependent on the geometry of the pontoon configuration are explained in the dynamic analysis for each barge separately.

In the analysis, the coupling between the six degrees of freedom is been considered. The analysis considers various nonlinearities produced due to change in the suspension cables tension. The wave forces on the submerged parts of the pontoon are calculated by using linear wave theory thereby ignoring the diffraction effects. Numerical studies are conducted to compare the coupled response of a Catamaran pontoon with that of a Semi-submersible barge to the impact of different parameters that influence the response.

7.2.2 MODEL

To be able to model the problem, some assumption has been made. The pontoon with the suspension cables has been treated as a single system. The analysis has been carried out for six degrees of freedom under uniform wave loads.

Both pontoons types are floating structures. The tension in the suspension cables is created by ballasting the tunnel element at the immersion site. The vertical suspension cables connect the tunnel element and the pontoons. Each floating body in the system has six degrees of freedom namely: surge, sway and heave as displacement in the x, y and z directions, and rotations about these axes resulting in the roll, pitch and yaw motions (see Figure 99(a)). For the calculations, a Cartesian coordinate system is used in which the positive x-direction coincides with the longitudinal direction of the pontoons. The (x,y) plane lies at the mean water surface. The positive y-axis is in the direction of the wave propagation. The oblique waves will have an angle μ with the y-axis. The positive z-axis is directed upwards (see Figure 99(b)).

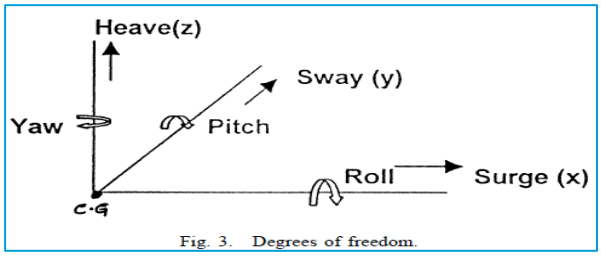

(a) Definition of the motional directions

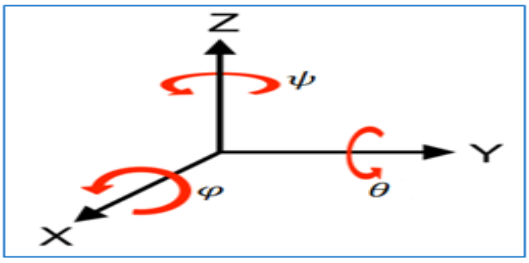

(b) Used coordinate system

Figure 99 degrees of freedom

7.2.3 ASSUMPTIONS

1) The initial pretention in all suspension cables has been assumed to be equal. However, the total pretension in the suspension cables changes with the motions of the pontoon.
2) In this part of the analysis, it has been assumed that during the immersion only the wave forces working on the system. The wave forces are estimated at the instantaneous equilibrium position. The wave forces are calculated with the linear wave theory. The wave diffraction and drift forces are neglected in this analysis.
3) Change in the pretention in the suspension cables is dependent on the position of the pontoon.
4) The pontoon is considered as a rigid body having six degrees of freedom as shown in Figure 99.
5) The pontoon is considered as a symmetrical body in surge and sway. Directionality to the wave approach has been neglected in the analysis. Only a uni-directional wave in the sway direction has been considered.
6) The damping matrix of the system has been assumed to be mass and stiffness dependent. And it depends on the initial values of the mass and the stiffness matrix

7.3 EQUATION OF MOTION

The equation of motion of the pontoons under regular waves can be presented as:

$$[\boldsymbol{M}+\boldsymbol{M_a}]\{\ddot{\boldsymbol{X}}(\boldsymbol{t})\}+[\boldsymbol{C}]\{\dot{\boldsymbol{X}}(\boldsymbol{t})\}+[\boldsymbol{K}]\{\boldsymbol{X}(\boldsymbol{t})\}=\{\boldsymbol{F}(\boldsymbol{t})\} \quad (126)$$

Where:

$[\boldsymbol{M}]$	The mass matrix of the system
$[\boldsymbol{M_a}]$	The added mass matrix
$[\boldsymbol{C}]$	The damping matrix.
$[\boldsymbol{K}]$	Stiffness matrix
$\boldsymbol{F(t)}$	The force vector consisting of Froud-Krilov components
$\boldsymbol{X(t)}$	Displacement vector of the system
$\dot{\boldsymbol{X}}(\boldsymbol{t})$	Velocity vector of the system
$\ddot{\boldsymbol{X}}(\boldsymbol{t})$	Acceleration vector of the system

To be able to determine the response of the system to the incident waves, the equation of motion has to be solved. First, the elements of the equation of motions are determined. Hereafter the characteristics of the system are used to solve the equation of motions and also to determine the motional behavior of the system.

7.3.1 MASS MATRIX

The structural mass of the pontoon is assumed to be constant for each degree of freedom. Hence the mass matrix [M] is diagonal and is constant. The added mass [M_a] due to surrounding water is considered up to the mean water-level/sea-level. The fluctuating components of the added mass matrix [M_a] due to the variable submergence of the pontoon is disregarded in the calculations, depending upon whether the water surface is above or below the mean sea level. The coupling between surge and pitch, sway and roll and another way around has been taken into account.

$$M=\begin{bmatrix} m_{pontoon} & 0 & 0 & 0 & -\sum m_i z_K & 0 \\ 0 & m_{pontoon} & 0 & -\sum m_i z_K & 0 & 0 \\ 0 & 0 & m_{pontoon} & 0 & 0 & 0 \\ 0 & -\sum m_i z_K & 0 & I_{xx-pontoon} & 0 & 0 \\ -\sum m_i z_K & 0 & 0 & 0 & I_{yy-pontoon} & 0 \\ 0 & 0 & 0 & 0 & 0 & I_{zz-pontoon} \end{bmatrix} \quad \text{and} \quad M_a=\begin{bmatrix} a_{11} & a_{12} & a_{13} & a_{14} & a_{15} & a_{16} \\ a_{21} & a_{22} & a_{23} & a_{24} & a_{25} & a_{26} \\ a_{31} & a_{32} & a_{33} & a_{34} & a_{35} & a_{36} \\ a_{41} & a_{42} & a_{43} & a_{44} & a_{45} & a_{46} \\ a_{51} & a_{52} & a_{53} & a_{54} & a_{55} & a_{56} \\ a_{61} & a_{62} & a_{63} & a_{64} & a_{65} & a_{66} \end{bmatrix}$$

The equation of motion is coupled, this means that motion in direction i will cause a force in direction–j. The diagonal terms $a_{11}, a_{22}, a_{33}, a_{44}, a_{55}, a_{66}$ represents the uncoupled terms of the mass matrix. The other terms a_{ij} represents the coupled terms. In the analysis only the uncoupled terms and coupling in surge-pitch, sway and roll are considered.

7.3.2 STIFFNESS MATRIX

The coefficients of the stiffness matrix are represented as Kij. For the derivation of the stiffness matrix the same approach has been followed as in (S. Chandrasekaran , A.K. Jain, August 2000). The coefficients are derived from reaction forces by giving the system a unit displacement in the jth degree of freedom and determining the corresponding force in the ith degree of freedom by keeping all other degrees of freedom restrained. In the initial conditions, there is a pretension To in the cables. This pretension plays an essential role in the determination of the stiffness matrix. The relation between the weight of the structure, buoyancy force and pretension is given in equation (127). Further for the derivation of the stiffness matrix, a pontoon with four suspension cables is used. In the analysis, the dynamic behavior of four and two suspension cables is analyzed. That's why the number of the suspension cables in the equation is given as n_t (see also Figure 101).

$$F_b = n_t T_0 + m_{pontoon} \quad (127)$$

The mass of the suspension cables is neglected in the derivation. The pontoons are considered as a rigid body with 6 degrees of freedom, and they are modeled as quasi-static springs.

The pontoons are symmetric in the x and y-direction. The total stiffness of the pontoons can be divided into two components, namely:

- The conventional stiffness of the pontoons with an influence of the suspension cables.
- The hydro-elastic stiffness of the pontoon depending on the water plane area A_w.

The pontoon has like every other floating structure hydro elastic coefficients in heave, pitch and roll degrees of freedom. The hydroelastic stiffness of the pontoons is determined by the water plane area and its second moments of inertia. The secant stiffness matrix is derived with respect to the gravity center by applying the principle of; $= K * x$. The total stiffness of the pontoon is determined by summing up of the components in each degree of freedom.

Surge

The stiffness of the system is determined by giving the system a unit displacement in the x-direction and keeping all degrees of freedom restrained see Figure 100. All forces are analyzed; the increase in the pretension of the each suspension cables can be given as in equation (128):

$$dT_1 = \left(\sqrt{x_1^2 + l^2} - l\right) * \frac{AE}{l} \qquad (128)$$

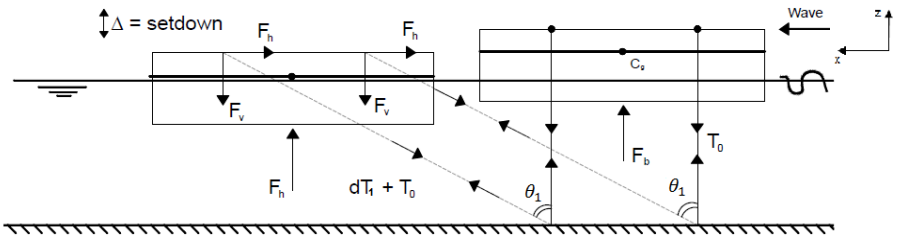

Figure 100 displacement in the surge direction

Forces and stiffness coefficients in the surge direction are formulated here next to it. The stiffness coefficients are determined by giving a displace x1 in the surge direction to the system and then determining the forces. Figure 100 shows the displaced position of the system. Due to the displacement x1, extra forces will be created in the suspension cables. And also the draft of the pontoon will be changed, the so-called set-down (Δ) is also depicted in the figure. The formulations of the forces are given in equations from (129) till equation (133). The same approach will also be used for the determination of the forces in the sway degree of freedom.

$$K_{11} = n_t * \frac{T_o + dT_1}{\sqrt{x_1^2 + l^2}} \qquad (129)$$

$$\Delta_1 = \frac{dT_1}{\rho_w * g * A_w} * n_t \qquad (130)$$

$$\cos(\theta_1) = l / \sqrt{x_1^2 + l^2} \qquad (131)$$

$$K_{31} = \frac{n_t}{X_1} * (T_o * cos(\theta_1) + dT_1 * cos(\theta_1) - T_o) \qquad (132)$$

$$K_{51} = K_{11} * z_1 \qquad (133)$$

From Figure 100 it can be concluded that by giving a displacement x1 to the system three forces are generated. Namely, the forces are generated in the surge, heave and pitch directions. The displacement x1 does not influence the other degrees of freedom.

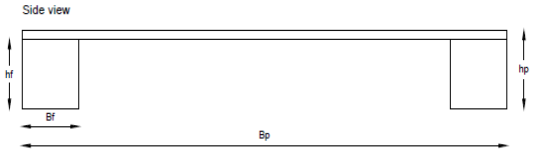

Figure 101 Top and side view pontoon (used for the derivation of the stiffness matrix)

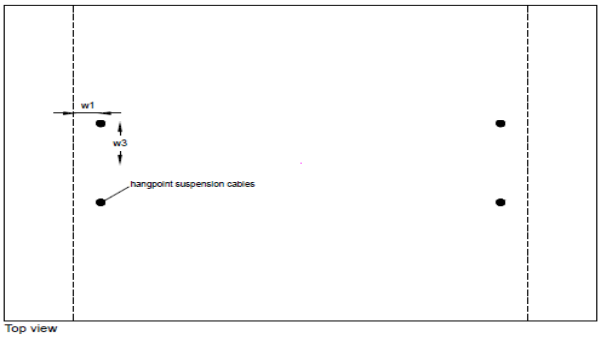

Sway

The forces in the sway degree of freedom are determined in the same manner as the force in the surge. To identify the forces, the pontoon is displaced in the y-direction. The system undergoes a displacement x2 in the y-direction. Also from the new equilibrium position, the forces are determined. The forces are given from equation(134)(140) till equation (139).

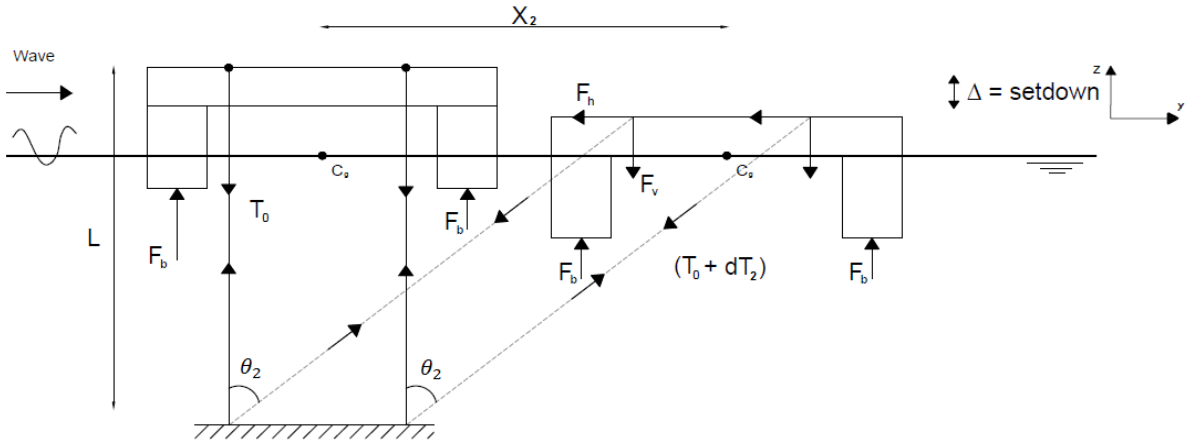

Figure 102 unit displacement in the sway direction.

The force $K_{22}\cdot z_2$ acts at the top of the pontoon and gives rise to the moment in the roll degree of freedom which is considered at the gravity centr of the pontoon. The positive sign occurs due to the counterclockwise character of the moment. By giving a unit displacement, there will be no moment in the pitch or yaw directions. That's why this component of the stiffness matrix remains unfilled.

$$dT_2 = \left(\sqrt{x_2^2 + l^2} - l\right) * \frac{AE}{l} \quad (134)$$

$$K_{22} = n_t * \frac{T_o + dT_2}{\sqrt{x_2^2 + l^2}} \quad (135)$$

$$\Delta_2 = \frac{dT_2}{\rho_w * g * A_w} * n_t \quad (136)$$

$$\cos(\theta_2) = \frac{l}{\sqrt{x_2^2 + l^2}} \quad (137)$$

$$K_{32} = \frac{n_t}{X_2} * (T_o * \cos(\theta_2) + dT_2 * \cos(\theta_2) - T_o) \quad (138)$$

$$K_{42} = K_{22} * z_2 \quad (139)$$

Heave:

To be able to determine the forces in the heave direction, a unit displacement is given to the pontoon in the vertical direction. All other degrees of freedom remains unchanged. From Figure 103 it can be concluded that by giving a displacement in the heave directions only the forces in the vertical direction will be affected. From the equilibrium of forces in the heave direction the expression for the vertical stiffness parameterK_{33} can be derived as in equation (140):

$$K_{33} = n_t * \frac{AE}{l} + \rho_w * g * A_w \quad (140)$$

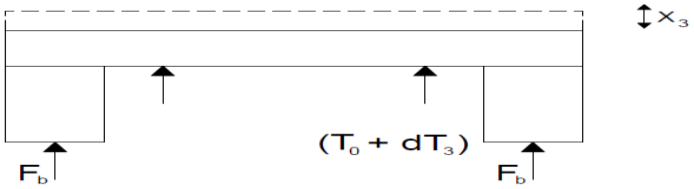

Figure 103 displacement in the heave direction

Roll

The coefficients of the fourth column of the stiffness matrix are obtained by giving an arbitrary rotation ϕ in the roll degree of freedom about the x-axis with all other degrees of freedom restrained. Summations of moments due to the resulting forces about x-axis are given in Figure 104. By giving an arbitrary rotation φ in the roll degree of freedom, the change in the initial pretension, in each cable is given by:

$$dT_4 = \frac{AE}{l} \cdot \left(\frac{B_p}{2} - B_f - tolerance - \frac{W_1}{2}\right) \cdot \cos(\varphi) \cdot \varphi = \frac{AE}{l} \cdot W_2 \cdot \cos(\varphi) \cdot \varphi \quad (141)$$

As a result of this, the small angle approximation is applied. From the equilibrium in the heave direction the spring stiffness in the vertical direction can be found:

$$K_{34} = n_t \cdot \frac{AE}{l} \cdot W_2 \cdot \cos(\varphi) \quad (142)$$

By giving a displacement ϕ no force is generated in surge or sway directions. Therefore, the elements K_{14} and K_{24} are equal to 0. In the equations above ϕ is arbitrary rotation in the roll degree of freedom, dT_4 is the increase in the suspension cable force. The stiffness in the roll degree is determined by the summation of the roll moments and dividing by the angle ϕ. The roll stiffness can be expressed as:

$$K_{44} = \left(I_{xx} \cdot \rho_w \cdot g - BG \cdot m_{pontoon} \cdot g\right) + \frac{n_t}{\varphi} * T_o * \left(h_p + 1 - KG\right) * \sin(\varphi) + n_t * \frac{AE}{l} * W_2 * \cos(\varphi) \quad (143)$$

Here in is the I_{xx} is the second moment of area of the cutwater the plane, BG is the distance between the centr of buoyancy and centr of gravity. The distance BG is calculated in section 4.6 Static Stability. From Figure 104 it can be concluded that there are no moments develop along the pitch and yaw degrees of freedom.

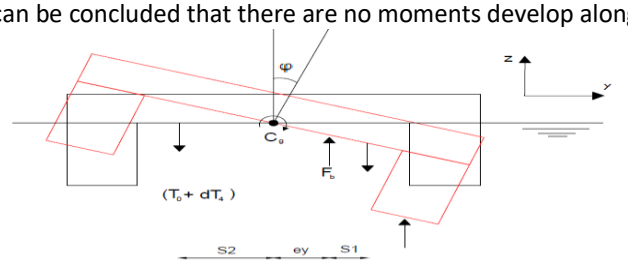

Figure 104 displacement in the roll degree of freedom

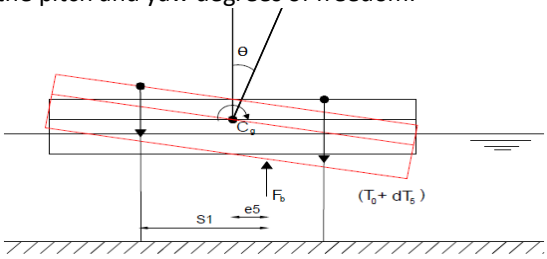

Figure 105 displacement in the pitch degree of freedom

Pitch:

The coefficients of the fifth column of the stiffness matrix are obtained by giving an arbitrary rotation θ in the pitch degree of freedom about the y-axis with all other degrees of freedom restrained. Summation of moments due to the resulting forces about the y-axis is given in Figure 104.The same procedure is followed as for roll degree of freedom to obtain the stiffness coefficients.

$$dT_5 = \frac{AE}{l} \cdot (W_3) \cdot \cos(\theta) \cdot \theta \quad (144)$$

$$K_{35} \cdot \theta = nt \cdot dT_5 \quad (145)$$

$$K_{35} = n_t \cdot \frac{AE}{l} \cdot W_3 \cdot \cos(\theta)$$

Again dT_5 is the change in the pretention of the suspension cables due to the rotation θ. In the equation above W_3 is the distance of the point of the suspension cables from the rotation point. Due to symmetry, the rotation point coincides with the center of gravity in the (x,y) plane. The force in the heave is given by equation (145). And the stiffness in the pitch direction can be expressed as:

$$K_{55} = \left(I_{yy} \cdot \rho_w \cdot g - BG \cdot m_{pontoon} \cdot g\right) + \frac{n_t}{\theta} * T_o * \left(h_p + 1 - KG\right) * \sin(\theta) + n_t * \frac{AE}{l} * W_3 * \cos(\theta) \quad (146)$$

When an arbitrary rotation is given in the pitch direction, no moments develop along the roll, yaw and sway directions.

Yaw :

By giving an arbitrary rotation ψ see also Figure 106 the suspension cable will be elongated. The extended length of the cables is expressed by equation

$$l_6 = \sqrt{\left((W_2^2 + W_3^2) \cdot \psi^2\right) + l^2} \quad (147)$$

- The change in of the pretension force in the suspension cables is given by equation (148).

$$dT_6 = \frac{AE}{l} \cdot (l_6 - l) \quad (148)$$

- The force in the heave direction due to the rotation ψ is given by equation (149).

$$K_{36} = n_t \cdot T_0 \left(\frac{l}{l_6} - 1\right) + n_t \cdot dT_6 \left(\frac{l}{l_6}\right) \quad (149)$$

- When the pontoon undergoes a rotation, ψ no moments will develop in pitch and roll direction. The moment in the Yaw direction is given by equation (150).

$$K_{66} = n_t \cdot \frac{(T_0 + dT_6)}{l_6} \cdot (W_3^2 + W_2^2) \quad (150)$$

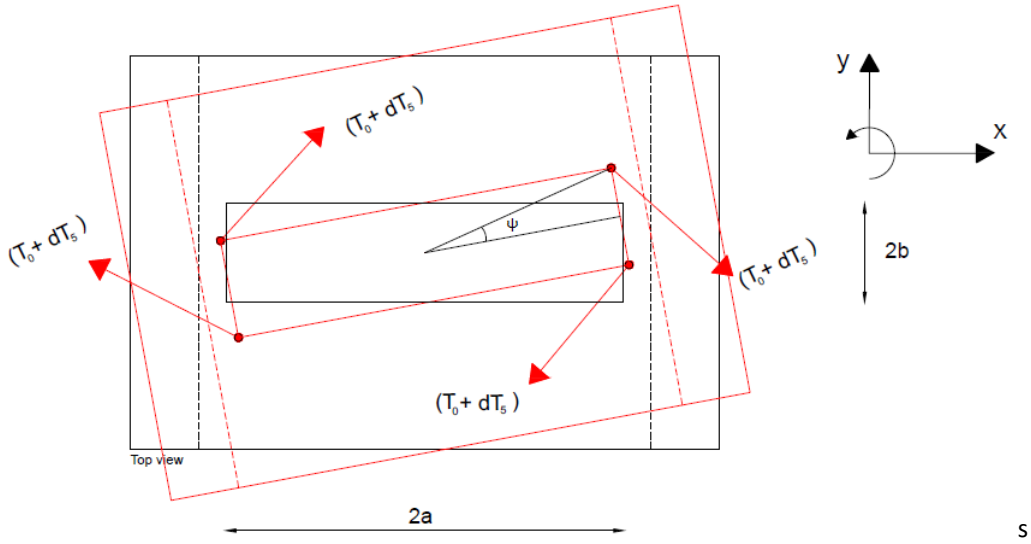

Figure 106 displacement in the yaw degree of freedom

The total stiffness matrix can be expressed as:

$$K = \begin{bmatrix} K_{11} & 0 & 0 & 0 & 0 & 0 \\ 0 & K_{22} & 0 & 0 & 0 & 0 \\ K_{31} & K_{32} & K_{33} & K_{34} & K_{35} & K_{36} \\ 0 & K_{42} & 0 & K_{44} & 0 & 0 \\ K_{51} & 0 & 0 & 0 & K_{55} & 0 \\ 0 & 0 & 0 & 0 & 0 & K_{66} \end{bmatrix}$$

From the presented stiffness matrix it can be seen that there is coupling between the various degrees of freedom. The off-diagonal terms in the matrix reflect the coupling effect between the multiple degrees of freedom. Especially the coupling is most active in the heave degree of freedom. From the matrix, it can be concluded that motion in each degree of freedom will have an influence on the movement in heave. The components of the stiffness matrix also include nonlinear terms.

The nonlinear terms are related to the displacement of the pontoon. The coefficients in the stiffness matrix are dependent on the force change in the suspension cables. This change also affects the buoyancy of the pontoons. Hence it can be stated that the stiffness matrix is response-dependent. And therefore the coefficients are time-dependent.

For each time value when the displacement is changed. The coefficients of the matrix will vary correspondingly. In the course of time, the values are replaced by a new value depending on the response value. Due to nonlinearities, the equation of motion can only be solved in the time domain.

7.3.3 Damping Matrix

The damping matrix is assumed to be proportional to the mass matrix [M] and stiffness matrix [K]. Also, it's assumed that the damping matrix is a diagonal matrix. In reality, the hydrodynamic damping matrix is a (6x6) matrix. The coupling effects are also present.

The coupling coefficients of the damping matrix can only be calculated with the aid of diffraction analysis, or they can be measured in a model test. Nevertheless, for now, the damping matrix is assumed to be a diagonal matrix. The orthogonal terms of the modal damping matrix can be expressed as:

$$E \cdot C \cdot E^T = 2 \cdot \xi_i \cdot \omega_i \cdot m_i \quad (151)$$

Where

E	Eigen matrix of the system
ξ_i	Critical damping ratio in the ith degree of freedom (taken as 0.05)
ω_i	Natural frequency in the ith degree of freedom
m_i	Modal mass in the ith degree of freedom

7.3.4 Force Vector

The wave forces are evaluated by using Airy's linear wave theory. To be able to use linear wave theory the wave height has to be small in comparison to its length, L. During the normal conditions in the Fehmarnbelt this is also the case. By knowing the water particle kinematics, the hydrodynamic force vector can be calculated in each degree of freedom. According to the linear wave theory, the undisturbed wave potential for the regular waves with propagation direction μ can be expressed as:

$$\phi_o = \frac{\zeta_a \cdot \omega}{k} \cdot \frac{\cosh[k \cdot (h+z)]}{\sinh(k \cdot h)} \cdot \cos(\omega t - kx \cdot \cos(\mu) - ky \cdot \sin(\mu)) \quad (152)$$

The pressure of the undisturbed wave can be expressed as:

$$P = -\rho \frac{\partial \phi}{\partial t} - \frac{1}{2}\rho \cdot (u^2 + w^2) - \rho g z \quad (153)$$

In the above equation, u and w represent the horizontal and vertical velocities of the water particle and z is the elevation. From Archimedes, it follows that the buoyancy force is equal to the weight of the pontoon. This static component is not taken into account in the dynamic analysis. The dynamic force component consists of three translational and three rotational forces and moments working on the system. The dynamic force components operating on the pontoon due to Froude-Krilov pressure can be expressed as:

$$\begin{aligned} P &= -\rho \frac{\partial \phi}{\partial t} \\ &= \rho \cdot \zeta_a \cdot g \cdot \frac{\cosh[k \cdot (h+z)]}{\sinh(k \cdot h)} \cdot \sin(\omega t - kx \cdot \cos(\mu) - ky \cdot \sin(\mu)) \end{aligned} \quad (154)$$

Due to the dynamic pressure gradient, a force will be applied to the submerged parts of the pontoons. When the acceleration varies over the body, then the total Froude-Krilov force may be calculated as the volume integral.

$$F_{FK} = \rho \int \ddot{x} \cdot dV \quad (155)$$

Alternatively, the Froude-Krilov force may be calculated by the surface pressure integration. For the analysis, the surface pressure integration is used in conjunction with the volume integration method. The vertical pressures are calculated by the pressure surface integration. For the long prismatic members as the floaters, it is more convenient and physically representative for the actual force application, to use the pressure integration for the axial forces over the members ends. And for the transverse forces is the volume integration method is applied. The forces are calculated by taking an integral till the still water level.

The surface elevation of a wave with amplitude ζ_a at any instant of time t traveling horizontal and transversal direction x,y with an angle μ can be denoted as:

$$\zeta(x, y, t) = \zeta\_a \cdot cos(kx \cdot \cos(\mu) + ky \cdot \sin(\mu) - \omega t) \quad (156)$$

The horizontal and vertical accelerations at the position z measured from the mean water level in depth of water h are given by:

$$\ddot{u}(x,y,t) = \zeta_a \cdot \omega^2 \cdot \frac{\cosh[k \cdot (h+z)]}{\sinh(k \cdot h)} \cdot \cos(kx \cdot \cos(\mu) + ky \cdot \sin(\mu) - \omega t) \quad (157)$$

$$\ddot{z}(x,y,t) = \zeta_a \cdot \omega^2 \cdot \frac{\sinh[k \cdot (h+z)]}{\sinh(k \cdot h)} \cdot \sin(kx \cdot \cos(\mu) + ky \cdot \sin(\mu) - \omega t) \quad (158)$$

By assuming deep water, $water\ depht = h > {}^{\lambda}/_{2}$ and a propagation angle of μ=0 the surface elevation, wave pressure and water particle accelerations can be expressed as:

$$\zeta(x,t) = \zeta_a \cdot cos(kx - \omega t) \quad (159)$$

$$P(x,t) = \rho \cdot \zeta_a \cdot g \cdot e^{k \cdot z} \cdot \cos(kx - \omega t) \quad (160)$$

$$\ddot{u}(x,t) = \zeta_a \cdot \omega^2 \cdot e^{k \cdot z} \cdot \cos(kx - \omega t) \quad (161)$$

$$\ddot{z}(x,y,t) = \zeta_a \cdot \omega^2 \cdot e^{k \cdot z} \cdot \sin(kx - \omega t) \quad (162)$$

Finally, the force vector can be given as:

$$F_{FK} = \begin{bmatrix} F_{surge} \\ F_{sway} \\ F_{heave} \\ M_{roll} \\ M_{pitch} \\ M_{yaw} \end{bmatrix}$$

Now all the components of the equation of motion are known, it can be solved, and the movements of the pontoons can be predicted in 6 degrees of freedom under different loading conditions. However, we saw already that the stiffness matrix contains nonlinear elements. This means that the concept of the RAO's is not applicable. The stiffness matrix is response-dependent at each instant of time. Also, the added mass and the radiation damping terms are fluctuating with the frequency, and they are not constant. However, in the model, they are assumed as constant. This is a rough approximation. The non-diagonal and frequency dependent terms of the added mass and radiation-damping matrices can be solved by the aid of Diffraction analysis. Due to nonlinear terms in the stiffness matrix, the equation of motion can only be solved in the time domain by using a numerical integration procedure.

There are several procedures available, one should be chosen which incorporates changes in spring coefficients which vary with suspension cable tension. From literature survey, it appears that the Newmark's β time integration procedure can be used to solve the equation of motion. At each time step, the stiffness matrix and the force vector should be updated, and the equation of motion should be solved for each time step.

To analyze the dynamical behavior of the system, first, the natural frequencies for the both pontoons are determined. Then, the calculated natural periods of the barges are used to adjust the added mass matrix with the aid of the provided data by Vughts (1969). Subsequently, the system behavior is calculated for different wave periods in beam waves. The equation of motion is solved in the time domain by applying the Newmark Beta Method. After evaluation of the dynamic behavior of the system in the time domain, the RAO's of the system are determined by taking only the linear part of the of the stiffness matrix in into consideration. The RAO's are used to predict the dynamic behavior of the pontoons for waves in different environmental conditions.

7.4 SOLUTION OF EQUATION OF MOTION IN TIME DOMAIN

In this part of the report, the dynamic behavior of the pontoons is analyzed in the time domain. Before performing this calculation, the natural frequencies of the barges were calculated. See also section 8.2.1 and 8.3.1. The force vector has been determined by using the Linear wave theory. The equation used for the force calculation has already been discussed.

The procedure which has been followed to calculate the wave forces on pontoons is in detail described in section 8.3 The focus in this section will be on the time domain calculations and the interpretation of the results.

The numerical studies conducted to obtain the natural frequencies and natural periods are described in section 8.2.1 and 8.3.1. Table 37 and Table 48 show the geometrical and mass properties of the pontoons. Water particle kinematics are evaluated using Linear wave theory. The primary assumption made for the force calculations is that the waveform is such that the wave height (H), is small in comparison to its length (L) and that the wave height is much smaller than water depth (h). The force vector is calculated for beam waves (90°). That means that the force is mainly active in sway, heave, and roll degrees of freedom. Further, the wave forces on the suspension cables are disregarded in the calculations..

Numerical integration

The equation of motion, having time-dependent components and motion dependent components in the stiffness matrix, can only be solved by using a numerical time integration procedure. There are different procedures available to solve the equation. One should be chosen, which could incorporate the change of the stiffness matrix in each time step.

The most general approach to solve the equation of motion in the time domain is the direct numerical integration of the dynamic equilibrium equations. The main idea behind this approach is that when the solution is defined as time zero then the next time step is calculated and the solution must satisfy the boundary conditions. Most of the available methods use a constant time step Δt, 2Δt …n•Δt increase for the each calculation. The primary distinction between the methods is that almost all the available techniques can be divided into two groups and may be classified as explicit or implicit time integration methods.

Explicit methods use the differential equation at a time step t to predict the dynamic behavior of the structure at the time step t+Δt. To account the stiff behavior of the real structures, a very small time step is required to obtain a stable solution. The implicit time integration methods use a set of linear equations at time step t+Δt to satisfy the equation of motion after the solution was found at the time step t+Δt. This technique requires the solutions of a set of linear equations at each time step. But larger time steps can be used to solve the equation of motion. To use a numerical time integration method, three requirements have to be met. The conditions can be summarized as:

1) As the time step decreases, the solution should approach the exact solution.
2) The numerical solution should be stable in the presence of the round-off errors.
3) The procedure should provide results which could be close to the exact solution of the system.

Two numerical time integration methods were used to predict the dynamic behavior of the pontoons namely: The explicit Newmark beta method and the implicit Newmark beta method. For the explicit time integration method, integration at each time step is done to obtain the dynamic force balance. The displacement and the velocity were assumed at the time step t=0 to be zero. The acceleration vector is determined for the t=0 by taking the force balance at t=0. The displacement, velocity, and acceleration for the time step t+1 were calculated by using the following set of equations.

$$X_{t+1} = X_t + \dot{X} \cdot \Delta t + [(0.5 - \beta) \cdot \ddot{X}_t + \beta \ddot{X}_{t+1}] \cdot \Delta t^2 \quad (163)$$

$$\dot{X}_{t+1} = \dot{X}_t + [(1 - \lambda) \cdot \ddot{X}_t + \lambda \ddot{X}_{t+1}] \cdot \Delta t \quad (164)$$

$$\ddot{X}_{t+1} = \boldsymbol{M}^{-1}[F_{t+1} \cdot \Delta t - \boldsymbol{C} \cdot \dot{X}_t - \boldsymbol{K} \cdot X_t] \quad (165)$$

Where

$\boldsymbol{M}$	Mass matrix
$\boldsymbol{K}$	Stiffness matrix
$\boldsymbol{C}$	Damping matrix
X_{t+1}	Displacement vector at time step $(t+1)$
$\dot{X}_{t+1}$	Velocity vector at time step $t+1$
$\ddot{X}_{t+1}$	Acceleration vector at $t+1$
F_{t+1}	Force vector at time step $t+1$
λ	Newmark constant $= 1/2$
β	Newmark constant $= 1/4$

In order to meet the requirements mentioned before a convergence criterion for the displacement was used:

$$\frac{X_{t+1} - X_t}{X_{t+1}} < 0.2\ \% \qquad (166)$$

If the convergence criterion was not met, then the computation was repeated till the convergence criterion was met. But it was found that for some time steps the convergence criterion was not met even by doing more than 30 iterations. To get some plausible results the time step was chosen very small Δt=0.001. The calculation time was very long. To calculate the displacement vector for 50 seconds a computation time more than half hour was required. Therefore, this method has not been found to be suitable for the further elaboration of the solution.

That's why an implicit Newmark beta method was used to predict the dynamic behavior of the pontoons in waves. This method determines the solution at time t+1 from the equation of motion at time t+1. Because the resisting force K_{t+1} is an implicit nonlinear function of the unknown displacement X_{t+1} iteration is required in this method. For the iteration, Newton-Raphson iterative procedure was used. As convergence criteria again equation (166) was used. At each step, the force vector is updated to take into account the change of the force in the suspension cable.

The primary assumption by applying this methodology is: the motion quantities of the system at the time (t) are known, and that those at the time (t+1) can be computed. Calculations start at the time t=0 at which the system is subjected to known initial conditions, and the calculations are carried out for each time step. Until the entire time-history of the motions, accelerations, and velocities are computed.

Again at the time t=0 the motions and the velocity of the system assumed to be zero. The initial acceleration vector has been calculated by equation (167) The stiffness matrix K(X,t) has been described such that its values are known at the time t=0 and the values of the matrix at (t+1) are computed by the Newmark integration scheme. Newton-Raphson iteration is applied to meet the convergence criterion.

$$\ddot{X}_0 = \boldsymbol{M}^{-1}[F_1 \cdot \Delta t - \boldsymbol{C} \cdot \dot{X}_0 - \boldsymbol{K_0} \cdot X_0] \qquad (167)$$

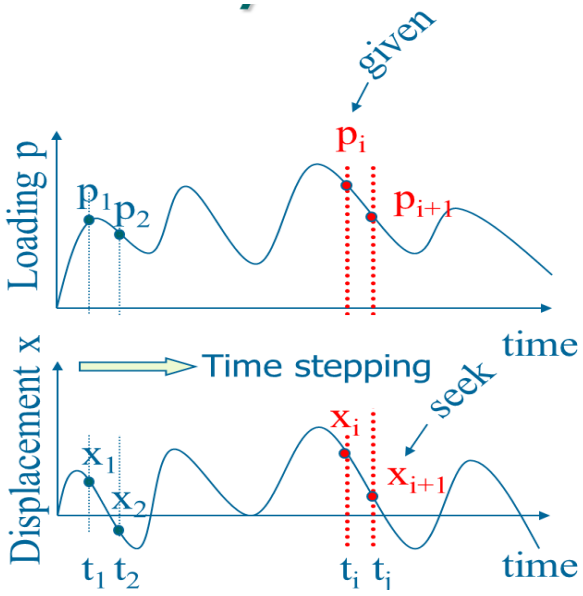

Figure 107 Principle of Newmark-beta method (Aurel Stratan, 2014)

For the calculations, the following scheme is followed to evaluate the dynamic behavior of the pontoons in beam waves.

Step		Action
1	a	Assuming the values of the displacement vector and velocity vector $X_0 = [0]$ and $\dot{X}_0 = [0]$
	b	Determining the Mass matrix and damping matrix $\boldsymbol{M}$ and $\boldsymbol{C}$
	c	Determining the initial value of the stiffness matrix $\boldsymbol{K_0}$
	d	Computing the values of acceleration vector $\ddot{X}_0 = \boldsymbol{M}^{-1}[F_1 \cdot \Delta t - \boldsymbol{C} \cdot \dot{X}_0 - \boldsymbol{K_0} \cdot X_0]$
2	a	Selecting proper time step Δt for the calculations presented here, time step was selected as 0.1 [s]
	b	Selecting the integration constants $\lambda = \frac{1}{2}$ and $\beta = \frac{1}{4}$
	c	Calculating the constants $a = \frac{M}{\beta \cdot \Delta t} + \frac{\lambda \cdot C}{\beta}$ and $b = \frac{M}{2\beta} + \Delta t \left(\frac{\gamma}{2\beta} - 1\right) \cdot C$
3	a	Calculating the effective force vector $\Delta \widehat{P_i} = (F_{i+1} - F_i) + a \cdot \dot{X}_i + b \cdot \ddot{X}_i$
	b	Calculating the effective stiffness matrix $\widehat{K_i} = K_i + \frac{\gamma}{\beta \Delta t} \cdot C + \frac{1}{\beta \cdot \Delta t^2} \cdot M$
4	a	Calculating the increment of the motion vector $\Delta X_i = \frac{\Delta \widehat{P_i}}{\widehat{K_i}}$
		Calculate the new value of the displacement vector $X_{i+1} = X_i + \Delta X_i$
	b	Check the convergence $\frac{X_{t+1} - X_t}{X_{t+1}} < 0.2\ \%$ → if the convergence is met then go to step 5 else perform the Newton-Raphson iteration (4.c)
	c	Newton-Raphson iteration (iteration j=1,2,…) $\Delta X_j = \frac{\Delta R_j}{\widehat{K_T}}$ → $\Delta R_j = \Delta \widehat{P_i}$
	d	Calculate the tangential stiffness matrix $K_T = K_i \cdot \Delta x_i$
	e	Calculating the effective tangential stiffness matrix $\widehat{K_T} = K_T + \frac{\gamma}{\beta \Delta t} \cdot C + \frac{1}{\beta \cdot \Delta t^2} \cdot M$
	f	Calculate tangential stiffness vector $\Delta f_j = f_j - f_{j-1} + \left(\widehat{K_T} - K_T\right) \cdot \Delta x_j \Delta R_{j+1} = \Delta R_j - \Delta f_j$
	g	Calculate the new motional displacement vector $X_{i+1}{}^{j} = X_{i+1}{}^{j-1} + \Delta X_j$
5	a	Calculate the incremental of the acceleration vector $\Delta \ddot{X}_i = \frac{1}{\beta \Delta t^2} \cdot \Delta X_i - \frac{1}{\beta \Delta t} \cdot \dot{X}_i - \frac{1}{2\beta} \cdot \ddot{X}_i$
	b	Calculate the incremental of the velocity vector $\Delta \dot{X}_i = \frac{\gamma}{\beta \Delta t} \cdot \Delta X_i - \frac{\gamma}{\beta} \cdot \dot{X}_i - \Delta t \left(1 - \frac{\gamma}{2\beta}\right) \cdot \ddot{X}_i$
	c	Calculate the new value of the acceleration vector $\ddot{X}_{i+1} = \ddot{X}_i + \Delta \ddot{X}_i$
	d	Calculate the new value of the velocity vector $\dot{X}_{i+1} = \dot{X}_i + \Delta \dot{X}_i$
6	a	Update the stiffness matrix and go to step 3.

Table 32 Newmark-ß Method Scheme [(Andrea Calabrese and Giorgio Serino), (Lyngs, 2008)]

7.5 RESULTS AND DISCUSSION

Numerical studies are conducted to compare the dynamical behavior of Catamaran pontoon with that of Semi-submersible. The dynamic behavior of both barges is analyzed close to the natural frequencies for each barge for wave heights of 1, 1.2 and 2 m and the position of tunnel element 1 m below the sea surface. Also, the effect of the wave periods is being taken into account by calculating the dynamical behavior for different wave periods. In this way, the near-resonating behavior and motional characteristics in various environmental conditions are analyzed.

7.5.1 SEMISUBMERSIBLE PONTOON

The motions for the Semi-submersible pontoon are given for a wave period T_p 13 [s] and a wave height of 1 [m] in Figure 108 and Figure 109. For the calculations, the presented scheme in table Table 32 is used. A computer program in Maple software has been developed for this calculations. This program is given in Appendix7. First, the results for a pontoon with four suspension cables are discussed, subsequently, the results for a pontoon with two suspension cables are presented.

As we can see from the results, the motions in soft degrees of freedom are relatively small. Even for very long waves. The wavelength for a T_p of 13 [s] is approximately 264 m. For very long waves the pontoon is quite stable in the soft degrees of freedom. The motional limits do not exceed. However, in the stiff degrees of freedom, the motions become problematic, and there is the possibility of breaking of the suspension cable. Also from the results, it can be concluded that the movements in the surge yaw and pitch are low. That was also expected. Because, in beam seas these degrees of freedom are not attacked by waves.

Due to coupling the motions in these degrees of freedom are very small and can be considered as insignificant and can be neglected. In Figure 110 the motions are given for a wave period of 13 s and a wave height of 2 m. Again the movements in the soft degrees of freedom still quite small compared to those in stiff degrees of freedom. Especially the motions in heave are exceeded by a factor 15. It is evident that the tunnel element cannot be immersed in these conditions. From the results, it can be concluded that for the Semi-submersible pontoon in long waves the motions in the stiff degrees of freedom are determinative for immersion operation.

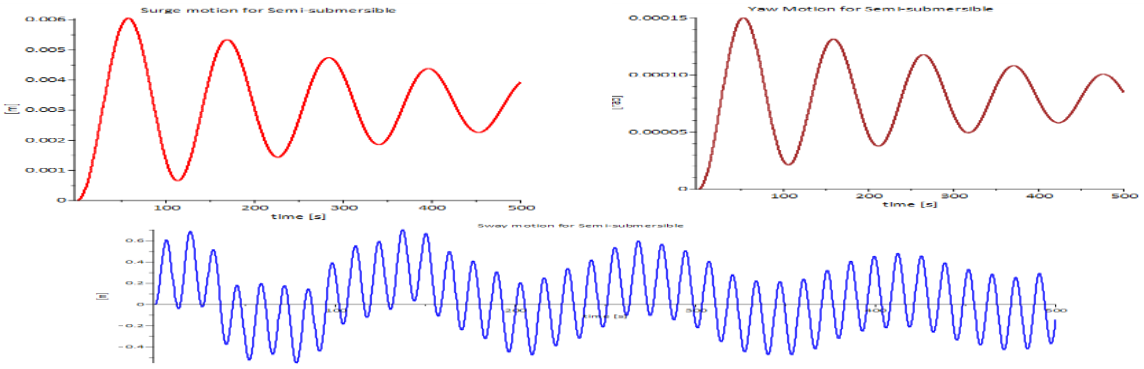

Figure 108 Motions of Semi-submersible in 'soft' degrees of freedom for Tp=13 [s] and H=1m

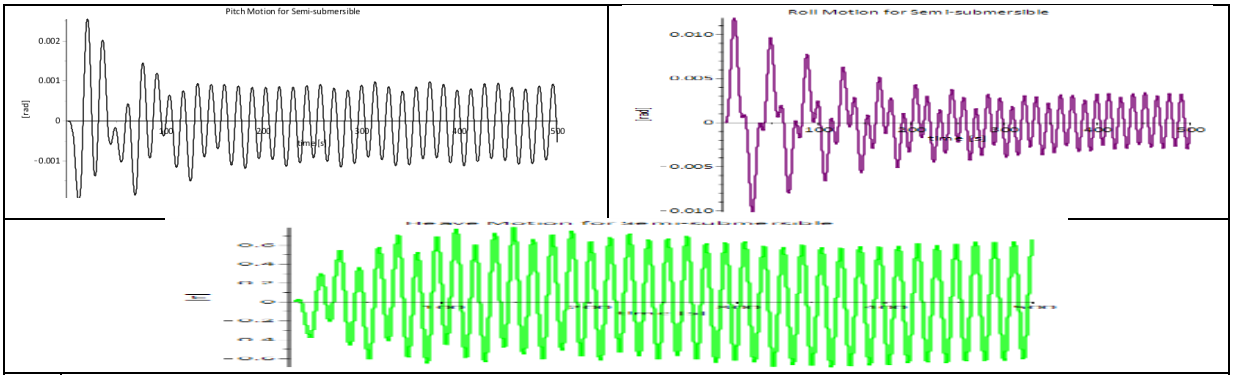

Figure 109 Motions of Semi-submersible in 'stiff' degrees of freedom for Tp=13.1 [s] and H=1m

The natural frequencies in the stiff degrees of freedom are relatively small. For heave, roll and pitch the pontoon has respectively the following natural frequencies: T_{heave}=3.82[s], T_{roll}=1.28[s] and T_{pitch} = 7.80[s]. For this periods is the dynamic behavior also has been investigated. It appears that the pontoon is quite insensitive for short waves. The motions are negligible. In Figure 111 the motions are given for the near-resonant behavior in heave. As from the figure it can be seen that the motions are negligible. The pontoon will undergo motion with small amplitude and high frequency.

Also, the accelerations have been calculated. The accelerations in sway, heave and roll are given Figure 112. As we can see the accelerations in sway already exceeds the limit values in SLS (see also section 4.7). This means that the accelerations of the pontoons are dependent on the wave height. Even for lower wave heights, the acceleration limit in sway are exceeded. It appears from the calculations that for a wave height of 1m the accelerations in sway do not exceed the limit value. From the point of view of operability, a wave height larger than 1m can be considered as not workable. The operability is discussed in detail in chapter 8.

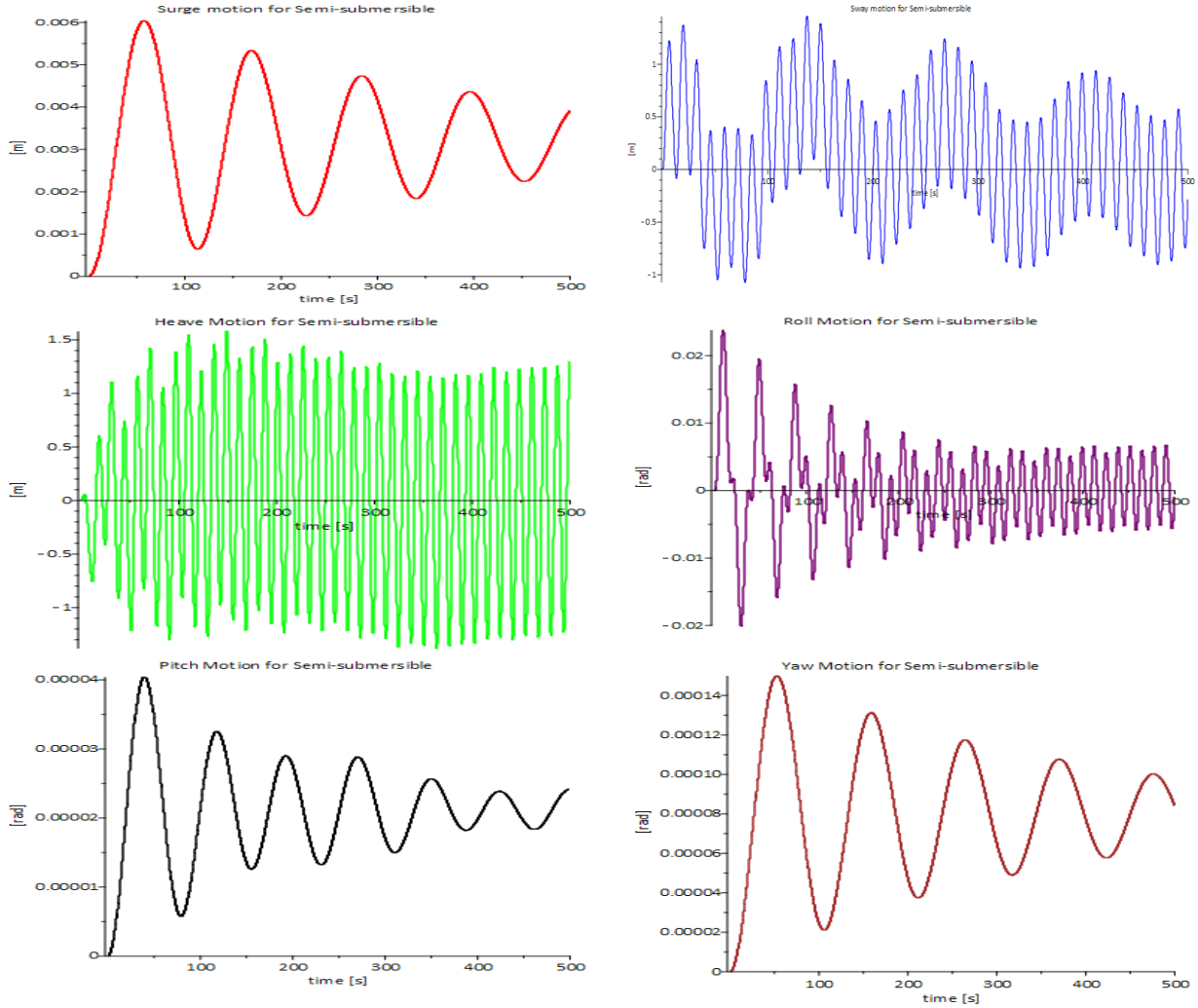

Figure 110 Motions of Semi-submersible in 6 degrees of freedom for Tp=13 [s] and H=2m

When applying two suspension cables as traditionally done, the natural frequencies in pitch increases from 7.80[s] to 12.4 [s]. Also, the natural frequency in yaw increases slightly from 14.7 [s] to 15.1 [s]. Due to small waterplane area (Aw), the effect of applying of two suspension cable in yaw degree of freedom is relatively lower than for the Catamaran as it is discussed later. If we compare Figure 108, and Figure 109 to the Figure 113 it can be seen that the motions of the pontoon increase slightly, when applying two suspension cables. In both cases, the motions in heave are the most sensitive to the near resonating behavior. From the calculations, it can be concluded the motional limits in heave are exceeded by a factor seven and in roll by a factor two. Also, the acceleration in heave are five times greater than limit values. From the results, it appears that it is not possible to immerse tunnel element safely during the conditions with long wavelengths.

However, very long waves are not likely to occur in Fehmarnbelt. To assess the dynamic characteristics of the Semi-submersible barge for waves in Fehmarn belt. The motions are calculated for a wave with a wave height of 1.2 m and period of 6.5 s. This wave is not exceeded in 95% of the time in the studied area. The calculations are performed for a 2-wire and a 4-wire pontoon. The results are presented Figure 114. The motions for two cable configurations are given in green and the motions of four cable configurations are given in red.

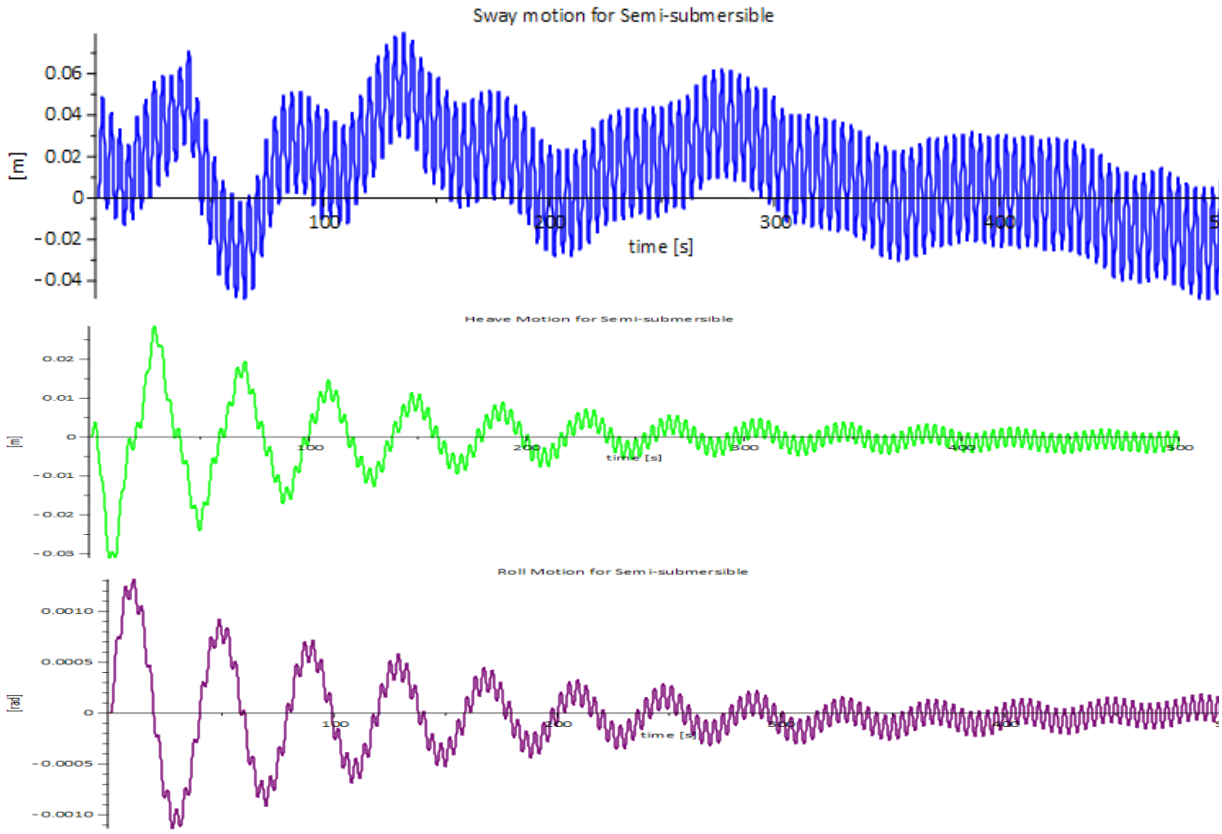

Figure 111 Motions of Semi-submersible in sway, heave and roll degrees of freedom for Tp=3.82 [s] and H=2m

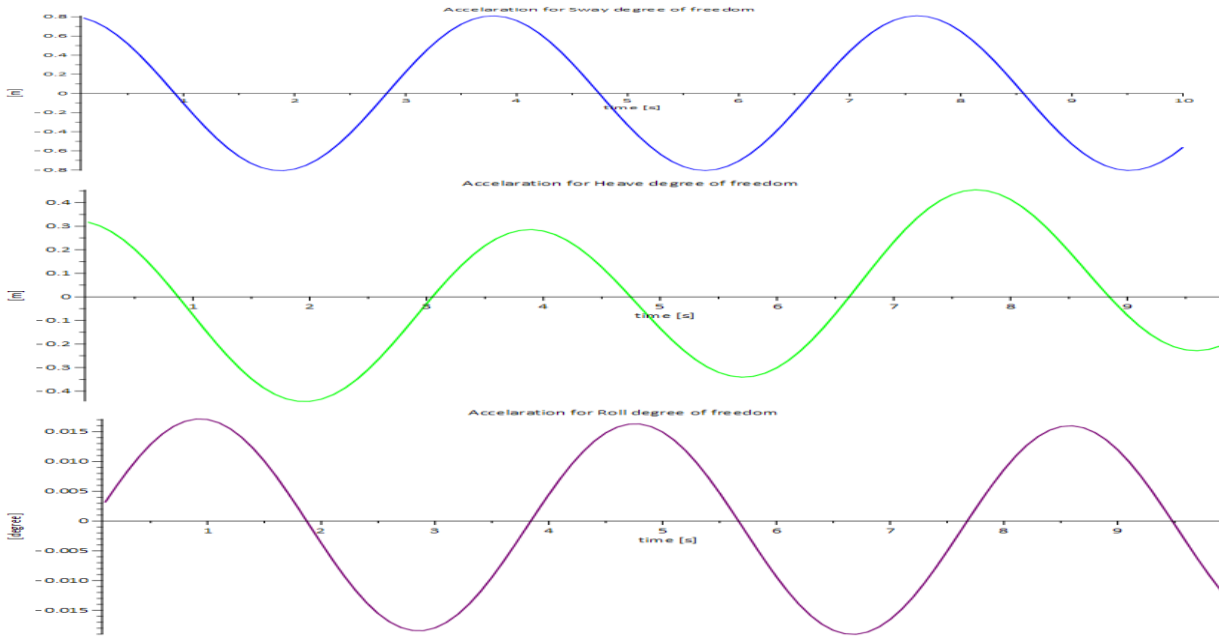

Figure 112 Accelerations of Semi-submersible in sway, heave and roll degrees of freedom for Tp=1.4 [s] and H=2m

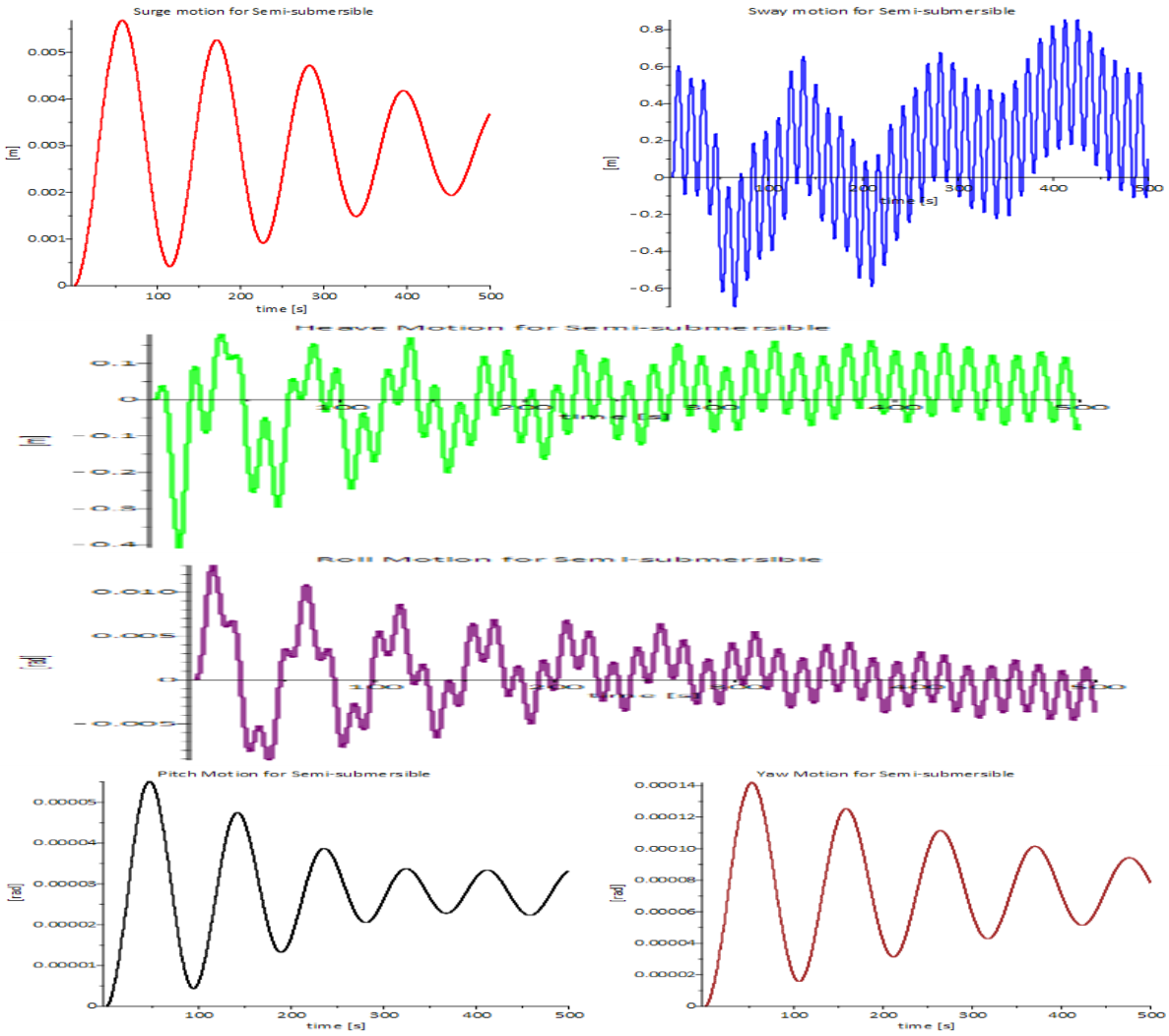

Figure 113 Motions of Semi-submersible in 6 degrees of freedom for T=13 [s] and H=1m (2 suspension cables applied)

From Figure 114 we can see that the cable configuration most influences the motions in pitch and yaw and sway and surge degrees of freedom. The last three are the so-called soft degrees of freedom. Motions in heave and roll are less sensitive to the cable configuration. The overall conclusion related to the suspension cable configuration is that the pontoon with the two-cable arrangement is more sensitive in soft degrees of freedom to waves.

By comparing the forces in the suspension cables and accelerations, it appears that a pontoon with four suspension cables has in heave almost have the same force fluctuation as a pontoon with two suspension cables. From this, it can be concluded that the capacity of the wires should be doubled to handle the force fluctuations. Also, a pontoon with four suspension cables has larger acceleration amplitudes. The amplitude in heave even exceeds the limit value. In general, it can be stated that a barge with four suspension cables has larger accelerations and force fluctuation in heave than a pontoon with two suspension cables.

For very short waves T = 1 [s] the motions and accelerations of the pontoon are negligible. For example, waves close to the natural frequency in the roll degree of freedom are of minor importance. The wave force decreases drastically for high frequencies. This means that for higher frequencies the wave impact on the motions of the pontoon is negligible.

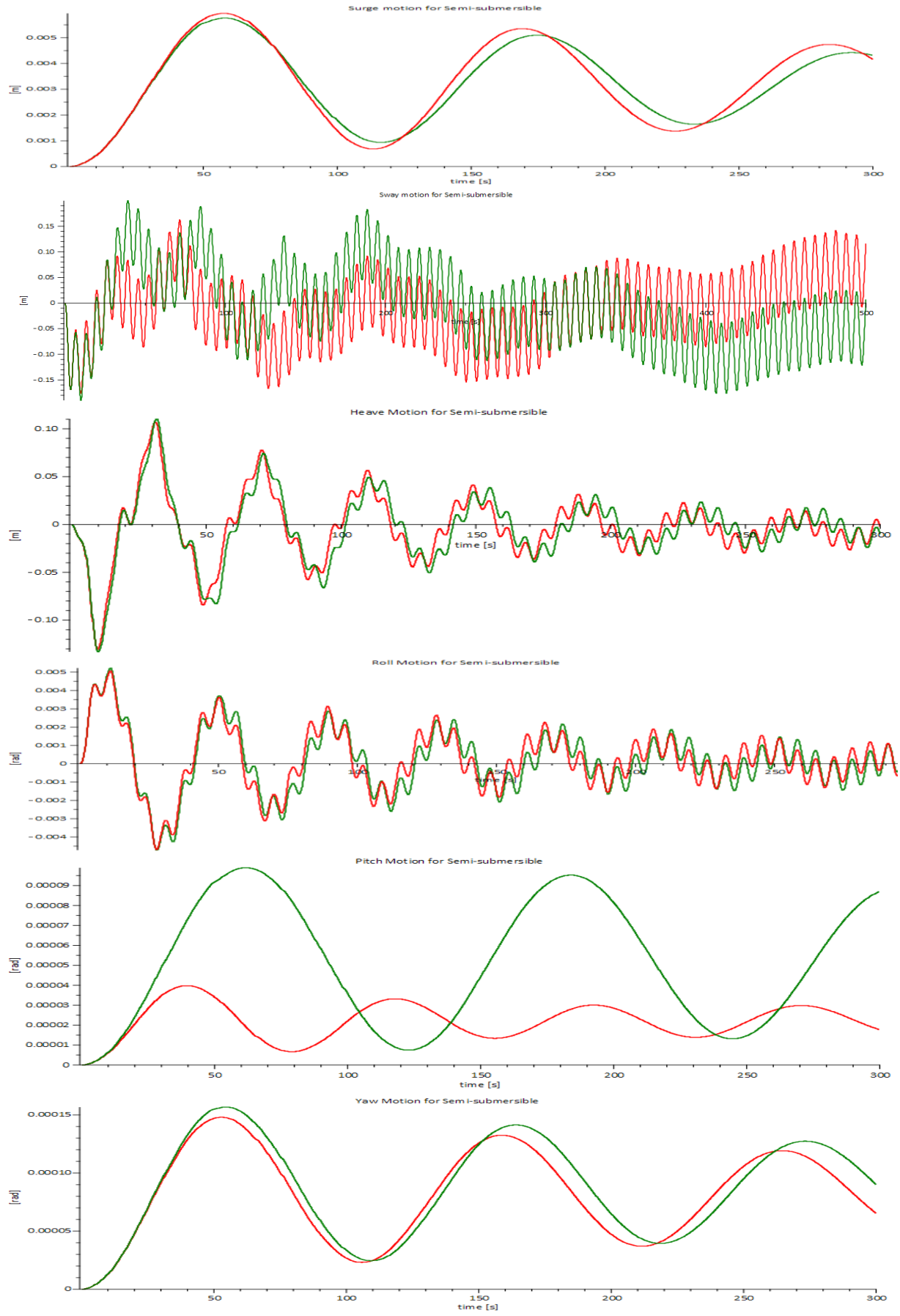

Figure 114 Motions of Semi-submersible in 6 degrees of freedom for T=6.5 [s] and H=1.2m
red = 4 suspension cables, green= 2 suspension cables applied)

7.5.2 CATAMARAN PONTOON

The primary natural frequencies of the Catamaran pontoon are given in tables Table 49 and Table 50. Also for the Catamaran pontoon is the near-resonant behavior has been determined using choosing the wave period near the natural frequencies. In Figure 117 the motions are given for a wave period of 11.05 [s], and a wave height of 1 m for a pontoon with four suspension cables and in Figure 115 the motions for a barge with four suspension cables are given. The same pattern can be observed as for the Semi-submersible pontoon.

Also for the Catamaran pontoon, it can be said that the stiff degrees of freedom are more determinative for the motions in the waves. The movements in soft degrees of freedom are less sensitive to waves, even for longer wavelengths. The motions in soft degrees of freedom stay entirely below the motions in the limit conditions. While the motions in the stiff degrees namely, heave and roll the limit values exceeds. Pitch can be treated as stiff or as the soft degree of freedom. It depends which configuration for suspension cable is used. By applying four wires, it can be interpreted as a stiff degree of freedom with high frequency. When two suspension cables are employed, the natural frequency becomes close to the natural frequency of sway. Therefore, it can be treated as the soft degree of freedom.

In the presented analysis only the beam waves are considered, if the waves attack the pontoons with an angle (μ) the motions in the surge, pitch and yaw will be more substantial because of, the force excitation will be larger than it is in the case for beam waves. But the motion in sway and roll are expected to be smaller than the presented values because the wave force will be smaller. It has to be mentioned that this principle is only valid when the wave period and the wave height is kept the same. For other combinations also different values will be calculated.

Also for the Catamaran pontoon, the near-resonant behavior of the pontoon in short waves is investigated. The wave frequency is chosen close to the roll frequency. The roll frequency of the Catamaran pontoon is very short. The natural frequency in roll is equal to 0.93 [s].In Figure 116 the motions for a wave period of 0.93 [s] are given. From the figure, it can be concluded that also Catamaran pontoon is insensitive for very short waves.

It is clear that both pontoons are sensitive to longer waves and large wave periods. The motions in the soft degrees of freedom are quite small. The movement in the stiff degrees is limitative. For relatively long waves T >10 [s] the motional limits for heave and roll are exceeded. The motional limit for heave is exceeded for a wave period of 11.05 [s] with a factor 4. So if the tunnel element will be immersed in these conditions, it is more likely that one or more suspension cables will break. Also, the accelerations are exceeded by a factor 4. The overall conclusion is that the tunnel element cannot be immersed safely in these wave conditions.

7.6 COMPARISON BETWEEN THE TWO DIFFERENT TYPE PONTOONS

The local wave data are provided by the owner of the project. In the sequel, the dynamic behavior for both pontoons will be compared to each other. The wave data are presented in Table 1. In order to compare the dynamic behavior for the environmental conditions of the Fehmarnbelt, the following five cases have been considered

	Wave height H [m]	Wave period [s]	Position TE under water [m]
Case I	1.2	3.5	1
Case II	1.2	6.5	1
Case III	1.2	5	15
Case IV	1.2	6.5	30
Case V	1.2	5	1

Table 33 Studies cases and environmental data

For all those cases the following parameters have been determined:

- Maximum motions in (surge, sway, heave, roll, pitch and yaw)
- Maximum force in the cables for due to motions
- Maximum acceleration in 6 degrees of freedom

The calculated results are presented in Table 34-Table 36. The results for both type barges are compared to a 4-cable pontoon configuration. Due to a large amount of data only the maximum values are given. The parameters are subdivided into three groups as mentioned above. In each table is one group of parameters has been presented for both type pontoons.

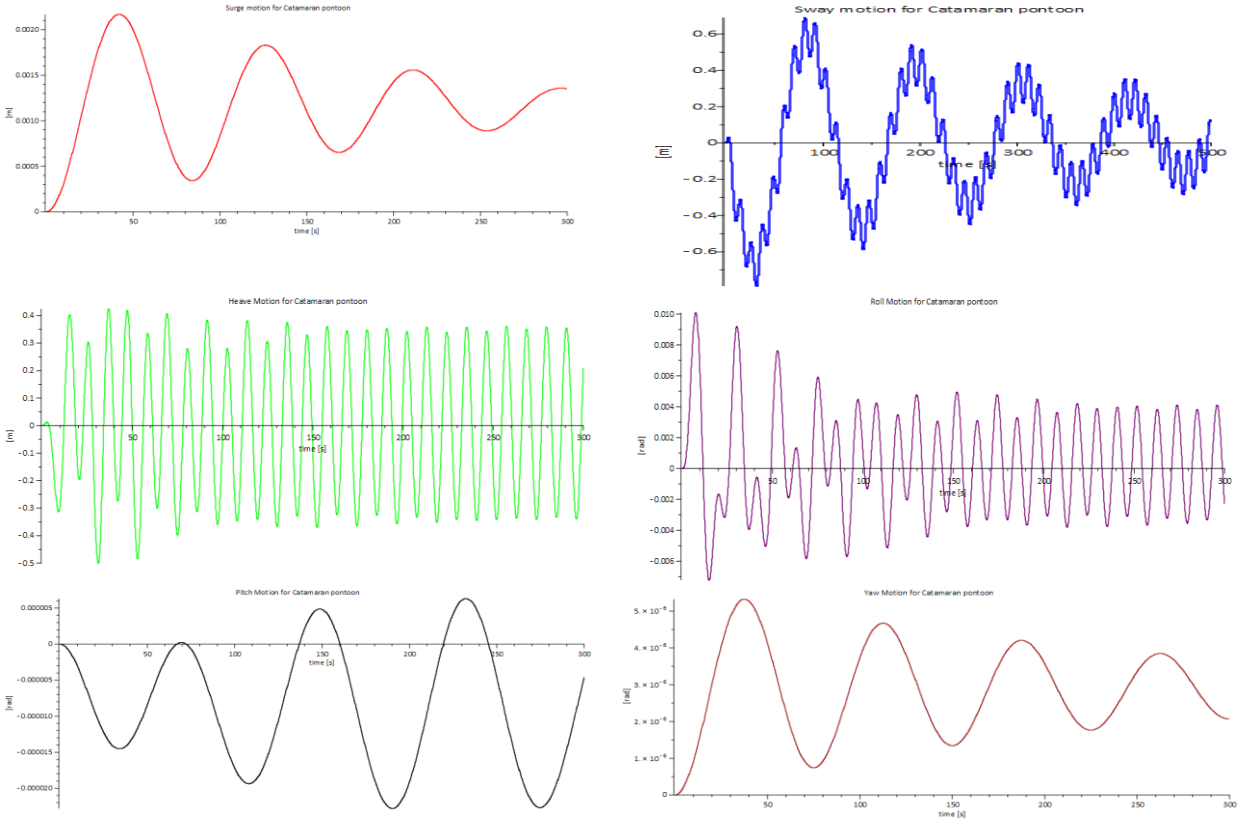

Figure 115 Motions of Catamaran Pontoon in 6 degrees of freedom for Tp=11 [s] and H=1m (2 suspension cables)

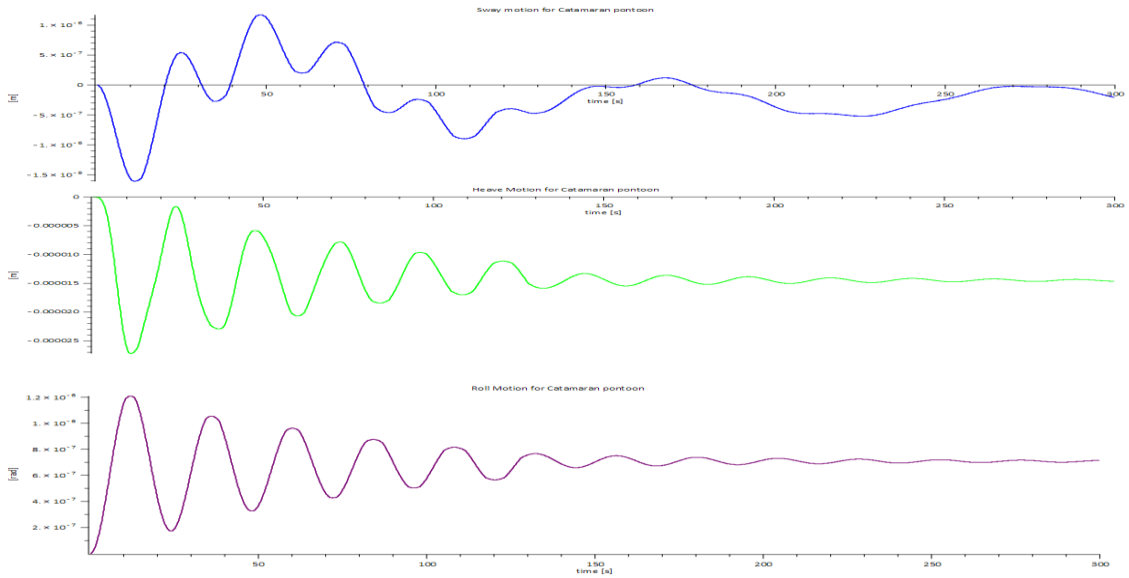

Figure 116 Motions of Catamaran Pontoon in 6 degrees of freedom for Tp=0.80 [s] and H=1m (2 suspension cables)

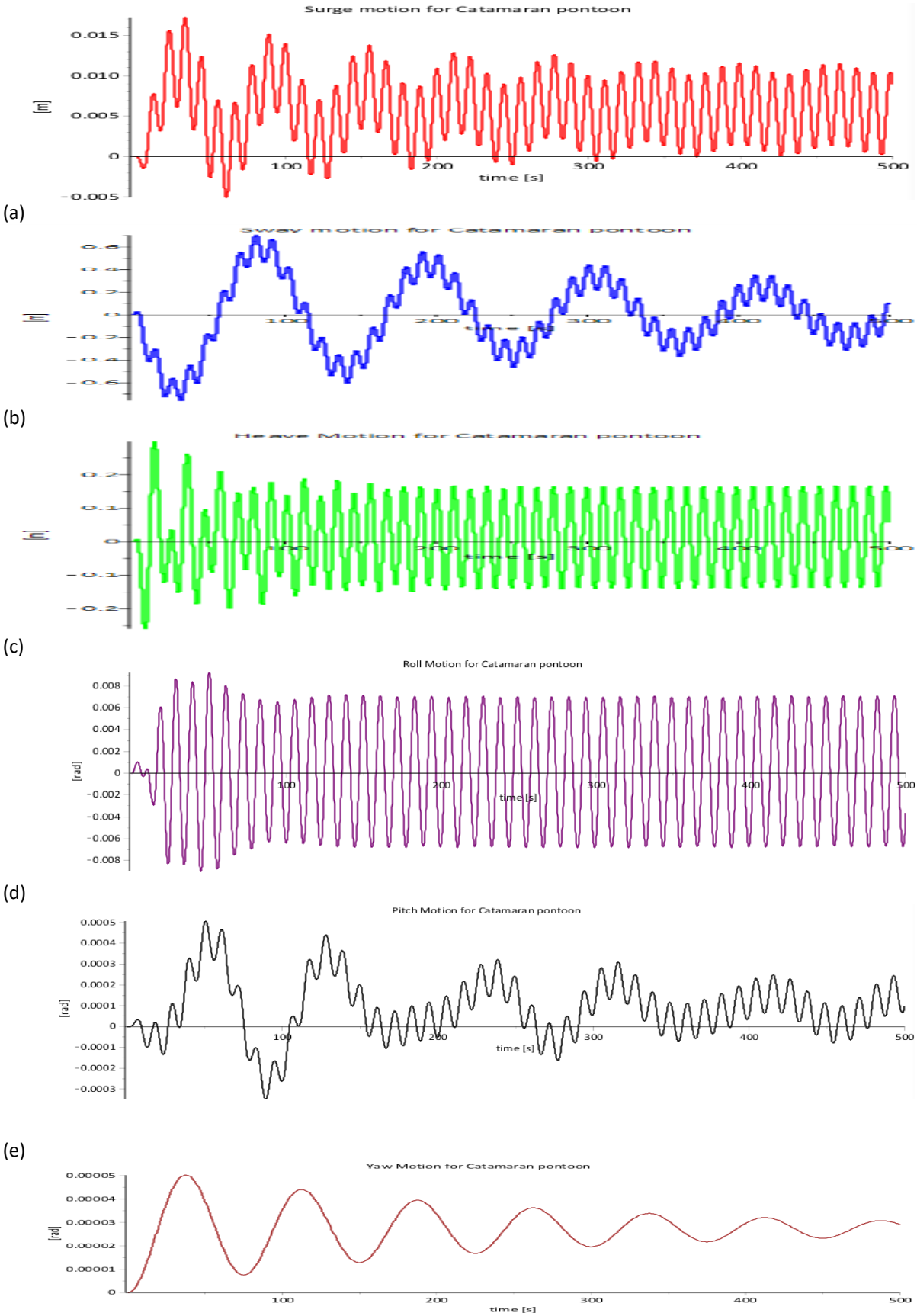

Figure 117 Motions of Catamaran Pontoon in 6 degrees of freedom for Tp=11 [s] and H=1m (4 suspension cables)

Motions in [m] and [rad]	Case I	Case II	Case III	Case IV	Case V
Catamaran Pontoon					
Surge	0	0.20	0.03	0.1	0.2
Sway	0.008	0.11	0.03	0.12	0.04
Heave	0.014	0.09	0.09	0.13	0.07
Roll	0.001	0.003	0.003	0.004	0.002
Pitch	0	0	0	0	0
Yaw	0	0	0	0	0
Semi-submersible Pontoon					
Surge	0	0.01	0.02	0.03	0
Sway	0.02	0.2	0.055	0.3	0.105
Heave	0.03	0.132	0.092	0.173	0.069
Roll	0.0012	0.005	0.0025	0.005	0.003
Pitch	0	0	0	0	0
Yaw	0	0	0	0	0

Table 34 Maximum motions for the 5 studied cases

Cable Force in [kN]	Case I	Case II	Case III	Case IV	Case V
Catamaran Pontoon					
Surge	3.1	2.8	0.1	0.1	2.5
Sway	0.4	78	5.8	93	10.3
Heave	605	4017	1153	974	3078
Roll	498	2760	751.36	607.67	2103
Pitch	-	-	-	-	-
Yaw	0.007	0.008	0.008	0.008	0.008
Semi-submersible Pontoon					
Surge	0.01	2.6	0.06	0.06	0.05
Sway	0.8	81	6.1	22	2.8
Heave	513	2238	579	649	1214
Roll	417	1681	470	517	971
Pitch	-	-	-	-	-
Yaw	0.02	0.03	0.02	0.02	0.02

Table 35 Maximum cable forces for the 5 studied cases

Acceleration	Case I	Case II	Case III	Case IV	Case V
Catamaran Pontoon					
Surge	0	0.03	0.	0.02	0
Sway	0.13	0.54	0.22	0.53	0.23
Heave	0.25	1.7	0.52	0.84	0.98
Roll	0.01	0.04	0.04	0.04	0.05
Pitch	0	0	0	0	0
Yaw	0	0	0	0	0
Semi-submersible Pontoon					
Surge	0	0	0	0	0
Sway	0.01	0.8	0.6	0.7	0.6
Heave	0.1	1.02	0.4	0.5	0.6
Roll	0.02	0.04	0.03	0.05	0.03
Pitch	0	0	0	0	0
Yaw	0	0	0	0	0

Table 36 Maximum pontoon accelerations for the 5 studied cases

It appears the most significant motions, and considerable force fluctuations in the suspension cables for both pontoons occur in Case II. Both barges seem to be sensitive to relatively long waves. The actual motions in the surge, pitch and yaw remain quite low in beam waves. The primary coupling of the modes is through the heave mode. However the influence is limited, the motions in the surge, pitch and yaw remain low. It is expected that for waves with an angle (μ) the motions in sway and roll will be smaller, but the motions for the surge, pitch and yaw are expected to be larger than presented here. In the above-shown tables, the exceeded values in SLS are given in yellow color, and the exceeded values in ULS in red.

It is also clear from the numerical analysis that the motions for the both pontoons in soft degrees remain small and far below the allowed movements in ULS and even SLS. The movements in stiff degrees of freedom namely, heave and roll, are determinative for the operations. The forces in the suspension cables in beam waves are determined by the motions in heave and roll. For both pontoons, the allowable force fluctuation is exceeded in case 2 and case 5. This exceedance will lead to direct failure of the cable. If it is desirable to immerse tunnel elements in wave conditions (T>5 s), then the capacity of the suspension cables should be enlarged.

For both pontoons, the acceleration in sway and heave directions appears to exceed the permitted values. This is true for both barges. However, Semi-submersible pontoon has favorable accelerations in heave and limit elegance in sway and for Catamaran pontoon is another way around.

If one considers the overall behavior of the pontoons in the wave conditions in Fehmarnbelt in beam waves, it appears that the Semi-submersible type pontoon has a favorable dynamic response in the expected wave conditions than the Catamaran pontoon. In Figure 118-Figure 120the motions, force fluctuations in the suspension cables and the accelerations are given for both types of barges for a Tp=6.5[s] and Hd =1.2 [m] when tunnel element is 1 [m] below the sea-surface. The data for Catamaran pontoon is given in red dashed line and for the Semi-submersible in green. From the results, it is clear that a Semi-submersible pontoon has favorable dynamic behavior in heave and roll in steady state. On the other hand, the transient motions are more significant compared to the Catamaran pontoon. When analyzing the force fluctuations, a Semi-submersible barge has better performance than the Catamaran pontoon. However, it is more significant accelerations in transversal direction compared to the Catamaran pontoon. Nevertheless, the difference is not very large. If one chooses a little larger SLS limit for the transversal acceleration, e.g. (0.7*g), than the limiting acceleration will be not exceeded for 95% annual wave conditions in Fehmarnbelt (Tp= 6.5 [s] and Hd= 1.2 [m]). Besides, the accelerations in heave are smaller than for Catamaran pontoon, which is also favorable for the workability.

It should be noted that on the other hand, the Catamaran pontoon has an improved static stability and a better floating capacity. That is why it can tackle greater force fluctuation in the suspension cables than the Semi-submersible barge. If one chooses for the Semi-submersible pontoon than the floating capacity and the static stability has to be improved (see also 4.6).

In the current design, only a force fluctuation of 50 [ton] is accounted in the analysis. Nevertheless, this aspect is not taken into account in this analysis. By increasing, the pontoons dimensions and submerging the floaters deeper under the sea level the dynamic behavior of the Semi-submersible pontoon can be further improved.

7.6.1 STATISTICAL ANALYSIS

The above presented time domain behavior is to illustrate how the pontoons behave in different wave conditions. However, for further analysis, the statistical approach is required to analyze the workability of both barges in various environmental conditions which can occur in the project area. To get statistical output (mean values, standard deviations, minimum and maximum) the extreme values for each simulation has to be

$$x_{design} = x_{mean} + \sigma_x \cdot \sqrt{2 \cdot \ln\left(\frac{N}{\alpha}\right)} \qquad (168)$$

determined. Instead, to use a single value from a simulation, it is more reliable to determine the extreme values for many simulations as it is described in (Hans Cozijn and Jin Wook Heo, 2009) and to obtain the most probable value of the required parameters. In formula form, this can be expressed by equation (168).

Where			
Parameter	**Meaning**	**Parameter**	**Meaning**
x_{design}	Design value of the parameter x	σ_x	standard deviation of parameter x
x_{mean}	Mean value of parameter x	N	Number of simulations
α	Coefficient (α~0.01)		

To obtain reliable design values for motions and to determine the workability many time domain simulations have to be performed. That is very time-consuming work. That is why for the workability analysis, an alternative approach has been chosen. This is discussed in the next chapter.

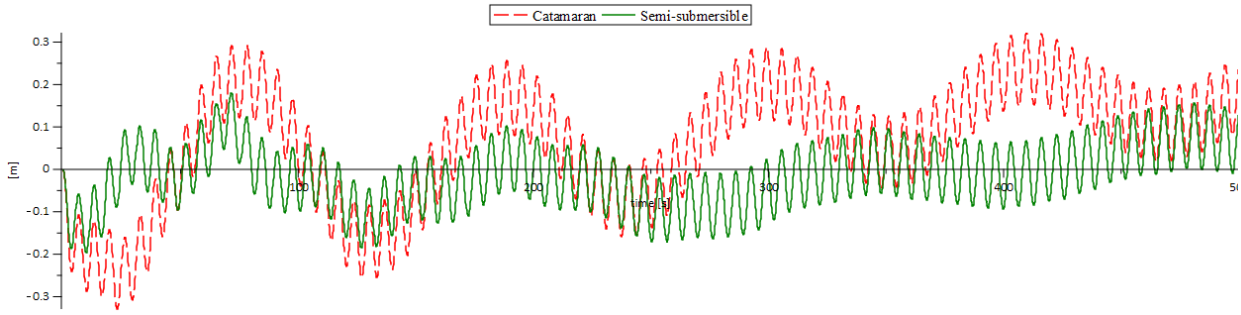

(a)

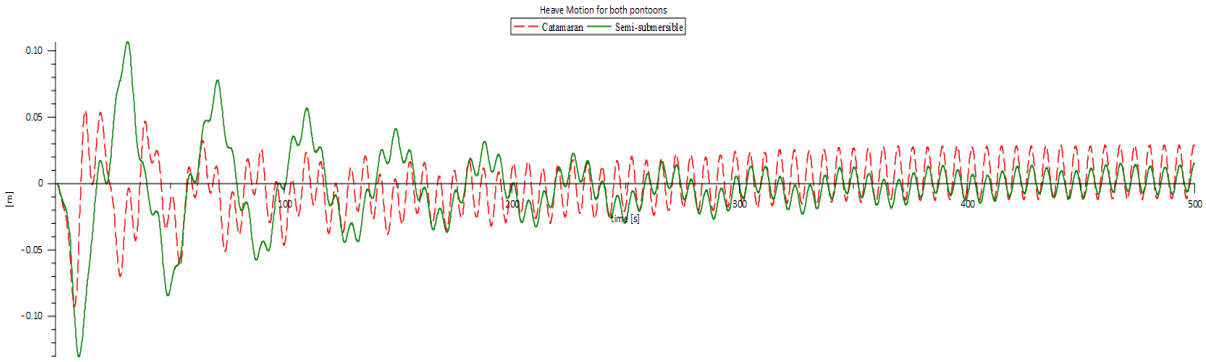

(b)

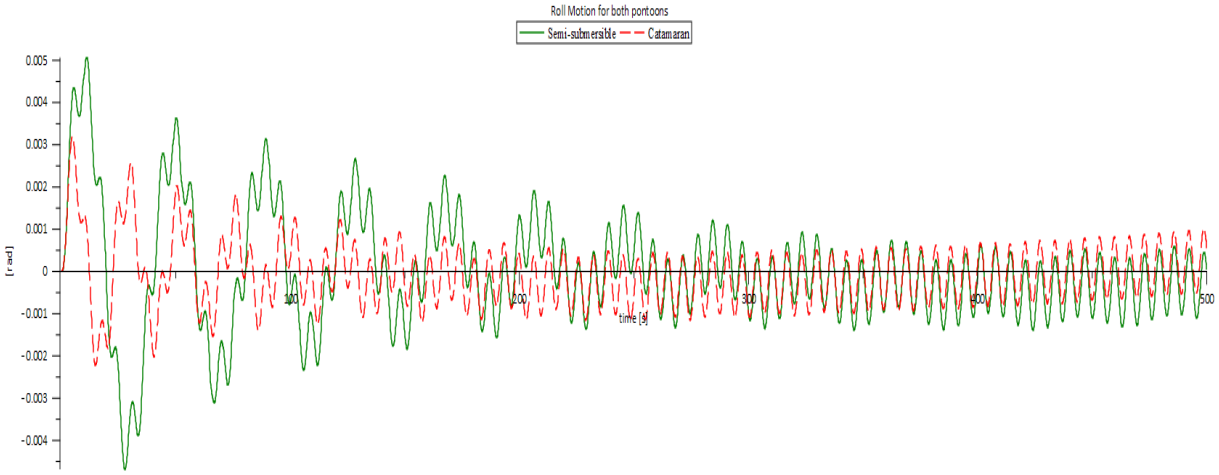

(c)

Figure 118 Motions of Catamaran and Semi-submersible pontoons in sway, heave and roll for Tp=6.5 [s] and Hd=1.2m (4 suspension cables)

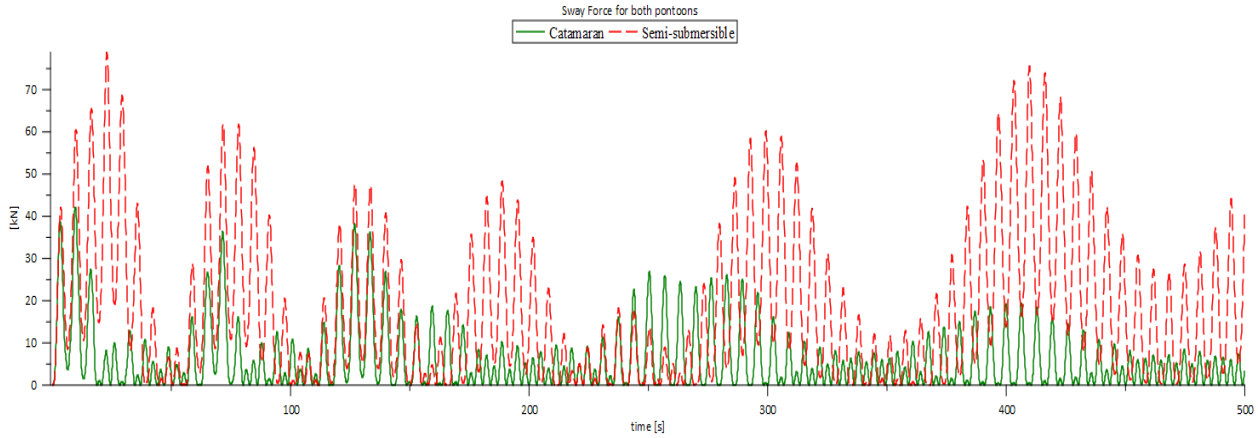

(a)

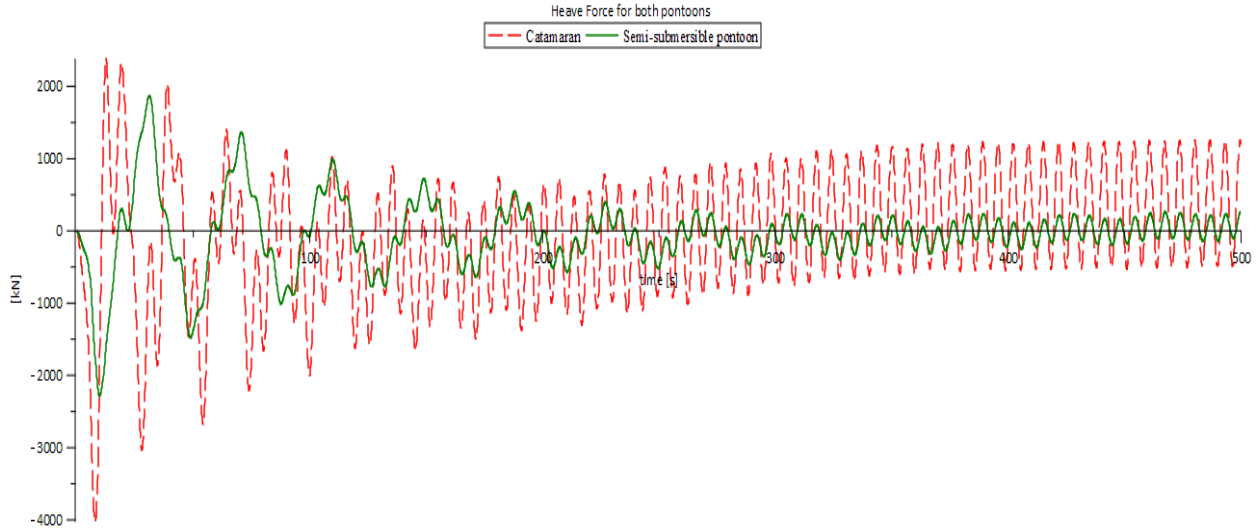

(b)

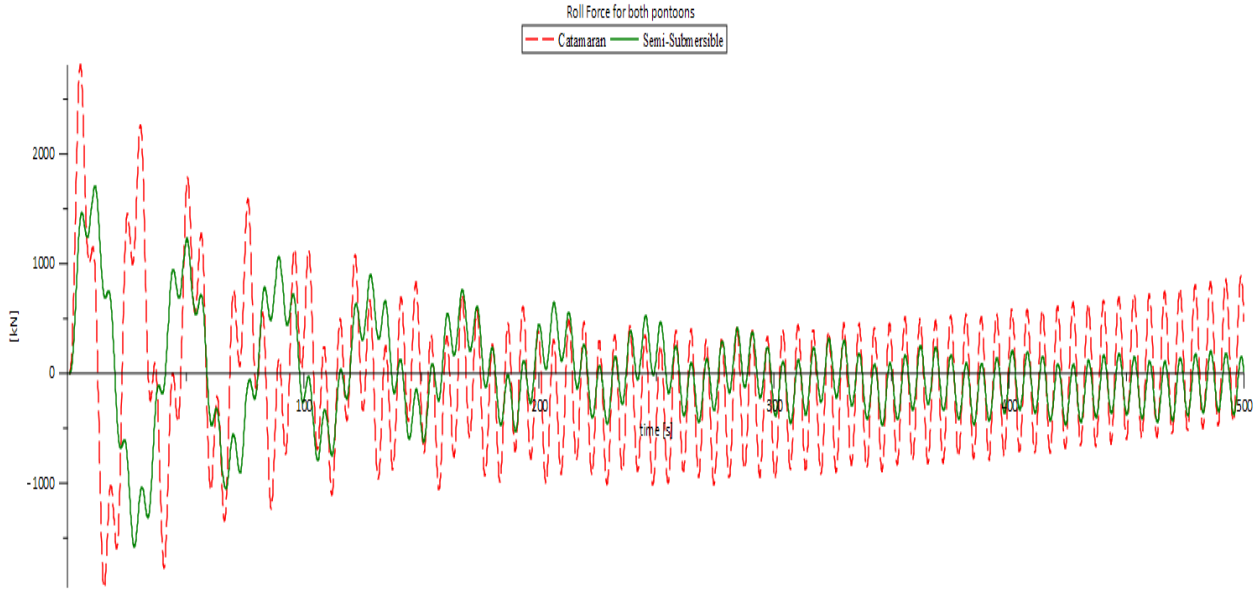

(c)

Figure 119 Force fluctuations in suspension cables of Catamaran and Semi-submersible pontoons in sway, heave and roll for Tp=6.5 [s] and Hd=1.2m (4 suspension cables)

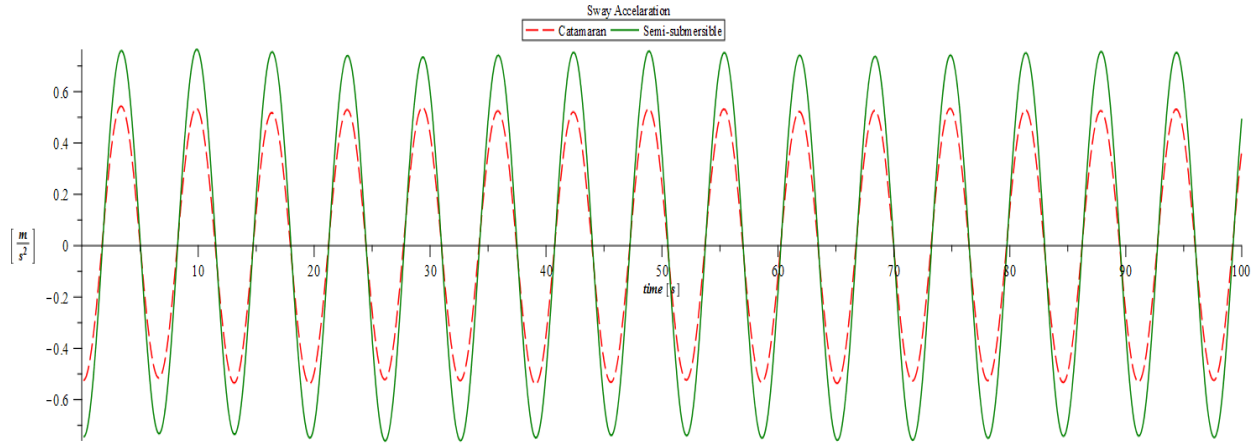

(a)

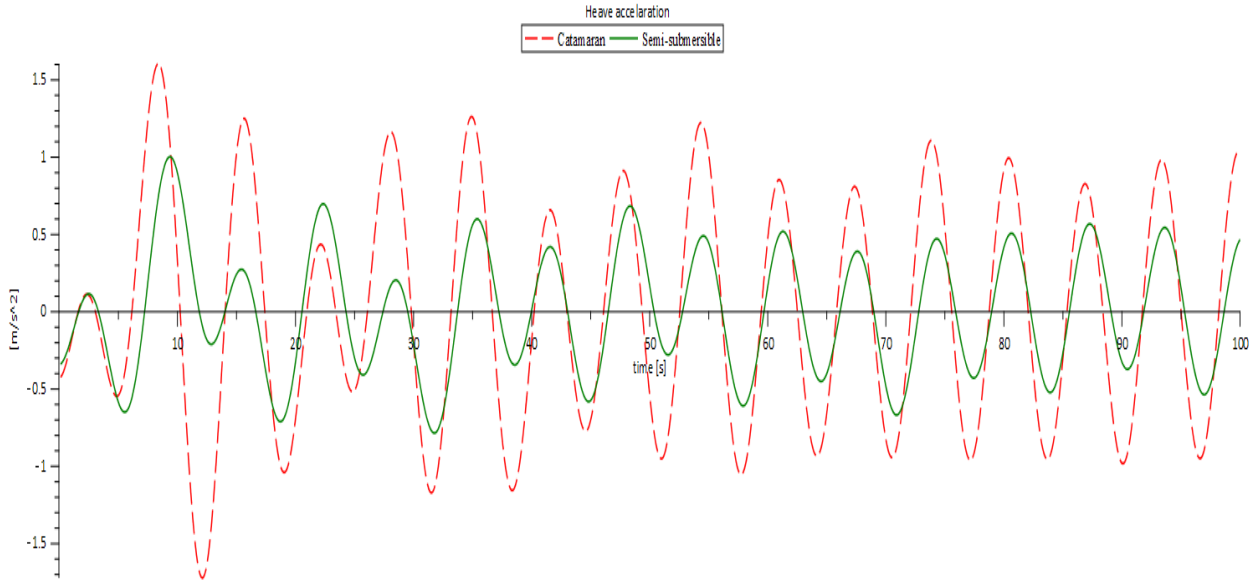

(b)

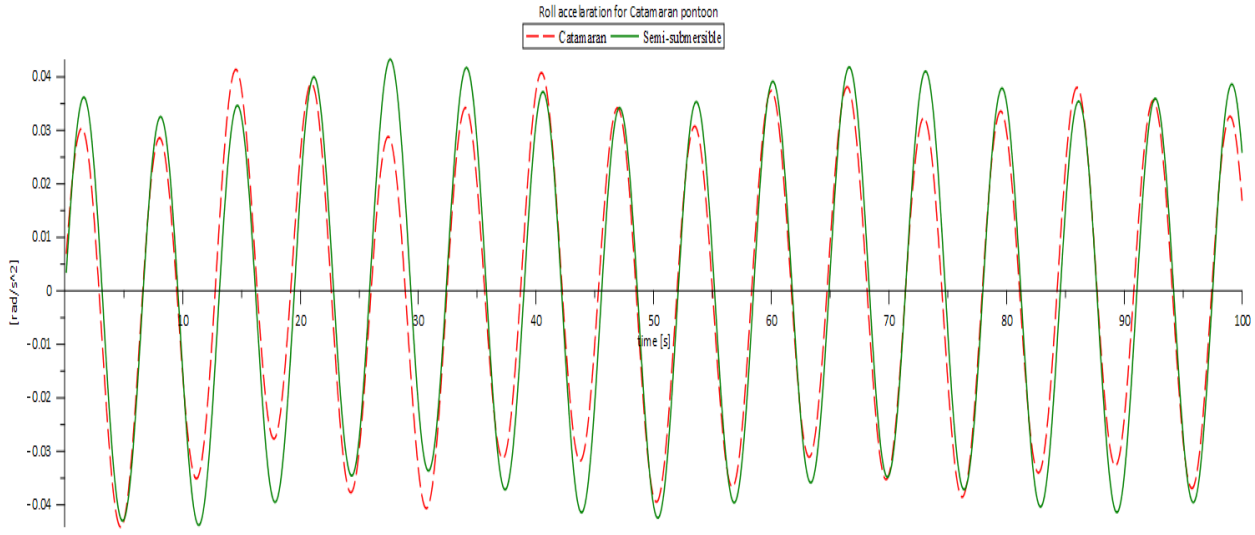

(c)

Figure 120 Accelerations of Catamaran and Semi-submersible pontoons in sway, heave and roll for Tp=6.5 [s] and Hd=1.2m (4 suspension cables)

7.7 VERIFICATION

In the previous sections of this chapter, calculations are performed in the time domain for several environmental conditions. For the calculations, the numerical procedure Newmark beta method has been used. Newmark beta method is a comprehensive procedure; mistakes can be easily made by using it. To be sure that this procedure is used correctly and that the results are reliable some verification calculations are performed. To verify the results of the model, a simple linear model has been set up. In this linear model, all the nonlinear terms in the stiffness are disregarded. The equation of motions is solved by using Fourier transforms. For different wave periods, the motional characteristics are calculated. The results are shown here below for the Semi-submersible pontoon.

The results are in good agreement with the obtained results from Newmark beta method. It can be concluded that the obtained results in the previous sections are reliable.

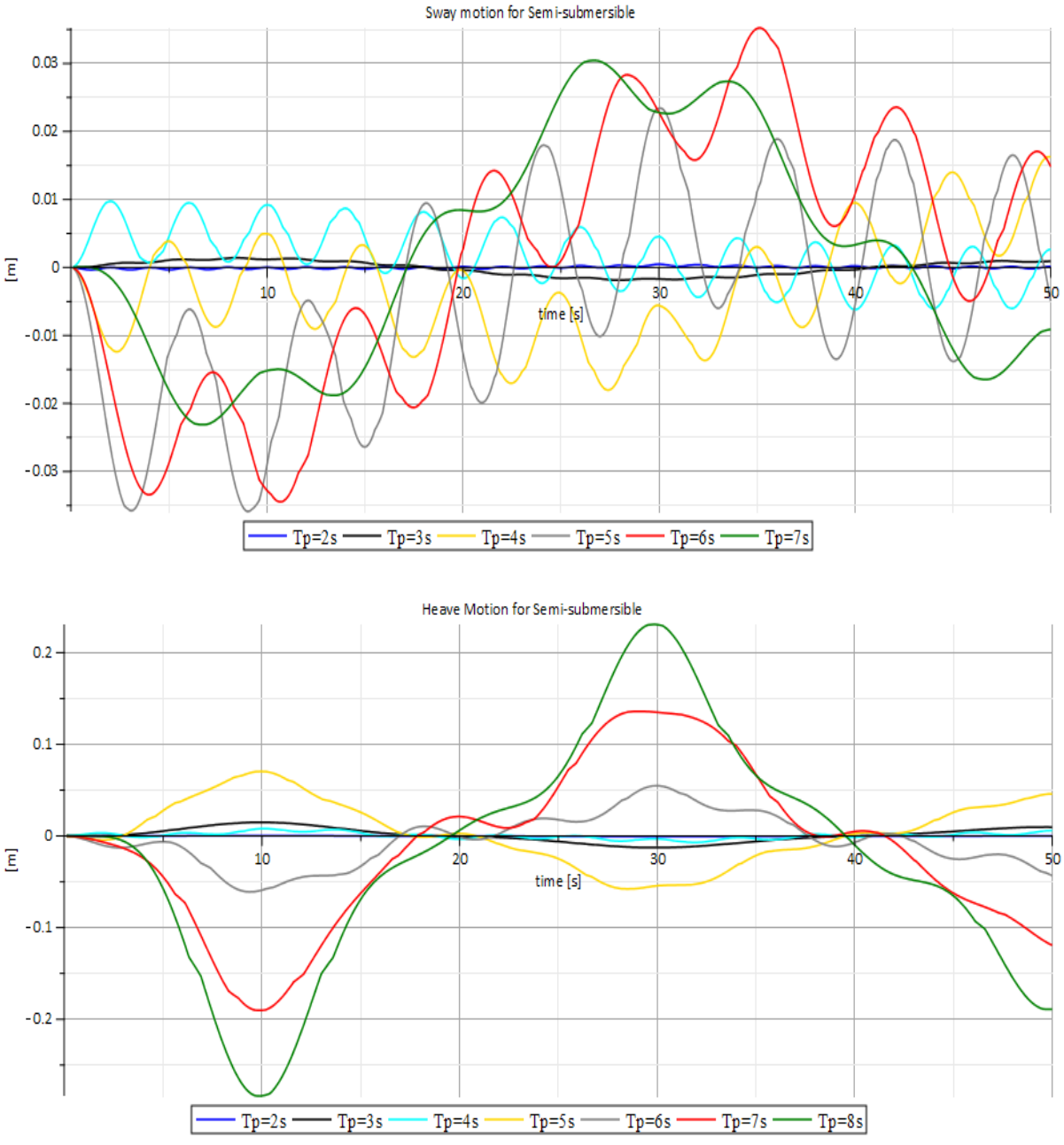

Figure 121 Motions Semi-submersible pontoon (Fourier analysis)

7.8 CONCLUSION

In the analysis the near-resonant behavior of the pontoons has been analyzed in the time domain. From calculations in beam waves, it appears that for both pontoons the motions in the soft degrees of freedom (sway, surge, and yaw) are very small compared to the limit values of the motions. Even for very long waves, the pontoons are quite stable. It can be concluded that the contribution of the first order wave forces to the pontoons motions in soft degrees of freedom is limited.

However, in the stiff degrees of freedom (heave, pitch, and yaw), the motions become problematic for long waves, and there is a possibility of breaking of the suspension cables. It can be concluded that for both type pontoons in long waves the motions in the stiff degrees of freedom are determinative. Also, the barges are more sensitive to long waves than for short waves. The motions in very short waves ($T \leq 1s$) are negligible. The pontoon will undergo in short waves $T \leq 3.53$ [s] motions with very small amplitude and high frequency. Besides, the accelerations do not exceed the limiting values.

It has to be mentioned that pitch can be treated as stiff or as a soft degree of freedom. It depends which configuration for suspension cable is used. By applying four wires, it can be interpreted as a stiff degree of freedom with high frequency. Nevertheless, when two suspension cables are applied the natural frequency becomes close to the natural frequency of sway. And it can be treated as a soft degree of freedom.

The number of applied suspension cables influences the motional characteristics. The pontoon with two suspension cables is more sensitive to longer waves than the pontoon with four suspension cables. When four suspension cables are applied, then the motions of the barges are smaller. From the results, it appears that the motions in pitch and yaw degrees are influenced by the applied cable configuration strongest. When using two suspension cables as traditionally done the natural frequencies in pitch increases considerably. Also, the natural frequency in yaw rises slightly. Due to small waterplane area (A_w), the effect of applying of two suspension cable in yaw degree of freedom is relatively lower for Semi-submersible than for the Catamaran pontoon.

The dynamic behavior of the system is only analyzed in beam waves, the modes in sway, heave, and roll of the pontoon will be excited by waves. Surge, pitch and yaw will not experience wave loads due to directional behavior of waves. The motions in these degrees of freedom are very small. Due to coupling, there are little motions in these degrees of freedom which can be almost neglected.

It is clear that both pontoons are sensitive to longer waves with large wave periods. The motions in the soft degrees of freedom are quite small. The movement in the stiff degrees is limitative. For relatively long waves $Tp > 5$ [s] the motional limits for heave and roll are exceeded. It can be concluded that both pontoons are sensitive to longer waves and less sensitive for short waves.

To be able to compare the dynamic behavior of the both pontoons, five cases have been studied. In the normative case, the wave period is chosen as 6.5 [s], which is not exceeded in 95% of the time in Fehmarnbelt in combination with the design wave height of 1.2 [m].

From the case studies, it appears that the Semi-submersible type pontoon has favorable dynamic behavior in the studied wave conditions than the Catamaran pontoon. From the results, it is clear that all two types of parameters namely: force fluctuations and accelerations the Catamaran pontoon has unfavorable dynamic behavior in waves than the Semi-submersible pontoon. It should be noted that on the other hand, the Catamaran pontoon has an improved static stability and a better floating capacity. That is why it can tackle greater force fluctuation in the suspension cables than the Semi-submersible barge. If one chooses for the Semi-submersible pontoon than the floating capacity and the static stability has to be improved. Nevertheless,

this aspect is not taken into account in this analysis. By increasing, the pontoons dimensions and submerging the floaters deeper under the sea level, the dynamic behavior of the pontoon can be further improved.

One of the boundary conditions for the immersion operation is that the suspension cables may not slacken due to the dynamic wave force (zero force in one of the suspension cables). Therefore the element will be extra ballasted such that it must always have tension in the suspension cables. The additional ballast force is calculated by a simple approximation: the dynamic wave force is proportional to the wave height and water cutting area of the pontoon. The dynamic forces which were taken into account for determination of the dimensions were for Semi-submersible: (607 and 303 KN for two and four cable configurations) and for Catamaran (3228 KN and 1614 KN).

The forces that are observed in the calculation are much higher than assumed values. For the Catamaran pontoon, a force fluctuation of (16400 KN in heave and 2760 in roll) and for Semi-submersible pontoon (9039 KN in heave and 1681 in roll) are observed. This brings us to a conclusion if one chooses to immerse the tunnel elements in sea conditions as mentioned above. More ballast has to be applied during the immersion than it was initially assumed. Besides, the pontoons must also have a larger floating capacity, which leads to bigger pontoon dimensions.

The mentioned numbers are the amplitude of the forces. These forces occur when the operation is being started. In the sequence, the amplitude of the forces decreases for Catamaran pontoon with (4 in heave and 2.5 in roll) for Semi-submersible pontoon the decreasing ratios are (15 for heave and 3 in roll). The amplitude of the most significant force terms are caused by the so-called transient motions, and in steady state, the magnitude of the forces decreases and stays within the limits of the values of ULS.

8 DYNAMIC ANALYSIS PONTOONS IN FREQUENCY DOMAIN

8.1 OPERABILITY

In this part of the report, the operationally of the pontoons in waves will be investigated. The operational limits already have been evaluated in section 4.7. The primary assumption for the determination of the limiting conditions is that the immersion operation can be carried out as long as the operational limits in the ULS are not exceeded. In the analysis, only the motional limits which are related to the allowable force in the suspension cables are considered for the ULS. The operational limits in SLS are also described in section 4.7. Off course for the total picture more aspects have to be taken into account, such as the motions of the tunnel element due to current excitation. But the primary object of this report is to determine the operational limits of the two types pontoons. That's why the other objects are disregarded in this analysis. The following approach is followed to determine the workability of the pontoon for the wave conditions in the Fehmarnbelt.

For this analysis, the dynamic response characteristics of the pontoons are presented as Response Amplitude Operators (RAO's). To apply the concept of RAO's the system is considered to be linear. This means that only the linear coefficients in the stiffness matrix are taken into account. The concept of linearity can only be applied if the motions are small enough and that the nonlinear terms in the stiffness matrix can be ignored. In the time domain analysis, it is already proved that for both pontoons the motions are small in the 'normal' conditions.

$$S_R(\omega) = (RAO)^2 \cdot S_L(\omega) \qquad (169)$$

$$m_n = \int_0^\infty S_R(\omega) \cdot d\omega \qquad (170)$$

When applying the RAO concept, it means that the principle of the superposition is valid. The response to the regular oscillatory force such as wave loading can be found by expressing the wave load as a Fourier series, and finding the corresponding Fourier series response for each component of the force and adding them together up will lead to the total response of the system. The RAO's are presented here as (amplitude of response/ amplitude of the wave) as a function of the wave frequency.

$$\mu(X_N) = \sqrt{m_0} \cdot \sqrt{2 \cdot \ln(\mathrm{N})} \qquad (171)$$

For the analysis the JONSWAP spectrum is used which is adjusted for the project location (see also (FEHY (Metocean Conditions), 2013)). The response spectrum of the motions is determined by multiplying the RAO's of the motions with the provided wave spectrum. The response spectrum is expressed by the equation (169). From the response spectrum, the spectral n^{th} spectral moment can be determined by the equation (170). For each given environmental condition is the most probable maximum of motion in N peaks is determined by the equation (171) for a given sea state.

Where	
$S_R(\omega)$	Response spctrum
RAO	Resonse Amplitude operator
$S_L(\omega)$	Wave Spectrum

For the calculations, it is been assumed that the immersion operation will take place in 3 hours. The average spectral peak period, in the project area, is 3,44 [s]. This means that during the immersion process about (3600·3/3.44) 3140 waves will pass the system. That is why for the calculations, N=3140 is taken into account.

Given the fact that the system can be assumed as linear, the equation of motion is solved in the frequency domain. Due to the character of the load (beam waves) only the response in three main activated modes namely, sway, heave and roll have been determined. First of all the components of the equation of motion are established for both type pontoons considered here.

Subsequently, the equation of motions is solved by using the Modal analysis. The RAO's are determined for sway, heave, and roll. The motional amplitudes are used for determination of the response spectrum.

The wave scatter diagram given in Appendix 2 is used for the determination of the workability of the pontoon in the given environmental conditions.

For each combination of the significant wave height and wave peak period the spectrum of the motion for each studied degree of freedom is calculated. If the most probable value of the motion exceeds the limit value, (which is already has been determined.) Then those conditions are considered as a not workable condition.

Presentation of the results

Due to a large number of data, not all the response spectra will be presented. The results of the calculations are presented in wave scatter diagram for the given wave conditions. Colors are used to indicate the systems operability. The workable conditions are given in green; the red color shows the conditions for which one of the limit state conditions in ULS are exceeded. Besides, yellow indicates the conditions for which one or more limits in SLS are exceeded. In the following sections first, the dynamic behavior of the pontoon is determined in the frequency domain. Subsequently is for each pontoon the workability presented using the wave scatter diagram.

8.2 DYNAMIC ANALYSIS SEMI-SUBMERSIBLE PONTOON IN FREQUENCY DOMAIN

In this part of the report, the dynamic behavior of the Semi-submersible pontoon will be analyzed. For the analysis, it is assumed that wave heights are small as mentioned previously with low steepness. This assumption allows us to apply linear wave theory and to avoid complicated calculations. The Semi-submersible pontoon has four columns and two floaters. The overall dimensions are given in Table 15 (see also Figure 49).

Parameter	Value	Units
Water depth	30	[m]
Mass of each column	20	[ton]
Mass of each floater	200	[ton]
Mass of the equipment	400	[ton]
Mass of ballast water	120	[ton]
Total force from suspension cables	480	[ton]
Amount of ballast in the pontoon	120	[ton]
Diameter suspension cables (4 cables)	55	[mm]
Diameter suspension cables (2 cables)	75	[mm]

Table 37 geometric properties of Semi-submersible pontoon

The methodology used here is equally valid for Catamaran pontoon. However, the waterplane area, the cable forces and the geometry of the pontoon differs. That's why the Catamaran pontoon will be analyzed separately in the following section.

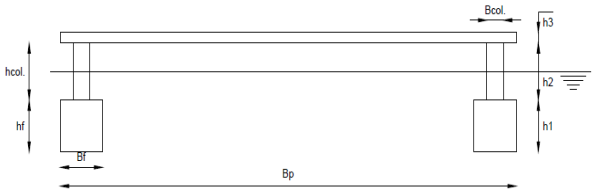

Figure 122 Semi-Submersible pontoon

Because of the large dimensions of the tunnel elements, also a pontoon with four suspension cables is analyzed. Traditionally two suspension cables configuration is applied for the immersion. Also, the two cables configuration is analyzed. The purpose of this analysis is also to determine what the effect of the number of the suspension cables is to the overall dynamic stability of the pontoon.

Characteristics of the pontoon and local data parameters

The principal dimensions and the local data that are used for the calculations have already been given in the report in different parts. For a better understanding of the calculations, they have repeated here again in Table 37. During the immersion, the pontoon will be ballasted such that it will have a draught of 4.52 m. The amount of ballast needed for that is 120 ton. The pontoon ballast is assumed to be uniformly distributed in the floaters. From the calculations of the static stability we get the following values for the parameters:

$$KG = \frac{\sum M \cdot z_k}{\sum M} = 8.15\ [m] \tag{172}$$

The distance of the center of buoyancy above the keel is:

$$KB = \frac{\sum V \cdot z_k}{\sum V} = 2.97\ [m] \tag{173}$$

The distance between G and B can be expressed as:

$$BG = KG - KB = 5.18\ [m] \tag{174}$$

The second moments of area of water plane area about the point of rotation are:

$$I_{xx} = 6.02 \cdot 10^4\ [m^4] \tag{175}$$

$$I_{yy} = 3.08 \cdot 10^4\ [m^4] \tag{176}$$

8.2.1 NATURAL FREQUENCY ANALYSIS:

For the analysis, the axis system presented in Figure 99 (b) is used. The x,y plane, and the origin are chosen at the mean water level. The natural periods for all 6 degrees of freedom are calculated. For the analysis first, the mass and the stiffness matrixes are determined. The mass matrix is split into two parts. Part 1 represents the structural mass, and part two represents the added mass terms.

Mass Matrix

The form of both matrixes is the same, namely: (6 x 6) matrix. Both matrixes specify the forces and moments required to accelerate the pontoon and the added mass in each degree of freedom.

$$F = M \cdot \ddot{x} \tag{177}$$

$$M = \begin{bmatrix} m_{pontoon} & 0 & 0 & 0 & -\sum m_i z_K & 0 \\ 0 & m_{pontoon} & 0 & -\sum m_i z_K & 0 & 0 \\ 0 & 0 & m_{pontoon} & 0 & 0 & 0 \\ 0 & -\sum m_i z_K & 0 & I_{xx-pontoon} & 0 & 0 \\ -\sum m_i z_K & 0 & 0 & 0 & I_{yy-pontoon} & 0 \\ 0 & 0 & 0 & 0 & 0 & I_{zz-pontoon} \end{bmatrix}$$

The axes and the degrees of freedom are shown in Figure 99. The structural mass matrix is expressed in SI-units (kg and m). The mass of the pontoon is not evenly distributed. This influences the shape of the mass matrix. Especially the mass is not evenly distributed in the z-direction, this has been taken into account in the model.

$$M_{structural} = \begin{bmatrix} 17{,}8{\cdot}10^4 & 0 & 0 & 0 & -6{,}4{\cdot}10^6 & 0 \\ 0 & 17{,}8{\cdot}10^4 & 0 & -6{,}4{\cdot}10^6 & 0 & 0 \\ 0 & 0 & 17{,}8{\cdot}10^4 & 0 & 0 & 0 \\ 0 & -6{,}4{\cdot}10^6 & 0 & 7{,}5{\cdot}10^8 & 0 & 0 \\ -6{,}4{\cdot}10^6 & 0 & 0 & 0 & 8{,}7{\cdot}10^7 & 0 \\ 0 & 0 & 0 & 0 & 0 & 1{,}2{\cdot}10^7 \end{bmatrix}$$

The coupling between surge and pitch, sway and roll and another way around has been taken into account. This means that due to acceleration in surge the structure will also experience a force in the pitch degree of freedom This principle also applies to the other degrees of freedom. There for also the non- diagonal terms has been taken into account. The $\sum m_i z_K$ indicates the sum of all the elementary masses times their z coordinate. By substituting the assumed values, the structural matrix is calculated.

The shape of the hydrodynamic mass matrix is assumed to be the same as that for the mass matrix. It should be noted that this is a very rough approximation. The added mass is one of the two hydrodynamic reactions because of the movement of the floating structure. Coupling between different degrees of freedom occurs. Resulting in off-diagonal terms in the matrix. The added mass is also depended on the frequency of the oscillations. The added mass terms could be theoretically calculated by using the diffraction theory.

$$M_a = \begin{bmatrix} 1{,}29{\cdot}10^5 & 0 & 0 & 0 & 1{,}33{\cdot}10^7 & 0 \\ 0 & 1{,}05{\cdot}10^6 & 0 & 1{,}33{\cdot}10^7 & 0 & 0 \\ 0 & 0 & 1{,}42{\cdot}10^6 & 0 & 0 & 0 \\ 0 & 1{,}33{\cdot}10^7 & 0 & 1{,}32{\cdot}10^7 & 0 & 0 \\ 1{,}33{\cdot}10^7 & 0 & 0 & 0 & 8{,}23{\cdot}10^8 & 0 \\ 0 & 0 & 0 & 0 & 0 & 6{,}47{\cdot}10^8 \end{bmatrix}$$

The added mass coefficients are dependent on motion direction, oscillation frequency and the geometry of the structure. The calculations are complex and require specified computer software to calculate the terms of the matrix. In this report, a simplified approach is followed to obtain the values of the added mass in different degrees of freedom. There are several methods of estimating the added mass and many experts in the field have released formulae for calculating the added mass coefficients. However, there are significant differences in the expected values. From the literature study, it can be concluded that a simple and useful estimation for the added mass is given in Baltrop, 1998 for the cylindrical shapes. For the analysis as a first approximation, the added mass is estimated by using Figure 123 and Figure 124 (from Baltrop, 1998). The total mass matrix is the sum of the two matrixes.

$$M_{total} = \begin{bmatrix} 1{,}91{\cdot}10^6 & 0 & 0 & 0 & 6{,}85{\cdot}10^6 & 0 \\ 0 & 2{,}83{\cdot}10^6 & 0 & 6{,}85{\cdot}10^6 & 0 & 0 \\ 0 & 0 & 3{,}2{\cdot}10^6 & 0 & 0 & 0 \\ 0 & 6{,}85{\cdot}10^6 & 0 & 7{,}63{\cdot}10^8 & 0 & 0 \\ 6{,}85{\cdot}10^6 & 0 & 0 & 0 & 9{,}1{\cdot}10^8 & 0 \\ 0 & 0 & 0 & 0 & 0 & 6{,}59{\cdot}10^8 \end{bmatrix}$$

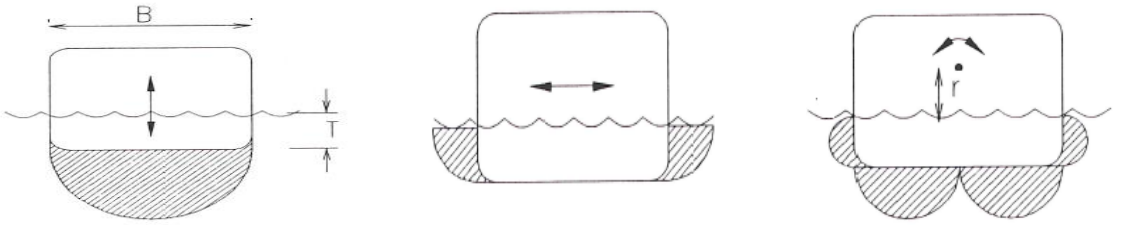

$$\frac{1}{2}\cdot\rho\pi\left(\frac{B}{2}\right)^2 \qquad \frac{1}{2}\cdot\rho\pi\cdot T^2 \qquad \rho\pi\left[\left(\frac{B}{4}\right)^2\cdot\left(\frac{B}{4}\right)^2+\left(\frac{T}{2}\right)^2\cdot\left(\frac{T}{2}+r\right)^2\right]$$

Figure 123 Estimate of added mass for water piercing parts (from Baltrop, 1998).

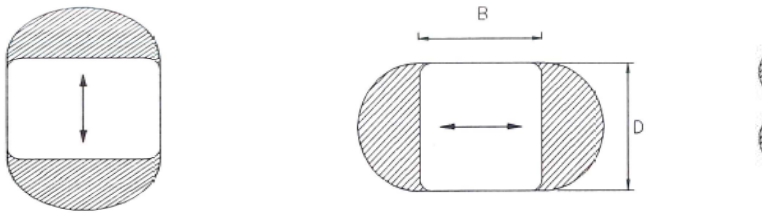

$$\rho\pi\left(\frac{B}{2}\right)^2 \qquad \rho\pi\cdot D^2 \qquad 5/2\cdot\rho\pi\left[\left(\frac{B}{4}\right)^4\cdot\left(\frac{D}{4}\right)^4\right]$$

Figure 124 Estimate of added mass for fully submerged parts (Baltrop, 1998). Copied from (Floating Structures:, 1998)

We have already seen that the stiffness matrix is not linear. The stiffness matrix is time and displacement dependent. For the calculation of the natural frequencies, all the nonlinear terms have been disregarded, and the matrix is determined at the time t=0. This approach can be justified since the natural frequencies are system properties and do not depend on the displacement. The linear part of the stiffness matrix is expressed here next to it.

$$K_{lin(2cables)}=\begin{bmatrix} K_{11} & 0 & 0 & 0 & 0 & 0\\ 0 & K_{22} & 0 & 0 & 0 & 0\\ 0 & 0 & K_{33} & 0 & 0 & 0\\ 0 & K_{42} & 0 & K_{44} & 0 & 0\\ K_{51} & 0 & 0 & 0 & K_{55} & 0\\ 0 & 0 & 0 & 0 & 0 & K_{66} \end{bmatrix}$$

The length of the suspension cables will change the position of the tunnel element in the vertical. Here next to the values of the stiffness matrix are given when the tunnel element is 1 [m] below the water surface. Then the length of the suspension cables is then 8 [m], assuming that the winches of the suspension cable are 1[m] higher on the deck of the pontoon.

$$K_{lin(2cables)}=\begin{bmatrix} 3.08*10^5 & 0 & 0 & 0 & 0 & 0\\ 0 & 3.08*10^5 & 0 & 0 & 0 & 0\\ 0 & 0 & 6.62*10^7 & 1.25*10^9 & 0 & 0\\ 0 & 1.03*10^6 & 0 & 1.78*10^9 & 0 & 0\\ 1.03*10^6 & 0 & 0 & 0 & 2.32*10^9 & 0\\ 0 & 0 & 0 & 0 & 0 & 1.14*10^8 \end{bmatrix}$$

When applying four suspension cables, the values of the stiffness matrix increases slightly. For the completeness also these values are presented here next to it. However, the cross-sectional area of the material in the wire rope is approximately the same, but the spring stiffness increases slightly by applying more suspension cables. Especially the spring stiffness in pitch degree of freedom increases strongest. This is caused by the fact, that in the case of four suspension cables also the cables are spread in the longitudinal direction leading to increase of the stiffness in the pitch direction.

$$K_{lin(4-cables)}=\begin{bmatrix} 3.07*10^5 & 0 & 0 & 0 & 0 & 0\\ 0 & 3.07*10^5 & 0 & 0 & 0 & 0\\ 0 & 0 & 7.10*10^7 & 1.34*10^9 & 3.50*10^8 & 0\\ 0 & 1.03*10^6 & 0 & 1.87*10^9 & 0 & 0\\ 1.03*10^6 & 0 & 0 & 0 & 5.82*10^8 & 0\\ 0 & 0 & 0 & 0 & 0 & 1.21*10^8 \end{bmatrix}$$

For the calculations, it is assumed that the longitudinal distance between the cables is 10 m. If this distance is increased, then the stiffness of the system will increase too in the pitch degree of freedom. But on the other hand, extra moments in the tunnel element will be introduced if the cable distance will be increased. So that's why 10 [m] is used for the analysis purposes. The natural frequencies ω_i of the pontoon are calculated by the square root of the eigenvalues of $\mathbf{(M^{-1}\cdot K)}$. The modes are surge, sway, heave, roll, pitch, and yaw.

Degree of freedom	Natural frequency ω_i [rad/s]	Natural period T_i [s]
Sure	0.428	14.7
Sway	0.344	13.0
Heave	4.72	3.92
Roll	1.63	1.29
Pitch	0.506	12.4
Yaw	0.416	15.1

Table 38 Natural periods of the pontoon and the Eigenfrequencies (for l=8m and 2 suspension cables)

Degree of freedom	Natural frequency ω_i [rad/s]	Natural period T_i [s]
Surge	0.428	14.7
Sway	0.342	13.1
Heave	4.90	3.82
Roll	1.68	1.26
Pitch	0.804	7.80
Yaw	0.428	14.7

Table 39 Natural periods of the pontoon and the Eigenfrequencies (for l=8m and 4 suspension cables)

The natural periods of the pontoon have also been calculated for a Semi-submersible pontoon with four suspension cables. Due to a slightly higher stiffness of the pontoon with four suspension cables, the natural periods are somewhat smaller than previously calculated values. The main difference occurs in the pitch degree of freedom. That natural period has been reduced significantly from 12.7[s] to 4.21[s]. Further, it appears that the stiffness in heave, roll, and yaw increases slightly. This leads to smaller natural periods in (heave, roll, and yaw). The results are given in Table 39.

From the results, it is evident that the natural periods of the pontoon in surge, sway and yaw are larger than waves of importance in the Fehmarnbelt. But the pontoon can be sensitive to the swell waves if they occur. The natural periods of the pontoon in surge, sway and yaw are pretty close the periods of swells. Also, the natural periods in pitch if two suspension cables are applied close to the swell periods.

If the tunnel element will be immersed in the environmental conditions in which swell weaves occur, then the pontoon will undergo large motions in the transversal directions and large rotation about the z axis. The effect of the mooring lines will be small on these motions. The mooring line is quite flexible, and it is not capable of resisting the first order motions of the pontoon. The only possibility is to increase the stiffness of the system. But also the effect of the stiffness is limited. By increasing the stiffness of the pontoon simply by putting more ballast in the tunnel element the natural period in surge and yaw decreases below the 10 seconds. But the natural period in sway will be pretty close the swell period.

The effect of the increased stiffness is being investigated by increasing the amount of pretension in the cables. Off course if more pretension will be needed than the dimensions of the pontoon and the suspension cables has to be adjusted. But this is disregarded in the calculations. The effect of increasing amount of ballast (extra stiffness) is investigated using two cases. In case 1 the total ballast is increased to a value of 1000 ton, and in case 2 the total amount of ballast has been increased to a value of 1500 ton. The natural periods for both cases are given in Table 40.

Degree of freedom	Natural periods T_i for Case 1 → T_o =1000 ton [s]	Natural period T_i for Case 2 → T_o =1500 ton [s]
Surge	8.85	7.91
Sway	9.78	8.52
Heave	4.38	4.85
Roll	1.34	1.42
Pitch	8.24	8.54
Yaw	7.32	6.00

Table 40 Natural periods of the pontoon (for l=8m, 4 suspension cables, To= 1000 [ton] or To=1500 [ton])

By increasing the initial pre-stress in the cables, the natural periods will decrease. The natural frequency of the yaw motion drops and becoming close the wind wave frequency. The Eigen matrix of the system with four and two suspension cables is given here below.

$$Eig._{2-cables} = \begin{bmatrix} -0.999988 & 00.989049 & 0 & 0 & 0 & 0 \\ 0 & 0 & 0 & 0.079378 & -0.999999 & 0 \\ 0 & 0 & 1 & 0 & 0 & 0 \\ 0 & & 0 & 0.996845 & 0.000245 & 0 \\ 0.004819 & 0.147584 & 0 & 0 & 0 & 0 \\ 0 & 0 & 0 & 0 & 0 & 1 \end{bmatrix}$$

The Eigen matrix of the system is when 2 suspension cables are applied:

$$Eig_{4-cables} = \begin{bmatrix} -0.999985 & 0.99768 & 0 & 0 & 0 & 0 \\ 0 & 0 & 0 & -0.925085 & 0.999999 & 0 \\ 0 & 0 & 1 & 0 & 0 & 0 \\ 0 & 0 & 0 & 0.37976 & 0.0000245 & 0 \\ -0.002565 & 0.06812 & 0 & 0 & 0 & 0 \\ 0 & 0 & 0 & 0 & 0 & 1 \end{bmatrix}$$

The Eigen matrix of the system is when 4 suspension cables are applied:

The columns of the Eigenmatrix are the mode shapes. Each column represents the mode shape of one natural frequency (surge, sway, heave, roll, pitch, and yaw). Note that in sway there is no coupling in roll because of the small accelerations. However, in roll mode, there is coupling to sway. The negative sign in sway indicates that the roll center is below the sea surface (in the case of four suspension cables). Moreover, in the case of two suspension cables is the pitch center below the water surface.

The value of the stiffness coefficients of the stiffness matrix is also dependent on the length of the suspension cables. During the immersion operation, the length of the wires will be changed by the position of the TE under sea level. Changing length will also cause changes in stiffness matrix. That's why the natural periods are recalculated for different positions of the TE under the sea level. The natural periods of the system for various positions of the TE underwater are given in Table 41 and Table 42.

Degree of freedom	Natural periods T_i for h =10 [m] [s]	Natural period T_i for h =15 [m] [s]	Natural period T_i for h =23 [m] [s]	Natural period T_i for h =30 [m] [s]
Surge	11.6	13.2	15.4	17.1
Sway	20.0	23.0	27.1	30.2
Heave	5.08	5.48	5.90	6.16
Roll	1.89	2.16	2.53	2.80
Pitch	10.7	11.3	12.0	12.5
Yaw	8.74	9.94	11.6	12.9

Table 41 Natural periods of the pontoon for different position of the TE under water (4 suspension cables)

Degree of freedom	Natural periods T_i for h =10 [m] [s]	Natural period T_i for h =15 [m] [s]	Natural period T_i for h =23 [m] [s]	Natural period T_i for h =30 [m] [s]
Surge	11.6	13.2	15.4	17.1
Sway	20.0	23.0	27.1	30.2
Heave	5.19	5.57	5.99	6.24
Roll	1.96	2.24	2.62	2.90
Pitch	15.0	15.0	15.0	15.0
Yaw	9.04	10.3	12.0	13.4

Table 42 Natural periods of the pontoon for different position of the TE under water (2 suspension cables)

It is also investigated what is the effect on the natural frequencies when putting less ballast in the TE. By placing less weight in the TE, the tension in the suspension cables will be reduced. And the system will become less stiff. Natural Periods for putting less ballast in the TE and the position of TE 1[m] below water table are given in Table 43 and Table 44.

Degree of freedom	Natural periods T_i for T_o =150 [ton] [s]	Natural periods T_i for T_o =200 [ton] [s]	Natural periods T_i for T_o =250 [ton] [s]	Natural periods T_i for T_o =300 [ton] [s]
Surge	18.4	16.1	14.7	13.6
Sway	23.2	20.2	18.3	16.80
Heave	1.31	1.32	1.33	1.34
Roll	0.99	1.02	1.04	1.05
Pitch	12.2	12.2	12.4	12.4
Yaw	19.6	16.9	15.1	13.8

Table 43 Natural periods of the pontoon for different amount of ballast in TE (2 suspension cables)

Degree of freedom	Natural periods T_i for T_o =150 [ton] [s]	Natural periods T_i for T_o =200 [ton] [s]	Natural periods T_i for T_o =250 [ton] [s]	Natural periods T_i for T_o =300 [ton] [s]
Surge	18.4	16.1	14.7	13.6
Sway	23.2	20.2	18.3	16.8
Heave	1.26	1.27	1.29	1.29
Roll	0.967	0.986	0.999	1.02
Pitch	4.21	4.24	4.24	4.24
Yaw	18.9	16.4	14.6	13.4

Table 44 Natural periods of the pontoon for different amount of ballast in TE (4 suspension cables)

8.2.2 FROUDE-KRYLOV FORCE

Only dynamic Froude-Krilov wave pressure is considered in the calculations. The wave pressure is expressed by equation (178).

$$P = \rho_w \cdot \frac{\partial \varphi_0}{\partial t} \tag{178}$$

The wave pressure works on all areas of underwater hull, which is in contact with water. The resulting dynamic force consists of 3 translational forces and three rotational moments. For the 30 [m] water depth and low wave, height as in the case of normal conditions, it occurs that the deep water equation can be applied for the wave force calculations. For the case of Fehmarnbelt with 30 m water depth till a wave period of 6 [s], deep water conditions can be assumed. The pressure of undisturbed unidirectional wave is given by equation (179).

$$P_{w-FK} = \rho_w \cdot g \cdot \zeta_a \cdot e^{kz} \cdot \cos(ky - \omega t) \tag{179}$$

$$F_{FK} = -\iint (P_{w-FK} \cdot \bar{n}) \cdot ds \tag{180}$$

$$M_{FK} = -\iint P_{w-FK} (\bar{r} \cdot \bar{n}) \cdot ds \tag{181}$$

In order to calculate the wave pressure, it is assumed that the waves are long compared to the cross-sectional dimensions of the floaters and columns. But the waves are not long compared to the overall transversal and longitudinal dimensions of the pontoons B_p and L_p. The relevant parts of the pressure integration are given in Figure 125. The pressures and water particle accelerations are integrated over the area to obtain the wave forces and moments.

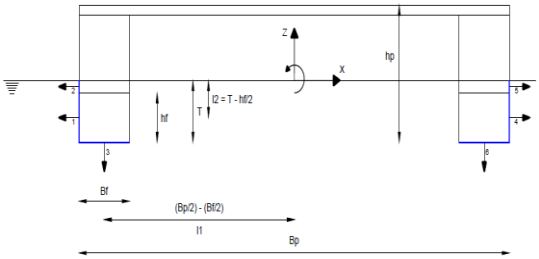

Figure 125 parts of the pressure integration for the wave force calculations

For the calculation of these Froude-Krilov forces and moments a wave traveling in the y-direction is analyzed (beam waves). Only pressure due to undisturbed wave, acting on the parts of the structure is taken into account. The forces and the moments are obtained by integrating the pressures over the area normal to the flow. The forces/moments from the pressures integration are expressed by the equations (180) and (181).

In order to calculate the forces and the moments first, the input variables are determined and subsequently the forces and the moments are calculated. Figure 126 gives the principle of the collocation point and the normal of a panel. These two variables for each panel, play an essential role in the force calculations. For each panel the pressure is determined in the collocation point, and this pressure is integrated over the whole area of the panel to get an estimate of the force. The Force direction is assumed to be opposite to the normal of the panel. For each panel given in Figure 126 the position of collocation point and the normal is determined.

The normal of the collocation point of each part is perpendicular to the panel at the intersection of the panel diagonals and has a direction into the fluid. The normal for part 1 till six are given in Table 45.

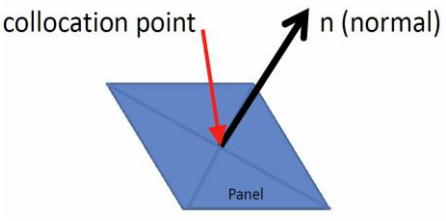

Figure 126 Collocation point and normal n

	n_i		
Pat	x		z
1	-1	0	0
2	-1	0	0
3	0	0	-1
4	1	0	0
5		0	0
	0	0	-1

Table 45 The normal of the 6 panels

The positions of the collocation point of the 6 panels are given in Figure 126.

In order to determine the force moments, the vector curl of each panel is determined. The vector curl, can be expressed as:

$$(\bar{r} \cdot \bar{n}) = ([r_2 \cdot n_3 - r_3 \cdot n_2], [r_3 \cdot n_1 - r_1 \cdot n_3], [r_1 \cdot n_2 - r_2 \cdot n_1]) \qquad (182)$$

The meaning of each parameter in the above-mentioned vector equation is given in Table 47. In the equation for the vector curl the terms represent the rotation arm about the axis-system.

The rotations are:

- The rotation arm about the x-axis.
- The rotation arm about the y-axis.
- The rotation arm about the z-axis.

As mentioned before, the calculations are performed for the beam waves traveling in the y-direction. The wave angle (μ) is assumed zero. It means that the force moment will act only about the x-axis on the system. No other force moment actions are taken into consideration. That's why the rotation arm about the x-axis is taken into account (see also Figure 125). The first term from the vector curl equation is used for the determination of the lever arm for the roll moment. By following the described procedure and filling in the determined parameters in the equations, the forces for beam waves are calculated.

For the calculations of the RAO's a wave amplitude of 1 [m] and water density of 1031 [kg/m^3] are used. The calculated forces in sway, heave and roll are given in Figure 127, Figure 128, and Figure 129 as a function of wave frequency. From the figures, it can be seen that most significant forces on the system will work in long waves with large periods. For short waves, the forces are significantly smaller. In waves with a period < 3 [s] the forces are much lower than those for waves with more considerable periods than 3 seconds. This fact has to be taken into account when selecting the proper immersion conditions. The statistical properties of the wave data for the different locations in the project area are given in Table 1. By observing the peak wave periods (T_p) in the project area, it can be concluded that the wave forces on the pontoons during the immersion operation can become quite large.

	n_i		
Part	x	y	z
1	$-B_p/2$	0	$T - \frac{h_f}{2}$
2	$-B_p/2$	0	$T - \frac{h_f}{2}$
3	$\frac{-B_p}{2} + \frac{B_f}{2}$	0	$-T$
4	$B_p/2$	0	$T - h_f/2$
5	$B_p/2$	0	$T - h_f/2$
6	$\frac{B_p}{2} + \frac{B_f}{2}$	0	$-T$

Table 46 collocation pint of the 6 panels

Coordinates			
Vectr	x	y	z
r	r_1	r_2	r_3
n	n_1	n_2	n_3

Table 47 Vector Curl

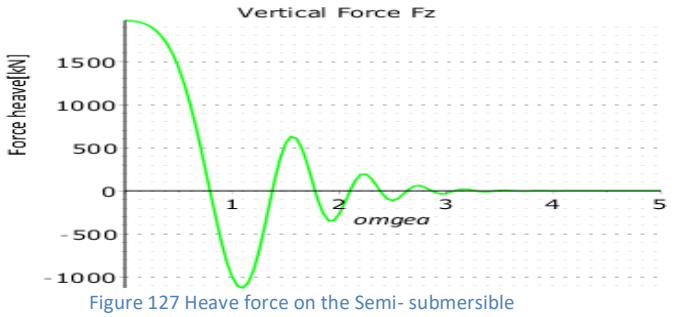

Figure 127 Heave force on the Semi- submersible

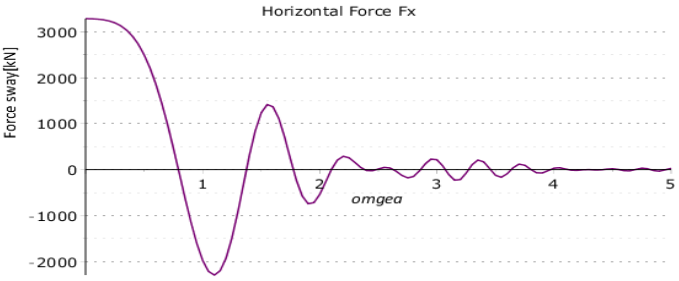

Figure 128 Sway force on the Semi- submersible

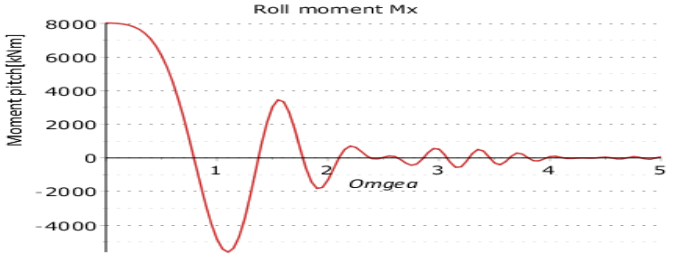

Figure 129 Roll moment on the Semi- submersible

8.2.3 FORCED EXCITATION SEMI-SUBMERSIBLE

The response of the system in regular waves can be calculated from the equation of motion. All the components of the equation of motion are determined. Damping of the system has been estimated as 5% of the critical damping of the system. Only the leading diagonal terms have been accounted in the calculations. For the calculations, the diffraction effects are neglected.

Only the Froude-Krilov force has been taken into account. The fluctuating effect of the water surface is disregarded in the calculations. The forces are determined by integrating the undisturbed wave pressure till the still water level. The equation of motions is solved in the frequency domain by the aid of modal analysis. The followed calculation procedure is given in Appendix7 Here only the results of the calculations are presented.

As we also saw in the time domain calculations, in beam waves only the motions in sway, heave, and roll matters. That's why for the workability analysis just these degrees of freedom are considered. In this section, only the results for Semi-submersible pontoon are given. The results of the Catamaran pontoon will be presented in the next section. The calculations are performed for the moment when the tunnel element is submerged 1m below the sea surface. In this position, the forces in the suspension cables are the largest. The resulting RAO's for the Semi-submersible pontoon are given Figure 130.

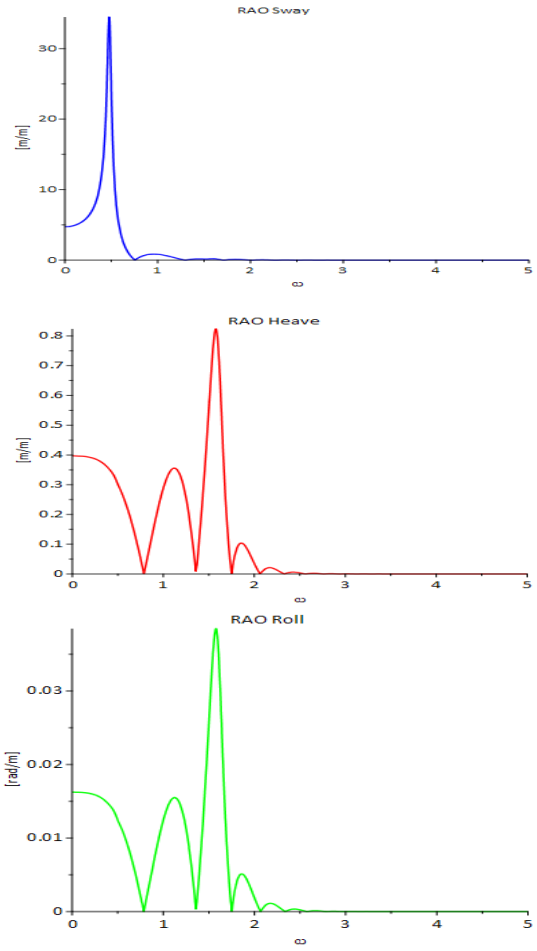

Figure 130 RAO's Semi-submersible pontoon in sway, heave and roll

8.2.4 OPERABILITY SEMI-SUBMERSIBLE PONTOON

To calculate the response in irregular waves the wave spectrum should be known. An energy density spectrum describes the random ocean waves. The wave energy spectrum represents the energy content of an ocean wave and its distribution over a frequency range of the random wave. Therefore, the random wave method of design is essential when evaluating the statistical properties if the response.

There are several spectrum formulas which can be used. The formulas are derived from the observed properties of ocean waves, and they are thus empirical. The most commonly used spectrum formulas are Pierson-Moskowitz and JONSWAP. The Pierson-Moskowitz (PM) spectrum is applicable in fully developed sea conditions only. The JONSWAP spectrum is derived from measurements in the North Sea and valid for developing seas.

$$S(\omega) = \alpha \cdot g^2 \cdot \omega^{-5} \cdot \exp\left(-1.25 \cdot \left\{\frac{\omega}{\omega_p}\right\}^{-4}\right) \cdot \gamma^a \qquad (183)$$

$$a = exp[-(\omega - \omega_p)^2/(2\sigma^2 \cdot \omega_p^2)] \qquad (184)$$

Where	
α	The Phillips constant, for the North Sea conditions it normally assume tobe equal to 0.0081.
ω	Wave frequency $(\omega = 2\pi/T_{wave})$
ω_p	Peak frequency $(\omega_p = 2\pi/T_p)$
γ	Peak enhancement factor $(\gamma = 3.3)$
σ	The with parameters, normally divided in two values namely: $\sigma_a = 0.07 \quad and \quad \sigma_b = 0.09$

In fact, JONSWAP spectrum is PM spectrum modified with peak enhancement factor which ensures the spectral peak. Therefore for the calculations, a JONSWAP spectrum is used. Which can be expressed by equations (183) and (184). For the Fixed Link corridor project, the values of σ and ϒ are determined from the actual wave frequency spectrum.

From the wave spectrum measurements, it appears that a JONSWAP spectrum represents well the majority of the fetch-limited sea states in Fehmarnbelt. The wave peak period which is required for the use of the JONSWAP spectrum can be estimated from the wave energy mean period T_{10} and is given by equation (185).

$$T_{10} = 0.9 \cdot T_p \quad (185)$$

From the provided data the width parameters and the peak enhancement factors are adjusted, and the spectrum is calculated with the values in equations (186) and (187).

$$\sigma_a = \sigma_b = 0.14 \quad (186)$$

$$\gamma = 2.44 \quad (187)$$

The response in irregular waves is found by using the transfer function of the motion and the wave spectrum. The irregular motional history in sway , heave and roll are obtained by adding up the regular components. The moments of the response spectra are given by:

$$m_n = \int_0^{\infty} S_n(\omega) \cdot \omega \cdot d\omega \quad (188)$$

$$with \qquad n = 1,2,..$$

The significant motional amplitude is calculated from the spectral density function of the motion as it is also done for waves. The significant motional amplitude is calculated by the aid of equation (189).

$$x_{1/3} = 2 \cdot \sqrt{m_o} \quad (189)$$

The mean period of the motion for given environmental conditions is calculated from the centroid of the spectrum with equation (190).

$$T_1 = 2\pi \cdot \frac{m_o}{m_1} \quad (190)$$

The wave frequency response in a sea state is obtained by combining the calculated RAO's with the wave spectrum. The RAO's/transfer functions are plotted in Figure 130 for the Semi-submersible pontoon as function of the wave frequency. The effect of the mooring lines and the contraction wires are disregarded in the RAO calculations. The response spectrum is calculated by multiplying the square RAO with the wave spectrum as in equation (169) has been given. It should be noted that the RAO's decreases by increasing wave frequency, also the peak of the response spectrum is moved to the lower frequencies.

The area m_o is the variance of the response, and the squared root of the variance is the standard deviation of the response. The mean zero crossing period is given by the equation (190) The most expected value for each degree is been calculated with the aid of equation (192)

The downtime analysis is carried out by evaluating the motional spectra for many combinations for wave height and wave periods. For every combination, the motional spectra in three degrees of freedom are calculated. For each degree of freedom, the mean motional period is calculated. The duration of the operation is assumed to be 3 hours. The number of cycles N is found by the following equation(191).

$$N_{cycles} = \frac{3600 \cdot 3}{T_{1,n}} \quad (191)$$

In the equation mentioned above $T_{1,n}$ represents the mean period of the response in nth degree of freedom.

For each combination of wave height and wave period, the most probable maximum is calculated for sway, heave, and roll in beam waves. Due to a significant amount of calculated data the results are presented in the wave scatter diagram. If one of the limit conditions is exceeded, then those conditions are marked as not workable. The results are shown in Figure 131 for a pontoon with two suspension cables and in Figure 132 for a pontoon with four suspension cables.

$$\text{most expected value} = \sqrt{m_0} * \sqrt{2 * \ln(N)} \quad (192)$$

T_p/H_s	0-0.1	0.1-0.2	0.2-0.3	0.3-0.4	0.4-0.5	0.5-0.6	0.6-0.7	0.7-0.8	0.8-1.0	1.0-1.2	1.2-1.4	1.4-1.6	1.6-1.8	1.8-2.0	2.0-2.2	2.2-2.4	2.4-2.6	2.6-2.8	2.8-3.0	3.0-3.2	3.2-3.4	3.4-3.6
0-0.25																						
0.25-0.5																						
0.5-0.75																						
0.75-1	9																					
1-1.25	247	60																				
1.25-1.5	1365	675																				
1.5-1.75	2035	4015	136																			
1.75-2.0	1581	5990	2930	25																		
2.0-2.25	740	4772	7078	1473	17																	
2.25-2.50	392	2570	5784	6464	702	17																
2.50-2.75	247	1019	2856	6895	5059	540	23															
2.75-3.0	201	224	1071	3068	6997	4192	510	35	4													
3.0-3.25	118	86	194	899	3137	6676	3991	543	33													
3.25-3.50	52	30	27	169	666	2765	6185	3959	903	4												
3.50-3.75	61	8	2	20	117	403	1857	4663	5006	148	4											
3.75-4.00	34	7	3	1	16	50	205	902	6924	1832	42	1										
4.00-4.25	18	2	1		1	4	23	70	1835	5395	732	33	1									
4.25-4.5	7					1	2	4	107	2190	3713	368	15	1								
4.5-4.75									4	70	1643	2412	241	4	1							
4.75-5.00										30	46	911	1340	216	7	1						
5.00-5.25										1		12	309	615	135	7						
5.25-5.50												1		51	205	102	11	1				
5.50-5.75															2	32	37	18	3			
5.75-6.00																	3	17	11	6		
6.00-6.25																			1	3	1	2
6.25-6.50																						1
6.50-6.75																						
6.75-7.0																						

Figure 131 Workable conditions Semi-submersible pontoon (2suspension cables applied)

T_p /Hs	0-0.1	0.1-0.2	0.2-0.3	0.3-0.4	0.4-0.5	0.5-0.6	0.6-0.7	0.7-0.8	0.8-1.0	1.0-1.2	1.2-1.4	1.4-1.6	1.6-1.8	1.8-2.0	2.0-2.2	2.2-2.4	2.4-2.6	2.6-2.8	2.8-3.0	3.0-3.2	3.2-3.4	3.4-3.6
0-0.25																						
0.25-0.5																						
0.5-0.75																						
0.75-1	9																					
1-1.25	247	60																				
1.25-1.5	1365	675																				
1.5-1.75	2035	4015	136																			
1.75-2.0	1581	5990	2930	25																		
2.0-2.25	740	4772	7078	1473	17																	
2.25-2.50	392	2570	5784	6464	702	17																
2.50-2.75	247	1019	2856	6895	5059	540	23															
2.75-3.0	201	224	1071	3068	6997	4192	510	35	4													
3.0-3.25	118	86	194	899	3137	6676	3991	543	33													
3.25-3.50	52	30	27	169	666	2765	6185	3959	903	4												
3.50-3.75	61	8	2	20	117	403	1857	4663	5006	148	4											
3.75-4.00	34	7	3	1	16	50	205	902	6924	1832	42	1										
4.00-4.25	18	2	1		1	4	23	70	1835	5395	732	33	1									
4.25-4.5	7					1	2	4	107	2190	3713	368	15	1								
4.5-4.75									4	70	1643	2412	241	4	1							
4.75-5.00										30	46	911	1340	216	7	1						
5.00-5.25										1		12	309	615	135	7						
5.25-5.50												1		51	205	102	11	1				
5.50-5.75															2	32	37	18	3			
5.75-6.00																	3	17	11	6		
6.00-6.25																			1	3	1	2
6.25-6.50																						1

Figure 132 Workable conditions Semi-submersible pontoon (4 suspension cables applied)

8.3 DYNAMIC ANALYSIS CATAMARAN PONTOON IN FREQUENCY DOMAIN

In this part, the operability of the Catamaran pontoon is analyzed. The pontoons consist of three parts, namely: two floaters and pontoon-deck (see also Figure 97). The same principles have been applied as for the Semi-submersible pontoon in the determination of the dynamic behavior. The steps and procedure are identical. For the analysis, the same local data has been used as previously. Only the geometry properties of the pontoon differ. All the calculations are performed in a computer program generated in Maple. For the calculations the main properties of the pontoon mentioned in Table 48 are used:

Parameter	Value	Units
The total weight of 1 pontoon	1500	[ton]
The weight of each floater	350	[ton]
Weight of the deck	400	[ton]
Weight equipment	400	[ton]
Position center of gravity above the keel	7.58	[m]
Positions Center of buoyancy above the keel	2.33	[m]
Distance KB	5.25	[m]
Total amount of pretension in the cables	984	[ton]
Diameter suspension cables (4 cables)	75	[mm]
Diameter suspension cables (2 cables)	100	[mm]
Length of the cable	6	[m]

Table 48 main parameters used for the calculations

8.3.1 NATURAL FREQUENCY ANALYSIS:

Mass matrix

The structural mass and the added mass matrices are given here next to it.

$$M_{structural} = \begin{bmatrix} 24{,}84\cdot10^5 & 0 & 0 & 0 & -7{,}523\cdot10^6 & 0 \\ 0 & 24{,}84\cdot10^5 & 0 & -7{,}523\cdot10^6 & 0 & 0 \\ 0 & 0 & 24{,}84\cdot10^5 & 0 & 0 & 0 \\ 0 & -7{,}523\cdot10^6 & 0 & 9{,}32\cdot10^8 & 0 & 0 \\ -7{,}523\cdot10^6 & 0 & 0 & 0 & 6{,}2\cdot10^7 & 0 \\ 0 & 0 & 0 & 0 & 0 & 1{,}855\cdot10^7 \end{bmatrix}$$

$$M_a = \begin{bmatrix} 4{,}65\cdot10^5 & 0 & 0 & 0 & 1{,}33\cdot10^7 & 0 \\ 0 & 2{,}52\cdot10^6 & 0 & 1{,}33\cdot10^7 & 0 & 0 \\ 0 & 0 & 1{,}51\cdot10^6 & 0 & 0 & 0 \\ 0 & 1{,}33\cdot10^7 & 0 & 7{,}48\cdot10^7 & 0 & 0 \\ 1{,}33\cdot10^7 & 0 & 0 & 0 & 3{,}82\cdot10^8 & 0 \\ 0 & 0 & 0 & 0 & 0 & 9{,}23\cdot10^8 \end{bmatrix}$$

There are several methods of estimating the added mass. Many experts in the field have released formulae for calculating the added mass coefficients. However, there are significant differences in the estimated values. From the literature study (Floating Structures:, 1998) it can be concluded that a simple and use full estimation for the added mass is given in Baltrop, 1998 for the cylindrical shapes. For the analysis as a first approximation the added mass is estimated by using Figure 123, and Figure 124 (from Baltrop, 1998) and (copied from (Floating Structures:, 1998)) has been used.

Subsequently, the estimated values are used in the calculation of the natural frequency. Then the calculated natural frequencies are used for determination of the added mass coefficients by (J.H.Vugts, 1971). The added matrix has been recalculated. This procedure has been repeated several times, till convergence was achieved.

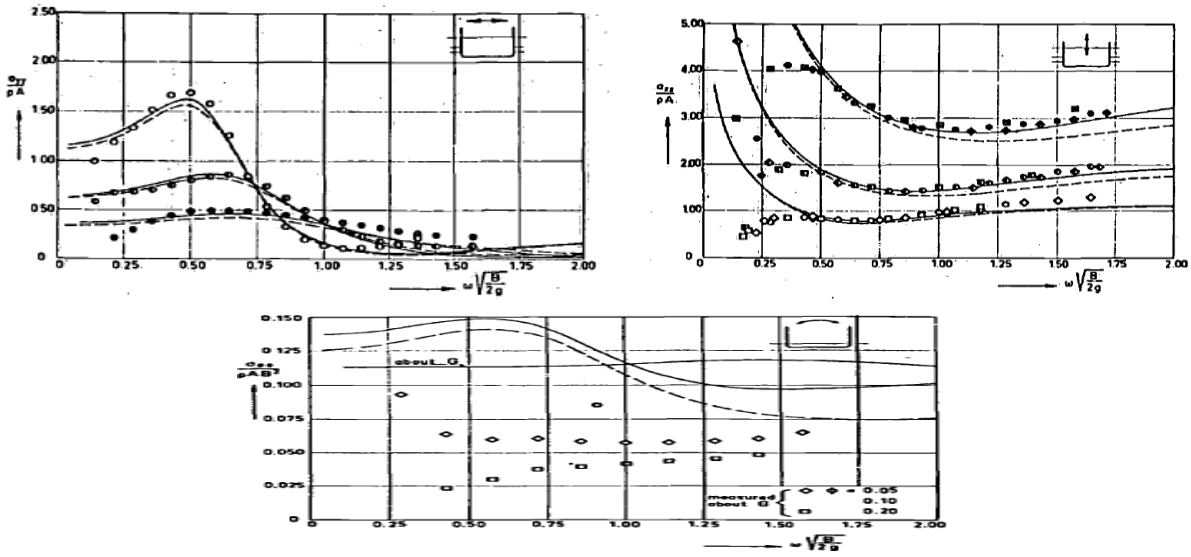

Figure 133 added mass for floating structures (J.H.Vugts, 1971)

The total mass and the linear stiffness matrices are given here below.

$$M_{tot} = \begin{bmatrix} 2{,}95{\cdot}10^{6} & 0 & 0 & 0 & 7{,}29{\cdot}10^{6} & 0 \\ 0 & 5{,}01{\cdot}10^{6} & 0 & 7{,}29{\cdot}10^{6} & 0 & 0 \\ 0 & 0 & 3{,}99{\cdot}10^{6} & 0 & 0 & 0 \\ 0 & 7{,}29{\cdot}10^{6} & 0 & 1{,}01{\cdot}10^{9} & 0 & 0 \\ 7{,}29{\cdot}10^{6} & 0 & 0 & 0 & 4{,}45{\cdot}10^{8} & 0 \\ 0 & 0 & 0 & 0 & 0 & 9{,}42{\cdot}10^{8} \end{bmatrix}$$

$$K_{lin} = \begin{bmatrix} 1.62{\cdot}10^{6} & 0 & 0 & 0 & 0 & 0 \\ 0 & 1.62{\cdot}10^{6} & 0 & 0 & 0 & 0 \\ 0 & 0 & 9.23{\cdot}10^{7} & 0 & 0 & 0 \\ 0 & 3.10{\cdot}10^{6} & 0 & 3.93{\cdot}10^{10} & 0 & 0 \\ 3.10{\cdot}10^{6} & 0 & 0 & 0 & 2.37{\cdot}10^{9} & 0 \\ 0 & 0 & 0 & 0 & 0 & 7.033{\cdot}10^{8} \end{bmatrix}$$

The natural frequencies and the natural periods are calculated for 1 m below the water surface for 4 and 2 suspension cables configuration.

Degree of freedom	Natural frequency ωi [rad/s]	Natural perid Ti [s]
Surge	0.740	8.490
Sway	0.568	11.06
Heave	2.420	2.420
Roll	6.332	0.990
Pitch	0.682	9.201
Yaw	0.838	7.402

Table 49 Natural periods of the Catamaran pontoon and the Eigen frequencies (for l=6m and 4 suspension cables)

Degree of freedom	Natural frequency ω_i [rad/s]	Natural period T_i [s]
Sure	0.740	8.49
Sway	0.568	11.06
Heave	6.704	0.93
Roll	2.67	2.35
Pitch	3.264	1.96
Yaw	0.864	7.27

Table 50 Natural periods of the pontoon and the Eigen frequencies (for l=6m and 4 suspension cables)

In table here below the natural frequencies are calculated when the pretension is increased in the suspension cables.

Degree of freedom	Natural periods T_i for T_o =1500 ton [s]	Natural period T_i for T_o =2000 ton [s]
Surge	7.046	6.05
Sway	9.496	8.399
Heave	0.916	0.876
Roll	2.513	2.592
Pitch	1.846	1.703
Yaw	5.407	4.238

Table 51 Natural periods of the pontoon and the Eigen frequencies (for l=6m and 4 suspension cables)

$$Eig_{(4-calbles)} = \begin{bmatrix} -0.999999 & -0.358383 & 1.44414{*}10^{-16} & 0 & 0 & 0 \\ 0 & 0 & 0 & -0.064247 & 0.999999 & 0 \\ 0.001014 & -0.9156833 & 1 & 1 & 0.002163 & 0 \\ 0 & 0 & 0 & 0.0426772 & -0.000010 & 0 \\ -0.000206 & 0.144034 & -3.45389{*}10^{-16} & 0 & 0 & 0 \\ 0 & 0 & 0 & 0 & 0 & 1 \end{bmatrix}$$

The Eigen-matrix when 4 suspension cables are applied:

$$Eig_{(2-cables)} = \begin{bmatrix} -0.999999 & -0.99689 & 0 & 0 & 0 & 0 \\ 0 & 0 & 0 & -0.0646562 & 0.999999 & 0 \\ 0 & 0 & 1 & -0.99701 & 0.0022878 & 0 \\ 0 & 0 & 0 & 0.042275 & -0.000011 & 0 \\ -0.000233 & 0.07868 & 0 & 0 & 0 & 0 \\ 0 & 0 & 0 & 0 & 0 & 1 \end{bmatrix}$$

Eigen-matrix when 2 suspension cables are applied

Natural period of the system for different lengths and pontoon with 4 suspension cables are:

Degree of freedom	Natural periods T_i for h =10 [m] [s]	Natural period T_i for h =15 [m] [s]	Natural period T_i for h =22 [m] [s]	Natural period T_i for h =30 [m] [s]
Surge	13.61	15.70	15.87	20.76
Sway	17.68	20.41	24.15	26.99
Heave	1.447	1.651	1.918	2.111
Roll	2.776	2.877	2.973	3.025
Pitch	3.016	3.423	3.947	4.319
Yaw	11.75	13.57	16.05	17.95

Table 52 Natural periods for different depths

Natural Periods for putting less ballast in the TE and the position of TE 1m below water table, 4 suspension cables are used:

Degree of freedom	Natural periods T_i for T_o=400 [ton] [s]	Natural periods T_i for T_o=450 [ton] [s]	Natural periods T_i for T_o=600 [ton] [s]	Natural periods T_i for T_o=700 [ton] [s]
Surge	12.401	11.786	10.43	9.782
Sway	15.463	14.755	13.22	12.488
Heave	0.994	0.993	0.995	0.995
Roll	2.082	2.109	2.185	2.233
Pitch	2.183	2.156	2.130	2.109
Yaw	12.38	11.601	9.840	8.988

Table 53 Natural periods for different tension values in cables

8.3.2 Froude-Kirov Force on the pontoon(Beam waves)

The force on the pontoon for different wave frequency is given in figure here below. The force has been calculated for a wave with amplitude of 1[m].

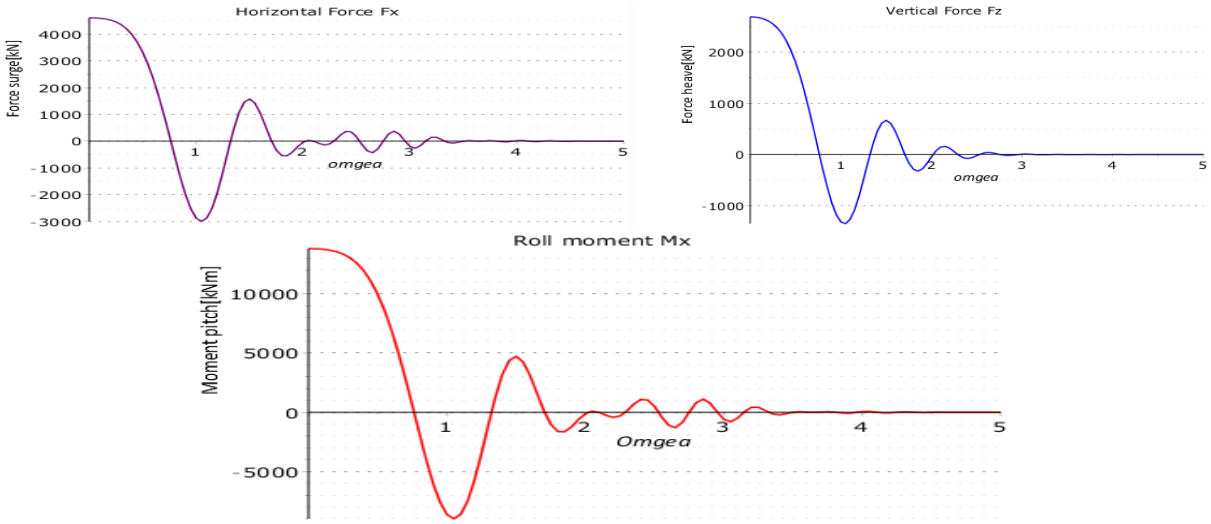

Figure 134 Froude-Krilov force on the Catamaran pontoon as function of the wave frequency

8.3.3 Forced excitation Catamaran

The RAO's of the catamaran pontoon has been calculated by following the same procedure as for the Semi-submersible pontoon. The results are given in Figure 135.

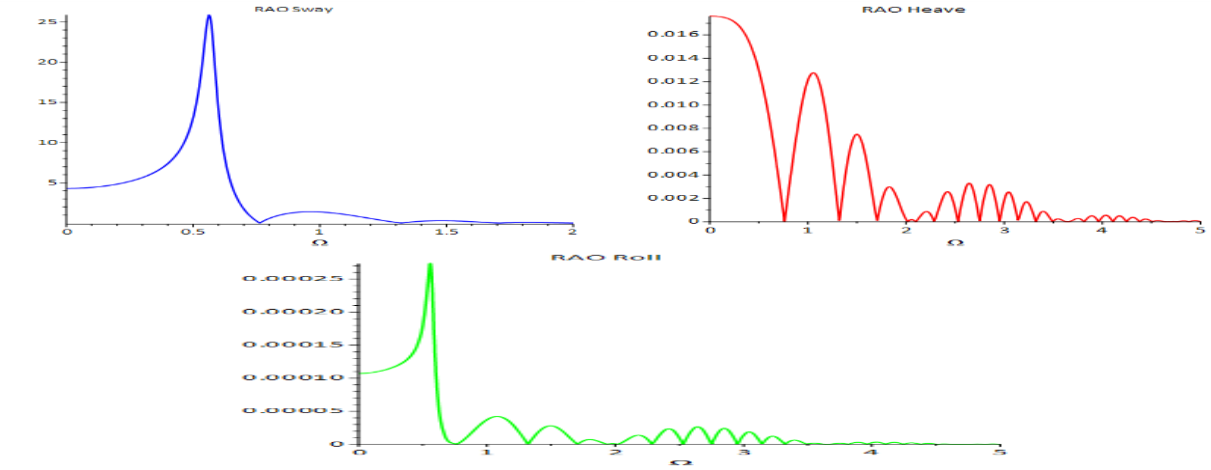

Figure 135 RAO's Catamaran pontoon

8.3.4 OPERABILITY CATAMARAN PONTOON

The same procedure is followed as for the Semi-submersible pontoon to calculate the operability for the Catamaran pontoon. For each combination of wave height and wave period, the most probable maximum is calculated for sway, heave, and roll in beam waves. Due to a large amount of computed data the results are presented in the wave scatter diagram. If one of the limit conditions is exceeded, then those conditions are marked as not workable. The results are shown in Figure 136 for a pontoon with two suspension cables and in Figure 137 for a pontoon with four suspension cables.

T_P /Hs	0-0.1	0.1-0.2	0.2-0.3	0.3-0.4	0.4-0.5	0.5-0.6	0.6-0.7	0.7-0.8	0.8-1.0	1.0-1.2	1.2-1.4	1.4-1.6	1.6-1.8	1.8-2.0	2.0-2.2	2.2-2.4	2.4-2.6	2.6-2.8	2.8-3.0	3.0-3.2	3.2-3.4	3.4-3.6
0-0.25																						
0.25-0.5																						
0.5-0.75																						
0.75-1	9																					
1-1.25	247	60																				
1.25-1.5	1365	675																				
1.5-1.75	2035	4015	136																			
1.75-2.0	1581	5990	2930	25																		
2.0-2.25	740	4772	7078	1473	17																	
2.25-2.50	392	2570	5784	6464	702	17																
2.50-2.75	247	1019	2856	6895	5059	540	23															
2.75-3.0	201	224	1071	3068	6997	4192	510	35	4													
3.0-3.25	118	86	194	899	3137	6676	3991	543	33													
3.25-3.50	52	30	27	169	666	2765	6185	3959	903	4												
3.50-3.75	61	8	2	20	117	403	1857	4663	5006	148	4											
3.75-4.00	34	7	3	1	16	50	205	902	6924	1832	42	1										
4.00-4.25	18	2	1		1	4	23	70	1835	5395	732	33	1									
4.25-4.5	7					1	2	4	107	2190	3713	368	15	1								
4.5-4.75									4	70	1643	2412	241	4	1							
4.75-5.00										30	46	911	1340	216	7	1						
5.00-5.25										1		12	309	615	135	7						
5.25-5.50												1		51	205	102	11	1				
5.50-5.75															2	32	37	18	3			
5.75-6.00																	3	17	11	6		
6.00-6.25																			1	3	1	2
6.25-6.50																						1

Figure 136 Workable conditions Catamaran pontoon (2suspension cables applied)

T_P /Hs	0-0.1	0.1-0.2	0.2-0.3	0.3-0.4	0.4-0.5	0.5-0.6	0.6-0.7	0.7-0.8	0.8-1.0	1.0-1.2	1.2-1.4	1.4-1.6	1.6-1.8	1.8-2.0	2.0-2.2	2.2-2.4	2.4-2.6	2.6-2.8	2.8-3.0	3.0-3.2	3.2-3.4	3.4-3.6
0-0.25																						
0.25-0.5																						
0.5-0.75																						
0.75-1	9																					
1-1.25	247	60																				
1.25-1.5	1365	675																				
1.5-1.75	2035	4015	136																			
1.75-2.0	1581	5990	2930	25																		
2.0-2.25	740	4772	7078	1473	17																	
2.25-2.50	392	2570	5784	6464	702	17																
2.50-2.75	247	1019	2856	6895	5059	540	23															
2.75-3.0	201	224	1071	3068	6997	4192	510	35	4													
3.0-3.25	118	86	194	899	3137	6676	3991	543	33													
3.25-3.50	52	30	27	169	666	2765	6185	3959	903	4												
3.50-3.75	61	8	2	20	117	403	1857	4663	5006	148	4											
3.75-4.00	34	7	3	1	16	50	205	902	6924	1832	42	1										
4.00-4.25	18	2	1		1	4	23	70	1835	5395	732	33	1									
4.25-4.5	7					1	2	4	107	2190	3713	368	15	1								
4.5-4.75									4	70	1643	2412	241	4	1							
4.75-5.00										30	46	911	1340	216	7	1						
5.00-5.25										1		12	309	615	135	7						
5.25-5.50												1		51	205	102	11	1				
5.50-5.75															2	32	37	18	3			
5.75-6.00																	3	17	11	6		
6.00-6.25																			1	3	1	2
6.25-6.50																						1

Figure 137 Workable conditions Catamaran pontoon (4 suspension cables applied)

8.4 CONCLUSION

In this chapter, the operability and motional behavior of the pontoons is studied in the frequency domain. The main conclusions from this chapter are listed here. The dynamic response of the barges is determined by the natural frequencies. In the analysis, the effect of different parameters has been taken into account. It is observed how the natural frequencies are influenced by changing several parameters.

When comparing the natural periods of the two pontoons to each other, it is clear that the Semi-submersible barge has larger natural frequencies than Catamaran pontoon. The natural periods of Semi-submersible pontoons are approximately a factor 1.4 larger than the natural periods of the Catamaran pontoon. Additionally, a pontoon with four suspension cables has a smaller natural period than a pontoon with two suspension cables. However, the difference is minimal.

For both pontoons, it can be concluded that the natural periods of the pontoon in surge, sway and yaw are larger than waves of importance in the Fehmarnbelt. However, the pontoons can be sensitive to the swell waves if they occur. The natural periods of the pontoon in surge, sway and yaw are close the periods of swells. Also, the natural periods in pitch if two suspension cables are applied are close to the swell periods.

By increasing the initial prestress in the cable, simply by putting more ballast water in the element the natural periods of the pontoons will decrease. The natural frequency of the yaw motion decreases and will be close the wind waves frequency. This is true for both pontoons. Catamaran pontoon is more sensitive to the pre-stress increase than the Semi-submersible. Also, the natural period in surge decreased to the wave periods for the Catamaran pontoon. There is more chance of occurring of resonance when Catamaran pontoon will be applied in combination with high prestress in the suspension cables.

During the immersion, the position of the tunnel element will change in the vertical alignment. The length of the suspension cables will change too correspondingly. The increasing length of the suspension cables has a favorable effect on the natural frequencies. From the results, it can be concluded that the pontoons are more sensitive to the wave loads when the tunnel element are positioned approximately 1 m below the water surface. Also, less pretension has a favorable effect on the natural frequencies of the system.

However, decreasing the prestress in the cables will enlarge the chance that the suspension cables may be slackening. If this happens then, the element will become uncontrollable with high risk to the safety of the operation. By observing the RAO's of the pontoons, it appears that a Semi-submersible pontoon is more sensitive to the long period waves than the Catamaran. The following observations are obtained from the calculations:

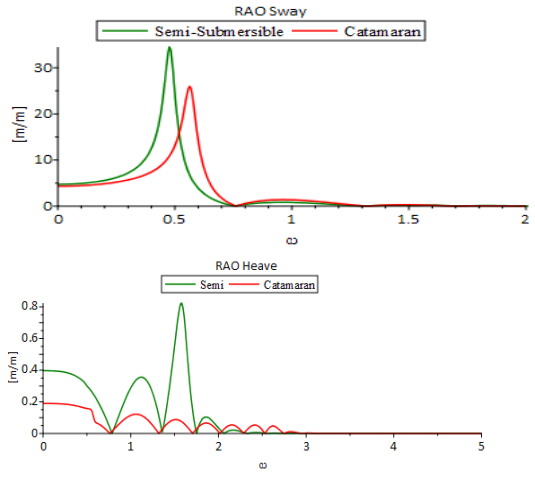

Figure 138RAO's for Semi-submersible and Catamaran pontoon

Degree of freedom	Factor	Wave frequency [rad/s]
Sway	1.4	0.5
Heave	2	From 0 till 0.4
Roll	2	0.4

Table 54 Difference in the RAO peaks for Semi-submersible and Catamaran Pontoons

It should be noted that in the calculations of the RAO's, the nonlinear term in the stiffness matrix are neglected. The difference in the RAO peaks can be declared due to larger inertia of the Catamaran Pontoon and larger stiffness of the suspension cables and more pretension of the cables. However, as we saw in the time domain calculations the motional behavior of the Semi-submersible pontoon is much more favorable than the Catamaran pontoon for the motions.

From the performed calculations for the workability, it is clear that for the Semi-submersible ULS limiting conditions are exceed more than for the Catamaran. The limit of the motions in the ULS was often exceeded for the Semi-submersible pontoon. From the observations of the RAO's and workability, it can be concluded that the dimensions of the Semi-submersible barge are not chosen optimally. By increasing, the pontoons dimensions and submerging the floaters deeper under the sea level the dynamic behavior of the Semi-submersible pontoon can be further improved. This was also done to optimize the dynamic behavior of the pontoon and to improve the static stability. The workability was recalculated for the new dimensions of the Semi-submersible pontoon.

Parameter	Value	Units
Water depth	30	[m]
Mass of each column	40	[ton]
Mass of each floater	400	[ton]
Mass of the equipment	400	[ton]
Total force from suspension cables	950	[ton]
Amount of ballast in the pontoon	250	[ton]
Diameter suspension cables (4 cables)	75	[mm]
Diameter suspension cables (2 cables)	100	[mm]
Length floaters	45	[m]
Width floaters	7	[m]
Draught (T)	7	[m]
Width pontoon	85	[m]
Pretension in cables	950	[ton]

Table 55 Altered dimensions Semi-submersible pontoon

T_p/H_s	0-0.1	0.1-0.2	0.2-0.3	0.3-0.4	0.4-0.5	0.5-0.6	0.6-0.7	0.7-0.8	0.8-1.0	1.0-1.2	1.2-1.4	1.4-1.6	1.6-1.8	1.8-2.0	2.0-2.2	2.2-2.4	2.4-2.6	2.6-2.8	2.8-3.0	3.0-3.2	3.2-3.4	3.4-3.6
0-0.25																						
0.25-0.5																						
0.5-0.75																						
0.75-1	9																					
1-1.25	247	60																				
1.25-1.5	1365	675																				
1.5-1.75	2035	4015	136																			
1.75-2.0	1581	5990	2930	25																		
2.0-2.25	740	4772	7078	1473	17																	
2.25-2.50	392	2570	5784	6464	702	17																
2.50-2.75	247	1019	2856	6895	5059	540	23															
2.75-3.0	201	224	1071	3068	6997	4192	510	35	4													
3.0-3.25	118	86	194	899	3137	6676	3991	543	33													
3.25-3.50	52	30	27	169	666	2765	6185	3959	903	4												
3.50-3.75	61	8	2	20	117	403	1857	4663	5006	148	4											
3.75-4.00	34	7	3	1	16	50	205	902	6924	1832	42	1										
4.00-4.25	18	2	1		1	4	23	70	1835	5395	732	33	1									
4.25-4.5	7					1	2	4	107	2190	3713	368	15	1								
4.5-4.75									4	70	1643	2412	241	4	1							
4.75-5.00										30	46	911	1340	216	7	1						
5.00-5.25										1		12	309	615	135	7						
5.25-5.50												1		51	205	102	11	1				
5.50-5.75															2	32	37	18	3			
5.75-6.00																	3	17	11	6		
6.00-6.25																			1	3	1	2
6.25-6.50																						1
6.50-6.75																						
6.75-7.0																						

Figure 139 Improved workability Semi-submersible pontoon (4 suspension when cables are applied)

From Figure 139 it is obvious that by submerging the pontoon deeper and increasing the stiffness in heave, the pontoon's dynamic behavior is improved. By increasing the length and the width of the floaters also the static stability and floating capacity is improved. The ULS conditions are not exceeded even for wave heights of 1.8 m and relatively larger wave periods. By changing the configuration of the pontoon, the dynamic behavior can further be improved. It should be noted, that for a wave height > 1.4 m the accelerations in sway become unacceptable large. For the mentioned wave height the expected value of accelerations in sway is above 1.5 m/s^2.

9 CONCLUSIONS AND RECOMMENDATIONS

Each of the previous chapters contains a conclusion on specific matter studied in this thesis report. By combining these outcomes, an answer to the research question is obtained. This section discusses the main findings. Besides, some recommendations are formulated for possible future research.

9.1 CONCLUSIONS:

In this report, a numerical model has been described to investigate the motional characteristics and stability during the construction stages transport and immersion of a floating tunnel element and twin barges which are also indicated as pontoons. The results of the model lead to the following conclusions:

Effect of the pontoon configuration on static stability:

The Semi-submersible barge is sensitive to the force fluctuation in the suspension cables. The pontoon can handle a force fluctuation of 160 ton per cable. When exceeding this value, there is a danger of not having enough freeboard during the operation. In extreme cases, the pontoon can be drawn by higher fluctuations. In general, it can be concluded that the Semi-submersible barge is more sensitive to the force fluctuation in the suspension cables than the Catamaran pontoon concerning the static stability and floating capacity. Especially the floating ability became problematic if the force fluctuations become larger.

Transport

During the transport, the floating element is stable, even with a very small freeboard of 0.2 [m].

Additionally, the results presented in this report demonstrate that the highest drag force on the floating element works during the fitting out of the element. The maximum force is calculated for a current angle of 50° with the longitudinal axis of the element. For larger current angles the drag force stays quite stable. Therefore, it can be concluded that when the current angle is larger than 40° the force will grow by a factor 1.65 and then staying quite stable.

Also, during the fitting out of the element, it will be subjected to a torque moment about the z-axis. The most significant moment occurs when the tunnel element makes an angle of 80°and then disappearing when the element will be positioned perpendicular to the flow direction. Also during the transport, the element is subjected to a torque moment about the z-axis. However, the magnitude is much smaller.

Towing velocity is decisive for the hydrodynamic stability during transport. Towing velocities higher than 1,0 [m/s] can only be applied when the water depth is larger than 12 [m] in a combination of a freeboard of 0,2 [m]. For shallow water depths < 12 [m], the element is only stable if the towing velocity is 1.0 [m/s] or smaller. By enlarging the freeboard, a higher towing velocity can be applied for shallow water depths.

During transport and immersion wind waves in the Fehmarnbelt are not of primary concern for the stability of a floating element. The natural periods of the floating element are sufficiently far enough from the wave periods. The smallest natural period (roll) of the floating element is 8s and the periods in heave and pitch are respectively around the 10s. The calculated periods are close to typically swell periods. Long periodic waves like swell play a small role in the climatology of the study area. Therefore, it can be concluded that there is little chance that resonance will occur due to wave loading.

Immersion

It appears that wave-induced motions of floating tunnel element are negligible during transport and immersion. The presented results demonstrate that the relatively small waves are not able to bring the heavy tunnel element into motions. On another hand, the relatively light pontoons are sensitive to wave loadings.

The element will prevent the movements of the barges. This prevention leads to higher force fluctuations in the suspension cables.

The current forces will also excite the tunnel element and the pontoons during the immersion. For the tunnel element length smaller than 140 m the natural periods of the system are reasonably far from the vortex-shedding periods. For the greater lengths than 150 m, the natural period in heave and pitch are becoming close to the vortex-shedding periods. This is only true for the Semi-submersible pontoon. An immersion system with Catamaran pontoons seems to be less sensitive to vortex shedding period. Despite that a system with the Catamaran pontoon has smaller natural periods in general, the natural frequencies are far enough from the vortex shedding periods, and that makes it less sensitive.

In the analysis, the near-resonant behavior of the pontoons has been analyzed in the time domain. From calculations in beam waves, it appears that for both barges the motions in the soft degrees of freedom (surge and yaw) are very small compared to the limit values of the motions. The motions in sway are considerable, but they do not exceed the limit values. Even for very long waves, the pontoons are quite stable. The contribution of the first order wave force to the pontoons motions in soft degrees of freedom is limited.

However, in the stiff degrees of freedom (heave, pitch, and roll), the motions become problematic for long waves, and there is a possibility of breaking of the suspension cable for the Catamaran pontoon during the transient motions of the pontoon. The suspension cable force is exceeded by a factor 2. However, the force fluctuations for the Semi-submersible barge are much smaller. It can be concluded that for both type pontoons in long waves the motions in the stiff degrees of freedom are determinative.

Also, the number of applied suspension cables influence the motional characteristics. The pontoon with two suspension cables is more sensitive to longer waves than the pontoon with four suspension cables. When four suspension cables are applied, then the motions of the pontoons are smaller.

One of the boundary conditions for the immersion operation is that the suspension cables may not slacken due to the dynamic wave force (zero force in one of the suspension cables). From the calculation, it appears if the tunnel element will be immersed in wave conditions: (T> 5 [s] and Hs > 1 [m]). Then the dynamic force fluctuations are much larger than it was initially assumed. This brings us to a conclusion if one chooses to immerse the tunnel elements in sea conditions as mentioned earlier, definitely more ballast must be applied during the immersion. Also, the pontoons must have a larger floating capacity which leads to bigger pontoon dimensions.

When comparing the natural periods of the two pontoons to each other, it is clear that the Semi-submersible barge has larger natural frequencies than Catamaran pontoon. The natural periods of Semi-submersible pontoons are approximately a factor 1.4 larger than the natural periods of the Catamaran pontoon. Additionally, a pontoon with four suspension cables has smaller natural periods than a pontoon with two suspension cables. However, the difference is minimal.

For both pontoons, it can be concluded that the natural periods of the barges in surge, sway and yaw are larger than waves of importance in the Fehmarnbelt. However, the pontoon can be sensitive to the swell waves if they occur. The natural periods of the pontoon in surge, sway and yaw are pretty close to the periods of swells. Also, the natural periods in pitch if two suspension cables are applied are close to the swell periods.

By increasing the initial prestress in the cables, simply by applying more ballast water in the element will lead to a decrease of the natural periods. The natural frequency of the yaw motion decreases and will be close the wind waves frequency. This is true for both pontoons. Catamaran pontoon is more sensitive to the pre-stress increase than the Semi-submersible. Also, the natural period in surge decreased to the wave periods for the

Catamaran pontoon. Therefore, there is more chance of occurring of resonance when Catamaran pontoon will be applied in combination with high pre-stress in the suspension cables.

During the immersion, the position of the tunnel element will change in the vertical alignment. The length of the suspension cables will vary too correspondingly. The increasing length of the suspension cables has a favorable effect on the natural frequencies. From the results, it can be concluded that the pontoons are more sensitive to the wave loads when the tunnel element is positioned approximately 1 m below the water surface.

Operability

For the determination of the operability the observed wave and current condition in the Fehmarnbelt were taken into account. The workability due to wave conditions is given in table here below. When the nonworkable conditions due to vortex shedding will be included, then the Semi-submersible barge is operable in 80% of the current conditions and Catamaran pontoon in 95 % in Fehmanrbelt. Both pontoons are sensitive to waves with a period T > 4 s, and wave height > 0.6 m.

The initially calculated dimensions of the pontoons were optimized with the aim to improve the workability of the pontoons. For the Semi-submersible pontoon it appears, when submerging the pontoon deeper and increasing the stiffness in heave, the pontoon's dynamic behavior is being improved.

By increasing the length and the width of the floaters also the static stability and the floating capacity is improved. The ULS conditions are not exceeded even for a wave height of 1.8 m and relatively larger wave periods. It should be noted, that for a wave height > 1.4 m the accelerations in sway become unacceptably large. Changing the dimension of the Catamaran pontoon do not lead to better operability. That's why it can be concluded that a Semi-submersible pontoon has better operability in waves than a Catamaran pontoon.

	Semisubmersible (2 cables)	Semisubmersible (4 cables)	Catamaran (2 cables)	Catamaran (4 cables)	Improved Semi-submersible
Workable condition	41.61	52.15	41.50	41.49	76.63
SLS lim. exceeded	13.85	10.23	44.04	48.62	22.94
ULS lim. exceeded	44.53	37.77	14.47	9.89	0.417
Total non-workable	58.39	48.05	58.51	58.51	23.36

Table 56 Operability in % of time for different pontoons

Conclusion

From the results presented in this report, it is clear that the most critical mode of motions is heave. The heave motions mainly affect the force fluctuations in suspension cables. When the tunnel element is immersed in wave conditions T>5 s and H > 1 m, then there is a significant danger that one of the suspension cables will break when applying Catamaran pontoon. If a Semi-submersible pontoon is used, then the tunnel element can be immersed in wave conditions T < 6.5 s and H < 1.8 m. However, for the workability of the pontoons, the transversal and vertical accelerations of the barges are important parameters. Both barges are sensitive to the wave forces and the related accelerations. For increasing wave heights and periods, the accelerations are exceeded for both pontoons. However, Catamaran pontoon is more sensitive to the wave force.

In total, a Semi-submersible pontoon has favorable operability in the waves and current conditions in Fehmarnbelt. Therefore, if the workability will be the primary objective, then it is better to apply a Semi-submersible pontoon with four suspension cables. Then in 77% of environmental conditions in Fehmarnbelt, the tunnel elements can be immersed.

9.2 RECOMMENDATIONS

The numerical model presented in this report gives a good insight into the hydrodynamic behavior of the immersion system. However, several simplifications and assumption are applied to get numerical results. Due to nonlinearities, it is difficult to predict some aspects described here with high accuracy. That's why for the final design stage a scale model tests are preferred. The scale model tests should reveal a better understanding of the magnitude of the forces and the motions in different environmental conditions.

In the dynamical analysis for determination of the global hydrodynamic response of the pontoons approximate methods are used which doesn't require complicated analysis. Thereby the motions of the tunnel element are ignored. The non-diagonal terms in the added mass and radiation damping matrices are ignored too. Besides, the dependency of the damping matrix on the motional frequency are also ignored. In reality, the motions of the three floating bodies will influence each other. For a better comparison of the motional behavior of the two pontoons and tunnel element, a sophisticated analysis is advised for the future research. If the very different response of the system from those presented here will be obtained; it is possible that the nonlinear effects have become dominant. In that situation model tests in a wave flume will give a better insight.

For the future research the following topics could be interesting:

1. Investigating the effect of the non-linear wave forces on the immersion system thereby including the diffraction forces in the model.
2. Studying the impact of passing ships on the system during the immersion operation.
3. Including the effect of the tunnel trench in the model.
4. The inclusion of the dynamics of the mooring system and their impact on the stability and workability of the system.
5. Economic optimization of the immersion operation, thereby taking the hydrodynamical behavior of the system into account.

BIBLIOGRAPHY

1) A. Glerum, B.P. Ritger, W.D. Eysinik, W.F. Heins. (1967). *"Heins,"Motorway Tunnels Built By The Immersed Tube Method".* Rijkswaterstaat.
2) ANSYS, Inc. (October 2012). *"AQWA User Manual".* Release 14.5.
3) B.P. Rigter. (April 1989). *"Krachten Op Drijvende Voorwerpen In Beperkt Water".* Technische Universiteit Delft.
4) CAPITA SYMONDS. (sd). Presentation (Fehmarnbelt Fixed Link).
5) CHEN Zhi-jie, WANG Yong-xue, WANG Guo-yu et al. (2009). *Frequency responses of immersing tunnel element under wave actions.* Journal of Hydrodynamics, Ser. B.
6) CHEN Zhi-jie, WANG Yong-xue, WANG Guo-yu et al. (2009). *Frequency responses of immersing tunnel element underwave actions.* Journal of Hydrodynamics, Ser. B, pp:739-749.
7) DHI. (sd). *ENVIRONMENTAL BACKGROUND STUDIES FOR THE FEHMARNBELT FIXED LINK*. Opgehaald van https://www.dhigroup.com/global/news/imported/2012/1/30/environmentalbackgroundstudiesforthefehmarnbeltfixedlink
8) DHI/IOW Consortium in association with LICengineering FEHY. (2013). *"Fehmarnbelt Fixed Link. Metocean Condition".* Report No E1TR0066.1068 pp. .
9) Donald J. Smith. (1996). *"Simplified First Order Motion Analysis of a Moored FPSO".* ISSN 01410814. Journal of the Society for Underwater Technology, Vol. 22, No. I, pp. 3-13.
10) Erik Jille en Daniëlle de Groot. (2009). *"Afzinken op Zee".* Cement 2009/8.
11) FEHMARN BELT CONTRACTORS. (2013). *Marine Works.*
12) FEHY (Metocean Conditions). (2013). *Fehmarnbelt Fixed Link, Metocean Conditions.* Report No E1TR0066. 1068 pp.
13) Femern A/S. (2013, January 12). WORK IN PROGRESS (Technical description of key issues of Tunnel solutions).
14) Femern A/S. (sd). *The Tunnel Across Fehmarnbelt*. Opgehaald van http://femern.com/en
15) Floating Structures:. (1998). *a guide for design and analysis.* Centre for Marine and Petroleum Technology.
16) Gijsbert W. Nagel. (2011). *""Dynamic behaviour of tunnel elements during the immersion process".* Delft Mastre Thesis.
17) Hans Cozijn and Jin Wook Heo. (2009). *""ANALYSIS OF THE TUNNEL IMMERSION FOR THE BUSAN-GEOJE FIXED LINK PROJECT THROUGH SCALE MODEL TESTS AND COMPUTER SIMULATIONS"".* Proceedings of the ASME 28th International Conference on Ocean, Offshore and Arctic Engineering OMAE2009 May 31 - June 5, 2009, Honolulu, Hawaii.
18) J.A van Santen. (1985). *"APROXIMATIVE FORMULAE FOR CALCULATING THE MOTIONS OF SEMI-SUBMERSIBLES".* Ocean Engng. Vol. 12, No.3 pp. 235-252.
19) J.H.Vugts. (1971). *"The hydrodynamic coefficients for swaying, heaving and rolling cylinder in a free surface".* Shipbuilding Laboratory, Technological University Delft.
20) J.M.J. Journée and Jakob Pinkster. (2002). *Ship Hydromechanics.* Delft: Delft University of Technology.
21) J.M.J. Journée and W.W.Massie. (First Edition, January 2001). *"OFFSHORE HYDROMECHANICS".* Ship Hydromechanics Laboratory, Delft University of Technology.
22) JØRGEN ANDERSEN, CLAUS IVERSEN and EELCO VAN PUTTEN. (June 2012). *"MARINE WORKS OPERATIONS AND ENVIRONMENTAL CONSIDERATIONS WHEN BUILDING THE FEHMARNBELT TUNNEL".* Terra et Aqua , Number 127.
23) Lyngs, J. H. (2008). *Model accuracy in aseismic design.* AALBORG UNIVERSITY.
24) M.Z. Voorendt, W.F. Molenaar, K.G. Bezuyen. (2011). *Hydraulic Structures (Caissons).* Delft University of Technology.
25) Molenaar, V.L. (1988). *"Applications of immersion technologies in underwater construction".* Tunneling and Underground Space Technology 3, no. 4 (1988): 353-358.

26) N. Haritos. (2007). *"Introduction to the Analysis and Design of Offshore Structures– An Overview".* EJSE Special Issue: Loading on Structures (2007), The University of Melbourne, Australia.
27) S. Chandrasekaran , A.K. Jain. (August 2000). *"Dynamic behaviour of square and triangular offshore tension leg platforms under regular wave loads".* Department of Civil Engineering, Indian Institute of Technology.
28) S.J. Callander and S.T. Schuurmans. (1991). *" Westerschelde-oeververbinding tracé 3 DI.I, Indicaties voor krachten op tunnel elementen".* Waterloopkundig Laboratorium.
29) Spijkers, J.M.J., A.C.W.M. Vrouwenvelder, and E.C. Klaver. (2006). *Dynamics of Structures; Part I Vibration of structures CT4140.* Delft.
30) Srinivasan Chandrasekaran. (2012). *"Dynamics of Ocean Structure, Dynamic Analysis of TLP's lectures 12, 13, 14".* Department of Ocean Engineering Indian Institute of Technology, Madras.
31) SYMONDS, C. (sd). Presentation (Oresund Tunnel).
32) TAISEI Corporation . (2014). *Annual Report 2014 (online)*. Opgehaald van http://www.taisei.co.jp/english/csr/annual_report_online2014/towards3.html
33) V.L. Molenaar. (1986). *"Immersed Tube Tunnelling Offshore: Execution of immersed Tube Tunnelling Projects Under Offshore Conditions, Based on Studies for the Euroroute Fixed Chanel Link Proposal".* Tunnelling and Underground Space Technology, Vol.1, No. ¾, pp. 289-296.
34) Volker Construction International (immersion team). (2013). *Technical Evaluation (Tunnel Coatzacoalcos).*
35) W.D. Eysink and R.J de Jong. (1993). *"Forces due to ship maneuvering during immersion of tunnels, Delft Hydraulics.*
36) W.D. Eysink. (maart 1981). *"Westerschelde-oeververbinding (krachten op en verplaatsingen van de tunnelelementen tengevolge van stroomdruk)".* REL.NR.1405, Rijkswaterstaat.
37) Wim Janssen. (2012, january 16). Presentation (Fehmarnbelt Fixed Link Tunnel).